USGS
science for a changing world

Prepared in cooperation with the U. S. Fish and Wildlife Service, Bureau of Land Management, California Department of Fish and Wildlife, Nevada Department of Wildlife, and the U.S. Forest Service

Population and Habitat Analyses for Greater Sage-Grouse (*Centrocercus urophasianus*) in the Bi-State Distinct Population Segment: 2018 Update

Open-File Report 2019–1149

U.S. Department of the Interior
U.S. Geological Survey

Cover: Greater sage-grouse hen on nest at Virginia Mountains field site in Nevada; photograph taken by Emmy Tyrrell, April 29, 2017.

Population and Habitat Analyses for Greater Sage-Grouse (*Centrocercus urophasianus*) in the Bi-State Distinct Population Segment: 2018 Update

By Peter S. Coates, Mark A. Ricca, Brian G. Prochazka, Shawn T. O'Neil, John P. Severson, Steven R. Mathews, Shawn Espinosa, Scott Gardner, Sherri Lisius, and David J. Delehanty

Prepared in cooperation with the U.S. Fish and Wildlife Service, Bureau of Land Management, California Department of Fish and Wildlife, Nevada Department of Wildlife, and the U.S. Forest Service

Open-File Report 2019–1149

U.S. Department of the Interior
U.S. Geological Survey

U.S. Department of the Interior
DAVID BERNHARDT, Secretary

U.S. Geological Survey
James F. Reilly II, Director

U.S. Geological Survey, Reston, Virginia: 2020

For more information on the USGS—the Federal source for science about the Earth, its natural and living resources, natural hazards, and the environment—visit https://www.usgs.gov or call 1–888–ASK–USGS.

For an overview of USGS information products, including maps, imagery, and publications, visit https://store.usgs.gov.

Suggested citation:
Coates, P.S., Ricca, M.A., Prochazka, B.G., O'Neil, S,T., Severson, J.P., Mathews, S.R., Espinosa, S., Gardner, S., Lisius, S., and Delehanty, D.J., 2020, Population and habitat analyses for greater sage-grouse (*Centrocercus urophasianus*) in the bi-state distinct population segment—2018 update: U.S. Geological Survey Open-File Report 2019–1149, 122 p., https://doi.org/10.3133/ofr20191149.

ISSN 2331-1258 (online)

Contents

Figures

Tables

Conversion Factors

Inch/Pound to SI

Multiply	By	To obtain
	Area	
acre	4,047	square meter (m^2)
acre	0.4047	hectare (ha)
acre	0.4047	square hectometer (hm^2)
acre	0.004047	square kilometer (km^2)

SI to Inch/Pound

Multiply	By	To obtain
	Length	
meter (m)	3.281	foot (ft)
kilometer (km)	0.6214	mile (mi)
meter (m)	1.094	yard (yd)
	Area	
square meter (m^2)	0.0002471	acre
hectare (ha)	2.471	acre

Acronyms and Abbreviations

AIC	Akaike's information criterion
AICc	bias-correted Akaike's information criterion
ΔAIC	difference between model of interest and most parsimonious model
BLM	Bureau of Land Management
CC	canopy cover
CDFW	California Department of Fish and Wildlife
CI	confidence interval
CRI	credible interval
DPS	distinct population segment
DSA	annual distributional areas
ESA	Endangered Species Act
GAMM	generalized additive mixed model
GPS	global positioning system
HSI	habitat suitability index
IPM	integrated population model
LADWP	City of Los Angeles Department of Water and Power
MCMC	Markov Chain Monte Carlo
MODIS	moderate resolution imaging spectroradiometer
MSE	mean squared error
NA	not applicable
NDOW	Nevada Department of Wildlife
NDVI	normalized difference vegetation index
PD	posterior distribution
PDF	probability density function
PJ-CC1	pinyon-juniper conifer cover class 1 (greater than 0 to 10 percent cover)
PJ-CC2	pinyon-juniper conifer cover class 2 (greater than 10 to 20 percent cover)
PJ-CC3	pinyon-juniper conifer cover class 3 (greater than 20 percent)
PMU	population management unit
QA/QC	quality control and assurance checks
RSF	resource selection function
SD	standard deviation
SE	standard error
SSM	state space model
UD	utilization distribution

USFWS	U.S. Fish and Wildlife Service
USGS	U.S. Geological Survey
VHF	very high frequency
WERC	Western Ecological Resource Center

Population and Habitat Analyses for Greater Sage-Grouse (*Centrocercus urophasianus*) in the Bi-State Distinct Population Segment: 2018 Update

By Peter S. Coates,[1] Mark A. Ricca,[1] Brian G. Prochazka,[1] Shawn T. O'Neil,[1] John P. Severson,[1] Steven R. Mathews[1], Shawn Espinosa,[2] Scott Gardner,[3] Sherri Lisius,[4] and David J. Delehanty[5]

Executive Summary

The Bi-State Distinct Population Segment (Bi-State DPS) of greater sage-grouse (*Centrocercus urophasianus*, hereinafter "sage-grouse") represents a genetically distinct and geographically isolated population that straddles the border between Nevada and California. The primary threat to these sage-grouse populations is the expansion of single-leaf pinyon (*Pinus monophylla*) and Utah juniper (*Juniperus osteosperma*) into sagebrush ecosystems, which fragments and reduces population connectivity and survival. Other important threats include low water availability during brood-rearing, particularly during drought, and increased predation by common ravens (*Corvus corax*), a generalist predator often associated with anthropogenic resource subsidies. Although the Bi-State DPS occurs at high elevations relative to sage-grouse range-wide, changes in historical wildfire cycles and the conversion of native shrubs to invasive annual grasslands still threaten these populations. The Bi-State DPS has undergone multiple federal status assessments and associated litigation. For example, in October of 2013, the Bi-State DPS was proposed for listing as threatened under the Endangered Species Act of 1973 by the U.S. Fish and Wildlife Service (USFWS), then withdrawn in April 2015. The withdrawal decision was challenged, and in May 2018, a Federal district court ordered the withdrawal decision to be vacated, and USFWS was required to re-open the October 2013 listing evaluation.

In response, the U.S. Geological Survey (USGS), with State and Federal collaborators, embarked on a multipronged analysis to provide current and best available science regarding population status of sage-grouse within the Bi-State DPS. Using data from a long-term monitoring program, we carried out six analytical study objectives. Here, we provide preliminary results of these analyses. First, we used integrated population modeling (IPM) to predict annual population abundance ($\hat{N}$) and annual finite rate of population change ($\hat{\lambda}$) for the Bi-State DPS, as a whole, and for each subpopulation between 1995 and 2018. Because sage-grouse exhibited population cycles (periodic increases and decreases in abundance across approximately 6- to 10-year wavelengths), we estimated trends across three nested temporal scales that represented one (11 years), two (18 years), and three (24 years) complete population cycles. Our model predicted population abundance ($\hat{N}_{total}$) for the Bi-State DPS during 2018 at 3,305 individuals (2,247–4,683), with the majority occupying Bodie Hills and Long Valley. The model also predicted cyclic dynamics in abundance through time with evidence of 24-year population growth and slight trends of decline over the past 18 years. Specifically, across the Bi-State DPS as a whole, we estimated annual average $\hat{\lambda}$ at 0.99, 0.99, and 1.02 over the one, two, and three population cycles, which equates to 9.6 percent decrease, 15.7 percent decrease, and 57.7 percent increase in abundance over the 11-, 18-, and 24-year cycles. Estimated abundance in 2018 had not reached numbers lower than those predicted during 1995. However, we observed spatial variation in population trends across the three cycles. The Bodie Hills subpopulation comprised the greatest $\hat{N}$ (1,521) and exhibited average annual $\hat{\lambda}$ greater than 1.0 across all periods resulting in average annual increases of 7 percent. This relatively large subpopulation has grown approximately 4 times larger than what was estimated in 1995 while experiencing cyclical dynamics within that period.

[1]U.S. Geological Survey.

[2]Nevada Department of Wildlife.

[3]California Department of Fish and Wildlife.

[4]Bureau of Land Management.

[5]Idaho State University.

Conversely, other smaller subpopulations within the Bi-State DPS exhibited average annual $\hat{\lambda}$ equal to or less than 1.0, resulting in 10-year extirpation risks ranging from 3.8 to 75.1 percent. In general, evidence of decline among smaller subpopulations was greatest for the most recent period (2008–18) compared to the period that encompassed three full population cycles (24-year). This difference coincides with an intense period of drought that began in 2012.

As part of our first objective, we conducted a comparative analysis for populations of sage-grouse within Nevada and California that occurred outside the Bi-State DPS. We developed a region-wide IPM using lek count data from Nevada Department of Wildlife (NDOW) and California Department of Fish and Wildlife (CDFW) databases, combined with telemetry data collected by USGS across 11 sage-grouse subpopulations. Our models predicted similar patterns in population cycling outside the Bi-State DPS but with evidence of long-term decline over the 24-year cycle. Specifically, average annual $\hat{\lambda}$ values were 0.94, 0.97, and 0.99 across the 11-, 18-, and 24-year time periods, respectively. These values equate to 46.1 percent, 40.4 percent, and 20.6 percent declines over the corresponding periods.

Second, we used lek count data in a state-space modeling framework to compare trends in population abundance across different spatial scales (that is, leks versus Bi-State DPS). This hierarchical framework allowed us to disentangle declines associated with climate conditions as opposed to other local level factors that might signal the need for management intervention. Specifically, we identified 7 leks that were declining and had recently decoupled from larger spatial scale trends that are typically governed by climatic conditions (referred to as soft or hard signals). The goal of this analysis was to provide an early warning system that might have implications for conservation actions at local scales.

Third, we developed phenological (spring, summer–fall, and winter) and reproductive life stage (nesting, early brood-rearing, and late-brood rearing) resource selection functions using various environmental covariates. We reported rankings of variable importance for each season and life stage, and developed habitat suitability index (HSI) maps. We binned categories representing low, moderate, and high suitability for each phenological season and life stage, and produced composite maps by phenological and reproductive stage to estimate annual habitat.

Fourth, we used $\hat{N}$ for each lek within the Bi-State DPS to carry out a spatial analysis that quantified substantial changes in the distribution of occupied habitat across long- (24-year) and short- (11-year) term periods. Owing to differences among available datasets, the long-term analysis primarily reflected spatial shifts among subpopulations comprising the majority of the Bi-State DPS (that is, Bodie Hills and Long Valley) while the short-term analysis also quantified changes among subpopulations along the periphery. Over long- and short-term periods, the overall distribution of occupied habitat (as measured by 99 percent utilization distributions intersecting any quantified habitat) was reduced by 20,573 ha and 55,492 ha, respectively. Occupied core areas (as measured by 50 percent utilization distributions intersecting any quantified habitat) over long-term periods were solely located in Bodie Hills and Long Valley. Although nearly all subpopulations experienced contractions in occupied overall and core distribution, Bodie Hills experienced spatial expansion that occurred with concomitant spatial contraction at Long Valley over both periods. Subpopulations at the northern (Pine Nuts), central (Sagehen) and southern (White Mountains) extents of the Bi-State DPS also experienced spatial contraction over the short-term period. These findings, coupled with those of population trends, indicate long-term patterns in redistribution of sage-grouse from Long Valley and peripheral subpopulations to Bodie Hills. That is, sage-grouse subpopulations at the periphery are declining while the largest population at the core is increasing, which could have meaningful impacts on overall metapopulation persistence. We provide evidence for loss of occupied habitat (reduced distribution) given local extirpation of subpopulations.

Fifth, we calculated percentages of selected phenological, life stage, and annual habitat that each subpopulation contributed to the Bi-State DPS. We then intersected these maps with a composite estimate of occupied habitat from the fourth objective and calculated percentages of selected habitat likely occupied by sage-grouse that each subpopulation contributed to the Bi-State DPS. These results indicate loss of occupied habitat and subsequent reductions in spatial distribution given reductions in abundance and, in some cases, extirpation of leks within subpopulations.

Lastly, we carried out an initial analysis of sage-grouse selection for irrigated pastures and wet meadows during the brood-rearing stage for the Long Valley subpopulation. This subpopulation represents a population core, representing 24.8 percent of total sage-grouse within the Bi-State DPS, and has exhibited long-term declines in abundance and distribution. The Long Valley subpopulation is also highly sensitive to precipitation and other factors that influence water availability. Models predicted higher use of the interior portions of irrigated pastures and wet meadows during the late brood-rearing period, representing a potentially risky use of habitat that was exacerbated during periods of low moisture (for example, drought, reduced water delivery, or both). Sage-grouse typically used edges of riparian areas and pastures, perhaps because the interior of these mesic areas consisted of considerably less overhead concealment cover (for example, shrubs) that may constitute a higher risk of mortality. We found that a lack of water delivery to pastures in the form of overwinter precipitation or diversion ditches increased the movements of sage-grouse to the interior of pastures. Although further investigation of water delivery impacts on chick survival are warranted, our initial findings regarding resource selection may explain recent population declines observed at Long Valley.

Background

Greater sage-grouse (*Centrocercus urophasianus,* hereinafter "sage-grouse") are a well-documented sagebrush obligate species (Patterson, 1952; Knick and others, 2013) whose population trends and resource requirements are widely used as an umbrella (Rowland and others, 2006) or surrogate (Runge and others, 2019) for the conservation of sagebrush ecosystems across 13 states and provinces in western North America. Sage-grouse have experienced long-term population declines across large spatial extents following the degradation and loss of sagebrush ecosystems arising from an array of stressors (Connelly and others, 2004; Schroeder and others, 2004; Doherty and others, 2016). Sage-grouse population declines have led to multiple assessments by U.S. Fish and Wildlife Service (USFWS) for listing under the Endangered Species Act (ESA) of 1973 and revisions to land use plans guiding national conservation policy (Bureau of Land Management, 2015; U.S. Fish and Wildlife Service, 2015).

An example of these efforts is illustrated by the nearly two-decade long evaluation of sage-grouse populations inhabiting the southwestern extent of the species' range, which occurs along the central border of California and Nevada and is known as the Bi-State population. Formal petitions for listing of the Bi-State population under the ESA by advocacy groups and subsequent evaluations of sage-grouse by the USFWS began in 2001. Geographic isolation and absence of contiguous sagebrush communities between the Bi-State population and the remainder of the species' range has resulted in genetic divergence of the Bi-State population from other populations within the Great Basin (Oyler-McCance and others, 2005, 2014). This geographic and genetic distinctiveness formed the basis for recognizing the Bi-State population as a Distinct Population Segment (Bi-State DPS) by the USFWS. In 2015, the Bi-State DPS was "warranted but precluded" for listing under the ESA (U.S. Fish and Wildlife Service, 2015). Prior to this decision, an evaluation for threatened status with section 4(d) rule designation of critical habitat occurred in October 2013 (U.S. Fish and Wildlife Service, 2013). That evaluation considered multiple threats to sage-grouse within the Bi-State DPS, namely reported declines and low abundances for some subpopulations, expansion and infill of single-leaf pinyon pine (*Pinus monophylla*) and Utah juniper (*Juniperus osteosperma*; hereinafter, "pinyon-juniper") into otherwise treeless sagebrush communities, climate-change related impacts on productivity (for example, drought) and hydrology of sagebrush ecosystems, changes in predator communities as a result of human activities, and an accelerated cycle of wildfire and invasive annual grass type conversion.

A collaborative effort between state and federal resource and science agencies identified a suite of targeted conservation measures and science-based adaptive management actions aimed at ameliorating threats to sage-grouse in the Bi-State DPS (Bi-State Action Plan, 2012). This was followed by a formal evaluation of population status using an integrated population modeling (IPM) approach developed by the U.S. Geological Survey (USGS; Coates and others, 2014b), which combines data across multiple sources (for example, demographic and lek count data) to better estimate population parameters and identify processes that influence population trends (Schaub and Abadi, 2011). The USFWS subsequently determined that the DPS was not warranted for listing, citing principally a lack of evidence for changing population trend from 2003 to 2012, and agency commitments to implement conservation-related management actions identified to benefit sage-grouse populations (U.S. Fish and Wildlife Service, 2015). Multiple actions were implemented subsequent to the USFWS decision. These actions included treatment of 53,000 acres of conifer encroachment within targeted sage-grouse habitat (Bi-State Technical Advisory Committee, 2019) prioritized partially by a quantitative conservation planning tool (Ricca and others, 2018). Continued long-term monitoring of the Bi-State DPS through standardized lek counts and tracking of telemetered sage-grouse was also critical for providing data to inform estimation of demographic rates, resource selection functions, movement parameters, predator impacts, population augmentation (Mathews and others, 2018), and further quantitative assessments of long-term rate of population change (λ) within the IPM framework (Coates and others, 2018; Mathews and others, 2018).

The 2015 decision not to list the Bi-State DPS was challenged by several non-governmental organizations and litigated through the U.S. District Court for the Northern District of California. In May 2018, the court vacated the warranted-but-precluded listing decision and required USFWS to re-open the listing evaluation process initiated during October 2013 (U.S. Fish and Wildlife Service, 2019).

The overarching objective of this research is to report timely best science aimed at helping to inform an updated status assessment by the USFWS for the Bi-State DPS. Here, the USGS with state and university partners applied substantial long-term datasets from lek counts, telemetry data from radio and GPS-marked sage-grouse, and habitat measurements to carry out six principle quantitative analyses designed to understand past and current states of sage-grouse within the Bi-State DPS:

1. We conducted comprehensive population analyses using lek counts and demographic rates informed by telemetered sage-grouse within an IPM framework. We estimated annual apparent abundance, $\hat{N}_{apparent}$, and then derived total abundance, $\hat{N}_{total}$, by adjusting for sightability (Coates and others, 2019), lek attendance (Wann and others, 2019), sex-ratios (Braun and others, 2015), and leks with unknown locations for each subpopulation and overall Bi-State DPS. We then predicted average annual rate of change ($\hat{\lambda}$) and averaged rates across short- (11-year), mid- (18-year), and long-term (24-year) time periods, which corresponded to 3 distinct population cycles largely driven by variation in annual precipitation. This was done for each subpopulation within the Bi-State DPS and across the region, as a whole. For comparative purposes, we estimate $\hat{\lambda}$ for populations falling within state boundaries of Nevada, but outside of the Bi-State DPS, using a state-wide lek count database and demographic estimates from 11 sampled populations in an IPM framework.

2. We expanded on a hierarchical framework for population monitoring that initially identifies biologically relevant spatial scales tied to population structure and function (Coates and others, 2017a). When combined with systematically collected population estimates (lek counts), the framework allows estimation of population trends across multiple spatial scales. We estimated empirical thresholds to detect change in $\hat{\lambda}$ and provide an early warning system for adaptive management that systematically integrates immediate scientific findings into management decisions (Walters, 1986). Here, our framework signals populations or subpopulations most likely declining in response to local-scale ecosystem perturbations, while accounting for environmental stochasticity governing changes in population abundance at larger spatial scales.

3. We developed spatially explicit maps of habitat selection from estimated resource selection function (RSF) parameters across the entire Bi-State DPS. We created maps that reflect selection across phenological periods (spring, summer–fall, and winter) that encompass all age and sex classes of sage-grouse, as well as specific life stage (nesting, early brood-rearing, late brood-rearing) maps for reproductive females.

4. We estimated spatially-explicit changes in occupied distribution across each time period for subpopulations and the Bi-State DPS as a whole. Specifically, we used $\hat{N}_{total}$ (Objective 1) to develop probabilistic relative abundance surfaces associated with distributions of leks (Doherty and others, 2016) and modeled the rate of change in areas and volume under the 99th and 50th percentile for each subpopulation and the Bi-State DPS during long and short-term time periods. Comparisons between predicted trends in population abundance with spatial distributions allow for a more complete evaluation of Bi-State DPS population status that might offer further insights into population persistence.

5. We calculated percentages of selected (from Objective 3) and likely occupied (as determined by intersections with composite spatial distribution estimates from Objective 4) phenological and life stage habitat that each subpopulation contributed to the Bi-State DPS.

6. We investigated the influence of precipitation and managed water delivery on sage-grouse selection for mesic habitat within the Long Valley subpopulation. Findings may help identify environmental mechanisms driving dynamics of other subpopulations within the Bi-State DPS and across the Great Basin during important life-history stages.

Study Areas

We studied all known sage-grouse subpopulations in the Bi-State DPS at different times from 1995 to 2018. Subpopulations comprised all the leks within Population Management Unit (PMU) boundaries defined by the Nevada Governor's Sage-Grouse Conservation Team (2004), and more localized subpopulations with specific management interest (for example, geographical isolation, low population size, possible reliance on managed water) nested within PMUs (fig. 1). For consistency, we herein define PMUs and nested subpopulations as subpopulations. From the northern region and progressing southward, we monitored sage-grouse subpopulations in the Pine Nut Mountains (Pine Nut PMU), Mount Grant (Mount Grant PMU), Desert Creek (Desert Creek/Fales PMU), Fales (Desert Creek/Fales PMU), Bodie Hills (Bodie Hills PMU), Long Valley (South Mono PMU), Sagehen (South Mono PMU), Parker Meadows (South Mono PMU), and White Mountains (White Mountains PMU) (fig. 1).

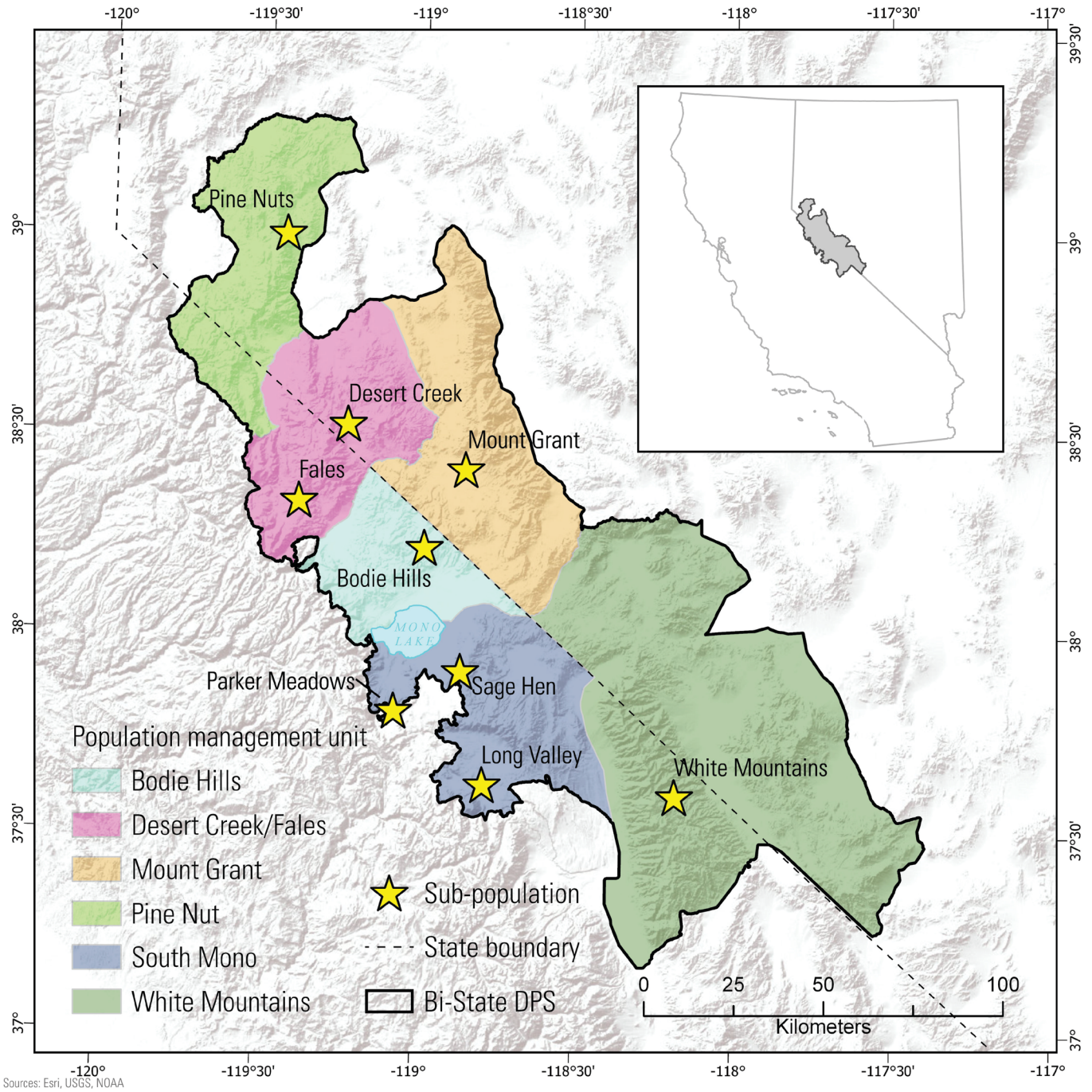

Figure 1. The Bi-State Distinct Population Segment (DPS) of greater sage-grouse (*Centrocercus urophasianus)* identified by population management units (PMUs) across Nevada and California. Stars indicate approximate center-points of subpopulations monitored: Pine Nut Mountains, Desert Creek, Fales, Mount Grant, Bodie Hills, Parker Meadows, Sagehen, Long Valley, and White Mountains.

Northern Region

The Pine Nut Mountains are located at the northernmost region of the Bi-State DPS within the Pine Nut PMU (fig. 1). The area is topographically diverse and encompasses 232,695 hectares (ha; Bi-State Local Planning Group, 2004) of the Bi-State DPS spatial extent. Dominant plant communities consist of sagebrush (*Artemisia* spp.) and mixed mountain shrub communities with extensive pinyon-juniper woodlands throughout the study area. Overstory of sagebrush communities is characterized by big sagebrush (*A. tridentata* spp.) and little sagebrush (*A. arbuscula*). Other shrub cover consists of a variety of rabbitbrush (*Chrysothamnus* and *Ericameria* spp.), Bailey's greasewood (*Sarcobatus baileyi*), and horsebrush (*Tetradymia* spp.). Mountain shrub communities are characterized by big sagebrush and a variety of mountain shrubs including Utah serviceberry (*Amelanchier utahensis*), common snowberry (*Symphoricarpos albus*), and desert bitterbrush (*Purshia glandulosa*). Dominant forbs consist of wooly mule-ears (*Wyethia mollis*), lupine (*Lupinus* spp.), and arrowleaf balsamroot (*Balsamorhiza sagittata*). Native perennial grasses include bluebunch wheatgrass (*Pseudoroegneria spicata*), crested wheatgrass (*Agropyron cristatum*), Great Basin wild rye (*Elymus cinereus*), needle-and-thread grass (*Hesperostipa comata*), and Indian ricegrass (*Achnatherum hymenoides*). Invasive annual grasses were dominated by cheatgrass (*Bromus tectorum*). The Pine Nut subpopulation is relatively geographically and genetically isolated relative to other subpopulations in the Bi-State DPS (Oyler-McCance and others, 2014), but emigration to other subpopulations in the Bi-State DPS has been documented (Coates and others, 2016a).

Mid-Northern Region

The mid-northern regions of the Bi-State DPS comprise subpopulations within the Mount Grant PMU and Desert Creek/Fales PMU (fig. 1). Mount Grant occurs at high elevation intermixed with pinyon-juniper on the Nevada side of the Bi-State DPS and is bordered by the Bodie Hills PMU (see "Central and Mid-Southern Region" section) on the California side. Desert Creek/Fales extends in a north-south orientation south of Wellington, Nevada, to Sweetwater Ranch, and east of the Sweetwater Mountains to west of State Highway 338. The subpopulation at Desert Creek occurs on the Nevada side of the Bi-State DPS and is bordered to the west by the subpopulation at Fales on the California side. Annual grasses, including cheatgrass, dominate parts of the ranchland and surrounding areas but eventually transition to a mix of shrubs and perennial grasses at higher elevations. Black (*A. nova)* and little sagebrush are the dominant dwarf sagebrush species. The western side of the Sweetwater Mountains towards Fales is characterized by shrubs, forbs, and perennial grasses at higher elevation sites such as Jackass Flat.

Central and Mid-Southern Region

The central and mid-southern regions of the Bi-State DPS in Mono County, Calif., comprise subpopulations within the Bodie Hills PMU and three subpopulations of management interest (Long Valley, Sagehen, and Parker Meadows) nested within the South Mono PMU (fig. 1). Bodie Hills is located approximately 13 kilometers (km) east of Bridgeport, Calif.; Long Valley is approximately 11 km southeast of Mammoth Lakes, Calif.; Sagehen is approximately 16 km southeast of Lee Vining, Calif., between Bodie Hills and Long Valley; and Parker Meadows is approximately 10 km south of Lee Vining between Bodie Hills and Long Valley. Vegetation available to all four subpopulations consists of sagebrush communities with major land cover types comprised of Wyoming (*A. t. wyomingensis*) and mountain big sagebrush (*A. t. vaseyana*), little sagebrush, rabbitbrush, bitterbrush, snowberry, and other non-sagebrush shrubs at lower elevation, as well as coniferous forests dominated by pinyon-juniper, and in many areas Jeffrey Pine (*Pinus jeffreyi*).

Southern Region

The southern region of the Bi-State DPS comprise subpopulations within the White Mountains PMU (fig. 1). The White Mountains lie along the border of Nevada and California and stretch for approximately 97 km, but the sage-grouse subpopulation is located primarily along a large plateau ranging from 3,048 to 3,962 meters (m), and extending for approximately 32 km (Elliott-Fisk, 1991), just south of White Mountain Peak (4,342 m). Sage-grouse on the Nevada side reside at low elevations, in habitat comprised of several species of conifer tree (bristlecone pine, *P. longaeva*; limber pine, *P. flexilis*; and pinyon-juniper) intermixed with stands of curl-leaf mountain mahogany (*Cercocarpus ledifolius*) and sagebrush. Various species of sagebrush and conifers make up the vegetation at high elevations. Little is known about sage-grouse behavior and ecology in this PMU, and locations for only a few sporadically monitored leks are known. Thus, we initiated a pilot study of sage-grouse movements on the California side of the PMU during the fall of 2016 and 2017 and launched extensive field study of demographic vital rates on both the California and Nevada sides beginning in spring of 2018.

Methods

Field Data Collection

Lek Counts

Personnel at California Department of Fish and Wildlife, Nevada Department of Wildlife, Bureau of Land Management, U.S. Forest Service, U.S. Geological Survey, Idaho State University, L.A. Department of Water and Power, University of Nevada Reno, Idaho State University, and University of Idaho used established protocols (Connelly and others, 2003) to count sage-grouse leks within Bi-State DPS and other Nevada and California populations spanning from 1995 to 2018. Lek counts were conducted each breeding season (March–May) on three separate and equally spaced occasions with the goal of capturing peak lek attendance by males. Counts were conducted between 30 minutes (min) before and 90 min after sunrise by ground observers using binoculars, spotting scopes, or both from suitable viewing locations. During a single survey morning, three counts were conducted spaced 10 min apart and the highest male count was recorded. From 2004 to 2018, leks within the central and southern Bi-State DPS, which included Fales, Bodie Hills, and Long Valley on the California side, were surveyed using a "saturation count" method, which required that all known active leks be counted simultaneously by experienced observers on a single day and then repeated across the lekking season. In some cases, primarily in Nevada, counts were conducted via aircraft and the total number of apparent males was recorded since assignment of sex could not be exact.

Capturing and Handling Sage-Grouse

Sage-grouse were captured near active leks in the spring and near late-summer water sources in the fall using published spotlighting techniques during nighttime (Wakkinen and others, 1992). Captured sage-grouse were fitted with necklace-style very high frequency (VHF) radio-transmitters (less than 3 percent body mass; Advanced Telemetry Systems, Isanti, Minnesota) or rump mounted Global Positioning System platform transmitting terminals (GPS; less than 5 percent body mass; GeoTrack, Apex, North Carolina). GPS-marked grouse also were fitted with a micro-VHF transmitter that allowed on-the-ground tracking (Severson and others, 2019). A unique aluminum leg-band with identification number was also deployed on each captured sage-grouse. All sage-grouse were classified by age and sex characteristics using published methodologies (Ammann, 1944). Sage-grouse were captured at six subpopulations within the Bi-State DPS spanning 2003–18, and across nine subpopulations within the Great Basin spanning 2009–18. All sage-grouse were captured and handled in accordance with the USGS Western Ecological Research Center (WERC) Animal Care and Use Protocol WERC-2015-02.

Radio and GPS Telemetry

We relocated individual VHF-telemetered sage-grouse using a three-element Yagi antenna (Advanced Telemetry Systems Inc., Isanti, Minn.) and a portable receiver (Communication Specialist Inc., Orange, Calif.). During reproductive periods (March–August), we sought to relocate birds at least three times per week. During the fall and winter months, fixed-wing aircraft were used on multiple occasions to relocate sage-grouse. Aircraft also were used to relocate sage-grouse that could not be found from the ground periodically during the reproductive period. We also tracked sage-grouse to inform reproductive status (nesting and brood-rearing) and mortality. To identify nest locations during the nesting period (March–June), we visually confirmed nesting status for females that occupied the same locations during two consecutive telemetry checks, indicating that incubation had begun. Care was taken to not flush nesting females. Nests were classified as successful if at least one chick hatched, as determined by visual assessment of eggshell remains or by observing one or more chicks in the nest bowl. Nests were considered unsuccessful when the entire clutch failed to hatch. Failed nests were classified as depredated (all eggs missing or destroyed), partially depredated and subsequently abandoned (at least one intact egg remaining in abandoned nest), or completely abandoned (abandoned, but clutch intact). Following hatch, we located females with broods every 10 days for up to 50 days during daylight or nocturnal hours. Nocturnal checks consisted of using spotlighting to confirm presence or absence of chicks affiliating with the marked female. At 50 days post-hatch, we flushed the entire brood and counted the number of chicks affiliated with each female that nested successfully to generate a final estimate of brood size.

Objective 1. Integrated Population Modeling and Estimated Abundance

Data Compilation

Lek count data underwent a series of objective screening criteria prior to inclusion in population modeling analyses. First, within the Bi-State DPS, leks were assigned to subpopulations based on intersections with subpopulations. Within the Great Basin, leks were assigned to the same population that fell within a 95-percent minimum convex polygon derived from telemetry locations for each study site (n = 11). Second, counts from satellite leks, which were transient and typically within 1.5 km of each other, were pooled with counts from the primary lek location to more accurately reflect maximum counts associated with a "true" lek and minimize effects of biasing counts low by including multiple years of zero-counts from infrequently visited satellites. In the DPS, satellite pooling was conducted in consultation with local agency (BLM, CDFW) biologists and members of the Technical Advisory Committee for the Bi-State DPS working group who collected the data. This group also conducted extensive quality control and assurance checks (QA/QC) of lek count data that enabled use of count data dating back to 1995 to be used for population model frameworks (see "IPM Formulation" section). Third, we selected the maximum male count observed for each lek each year. We summed all counts within a complex for each survey date and used the count on the date with the maximum total count. We also used the apparent-male counts taken from aerial surveys (less than 0.9 percent of all lek surveys) rather than tallying these leks with a zero-count value. These processes resulted in counts for 65 leks for the Bi-State DPS and 389 leks for the Great Basin.

Sage-grouse exhibit cyclic patterns in population abundance (Garton and others, 2015). Thus, estimates of averaged annual finite rate of population change in abundance (λ) may be sensitive to when the start and end points of population spans occurred relative to population cycles (fig. 2). Analyses that span equivalent cycle years (for example, nadir to nadir) will be less prone to leveraging effects relative to those that span nadir to apex or apex to nadir, for example. Estimates of averaged λ may also vary across multiple cycle periods or when cycles have varying length and amplitude (Row and Fedy, 2017). Thus, for the IPM analysis, we constructed three datasets encompassing three distinct periods that corresponded to years of population nadir identified within the DPS and Great Basin: long-term (1995–2018), mid-term (2001–18), and short-term (2008–18).

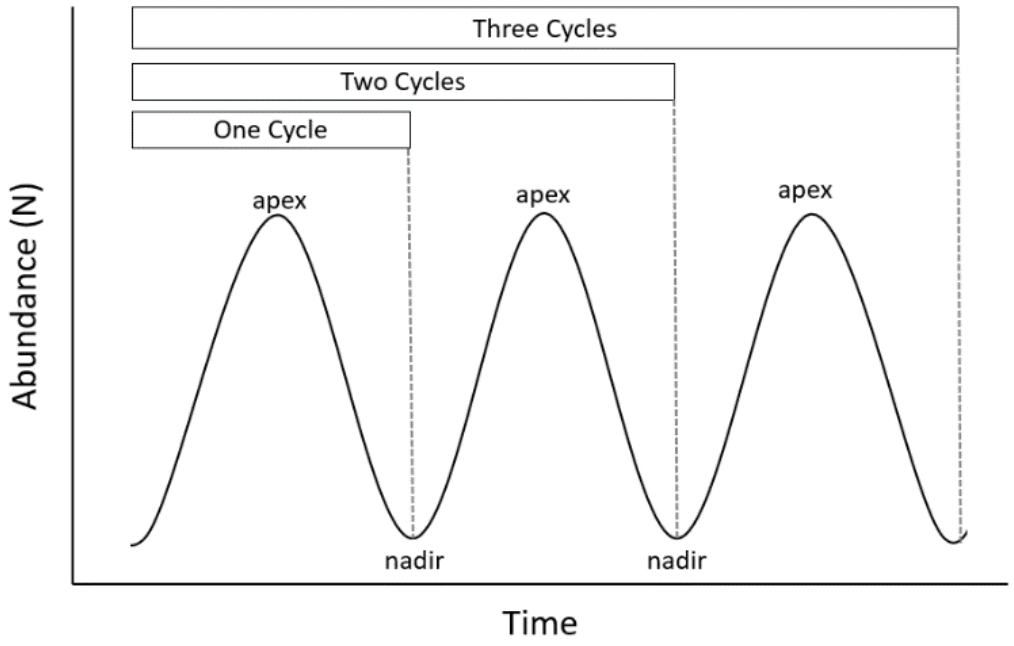

Figure 2. Complete cycles from nadir (trough) to nadir for a population that oscillates from increase to decrease in abundance (N) over time.

These cycles corresponded to 24-, 18-, and 11-year periods. We identified points of nadir dating back to 1990 given data for the Bi-State DPS and Great Basin by plotting averaged annual maximum counts and apparent abundance estimates from state-space model predictions (Kéry and Schaub, 2012). Bi-State DPS and Great Basin shared similar historic nadirs, so we used the same periods for both areas.

For each period, we only used leks that were active at least once during the entire period. We used the Nevada Department of Wildlife definition for active status, where at least two males must be observed on a lek at least twice during a 5-year sequence. We also accounted for rare cases of lek extirpation by replacing missing values with zero counts for active leks that became inactive (and were no longer counted) during a cycle period. Recent advances in coding IPM analyses (for example, multi-lek and multi-subpopulation model; see "IPM Formulation" section) allowed for predicting abundance ($\hat{N}$) and deriving annual λ for every lek. Thus, we derived annual average λ across each long-term, mid-term, and short-term population period to estimate overall population trends while accounting for populations experiencing cycles with approximate decade-long wavelengths. Data were sufficient to provide trend evidence of increasing, neutral, or decreasing populations (see fig. 3). While a strength of the IPM is estimation of $\hat{N}$ in years with missing data (for example, lek counts), predictions along a time series of excessively sparse data can exert strong leverage on overall means and ultimately bias estimates of population $\hat{\lambda}$ low or high. Thus, we removed leks with excessively sparse data as evidenced by apparent erroneous influence on estimates. Specifically, we developed an analysis to identify combinations of missing counts (NA values) within a time series that produced inaccurate estimates for each time period. If a lek consisted of the identified sequence of NA values, then it was removed for analysis of trends. This was an iterative approach, as a single iteration consisted of a sequence of NA values infilling observed counts throughout the time series so that all combinations of missing data were explored across iterations. To identify combinations of NA values evidenced as producing inaccurate estimates, we compared averaged $\hat{\lambda}$ between each NA value combination to the complete dataset counterpart for each time period. Thus, the complete data sequence served as the "truth," in that estimates can be reliable. If the NA combination produced estimates different from the full time series, then we stored the combination into an "NA key." We then cross-referenced back to each lek against the NA key (that is, sequences of missing data that likely produce spurious estimates) for each period and removed leks with missing data that matched the NA key. However, we relaxed this rule for Pine Nut, White Mountains (Nevada side), and Sagehen for the 2008–18 cycle period. These were subpopulations with fewer than five leks, with most failing the missing value key standard. To drop these leks would have resulted in excessive borrowing of information from other subpopulations and led to estimates that simply mirrored the DPS rather than observed site-specific counts. Hence, we allowed inclusion of leks from these subpopulations with at least 4 years of counts and accepted reduced confidence in our associated estimates of $\hat{\lambda}$ from 2008 to 2018. The goal of these combined steps was to produce a separate dataset for each period that minimized spurious effects from inconsistent sampling efforts and inactive leks.

IPM Formulation

Within an IPM framework, we unified two major data sources, lek counts and demographic data, to yield more precise $\hat{N}$ and $\hat{\lambda}$ (Schaub and Abadi, 2011; Kéry and Schaub, 2012) across the three different spatial scales of individual Bi-State DPS subpopulations, Bi-State DPS-wide, and Nevada-wide. Demographic data was collected in all subpopulations within the Bi-State DPS and at 11 separate subpopulations within Nevada. IPM-based estimates have informed previous assessments of population status for the Bi-State DPS (Coates and others, 2014b; Mathews and others, 2018) and the relationship of climatic variability with population flux (Coates and others, 2018). Ultimately, estimates were generated from formulation of a joint likelihood by modeling the observation process (observed counts) and state process (demographic data).

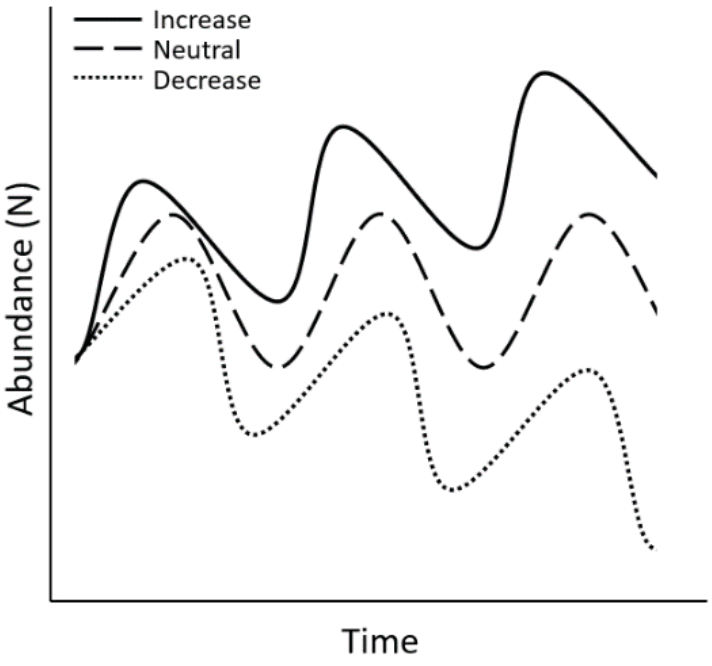

Figure 3. Population oscillations with increasing, neutral, or decreasing trends across complete cycles spanning periods of nadir to nadir.

Observation Process. The IPM consists of an underlying state-space model (Kéry and Schaub, 2012) that estimated observation error using time-series lek count data because detection of sage-grouse during lek counts is imperfect (Baumgardt and others, 2017). We improved on previously published IPMs (Coates and others, 2018; Mathews and others, 2018) by developing a multi-lek–multi-site hierarchical structure that allowed $\hat{N}$ at all leks, even those with missing counts provided they underwent QA/QC methods. We used Bayesian p-values to test the goodness of fit for different observation error distributions of normal, Poisson, and negative binomial, at lek *l*, subpopulation *i,* and year *j*. The normal distribution garnered the most support. Thus, model structure of maximum counts (*y*) took the form

$$y_{ijl} \sim \text{Normal}\left(\text{N}_{pijl}, \sigma^2_{subpopulation,i}\right) \quad (1)$$

$$\sigma^2_{subpopulation,i} \sim \text{Uniform}\left(0,\ 100\right) \quad (2)$$

The state process of the IPM was structured as a stochastic demographic matrix model, which consisted of age-structure (two classes: yearling or adult) and individual life stages (for example, annual fecundity and survival). We considered density dependence using the Ricker model that assumed constant linear decrease in the demographic rate as population size increases *N* (Ricker, 1954), and the Gompertz model (Dennis and Taper, 1994) that assumed constant linear decrease as a function of logarithmic transformation of *N*. We also fit different combinations of random effects (for example, subpopulation and year) to each life stage to allow for benefits of data sharing (for example, borrowing of strength) and to account for intraclass correlation which ultimately improves parameter estimation (Kéry and Schaub 2012). We modeled each vital rate separately and created five models with different random effect structures representing different spatiotemporal effects: null (no random effects), year only, subpopulation only, year and subpopulation additive, and year and subpopulation nested as described in Coates and others (2018). The most parsimonious random effect structure and density dependent structure for each subcomponent model was identified using WAIC, a fully Bayesian prediction accuracy assessment used for hierarchical models (Watanabe, 2010; 2013) and recommended for ecological modeling (Hooten and Hobbs, 2015). The IPM was written in BUGS language interfacing Program R (R-Core Team, 2018) with JAGS (Plummer, 2003; 2016).

State Process. The demographic processes that describe changes in abundance were separated into survival and fecundity (fig. 4). Based on telemetry movements, we assumed migration (emigration and immigration) between subpopulations had negligible impacts and were not estimated. However, because sage-grouse frequently move between leks within a subpopulation and we lacked data with sufficient spatiotemporal resolution to link variation in demographic rates to specific leks, we assumed that leks within the same subpopulation shared similar demographic rates. Detailed specification of each demographic subcomponent model was reported in appendix 1. Briefly, survival (*S*) of sage-grouse was modeled using Bayesian frailty analysis (Halstead and others, 2012) with monthly alive-dead encounter histories, where each interval allowed estimation of unit hazard rate given a Bernoulli process. Posterior distributions for annual survival were derived based on cumulative hazard across a 12-month period. Inferences of annual survival rates were based on VHF-marked sage-grouse owing to reduced survival probabilities in GPS-marked birds (Severson and others, 2019). Fecundity was decomposed into multiple subcomponent models, specifically first attempt nest propensity (*np*1), second attempt nest propensity (*np*2), first clutch size (*cl*1), second clutch size (*cl*2), first attempt nest survival (ns1), second attempt nest survival (*ns*2), hatchability (*h*), chick survival (*cs*), and juvenile survival (*js*). Specific error distributions and other model details for each fecundity subcomponent model are described in appendix 1. Given the posterior probability distributions for each subcomponent parameter, we derived fecundity (γ), which took the form

$$\begin{aligned}\gamma_{ija} = &\left(np1_a \times cl1_{ja} \times ns1_a \times h_{ija} \times cs_{ija} \times js\right) + \\ &\left(\left(1 - ns1_a\right) \times np2_{ija} \times cl2_{ja} \times ns2_a \times h_{ija} \times cs_{ija} \times js\right)\end{aligned} \quad (3)$$

where *i*, *j*, and *a* represent subpopulation, year, and age class, respectively. We divided *f* by 2 to represent a female-based demographic model with assumed equal sex ratios at hatch (Atamian and Sedinger, 2010a). Estimates of *f* were a stochastic process as the demographic matrix consisted of posterior distributions of individual population vital rates.

Joint Likelihood. For the Bi-State DPS, we obtained both lek count and demographic data for each subpopulation. Thus, we formulated a joint likelihood from all the subcomponent likelihoods to estimate apparent abundance ($\hat{N}_{apparent}$), as shown from the directed acyclic diagram in figure 5. Here, changes in a population state, $\hat{N}_{apparent}$, were informed by annual estimates of *s* and *f* from field data collected at each subpopulation, as well as informative priors (*np*1 and *js*) where data were not adequate for likelihood estimation. The state was mapped directly to the observed counts through the observation process, which was assumed to arise from a normal error distribution. Formulation of a joint likelihood allowed for demographic and lek count data to ultimately inform all modeled parameters. For example, not only did both forms of data influence $\hat{N}_{apparent}$, but fecundity and survival parameters were influenced by count data given observation error. For the Nevada-wide IPM, demographic data were sporadic and confined to 10 subpopulations that did not encompass all leks surveyed across the state.

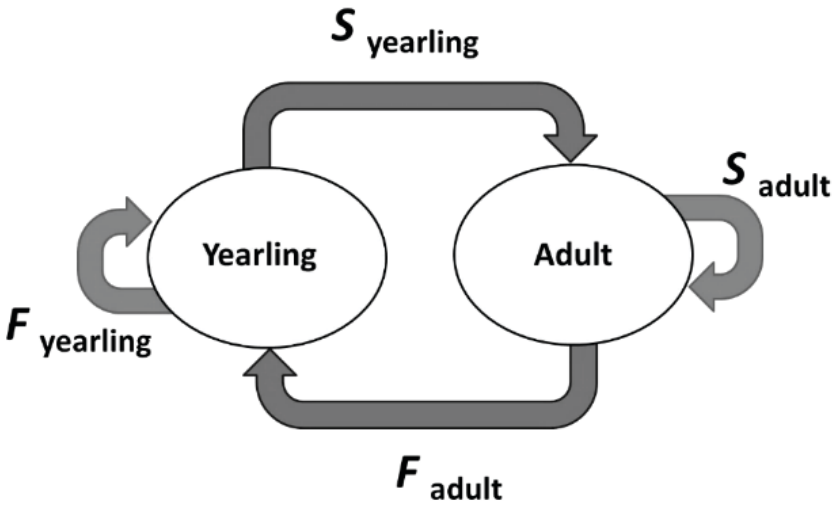

Figure 4. Age-structured demographic components of the integrated population model for greater sage-grouse (*Centrocercus urophasianus*) in the Bi-State Distinct Population Segment, California and Nevada. *F*, fecundity estimate; *S*, survival estimate.

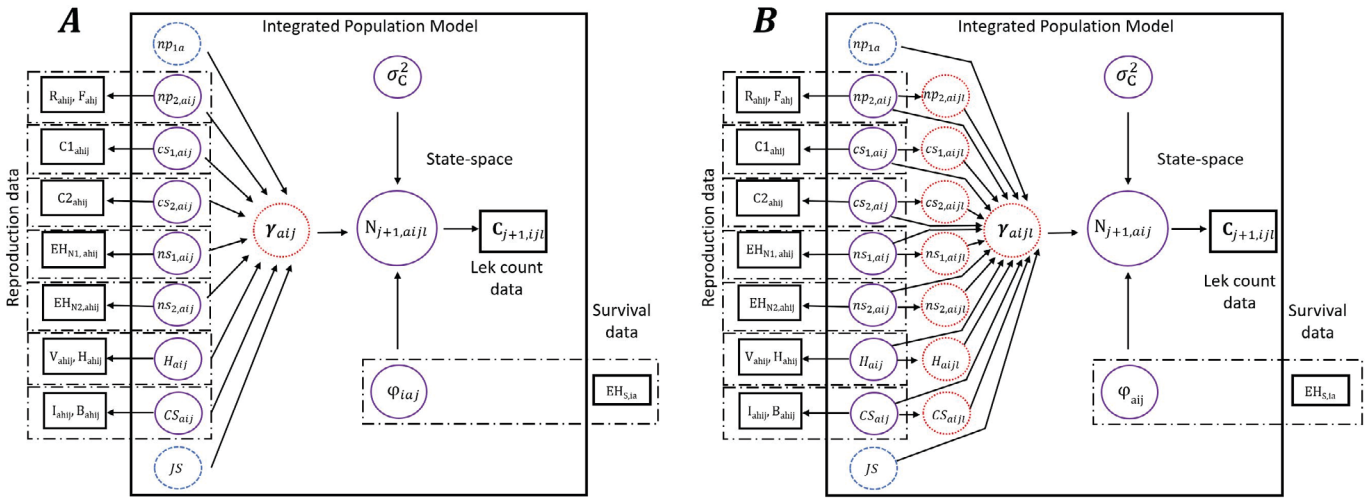

Figure 5. Integrated population model (IPM) components and data for greater sage-grouse (*Centrocercus urophasianus*) in the Bi-State Distinct Population Segment (*A*) and across state of Nevada (*B*). Large solid box represents IPM; small solid boxes represent data vectors; dashed boxes represent subcomponent models; solid circles represent estimated parameters; dashed circles represent informative priors; dotted circles represent derived parameters. R = number of sage-grouse available; F = number of sage-grouse nesting; C1 = clutch size of first nest; C2 = clutch size of second nest; EH = encounter histories for nest survival for first nests (N1), second nests (N2), and survival (S); V = number of eggs in clutch; H = number of eggs that survived; I = number of chicks that hatched; B = number of chicks that survived; *C* = observed lek count; *np* = estimated nest propensity; *cs* = estimated clutch size; ns = estimated nest survival; *H* = estimated hatchability; *CS* = estimated chick survival; *JS* = estimated juvenile survival; γ = derived fecundity; ϕ = estimated survival; σ^2 = observation error, N = estimated abundance; i = subpopulation, h = bird, k = month, j = year, l = lek, a = age.

Estimating Total Population Size

The IPM generates an estimate of abundance given, in part, by the observation process partitioned from time series counts of males attending leks. However, the state-space model component of the IPM cannot completely partition all sources of error from observation processes and account for potential biases associated with detection. Although lek counts are widely used as an index for population size, they do not represent total abundance (N_{total}). Lek counts are prone to error associated with proportion of males that are not attending a leks while surveyed (that is, attendance), proportion of males attending leks that were undetected during surveys (that is, sightability), and predicted proportion of males that are not counted because their lek locations are unknown. Furthermore, adult sage-grouse population sex-ratio are typically female-biased (Braun and others, 2015) owing to higher mortality of males.

Thus, we carried out a multiple-step iterative analysis to adjust estimated apparent abundance ($\hat{N}_{apparent}$) to derive total abundance ($\hat{N}_{total}$) while accounting for model parameter uncertainty. First, we accounted for male lek attendance because not all male sage-grouse attend lek during mornings (Wann and others, 2019), when surveys are conducted. Specifically, we divided each sample (n = 3,000) of the posterior probability distribution of $\hat{N}_{apparent}$ by a lek attendance rate (median = 0.848), which took the form

$$\hat{N}_{attend} = \frac{\hat{N}_{apparent}}{0.848} \quad (4)$$

This adjustment of 0.848 was informed by GPS-marked male-sage grouse visiting leks across multiple sites and years in the Great Basin and represented higher attendance during non-drought years that most closely matched conditions in 2018 (Wann and others, 2019). Third, only a proportion of sage-grouse are observed during a single survey among the total that attend leks and are available for observation (Fremgen and others, 2016), which is often referred to as observer sightability. Thus, we divided that resulting distribution by an equal number of samples drawn from a Beta distribution (parameters, $\alpha = 61.29$; $\beta = 9.97$) of sightability ($\tilde{\omega}$) for males on leks, which was informed by ground-based and aerial-infrared surveys calibrated with known abundance (median = 0.86, 95-percent credible interval [expressed as 0.025–0.975 quantile of the posterior distribution, CRI] = 0.77–0.93; Coates and others, 2019) that generated estimates similar to those from other studies (Fremgen and others, 2016; Baumgardt and others, 2017), which took the form

$$\hat{N}_m = \frac{\hat{N}_{attend}}{\tilde{\omega}} \quad (5)$$

Finally, to calculate total population size, we estimated the number of females, $\hat{N}_f$, in the population by multiplying the observation-process adjusted estimates of males, $\hat{N}_f$, by 3,000 samples drawn from a normal distribution describing variation in sex-ratios ($\tilde{\varsigma}$) for fall-harvested sage-grouse (median = 2.04 females:males, standard error [SE] = 0.30; Braun and others, 2015), which took the form

$$\hat{N}_f = \hat{N}_m \times \tilde{\varsigma} \quad (6)$$

We then added distributions of $\hat{N}_f$ to $\hat{N}_m$ for each lek, resulting in $\hat{N}_{f,m}$ at the lek level. Lastly, we estimated $\hat{N}$ at the subpopulation level while accounting for unknown leks and assuming 95-percent of all leks were known. Accordingly, for each year we divided the number of known active leks in each subpopulation by 0.95 to derive the total number of active leks (known and unknown) at each subpopulation. The 95-percent value was based on expert knowledge from members of an interagency technical advisory team for the Bi-State DPS. Inactive leks were excluded, though we included pending-active leks defined as leks with only one count of two or more male over a 5-year period within the recently counted White Mountains subpopulation to generate a more robust estimate for this extremely remote subpopulation. For each year, we then averaged the distributions, $\hat{N}_{f,m}$, across all leks at the subpopulation level and multiplied the averaged distribution $\hat{N}_{m,f}$ by the total number of active leks (known and unknown) within each subpopulation to obtain $\hat{N}_{total}$ for each subpopulation. $\hat{N}_{total}$ was derived at the Bi-State DPS level by summing the distributions across subpopulations.

Deriving λ. From the estimated posterior probability distributions of $\hat{N}_{total}$ (fig. 5), we derived λ (Caswell, 2001) for each lek (l) by year (k), which took the form

$$\lambda_{kl} = \frac{\hat{N}_{k+1,l}}{\hat{N}_{kl}} \quad (7)$$

where

k+1 represents the following year k.

We applied equation 7 to derive λ at the subpopulation (i) and DPS extents based on $\hat{N}_{total}$ at the respective extents. We report and plot $\hat{N}$ and $\hat{\lambda}$ for each subpopulation and for the entire Bi-State DPS. We also report and plot $\hat{\lambda}$ for the Great Basin-wide extent. Posterior probability distributions were summarized as median and 95-percent CRI. Posterior probability distributions of demographic rates were also reported as median and 95-percent CRI.

Comparison of Trends Across Varying Periods. We carried out comparisons in average annual $\hat{\lambda}$ between the Bi-State DPS and Nevada-wide across three periods that corresponded to years of population nadir: long-term (1995–2018), mid-term (2001–18); and short-term (2008–18), as described above. Based on modeled posterior probability distributions and allowing for stochasticity, we projected $\hat{N}$ across 11 years into the future for the DPS. For illustrative purposes, we set initial values of Nevada-wide and Bi-State DPS abundance to be the same and compared trajectory and cyclicity between the regions across the past 24 years as well as projected across the next 11 years.

Objective 2. Hierarchical Signal Analysis

Sage-grouse populations exhibit cyclical patterns in abundance and growth (Row and Fedy, 2017) and are highly influenced by climatic variation at broader spatial scales within the Bi-State DPS (Coates and others, 2018). Thus, we developed a novel hierarchical and spatially nested monitoring framework that compares $\hat{\lambda}$ across multiple spatial scales and can provide an early warning system for detecting population declines that are decoupled from broader spatial scales or larger populations of sage-grouse. This framework establishes the relevance of nested spatial and temporal scales, as well as the direction and magnitude of $\hat{\lambda}$ across space and time. This framework initially identified biologically relevant spatial scales tied to population structure and function, namely lek and Bi-State DPS region, and estimated whether leks at smaller spatial scales were trending similar to the Bi-State DPS, or whether trends between scales were decoupled. Decoupling from larger spatial scale trends signals potential local deterministic factors driving local population changes. Knowing leks that are declining and decoupling from the Bi-State DPS extent can help to identify areas for target management actions, especially those aimed at reversing population declines (fig. 6). Furthermore, identifying decoupling across scales helps to account for the effects of annual precipitation, which is known to influence strongly broad-scale sage-grouse population trends in the Bi-State DPS (Coates and others, 2018).

Data Compilation

We compiled time-series maximum counts for active leks at any time between 2001 and 2018. We did not use lek data prior to 2001 because too few leks provided enough repeated measures data for the hierarchical analysis. We did not impose the missing value key (see "Objective 1. Integrated Population Modeling and Estimated Abundance" section) because the analysis required greater temporal and spatial representation across nested scales. Lek count data still underwent several quality control checks by an Inter-Agency Technical Advisory Committee for the Bi-State DPS before data were compiled for use in our models. In addition to the committee's QA/QC, we developed a set of criteria that was similar to those criteria described in Coates and others (2018). For example, we used the number of males associated with the date of maximum saturation count across the Bi-State DPS (see "Objective 1. Integrated Population Modeling and Estimated Abundance" section). We added a value of 1.0 to the reported count to avoid division by zero, which yields an undefined calculation of $\hat{\lambda}$. Furthermore, a lek had to be counted a minimum of five times over the study period, and each lek had to be monitored for at least 2 out of the last 5 years to be included in our dataset. Leks that met the last criteria but had some counts missing from the time series received NA values in place of the missing counts.

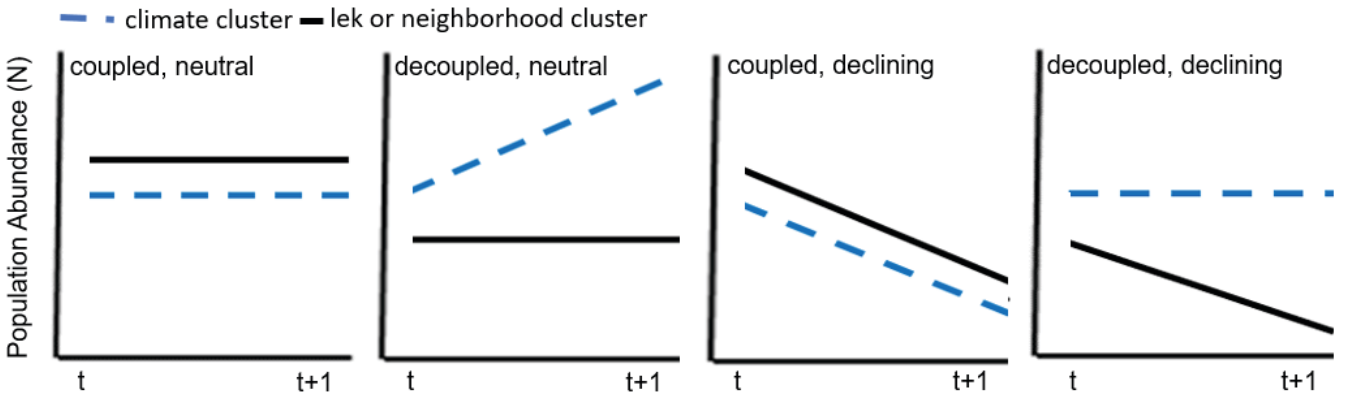

Figure 6. Four hypothesized outcomes in comparing trends between smaller scale (black solid line) and upper scale (blue dashed line).

Defining Multiple Spatial Scales

We defined spatially nested scales as single lek (local) and Bi-State DPS (regional). Leks represent population responses to local drivers of population change, whereas the regional Bi-State DPS more closely represents dynamics governed by region-wide climatic and habitat conditions. Hence, comparison of population trends at the lek versus regional extents help account for population changes driven by larger extent, and likely less manageable, environmental factors (fig. 6) versus local effects where local populations can benefit from targeted conservation actions within an adaptive management framework. We note that the original framework of Coates and others (2017a) included an intermediate "neighborhood cluster" quantitively comprised of adjacent leks largely closed to immigration and emigration so that population dynamics were primarily driven by births and deaths (O'Donnell and others, 2019). This scale has not been fully quantified for the Bi-State DPS, and subpopulations do not fully represent closed population units as evidenced by data from GPS marked sage-grouse (Coates and others, 2016a) and measures of genetic relatedness (Oyler-McCance and others, 2014). Hence, we only used the lek scale to estimate local dynamics.

State-Space Model Formulation

We developed Bayesian state-space models (SSM) using lek count data to estimate intrinsic rate of population change ($\hat{r}$) and derive $\hat{\lambda}$ (Kéry and Schaub, 2012; Coates and others, 2014b; Green and others, 2017; Monroe and others, 2017). We chose to use estimates from an SSM approach, as opposed to the IPM estimates, because thresholds established to indicate decoupling were determined previously (Coates and others, 2017a) using this approach across Nevada. Similar to IPMs, SSMs provide a means of separating process variance (that is, environmental flux) from observation error (Kéry and Schaub, 2012) by partitioning each variance component using a hierarchical structure. Although SSMs account for observation error, they do not explicitly estimate detection probability, and they assume constant or random variation in error. Nevertheless, under these assumptions, estimates from SSMs provide unbiased indices of $\hat{\lambda}$ (Monroe and others, 2019). We used a nested random effects structure (for example, lek nested within region) to derive posterior probability distributions for $\hat{\lambda}$ at each lek, as well as the Bi-State DPS population during each year of the time series. Model specifications are fully described in appendix 2.

We fit the model using Markov chain Monte Carlo (MCMC) sampling in program JAGS that interfaced with Program R (R-Core Team, 2018) using the rjags library (Plummer, 2016). MCMC settings consisted of three chains of 10,000 iterations each and a burn-in period of 100,000 iterations. Parameter inference was based on a subsample of the Markov chains, whereby every tenth sample was kept, and the rest discarded. This practice of thinning the Markov chain was done to reduce the degree of serial autocorrelation among the final set of inferential samples. The large number of parameters that were monitored precluded the use of the R-hat statistics (Gelman and others, 2014). Therefore, model convergence was assessed via visual inspection.

Evaluation of Posterior Probability Distributions

The posterior probability distributions of λ through time for each lek and the Bi-State DPS form the foundation for evaluating evidence of declining populations and decoupling across scales, which provides early warning for the potential need for management intervention. Following estimation of posterior probability distributions (PD) of $\hat{\lambda}$, we calculated the proportional density of the PD that was (1) decoupled from the region PD and decreasing; (2) coupled with the region PD, decreasing, but less than the median of the region PD; (3) coupled, decreasing, and greater than the median of the region PD; and (4) stable or increasing. Figure 7 displays amount of area under the curve for the four outcomes of intersecting PDs between two spatial scales. We then calculated the ratio of the PD representing evidence for decline and for decoupling to the PD representing evidence against decline and decoupling. We then took the natural log of the odds ratio (log-odds) and established thresholds for log-odds that represented significant evidence of decline and decoupling using a simulation approach employing a large dataset that spanned Nevada and California.

Developing Thresholds for Destabilization and Decoupling

We used 17 continuous years (2000–16) of annual lek count data across Nevada and California to inform retrospective simulation analyses designed to estimate (1) destabilizing thresholds to identify significant annual population decline by contrasting $\hat{\lambda}$ at the scale of interest relative to $\hat{\lambda}$ = 1.00 (stable population) and (2) decoupling thresholds to identify populations at the smaller scales that fall out of synchrony with those at larger scales by contrasting proportional differences in $\hat{\lambda}$ across nested scales. We required data at this much larger extent (beyond the DPS) to more accurately estimate these generalizable thresholds. To determine thresholds, we derived PD of $\hat{\lambda}$ for each lek, which represented the smallest spatial scale, and the regional scale. We then developed a method to describe the relationship of $\hat{\lambda}$ between the two extents calculated using log-odds ratios. Comparisons in $\hat{\lambda}$ were only made within the same year and between leks or subpopulations and regional scales.

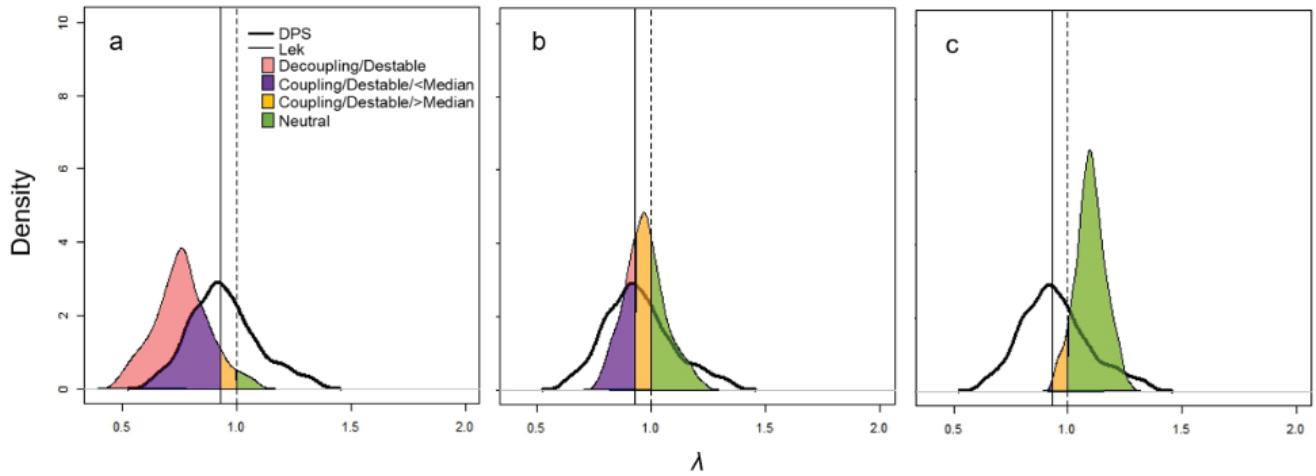

Figure 7. Strong evidence of decoupling and declining (*A*); coupled and evidence of stability (neutral; *B*); strong evidence of stability (*C*) based on intersection of posterior probability distributions of lambda for upper scale (thick distribution line) and scale of interest (for example, lek; thin distribution line). Solid vertical line represents median statistic of upper scale distribution (for example, Bi-State DPS), and dashed vertical line represents $\hat{\lambda} = 1$ (no increase or decrease).

We established two different thresholds for destabilizing and decoupling and associated warning signals to identify (1) slow thresholds that identify populations likely to experience a long-term decline and (2) fast thresholds that identify populations with precipitous declines and relatively high likelihood of near-term extirpation. Slow or fast warnings at a particular scale and year were activated *if and only if* (1) annual rates of change for sage-grouse populations at the population level of interest are determined lower than an identified destabilization threshold and (2) the proportional annual rates of change for sage-grouse populations were lower than the proportional changes at the next larger spatial scale, and thereby crossed a slow and fast decoupling threshold. Requiring crossing of both destabilizing and decoupling thresholds to activate a warning provides a spatial safeguard against implementing unnecessary management action that might arise from detecting local population declines that are most likely tracking unfavorable environmental conditions affecting the larger region.

We also employed temporal safeguards against prematurely implementing actions owing to short-term population dynamics, such as those arising from a single poor year of demographic performance or errors in lek counts. Accordingly, signals can be activated if warnings persist over a particular sequence of years, which provides an indicator of management intensity that may be needed to slow and ultimately halt population declines at the corresponding scale. Signal activation then can initiate adaptive management. Soft signals, such as those based on 2 consecutive years of activated slow warnings, identify the need for more intensive monitoring. Hard signals, such as those based on 3 out of 4 consecutive years of slow warnings or 2–3 consecutive years with activated slow or fast warnings, identify the need for management intervention aimed at stabilizing populations. Collectively, these rules facilitate detection of deleterious anthropogenic effects on local populations and distinguishing them from wider reaching environmental stochastic effects. Specific values for thresholds were identified using a simulation analysis from past lek count data, which measured increases in population growth under different signal thresholds given imposed management actions. Detailed description of simulation methodology to determine specific values for thresholds is reported in appendix 2.

Objective 3. Phenological Season and Reproductive Life-Stage Habitat Mapping

Delineating Seasons and Life Stages

We developed resource selection functions (RSF; Boyce and McDonald, 1999; Johnson and others, 2006) using data collected from telemetry locations from 2003 to 2018 (fig. 8). Patterns in RSF were partitioned into phenological seasons for all sage-grouse age and sex classes combined, and specific reproductive life-stages for reproductive females defined as nesting females and females with broods. For seasonal RSF mapping, we divided telemetry data into three seasons: spring from mid-March to June (locations, n = 13,853; birds, n = 654), summer from July to mid-October (locations, n = 11,028; birds, n = 490), and winter from late-October to early March (locations, n = 9,864; birds, n = 432). Importantly, the phenological-based RSFs included all age and sex classes of sage-grouse. Thus, the resulting spatially explicit predictions represented selection patterns by all sage-grouse combined during each season and did not explicitly represent habitat used by only reproductive females. Sage-grouse with fewer than two locations were removed from the dataset. For life stage mapping, we restricted the dataset to only reproducing females and estimated RSFs for three distinct periods: nesting (nest locations, n = 445), early brood-rearing (brood locations, n = 840; broods, n = 146), and late brood-rearing (brood locations, n = 1,341; broods, n = 152).

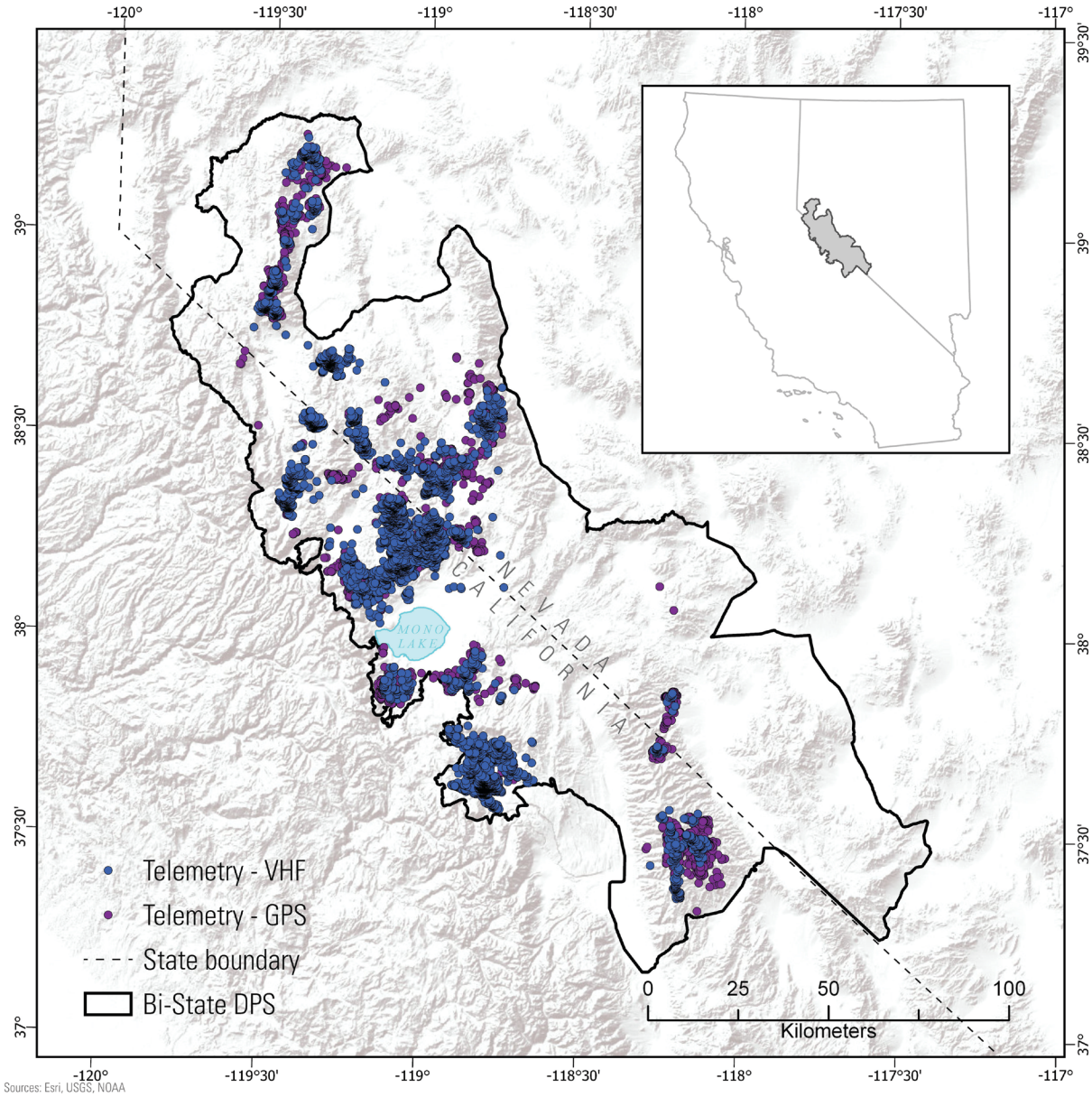

Figure 8. Locations for very high frequency (VHF) and global positioning system (GPS) telemetered greater sage-grouse (*Centrocercus urophasianus*) collected within the Bi-State Distinct Population Segment (DPS) used to estimate Resource Selection Functions across phenological seasons and reproductive life stages. Data were collected between 2002 and 2018.

Environmental Spatial Covariates

We quantified a broad suite of biotic and abiotic variables potentially associated with sage-grouse phenologically based and life-stage-based RSFs as spatially explicit environmental covariates. We used shrubland land cover types from the National Land Cover Database derived using fractional analyses (Xian and others, 2015) and updated to reflect conditions as of 2016 (https://www.mrlc.gov/data/type/shrubland), where each 900 m^2 resolution pixel represented a continuous percentage of cover. For our mapping and covariate extraction, we used layers depicting percent cover of bare ground; herbaceous annual and perennial vegetation; big sagebrush (such as mountain big sagebrush, Wyoming big sagebrush, or basin big sagebrush); little sagebrush (such as little sagebrush, black sagebrush); all sagebrush; non-sagebrush shrub (such as rabbitbrush, and bitterbrush); and all shrubs. For vegetation structure, we used layers depicting height of all sagebrush and all shrubs. In addition, we used a recently developed high-resolution (1 m^2) maps of conifer cover (Gustafson and others, 2018), whereby circular canopy extent was classified with object recognition algorithms in Feature Analyst™ (Overwatch Systems, Sterling, Virginia). The map rescaled to 900 m^2 resolution using a circular moving window with a 50 m radius (ArcGIS Spatial Analyst™, Environmental Systems Research Institute, Redlands, Calif.) that represented a continuous proportion of pinyon-juniper within each pixel. We also evaluated selection and avoidance of a proportion of areas that consisted of different conifer cover classes (CC1, greater than 0 to 10 percent cover; CC2, greater than 10 to 20; and CC3, greater than 20 percent). We provide descriptions of individual environmental covariates and the data source in appendix 3. We evaluated patterns of selection and avoidance of land cover variables at three different spatial scales relevant to sage-grouse movement patterns because sage-grouse often select habitat in a scale-dependent fashion (Casazza and others, 2011; Aldridge and others, 2012). Specifically, we calculated the proportion of each candidate land cover covariate within circular moving windows (neighborhood analysis tool, ArcGIS™ Spatial Analyst) with radii of 167.9 m (8.7 ha), 439.5 m (61.5 ha), and 1,451.7 m (661.4 ha), which represented averages of minimum, mean, and maximum daily distances traveled by sage-grouse, respectively. We included an additional, finer scale for analysis of nest site selection (radius = 75 m; 1.8 ha) to accommodate potential nest site selection based on landscape attributes more directly associated with the nest such as nest cover and average distance moved during nesting recess (Dudko and others, 2018).

We also investigated distance to and density of landscape features within the RSFs, including various water features and agricultural development. We measured distance to multiple water features compiled within the National Hydrography Dataset (U.S. Geological Survey, 2014), which included perennial streams, intermittent streams, springs, open water bodies, ditches, canals, and wells. We also evaluated distance to edge of multiple land cover covariates, including conifer cover classes, any forest type, and wet meadows. For all landscape features, linear distance was calculated as a simple Euclidean distance from a used or available point using the Distance tool in Spatial Analyst (ArcGIS™ 10.1). Distance-based predictors were transformed using an exponential decay function (Coates and others, 2016b, 2016c) such that the effect of the predictor decays with increasing distance, using $e^{-d/a}$ where α represented either the median value at all locations, broods, or nests, or 5 km, whichever was smaller. This decay function allowed for estimation of the degree to which the effect of a habitat feature strengthened or weakened with increasing distance from that feature.

Topographic characteristics were calculated to assess the probability of sage-grouse use with several indices derived from the National Elevation Dataset (U.S. Geological Survey, 2009) within 900 m^2 pixels. Elevation and slope were derived from digital elevation models. We also calculated topographic roughness expressed as variance in elevation change (Riley and others, 1999); surface curvature using a concavity versus convexity index (Bolstad and Lillesand, 1992); heat load index expressed as predominance of southwest-facing slopes while accounting for steepness (McCune and Keon, 2002); compound topographic index using a steady state wetness index (Gessler and others, 1995); and transformed aspect using a transformation of circular aspect to a zero to one value where one is hottest, driest, southwest-facing slopes (Roberts and Cooper, 1989) using the Geomorphometry and Gradient Metrics Toolbox (Evans and Oakleaf, 2012). All topographic characteristics were re-evaluated for each moving window size.

We included the Normalized Difference Vegetation Index (NDVI; Pettorelli and others, 2011) in our analysis to account for spatiotemporal variation in vegetation greenness and productivity. NDVI products were based on MODIS (Moderate Resolution Imaging Spectroradiometer) data obtained from the USGS collection of NASA land data products (Didan, 2015). NDVI images are released every 16 days with a spatial resolution of ~250 m. We averaged the images for each study year within each seasonal or life stage time window using cell statistics (ArcGIS™ Spatial Analyst) and extracted those values to the corresponding dataset. We also applied the larger moving window neighborhood sizes (radius = 439.5 and 1,451.7, respectively) to NDVI, omitting the smallest because it was smaller than the product's original spatial resolution.

Values of all landscape habitat features, distance metrics, and topographic indices were extracted from the GIS for input into the habitat selection analyses at used locations, defined as locations occupied by radio-marked sage-grouse, and random locations. The purpose of generating random locations was to characterize the environment available to sage-grouse. Ten random locations within a buffered minimum convex polygon generated from all locations used by a grouse were included to account for heterogeneity of available land cover types (Aldridge and others, 2012). Prior to analysis, we centered and standardized land cover variables that represented continuous values on the landscape such as index values or percent cover, using each variable's mean and standard deviation $(z = \frac{x - \mu_x}{\sigma_x})$. Because distance variables already were transformed to a scale of 0–1 by the exponential decay function, we centered those variables but did not further transform them.

Resource Selection Function Analyses

RSFs were used to characterize the study area in terms of selection versus avoidance for the *n*-dimensional combination of landscape predictors considered in this analysis. In the RSF analysis, selection versus avoidance for landscape features are estimated by contrasting measurements at used locations, such as adult grouse, brood, or nest locations, with measurements at random locations representing features available to grouse within a population as developed by Coates and others (2014a, 2016c). For each season and life stage, we estimated an RSF using generalized linear mixed models (GLMMs) with a binomial error distribution and logit-link function, where the environmental covariates were used to predict the response variable representing used (y = 1) versus random (y = 0) locations.

Variable Screening and Model Selection

A preliminary variable screening analysis was carried out to identify the most explanatory predictors among a broader set of correlated candidate predictors. Candidate predictors included all characterizations of the specific landscape features described above in the "Environmental Spatial Covariates" section. While considering multiple characterizations of landscape features (for example, multi-scale and distance-based metrics) helps to identify appropriate functional relationships between sage-grouse habitat selection and landscape features, it can also complicate conventional resource selection analysis by introducing collinear variables into RSF model selection, leading to models with redundant or confounded parameters. We performed variable screening for two primary reasons, first because including collinear variables within the same model structure can distort RSF estimation and prediction (Dormann and others, 2013), and second because the inclusion of a very large number of predictor variables (n = 100 in this case) can lead to model overfitting, with subsequent models that can be difficult to interpret (Grace and Bollen, 2005). Our iterative variable selection procedure therefore explores the performance of each candidate habitat predictor within a multivariate RSF framework while preventing models from including any pair or set of strongly correlated variables, defined as |r| greater 0.5. Our iterative preliminary variable screening procedure is detailed in appendix 4.

Following the completion of the variable screening procedure for each season and life stage, we selected a final model based primarily on delta-AIC rank (ΔAIC; see appendix 4) while removing variables that had $|r|$ greater than 0.5 with any variable that ranked higher in terms of ΔAIC. We did not consider any variables that had ΔAIC < 2 when compared to models fit without that variable (see appendix 4). We then fit a full RSF model from all grouse or broods with at least two used locations, or all nests for the nest dataset, and all predictors in the final list of top-ranked, uncorrelated habitat predictor variables. We used generalized linear mixed models with binomial family of distributions to account for unavoidable unbalanced data structure across sites and years when analyzing the full dataset (Gillies and others, 2006; Bolker and others, 2009) and we added a random intercept for grouse or brood, respectively, and a random intercept for site-year in the final model. We also considered 2nd order polynomial terms such as quadratic, or peaked effect terms for topographic variables such as elevation, roughness, and slope, if they were identified as important within the variable screening procedure. This was based on prior knowledge that grouse typically used habitats at intermediate elevations which tend to exhibit moderate topographic slope and ruggedness.

Because the inclusion of a complete set of predictors can influence each predictor's explanatory power and relative importance, we considered our model-building to be exploratory and sequentially culled any remaining uninformative parameters from the final model based on $abs(\hat{\beta} / \mathrm{SE}(\hat{\beta})) > 1.44$, which approximately corresponds to an 85 percent confidence interval (CI) around the coefficient estimate (Pagano and Arnold, 2009; Arnold, 2010; Austin and others, 2017). Arnold (2010) justifies the statistical relevance of the 85 percent CI as a cutoff point at which a parameter fails to add meaningful information to a model when included. We fit the final model for each life stage or season in R using the package "lme4" (Bates and others, 2015) in Program R (R-Core Team, 2018). If necessary, we updated the final model using starting values from a previous model fit and increased model function evaluations to 100,000 to achieve model convergence.

Habitat Selection Index

For each season and life stage, the final RSF took the form

$$w(x) = \exp\left(\beta_1 x_1 + \beta_2 x_2 + \ldots + \beta_k x_k\right) \quad (8)$$

where

$w(x)$ is the resource selection function (RSF) and

β represents the coefficient estimate for each predictor ($x_1 \ldots, x_k$) (Manly and others, 2002; McDonald, 2013).

The RSF is not an absolute probability because random locations do not represent true absence, but RSFs have utility as relative measures of the probability of selection when appropriately conditioned on available habitat (Johnson and others, 2006; McDonald, 2013; Northrup and others, 2013). For each of the six models (spring, summer–fall, winter, early brood-rearing, late brood-rearing, nesting), we applied the final RSF equation across all pixels in the Bi-State DPS spatial extent using Raster Calculator in Spatial Analyst (ArcGIS™ 10.4). Then, following Coates and others (2014a, 2016c), we transformed the RSF to a habitat selection index (HSI), which took the form

$$\text{HSI} = \frac{w(x)}{1 + w(x)} \quad (9)$$

HSI surfaces indicate relative habitat quality for each pixel (Coates and others 2014a, 2016c) and are equivalent to a logistic transformation on *w(x)* but were only used to express relative habitat use proportional to availability on a scale of 0–1. HSI values represent relative (not absolute) probabilities, where an increase in HSI corresponds to an increase in probability of selection.

We performed a covariate sensitivity analysis for each model to identify the strongest predictors with respect to their influence on the HSI. We used the HSI values for this analysis because they are less prone to extreme values and more appropriate for identifying effect sizes in terms of relative probability. We calculated a delta-HSI score for each predictor in the final model as follows. First, we set all predictors to their median values. Next, for the single predictor of interest, we generated HSI scores ranging from the predictor's 2.5th percentile value to its 97.5th percentile value, thus encompassing 95-percent of the available distribution, and subtracted the minimum predicted HSI value from the maximum HSI predicted value across this range. For predictors with linear effects, this corresponded to a difference in HSI across the range of values from the 2.5th to 97.5th percentile for the predictor. However, for non-linear effects such as quadratic terms for topographic variables, the delta-HSI indicated the difference between the highest and lowest points of the distribution, thereby reflecting the potential magnitude of the effect between any two potential values. The sign (positive versus negative) of the coefficient was used to indicate whether the predictor's delta-HSI represented a positive or negative influence on relative probability of selection.

Phenological Season, Life Stage, and Annual HSI Mapping

With respect to each seasonal or life stage RSF, we categorized the Bi-State DPS study area into four binned classes that represent a habitat selection index at larger spatial scales. This also simplified interpretation of output HSI values because it ranks HSI values based on the number of sage-grouse locations, brood locations, or nests that fall into each class. To accomplish this, we followed the previously established methodology of Coates and others (2014a, 2016c), with the exception that we used all model data for classification rather than an independent subset. This was done because fewer birds with adequate numbers of locations across seasons and life stages were monitored within the Bi-State DPS. We first determined the mean HSI value at all used locations ($\overline{x}_{used}$) for adult grouse, brood, or nest, depending on season or life stage, respectively. Assuming HSI values at used locations were approximately normally distributed, the highest ranked habitat selection class comprised of HSI values within 0.5 standard deviations (σ^2) below the mean ($\overline{x}_{used} - 0.5*\sigma^2$), moderate selection was HSI values from greater than 0.5 to 1.0 standard deviations (SD) below $\overline{x}_{used}$, and low selection habitat comprised HSI values from greater than 1.0 to 1.5 SD below $\overline{x}_{used}$. Any values less than 1.5 SD from the mean HSI were regarded as generally unsuitable habitat, a categorization that described less than approximately 8 percent of all used locations. We applied this methodology to define habitat selection cut-points and subsequent classes for each seasonal or life stage region-wide HSI.

Objective 4. Spatially-Explicit Distributional Analysis

To better understand gains and losses in sage-grouse distributions through time, among subpopulations, and across the Bi-State DPS as a whole, we estimated annual distributional areas (DSA) which represented information about IPM-derived estimates of abundance ($\hat{N}$, see "Objective 1. Integrated Population Modeling and Estimated Abundance" section) and habitat indices (see "Objective 3. Seasonal and Life History Stage Habitat Mapping" section). DSAs accounted for lek configuration, distance to leks, and $\hat{N}$ associated with each lek, and extractions at the 99 and 50 percent isopleths represented overall and core distributions of habitat, respectively, predicted to be occupied by sage-grouse during at least one phenological or life-history season.

The DSA approach distinguishes these likely occupied habitats from "potential" selected habitats with predicted low or no occupancy. Low or no occupancy in potential selected habitat may occur for multiple reasons. For example, these habitats may be located in areas that have resources selected by sage-grouse but are too far from existing subpopulations centered around leks to be colonized readily. Such areas also may represent historically occupied areas that have undergone local extirpation. Importantly, it is also possible that seemingly suitable habitat contains remnant populations that have gone undetected due to very low abundance.

Our primary objective was to investigate trends of gains or losses in DSA within subpopulations and across the Bi-State DPS with respect to the long- and short-term time periods encompassing three and one population cycles, respectively (see "Objective 1. Integrated Population Modeling and Estimated Abundance" section). We also explored spatial variation among subpopulations and identified potential redistribution of sage-grouse occupancy through time. To accomplish these objectives, we carried out multiple steps. First, we followed published methodological techniques to create a probability density function (PDF) across the Bi-State DPS using lek locations from standardized kernel point density models (Doherty and others, 2016). Second, we calculated a 99 and 50 percent isopleth of the PDF to estimate boundaries of overall and core sage-grouse utilization, respectively. We then removed non-habitat areas within these boundaries by intersecting these areas with areas of sage-grouse habitat defined in objective 3 within 10.6 km of lek with an associated IPM-estimated $\hat{N}$ from the respective long or short-term period. The intersected areas represented DSAs. We calculated the amount of each DSA within subpopulations, as well as Bi-State DPS, by year. We also calculated a generalized DSA using the average IPM-estimated abundances for each lek over the short-term period (2008–18) as the weighting factor for management application, see Objective 5. Region-Wide Habitat Indices of Selected and Occupied Habitats for Conservation Planning. Further analytical details are as follows.

Data Compilation

Following the "Integrated Population Modeling and Estimated Abundance" section, we compiled median $\hat{N}$ for each individual lek by year across long- and short-term periods, largely because the PDF from kernel estimators relies on single point density values (see 'Kernel Density Function'). Similar to the trend analysis (see "Objective 1. Integrated Population Modeling and Estimated Abundance" section), not all subpopulations had enough lek surveys with associated IPM derived $\hat{N}$ to estimate DSAs across all periods. Thus, DSAs should be considered relative values (that is, not absolute distributions) that are useful for comparing annual trends in gains or losses of occupied habitat within each subpopulation across different time periods. For the long-term period (1995–2018), data were only sufficient for spatial estimation across the Bodie, Fales, Long Valley, and Sagehen subpopulations. For the short-term period, data were sufficient for spatial estimation for all subpopulations across the Bi-State DPS using the following adjustments. We included active leks that were removed from the short-term trend analysis based on identification from the NA key identified in objective 1. We spatially accounted for these leks by assigning median IPM-derived $\hat{N}$ values from estimated active leks within the same subpopulation and year. Thus, we assumed that the rate of change in DSA through time for leks with missing data was similar to the average rate of change for estimated leks within the same subpopulation. In this spatial analysis, it was appropriate to include these leks to help reduce potential biases of underestimating DSA in areas of missing lek data. For example, this procedure helped prevent "holes" in the estimated DSA associated with missing data. Missing data for leks that were considered inactive or extirpated did not receive a value.

Kernel Density Function

Kernel density estimation has been commonly used in ecological studies to calculate home ranges (Worton, 1989), individual- and population-level utilization distributions (Coates and others, 2013; Doherty and others, 2016), and large-scale breeding core areas (Doherty and others, 2010). Kernel estimators are non-parametric analyses that place no constraint on the shape of a PDF, given input point locations, and allow inference of animal utilization among points. Although location data from individual animals are typically used to approximate PDFs, point location of breeding sites (that is, leks) can provide an index of population-level density and distribution, given that abundance data associated with each lek are available (Coates and others, 2016e; Doherty and others, 2016). A parameter h represents the bandwidth of the kernel function and controls the degree of smoothing between point locations (Gitzen and others, 2006). Because kernel density functions were used to approximate population distribution at broader scales in this analysis, similar to those conducted in Doherty and others (2016), we developed two PDFs based on input of two separate h to reflect previously reported estimates of population-level distribution patterns of telemetered sage-grouse associated with lek sites within the Bi-State DPS (Coates and others, 2013). Specifically, we used values of 6.0 and 10.6 km based on breeding season and year-round utilization distributions, respectively, informed by locations for telemetered sage-grouse in relation to lek sites. To evaluate spatiotemporal changes in distribution, we weighted each lek point-location by its corresponding median $\hat{N}$ for each year, which provided variation in spatial distribution based on variation in abundance among leks. To derive a sage-grouse kernel index for each year, we standardized the probabilistic density surfaces and averaged the values for each pixel, which took the form

$$Kernel\ Index = \left(6.0\ km\ PDF + 10.6\ km\ PDF\right)/2 \quad (10)$$

Averaging kernels across both spatial scales appropriately accounted for use of breeding areas and other seasonally-used areas in the distributional model. This multi-scale density process was intended to reflect the use of areas around sage-grouse leks with ecologically meaningful spatial scales.

To minimize inclusion of habitats rarely used by sage-grouse in DSA estimates (for example, rocky alpine habitats, salt flats), we created a geospatial mask comprised of any pixel that did not represent selected habitat (that is, greater than or equal to the low selection category) during at least one phenological season or reproductive life stage within 10.6 km of a lek, and removed masked pixels from DSA estimates. We then calculated the amount of total area and proportional volume of DSA within 99 and 50 percent extrapolated and habitat-masked isopleths for each year by each subpopulation and entire Bi-State DPS. As a validation, we calculated the proportion of leks falling within the 2018 DSA at the 99 percent isopleth. Only one out of 57 leks (1.8 percent) fell outside 2018 DSA, which comprised a now extirpated lek in the Pine Nuts.

Modeling Changes in Sage-Grouse Distribution

We used linear mixed effects models in a Bayesian modeling environment to evaluate changes in distribution of DSA by total area and proportional volume across the long- and short-term periods for each subpopulation and Bi-State DPS. For total area, we analyzed subpopulation-specific trends on a common scale by standardizing the annual area for each subpopulation around its mean and standard deviation for the overall time series. This was done to balance the model so that trend estimates would be comparable among sites. Proportional area did not require standardization because it was bounded between zero and one. The DSA total area model was expressed as

$$DSA(a)_{ij} = \alpha_i + \beta_i X_{ij} + \varepsilon_{ij} \quad (11)$$

$$\varepsilon_{ij} \sim Normal\left(0, \sigma^2\right) \quad (12)$$

$$\alpha_i \sim Normal\left(\mu_\alpha, \sigma_\alpha^2\right) \quad (13)$$

$$\beta_i \sim Normal\left(\mu_\beta, \sigma_\beta^2\right), \quad (14)$$

and the DSA volume proportion model was expressed as

$$DSA(v)_{ij} \sim Beta\left(rq_{ij}, r\left(1-q_{ij}\right)\right) \quad (15)$$

$$r \sim Gamma\left(0.1, 0.1\right) \quad (16)$$

$$logit\left(q_{ij}\right) = a_i + \beta_i X_{ij} \quad (17)$$

$$\alpha_i \sim Normal\left(\mu_\alpha, \sigma_\alpha^2\right) \quad (18)$$

$$\beta_i \sim Normal\left(\mu_\beta, \sigma_\beta^2\right), \quad (19)$$

where

$DSA(a)_{ij}$ or $DSA(v)_{ij}$ for each subpopulation (i) and year (j) was modeled as a deterministic function of year, represented by X_{ij}, and

error, ε_{ik} was assumed to arise from a normal distribution with mean of 0 and variance σ^2.

The Beta distribution was used for $DSA(v)_{ik}$ to bound estimates between 0 and 1, $DSA(v)_{ik} \in [0,1]$, which is appropriate for proportions (Ferrari and Cribari-Neto, 2004). The Beta distribution has an additional parameter, $r > 0$, that controls the concentration around the value, q_{ik}, which is modeled on the logit scale as a function of covariates and other random effects parameters. For both models, we fit random intercept, a_i, and slope, β_i, by subpopulation to make conditional inference of effect, and estimated trend using the marginal distribution of the time effect per subpopulation, where a negative or positive sign would indicate either a declining or increasing trend, respectively. Random intercepts and slopes were assumed to arise from a normal distribution around the mean of subpopulation intercepts, μ_a, and slopes, β_i, respectively, with variances σ_α^2 and σ_β^2, respectively. The hyperparameter of the assumed distributions of the random effects allowed for inference at the Bi-State DPS-wide scale. Differences in distribution between the initial (1995 or 2008) and the final study year (2018) were used to estimate net gain and loss for each subpopulation. A posterior distribution of total gain and loss was derived from the area model, where gains and losses based on the trend estimated for each subpopulation were summed across all subpopulations studied from each dataset (three and one population cycles). Per subpopulation and across the Bi-State DPS, we report model estimates of net gain/loss (ha), rate of gain/loss (β_i), and probability (P) of $|\beta_i| > 0$ for each of the three time periods. We evaluated evidence of net gain/loss based on predicted posterior distributions.

Objective 5. Region-Wide Habitat Indices of Selected and Occupied Habitats for Conservation Planning

To further describe spatial distribution of habitats, we present overlays of phenological seasonal and life stage maps to identify areas where conditions selected by all sage-grouse regardless of sex or reproductive status were also selected by reproductive female sage grouse. Overlays consisted of spring with nesting, spring and summer–fall with early brood rearing, and summer–fall with late brood rearing. We also created a composite map of habitats selected on an annual basis through the geospatial union of all phenological and life stage pixels identified as low, moderate, or high selected habitat.

We calculated percentages of selected phenological, life stage, and annual habitat that each subpopulation contributed to the Bi-State DPS. Using the methods described for Objective 4, we produced a composite and generalized DSA using the average IPM-estimated abundances for each lek over the short-term period (2008–18) as the weighting factor. We extracted the generalized DSA at the 99 percent isopleth and intersected with maps of selected phenological, life stage, and annual habitat. Products of these intersections yielded selected habitat likely occupied by sage-grouse and percentages of selected versus occupied habitat that each subpopulation contributed to the Bi-State DPS throughout their most recent population cycle by incorporating years of relatively high and low abundance. Values for the ratio of occupied to selected habitat that were less than, equal to, and greater than 1.0 indicated under-utilization, equivalent, or disproportionate use, respectively.

Objective 6. Effects of Precipitation and Managed Water Delivery on Brood Habitat

Sage-grouse in Long Valley occupy greater than 15 percent of land managed by Los Angeles Department of Water and Power (LADWP), an agency with water rights to much of the southeastern Sierra and Owens River watersheds. Much of this area contains wet meadows and irrigated pastures on the western and northern ends of Lake Crowley. Historically, LADWP generally allowed a portion of surplus water to irrigate managed pastures in Long Valley in an effort to balance the water needs for Los Angeles, Calif., with needs of ranching operations and wildlife. However, recent prolonged drought and increased urban water demand reduced the volume of surplus water available for pasture irrigation, likely contributing to reduced productivity and greenness in Long Valley (fig. 9). Such limitations could negatively impact sage-grouse, particularly during the brood-rearing period when green forbs and associated insects are needed for chick growth and survival (Drut and others, 1994; Atamian and others, 2010b; Casazza and others, 2011).

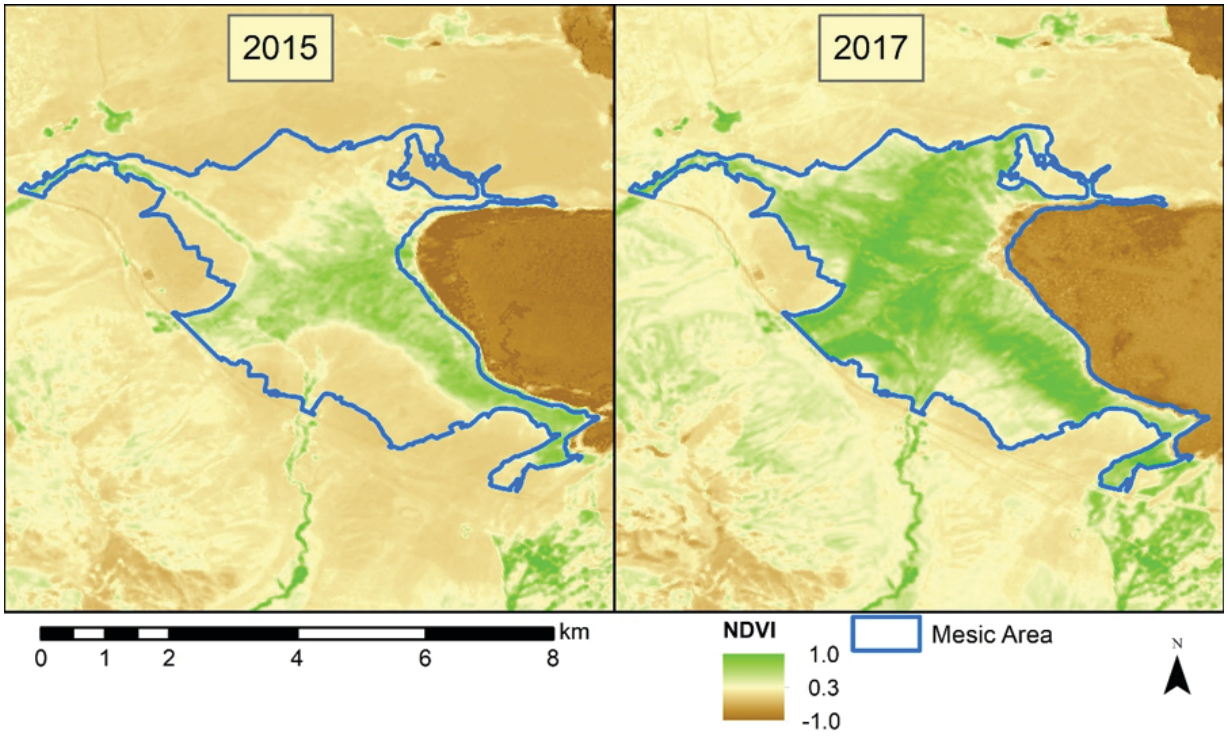

Figure 9. Normalized Difference Vegetation Index (NDVI) between two extreme years of precipitation, 2015 and 2017, for the Convict Creek mesic area in Long Valley within the Bi-State Distinct Population Segment of greater sage-grouse (*Centrocercus urophasianus*). High values (green) reflect abundant and green vegetation, low value reflects more senesced and less abundant vegetation.

Because of the significance of Long Valley to the overall status of the Bi-State DPS and the continued threat of prolonged drought, additional site-specific research that identifies management solutions to help mitigate effects of water management on sage-grouse at this site are warranted. Hence, we conducted an analysis using female sage-grouse with broods in Long Valley to estimate selection of (1) all available mesic resources (for example, wet meadows, upland seeps, irrigated pasture) and (2) irrigated pastures, specifically, the Convict Creek mesic area (fig. 10).

Data Compilation

We used locations from radio-marked female sage-grouse with broods collected from approximately June–August between 2003 and 2005, 2007–11, and 2016–18. Sequential day and night locations were obtained every 10 days until brood failure or independence, which occurs at approximately 50–70 days following hatch. For each location, we attempted to observe the female or chicks directly but without causing them to flush. The exception to this procedure was at the 50-day location where observers intentionally flushed the female and any associated chicks in order to count chicks and verify brood success to day 50. We allowed habitat space availability to vary annually by calculating a 99 percent kernel density utilization distribution (UD) for each year using the "kernelUD" function in the "adehabitatHR" package (Calenge, 2006) in the Program R (R-Core Team, 2018). We estimated the bandwidth using likelihood cross validation with the "bw.ppl" function in the "spatstat" package (Baddeley and others, 2016) and removed the water surface of Lake Crowley from the UDs. We then generated a number of random locations within each annual UD equal to 10 times the number of brood locations for each year using the "spsample" function in the "sp" package (Bivand and others, 2013).

We digitized all major meadows and pastures in Long Valley visually from aerial photographs. Irrigated pastures often were delineated by irrigation canals, while the other mesic resources were delineated by an upland shrub edge. For each year, we calculated an average NDVI for all 900 m^2 pixels from radiometrically and geometrically corrected (Dwyer and others, 2018) and cloud-free Landsat 5, 7, and 8 satellite images recorded during July and August. Landsat-derived NDVI values agree well with ground-based measurements of mesic areas in sagebrush communities (Snyder and others, 2019). For each used and random location, we then assigned the corresponding NDVI pixel value for that location, and the average NDVI with a 100, 400, and 1000 m radius of the location. Within those radii, we also calculated the proportion of the area with greater than 0.3 NDVI, which has been identified as a potential threshold for mesic resources in good condition (Donnelly and others, 2016). In addition, we calculated the average NDVI and proportion of area greater than 0.3 NDVI of the entire mesic resource and the area within 100 m of the edge of the mesic resource for each year. We also measured the distance of each location to the edge of the nearest mesic resource such that locations occurring within the mesic resource received a negative distance to edge. While we acknowledge that other covariates such as terrain features, shrub cover, and roads affect sage-grouse space use, availability of these features was assumed to be constant across the study period. Therefore, we focused our analysis on NDVI and proximity to mesic resources metrics to assess temporal changes in sage-grouse selection patterns as a function of variation in mesic habitat conditions as indexed by NDVI and associated proximity.

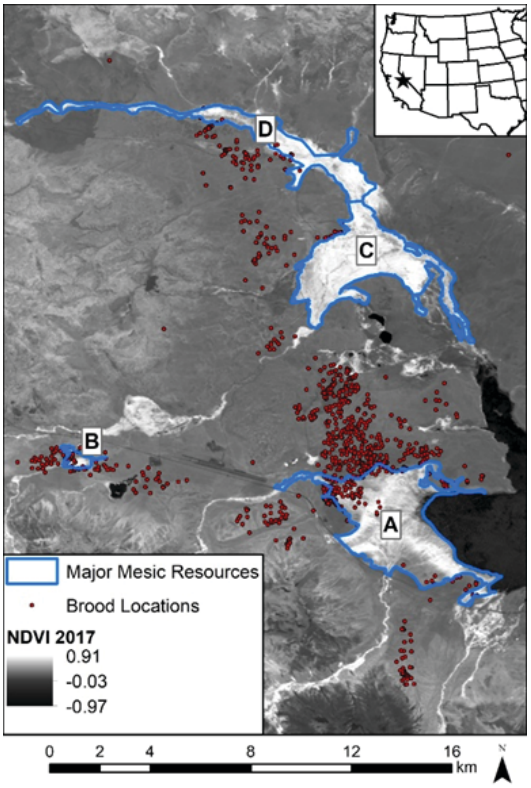

Figure 10. Study areas used to assess the selection of greater sage-grouse (*Centrocercus urophasianus*) broods relative to major mesic resources in Long Valley, California, from 2003 to 2018. *A*, Convict Creek mesic area; *B*, Laurel Creek mesic area; *C*, Hot Creek mesic area; and *D*, Owens River mesic area. Base map is a normalized vegetation difference index (NDVI) averaged during July and August 2017. Background image was produced from Landsat Analysis Ready Data; Dwyer and others, 2018.

Modeling Approach

We modeled resource selection with binomial generalized additive mixed models (GAMM) using the "gam" function in the "mgcv" package (Wood, 2019) in R with used and available locations as the binomial response. The model took the form

$$g\left(E\left(Y\right)\right) = \alpha + f_1 x_1 + \ldots + f_k x_k \quad (20)$$

where

$E(Y)$ is the expected response value given a logit function $g(Y)$ to link with each predictor variable $x_1, \ldots x_k$, α is the intercept, and $f_1 x_1, \ldots f_k x_k$ represent smoothed non-parametric functions.

We fit year and individual bird as random effects and supplied weights of 0.1 and 1.0 to the available and used locations, respectively, to account for the unequal sample sizes in the response classes. We fit all additive non-parametric functions as thin plate regression splines and estimated the appropriate number of knots using maximum likelihood. We set the maximum number of knots to 5 to avoid overfitting and allowed the knots to be able to shrink to 2, indicating a linear fit. We fit multiplicative non-parametric functions as tensor product smooths of the cubic regression splines and estimated the number of knots without restriction using maximum likelihood. Fitting GAMMs allowed for more interpretable estimation of non-linear effects (Wood, 2019) that we expected in our more focused and site-specific analysis of sage-grouse response to changing mesic resource availability throughout the brood rearing period. All candidate models were compared using Akaike's information criterion corrected for small sample sizes (AICc; Burnham and Anderson, 2002).

For selection of all available major mesic resources, we used a 3-step approach using AICc, and with no explanatory variables exceeding the collinearity threshold of |r| greater than 0.55. Step 1 identified the best fitting NDVI-scale (for example, 30, 100, 400, 1000 m) to carry forward. These scales were slightly modified from the seasonal modeling scales to approximate brood movements. The smallest scale of 30 m was also included in this analysis to reflect short movements. Step 2 assessed biologically relevant model structures including: combinations of the selected NDVI scale from step 1; the distance to the nearest mesic resource; ordinal day of the year; the NDVI of the nearest mesic resource; and the NDVI of the entire study area other than the mesic resources. Step 3 reassessed the appropriate NDVI scale using the overall model structure selected from step 2 to ensure that even weak correlations between distance to mesic resource and NDVI did not confound scale selection.

For selection of irrigated pastures, we used sage-grouse brood locations closest to the Convict Creek mesic area, which is a large pasture managed primarily by sheet flow (that is, flood) irrigation pumped from diversion ditches from Convict Creek. The pasture is irrigated for cattle and wildlife. We examined how variation in pasture characteristics that respond to changes in water management influence sage-grouse resource selection. We primarily assessed interactions between sage-grouse distance to the pasture with pasture greenness indices described by the overall average NDVI in the pasture, NDVI within 100 m of the pasture edge, proportion of the overall pasture with greater than 0.3 NDVI, and proportion of the area within 100 m of the pasture edge. We included the condition of the pasture edge because as upland vegetation desiccates in the summer, sage-grouse use the edges of mesic habitat in close proximity to both food in the mesic area and cover in the uplands (Casazza and others, 2011). Braun and others (1977) also recommended protection of a 100 m buffer at the edge of mesic resources for sage-grouse. We also assessed an interaction with the entire study area NDVI, reasoning that if the uplands exhibited substantial greenness as indicated by high NDVI, sage-grouse broods may not need to use the pasture. Lastly, we included a covariate for season that distinguished early brood-rearing from late brood-rearing. We used before, versus on or after, 1 July, as the temporal demarcation for early- versus late-brood rearing, which was guided by the analysis for all mesic resources. This analysis focused on Convict Creek comprised just one step because the NDVI scale was not relevant to this question. All candidate models were contrasted using AICc.

Relations Between Precipitation, Water Delivery, and NDVI

We conducted additional preliminary analyses aimed at the Convict Creek mesic area to further identify relationships between edge greenness as measured by NDVI and (1) relative contributions of managed versus unmanaged water sources and (2) amount of water delivery in managed drainages resulting in peak, non-increasing greenness. We used archived records from LADWP and livestock operators spanning 1990–2017 to estimate annual acre-feet water deliveries from two primary ditches (Diversion 26 and Diversion 27) used to sheet-flow irrigate the Convict Creek mesic area. We used acre-foot estimates spanning the entire growing and livestock grazing season for each year. One caveat of this analysis is that we have no information regarding the timing or pulses of water delivery on NDVI greenness. Available water from natural watershed runoff was estimated annually for the same years using data from PRISM (Daly and others, 2008).

Available water from winter precipitation was estimated from January–April measurements across the Owens River watershed that fell primarily as snow releasing meltwater during spring and summer. Rainwater that fell within Long Valley during spring and summer (May–August) comprised local pulses of moisture. We used random forest models, a machine learning approach based on classification and regression trees, with the "randomForest" package (Liaw and Wiener, 2002) in Program R to identify the water source with the highest importance rank as measured by the percent increase in mean squared error (MSE) when each water source is removed from the model (Baruch-Mordo and others, 2013). We used segmented regression with the "segmented package" (Muggeo, 2008) in Program R to identify thresholds where increases in managed water delivery to Convict Creek did not result in concomitant increases in greenness within 100 m of the edge. We used two response variables for this analysis: (1) the proportional area within 100-m of the edge with NDVI greater than 0.3 and (2) the average NDVI within 100 m of the edge.

Preliminary Results and Interpretation

Objective 1. Integrated Population Model

Data Sample Sizes

We compiled thousands of historic intra-annual lek surveys and underwent QA/QC, which resulted in a total of 803 maximum male counts across 65 leks spanning the entire Bi-State DPS from 1995 to 2018. After screening these data for active status and excessive missing values, 376 counts across 16 leks, 404 counts across 23 leks, and 356 counts across 37 leks informed IPM estimation for the long (24 year), mid (18 year), and short (11 year) cycle periods, respectively. These data provided information about changes in observed population sizes while informing the observation error. The state process, which was informed by individual-based life history data consisted of individually marked sage-grouse using VHF (n = 611) and GPS (n = 18) telemetry across the study duration. Sample sizes of sage-grouse varied in estimation of demographic posterior probability distributions (*s*, n = 467; *c*, n = 194; *ns*, n = 374; *h*, n = 208; *cs*, n = 268; *np2*, n = 200).

Estimating Total Population Size

After accounting for variation in lek detection, male lek attendance and sightability, and sex-ratios, the IPM informed by data spanning 2008–18 produced $\hat{N}$ for Bi-State DPS, as a whole, at 3,305 (95 percent CRI = 2,247–4,683) sage-grouse. Using posterior probability distributions of $\hat{N}$ and derived $\hat{\lambda}$, we estimated 10-year extirpation probability at 1.1 percent based on the proportion of MCMC iterations that resulted in *N* of zero. Subpopulation median $\hat{N}$ with 95-percent credible limits, proportion of sage-grouse representing DPS, and 10-year extirpation probabilities are listed in table 1. Summarized demographic rate with age structure for DPS are listed in table 2. Specific demographic rates for models based on support of random effect structures are listed in appendix 5.

Population Trends Across the Bi-State DPS

Bi-State DPS Population Trends. Our models indicate population trends within the Bi-State DPS, in its entirety, did not exhibit evidence of a decreasing or increasing trend over the course of three distinct time periods: 1995–2018 (24 years), 2001–18 (18 years), and 2008–18 (11 years), which corresponded to nadir to nadir projections for 3, 2, and 1 complete population cycles. Specifically, we estimated average annual $\hat{\lambda}$ at 1.02 (95 percent CRI = 0.74–1.42), 0.99 (95 percent CRI = 0.68–1.34), and 0.99 (95 percent CRI = 0.70–1.30) over the three respective periods (table 3). These values resulted in an estimated 57.7 percent increase since the nadir 24 years ago, 15.7 percent decrease from the nadir 18 years ago, and 9.6 percent decrease over the past 11 years. Meaning, the 2018 estimated $\hat{N}$ was greater than the estimate at the nadir of 1995 (fig. 11*A*), and slightly less than estimates during nadirs of 2001 (fig. 11*B*) and 2008 (fig. 11*C*). Derived $\hat{\lambda}$ from the estimated $\hat{N}$ are displayed in figs. 11*D–F*. Although the Bi-State DPS has experienced substantial declines over the past 6 years, these declines have been nearly offset by 4 years of previous population growth during 2008–11. Importantly, the Bi-State DPS experiences cyclical patterns in abundance over time, which is typical of sage-grouse populations in other portions of their range (Row and Fedy, 2017). The 6- to 11-year wavelength of our observed oscillations are consistent with those reported elsewhere in sage-grouse range (Fedy and Doherty, 2011), although these period lengths have shortened relative to 50-year patterns (Row and Fedy, 2017). Such interannual variation in abundance is driven deterministically by interannual variation in demographic processes (Dahlgren and others, 2016; Coates and others, 2018), but are also apparently influenced by interannual variation in lek attendance rates that themselves vary with winter precipitation (Wann and others, 2019). However, the integrated approach that combines demographic with observation data likely helps to guard against any potential confounding effects of variation in attendance that might influence variation in observation error. Research that investigates confounding effects of attendance on inferences of $\hat{\lambda}$ would be beneficial (for example, Monroe and others, 2019), especially studies that disentangle differences in inferences from lek-based approaches versus those that integrate other forms of data (such as IPMs).

Table 1. Median sample of posterior probability distribution of predicted abundance ($\hat{N}$) with 95-percent credible intervals (2.5th and 97.5th percentiles of distribution) during 2018, proportion of greater sage-grouse (*Centrocercus urophasianus*) in each subpopulation within Population Management Units (PMUs) of Bi-State Distinct Population Segment (DPS), and associated proportional abundance contributions and 10-year extirpation probabilities (that is, percentile of distribution intersecting zero at a 10-year projection).

[$\hat{N}$ was adjusted for sightability, lek attendance rate, predicted proportion of unknown leks, and sex ratios]

Subpopulation*	Median	95 percent credible interval		Prop. of DPS	Percent extirpation probability
		Lower	Upper		
Bi-State DPS	3,305	2,247	4,683	1.00	1.1
Pine Nuts PMU	33	0	73	0.01	69.7
Desert Creek/Fales PMU	447	218	750	0.14	9.0
Fales	121	54	208	0.04	38.4
Desert Creek	325	163	542	0.10	23.4
Bodie Hills PMU	1,521	1,181	1,941	0.46	2.4
Mount Grant PMU	374	205	619	0.11	24.6
South Mono PMU	885	634	1,214	0.27	3.8
Sagehen	20	0	75	0.01	74.8
Long Valley	818	614	1,053	0.25	7.9
Parker Meadows	48	21	86	0.01	64.3
White Mountains PMU	45	9	86	0.01	75.1

*Subpopulations comprise either PMUs that contain all the leks within boundaries defined by the Nevada Governor's Sage-Grouse Conservation Team (2004), or more localized subpopulations with management interest nested within PMUs.

Table 2. Summary of posterior distributions of derived population vital rate parameters (median and 95 percent credible intervals defined by 2.5th and 97.5th percentile of distribution) using an integrated population model for greater sage-grouse (*Centrocercus urophasianus*) in Bi-State Distinct Population Segment, California and Nevada.

Age class	Median	Lower CRI	Upper CRI
Nest propensity (np1)			
Yearling	0.884	0.810	0.938
Adult	0.954	0.902	0.984
Nest propensity (np2)			
Yearling	0.130	0.024	0.376
Adult	0.235	0.059	0.459
Nest survival (ns1)			
Yearling	0.494	0.368	0.622
Adult	0.379	0.313	0.451
Clutch size (c1)			
Yearling	6.443	5.746	7.195
Adult	6.912	6.280	7.472
Nest survival (ns2)			
Yearling	0.663	0.470	0.808
Adult	0.562	0.380	0.732

Age class	Median	Lower CRI	Upper CRI
Clutch size (c2)			
Yearling	6.058	5.022	7.336
Adult	6.489	5.443	7.663
Hatchability (h)			
Yearling	0.875	0.722	0.945
Adult	0.867	0.713	0.939
Chick survival (cs)			
Yearling	0.403	0.305	0.517
Adult	0.364	0.283	0.466
Fecundity (f)			
Yearling	0.403	0.257	0.588
Adult	0.349	0.240	0.496
Survival (s)			
Juvenile	0.748	0.672	0.818
Yearling	0.687	0.556	0.789
Adult	0.682	0.578	0.769

Table 3. Median sample of posterior probability distribution of predicted average annual rate of population change in abundance ($\hat{\lambda}$) with 95-percent credible intervals (2.5th and 97.5th percentiles of distribution) across three (1995–2018), two (2001–18), and one (2008–18) complete population cycles for greater sage-grouse (*Centrocercus urophasianus*) within the Bi-State Distinct Population Segment (DPS), each studied subpopulation of the Bi-State DPS, and a sample of 11 subpopulations within the Great Basin.

Subpopulation	1995–2018			2001–18			2008–18		
	Median	Lower CRI	Upper CRI	Median	Lower CRI	Upper CRI	Median	Lower CRI	Upper CRI
Bi-State DPS	1.018	0.737	1.418	0.989	0.677	1.343	0.988	0.704	1.304
Pine Nuts PMU	na	na	na	na	na	na	0.835	0.234	1.94
Desert/Fales PMU	0.999	0.59	1.641	0.955	0.457	1.387	0.947	0.441	1.361
Fales	0.999	0.59	1.641	0.984	0.539	1.525	0.965	0.544	1.397
Desert Creek	na	na	na	0.939	0.348	1.499	0.938	0.337	1.535
Bodie PMU	1.07	0.76	1.758	1.029	0.74	1.457	1.061	0.783	1.471
Mt. Grant PMU	na	na	na	na	na	na	0.989	0.551	1.536
S. Mono PMU	0.995	0.677	1.421	0.982	0.656	1.4	0.961	0.681	1.344
Sagehen	0.916	0.282	1.964	0.844	0.18	1.819	0.834	0.222	1.658
Long Valley	0.996	0.676	1.427	0.986	0.655	1.433	0.96	0.68	1.361
Parker Meadows	na	na	na	0.968	0.254	7.16	1.048	0.361	5.814
White Mtns PMU	na	na	na	na	na	na	0.85	0.343	1.957
Great Basin	0.99	0.92	1.04	0.97	0.85	1.1	0.94	0.92	0.97

*Subpopulations comprise either PMUs that contain all the leks within boundaries defined by the Nevada Governor's Sage-Grouse Conservation Team (2004) or more localized subpopulations with management interest nested within PMUs.

Within the Bi-State DPS, population cycling is governed by changes in precipitation during the spring, summer, and fall of the previous year (Coates and others, 2018). Specifically, Coates and others (2018) found a 50 percent increase in precipitation between year *k* and *k+1* corresponds to a 15.5 percent growth in $\hat{\lambda}$ during year *k+1*, which leads to an increase in sage-grouse abundance during year *k+2*. Multiple studies have found that annual precipitation is associated with specific demographic rates (Blomberg and others, 2012; Blomberg and others, 2014; Gibson and others, 2017), which are the processes that deterministically influence $\hat{\lambda}$ (Taylor and others, 2012; Dahlgren and others, 2016). For example, relatively high levels of precipitation during the spring growing season provide valuable cover (grasses and forbs), food (forbs and invertebrates), and water resources for chicks by delaying plant senescence and desiccation within upland riparian habitats and surrounding areas (Blomberg and others, 2014).

Conversely, relatively low levels of precipitation have resulted in short-term declines in population abundance (Coates and others, 2018), and such declines can be extreme under drought conditions. One clear example of this phenomenon was the severe drop in $\hat{N}$, and subsequent decrease in $\hat{\lambda}$, during each year of a severe drought between 2012 and 2016. Nevertheless, despite these substantial effects of climatic condition on $\hat{N}$ and $\hat{\lambda}$, trends across longer time frames that encompass multiple population cycles indicate neutrality (that is, long-term stability).

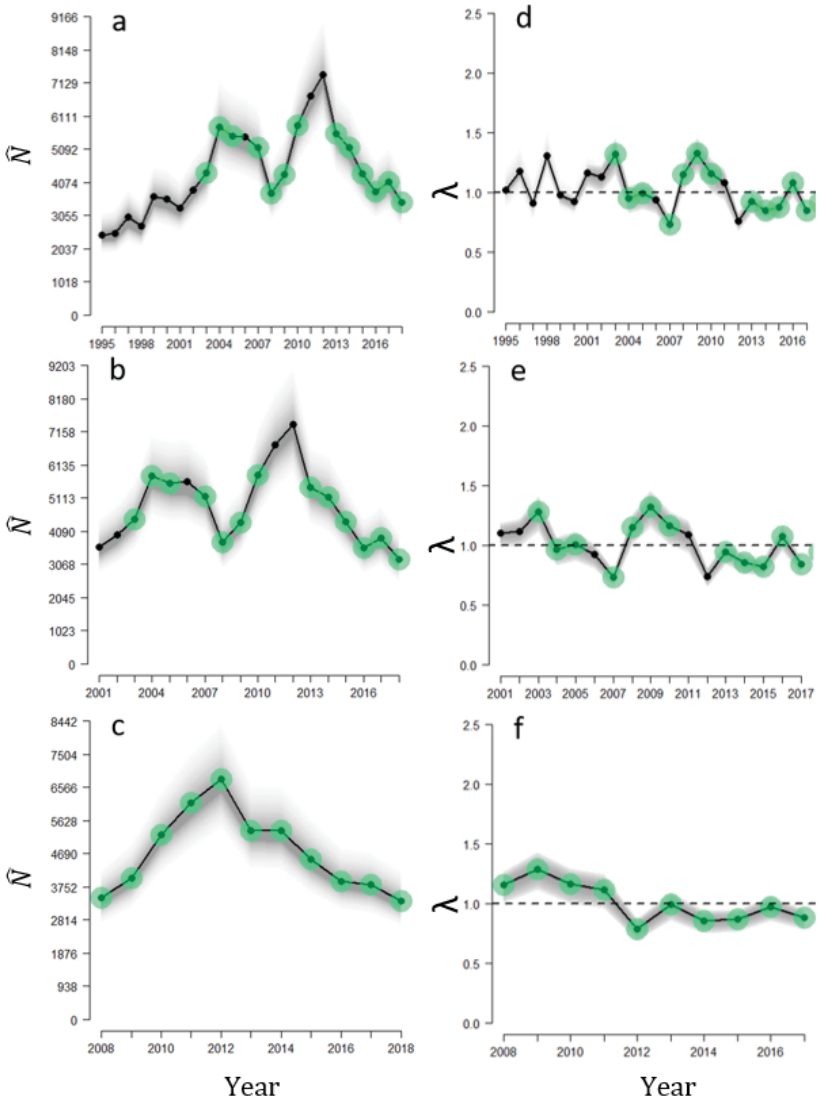

Figure 11. Median (solid lines) and sampled posterior predictions (grey lines) of total population abundance $\hat{N}$ for modeled periods (*A*) 1995–2018, (*B*) 2001–18, and (*C*) 2008–18, which were adjusted for sightability, lek attendance rate, predicted proportion of unknown leks, and sex ratios, as well as the annual rate of change in abundance $\hat{\lambda}$ for respective periods (*D*–*F*) for greater sage-grouse (*Centrocercus urophasianus*) within the Bi-State Distinct Population Segment. Estimates were generated from an integrated population model that consists of lek count observations and demographic rates from telemetry data collected across all subpopulations. Grey lines represent samples from the posterior distribution and green dots represent years of demographic rate estimates for one or more subpopulations.

Trend Comparison Between the Bi-State DPS and Nevada-wide. In comparing trends between the Bi-State DPS and Nevada-wide, we found the Nevada-wide showed stronger evidence of decline across all three time periods, especially the single cycle short-term period (fig. 12). Specifically, the estimated averaged annual $\hat{\lambda}$ (median estimates of the annual posteriors) for the Nevada-wide model was 0.99 (95 percent CRI = 0.92–1.04), 0.97 (95 percent CRI = 0.85–1.10), and 0.94 (95 percent CRI = 0.92–0.97), corresponding to 20.6 percent, 40.4 percent, and 46.1 percent declines across the long- (1995–2018), mid- (2001–18), and short- (2008–18) term periods (fig. 12). Differences in trends, especially during short-term, among the two regions can be explained by three hypotheses, which may not be mutually exclusive. First, subpopulations in Bi-State DPS and Nevada are impacted by changes in climatic conditions, but the Nevada subpopulations appear to consist of more substantial disturbances, resulting in loss and fragmentation of habitat. For example, Nevada populations may be more subjected to the adverse impacts of an accelerated positive feedback loop between wildfire and invasive grasses (Coates and others, 2018), which is rapidly converting sagebrush communities into exotic annual grasslands (Brooks and others, 2004; Chambers and others, 2014). Much of Nevada occurs at lower elevation than the Bi-State DPS, with drier and warmer soils that are more susceptible to increased wildfire frequency and higher probability of megafires, that kill sagebrush and allow for permanent occupation of annual grasses. Conversely, within the Bi-State DPS, sage-grouse habitat consists of cooler and wetter soil profiles at relatively high elevations, resulting in greater levels of resilience following disturbance and resistance to exotic species invasion (Maestas and others, 2016), with exception of the Pine Nut Mountains (see "Inferences for Population Management Units and Subpopulations" section).

A second hypothesis is that differences in trends between Bi-State DPS and Nevada are attributed to differences in the severity of droughts. Drought has been increasing in severity and duration through time within Nevada (Seager and others, 2007; Mensing and others, 2008). However, the Bi-State DPS typically receives more annual precipitation than much of Nevada and, perhaps, this provides a buffer from severe losses in abundance across cyclical nadirs. These two hypotheses of stressor by wildfire and drought are not mutually exclusive. Indeed, a recent study indicates that lack of precipitation and wildfire act multiplicatively to drive long-term declines in sage-grouse populations (Coates and others, 2016d).

A final hypothesis for the observed differences in population trends involves conservation efforts. For example, numerous conservation actions have been carried out in the Bi-State DPS over the past six years with a goal of increasing abundance by providing more sage-grouse habitat. Most conservation actions in the Bi-State DPS were focused on removing conifers using a data-driven conservation planning tool that predicted benefits to sage-grouse populations (Ricca and others, 2018) and expertise from numerous multi-level interagency working groups (Duvall and others, 2017). Conifer removal projects were prioritized because conifer expansion was considered the greatest threat to DPS sage-grouse by the USFWS (U.S. Fish and Wildlife Service, 2013), as trees adversely impact sage-grouse movements (Prochazka and others, 2017), survival of individuals (Coates and others, 2017b), and lek persistence (Baruch-Mordo and others, 2013). Removing conifers from otherwise intact sagebrush communities has increased demographic and population growth rates (Severson and others, 2017). Since 2012, 53,000 acres of conifer encroached sage-grouse habitat has been treated (conifers removed) across the Bi-State DPS (Bi-State Technical Advisory Committee, 2019). It is possible that removal activities have provided a lift in population performance that might offset negative impacts of drought within the Bi-State DPS.

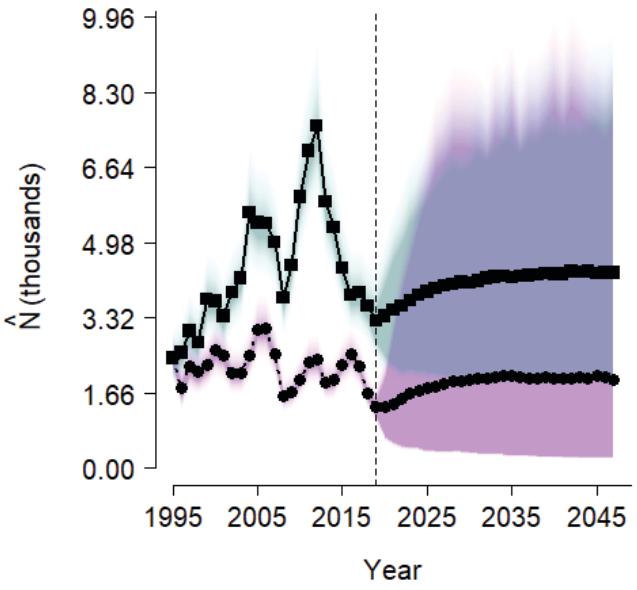

Figure 12. Median values of total abundance ($\hat{N}$) of Bi-State Distinct Population Segment (DPS; denoted as squares) with sampled posteriors (cyan) and 11 subpopulations from the Great Basin (denoted as circles) with sampled posteriors (purple). Dashed vertical line reflects 2018 as the year of final data collection, so modeled predictions are illustrated to the right of line. Initial abundance for the Great Basin was set at Bi-State DPS estimated $\hat{N}$ for comparative purposes in trends and 10-year predictions. Estimates were generated from an integrated population model that consists of lek count observations and demographic rates from telemetry data collected across all measured subpopulations.

Synthesis With Other Bi-State DPS Population Studies. Although substantially different in methodology, our results were consistent with range-wide analyses that employed population reconstruction approaches (Garton and others, 2011, 2015), which concluded that two Bi-State subpopulations (Bodie Hills and Long Valley) had low to moderate probabilities of falling below effective population sizes over the next 30 and 100 years. Garton and others (2015) reported that Bodie Hills subpopulation exhibited evidence of increases through time, similar to our findings. A mixed-effects model analysis of trends between 1965 and 2008 by the Sage and Columbian Sharp-Tailed Grouse Technical Committee (2008) also reached similar conclusions using these two subpopulations. Our modeling effort using IPMs expanded on these two earlier approaches in multiple ways. First, we included additional recent years of data. This allows for further investigation of years following a severe drought on longer term trend patterns. Second, the IPM approach integrated demographic data collected directly from tracking sage-grouse with telemetry over a 16-year period, as well as lek count data dating back to 1995. Unifying these datasets allowed for a more thorough investigation of $\hat{N}$ and $\hat{\lambda}$, as well as the demographic rates (that is, processes) that drive such patterns. Third, other statistical analyses were limited to Bodie Hills and Long Valley subpopulations, whereas our analysis comprised all subpopulations, which provides better spatial representation of the Bi-State DPS and facilitates a thorough investigation of spatiotemporal variation in $\hat{\lambda}$ and demographic rates across the Bi-State DPS. Lastly, the other approaches used population reconstruction and mixed effects models that relied solely on lek count data, whereas the IPM incorporated demographic data from telemetry methods to refine estimates of $\hat{N}$ and $\hat{\lambda}$. Nevertheless, all studies independently demonstrate consistent patterns in trends through time.

The trends and demographic estimates reported here are also consistent with previous IPM analyses carried out in the Bi-State DPS. For example, the initial reported average annual $\hat{\lambda}$ was 1.00 (95 percent CRI = 0.88–1.41) with similar substantial spatiotemporal variation in $\hat{\lambda}$ and demographic rates between years 2002–12 (Coates and others, 2014b). This analysis encompassed one full population cycle, such that the beginning and ending years of study represented two adjacent apexes (that is, peak to peak). Thus, although limited to a single cycle for inference, the inferences of long-term trends were not influenced by sensitivity to start and end years across a cycling population. However, a second published IPM model for the DPS concluded that average annual $\hat{\lambda}$ was 0.98 (95 percent CRI = 0.69–1.25) across 2002–15, and the authors attributed a sharp decline from 2012 to 2015 to severe drought (Coates and others, 2018). A similar average annual $\hat{\lambda}$ of 0.98 was reported in Mathews and others (2018) representing trends across 2002–17. However, average annual $\hat{\lambda}$ reported in Coates and others (2018) and Mathews and others (2018) could not be interpreted to represent true long-term trends because they were not corrected for cyclical patterns and time scales. For example, both studies begin at a population size apex (that is, 2001) and end at the nadir (that is, 2015 and 2017, respectively). Thus, both studies have greater temporal representation of declining years than increasing years, simply based on beginning and ending years within a cycling population. Importantly, estimates from the Coates and others (2014b) study that helped inform the 2015 listing decision of not warranted (U.S. Fish and Wildlife Service, 2015) did not overlap periods of extreme drought that occurred subsequently, for which we now have evidence of driving sage-grouse population cyclicity in the Bi-State DPS (Coates and others, 2018) and Great Basin (Coates and others, 2016d).

Here, we expanded on these previous IPM analyses with the goal of correcting for cyclicity to better estimate long-term trends. First, adjusting the beginning and ending dates of analysis to correspond to points of nadir removed potential misleading trends otherwise associated with start and end years in previous analyses. Second, we estimated average annual $\hat{\lambda}$ across three, two, and one full population cycles; this provides more temporal representation in properly inferencing annual average $\hat{\lambda}$. Previous versions of the IPM relied on a count index, which consisted of averaged annual lek counts across subpopulations (Coates and others, 2014b; Coates and others, 2018; Mathews and others, 2018). Averaging techniques could be prone to biases associated with removal of inactive leks through time, which tends to increase averages as leks are removed. With recent advances in IPM analyses, our third improvement was employing a multi-lek–multi-site analysis, which allowed for estimation of $\hat{N}$ and a derived $\hat{\lambda}$ for every lek, removing potential biases associated with averaging. Fourth, although previous versions of the IPM had good spatial representation, they did not incorporate lek and demographic data from all subpopulations based on data collection limitations. With more field efforts in data collection and QA/QC improvements on historic lek counts, all subpopulations were represented in this version to estimate $\hat{N}$ (fig. 13) and derive $\hat{\lambda}$ (fig. 14) across the Bi-State DPS. Lastly, using estimates and variances of factors that influence observation error, such as sightability, lek attendance, unknown leks, and sex ratios, we provide estimates of true abundance, $\hat{N}_{total}$, rather than an apparent abundance that was otherwise biased low.

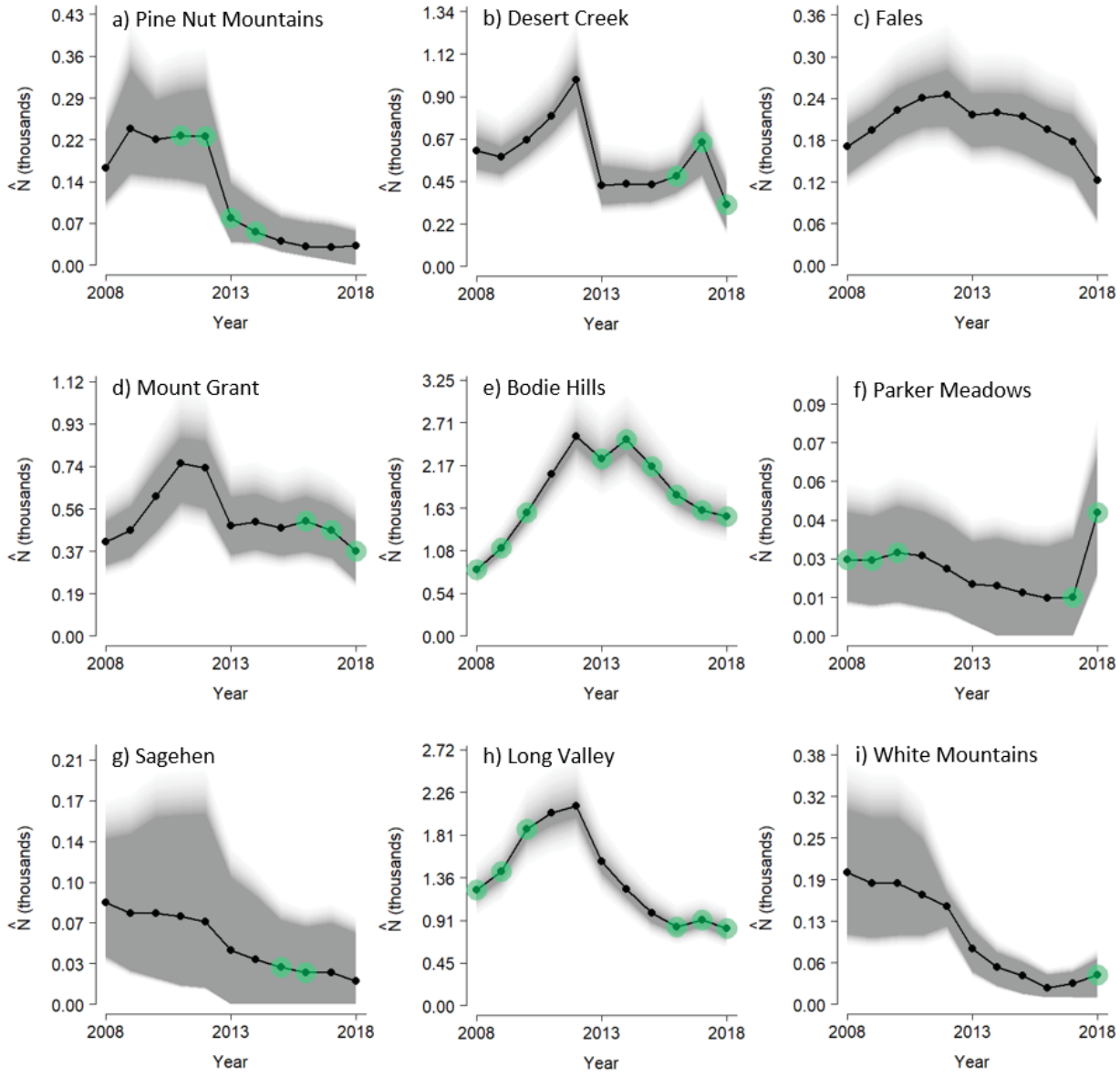

Figure 13. Median (solid lines) and sampled posterior predictions (grey lines) of $\hat{N}$, adjusted for sightability, lek attendance rate, predicted proportion of unknown leks, and sex ratios for greater sage-grouse (*Centrocercus urophasianus*) within the Bi-State Distinct Population Segment. Estimates were generated from an integrated population model that consists of lek count observations and demographic rates from telemetry data collected across all subpopulations. Green dots represent years of demographic rate estimates for each subpopulation.

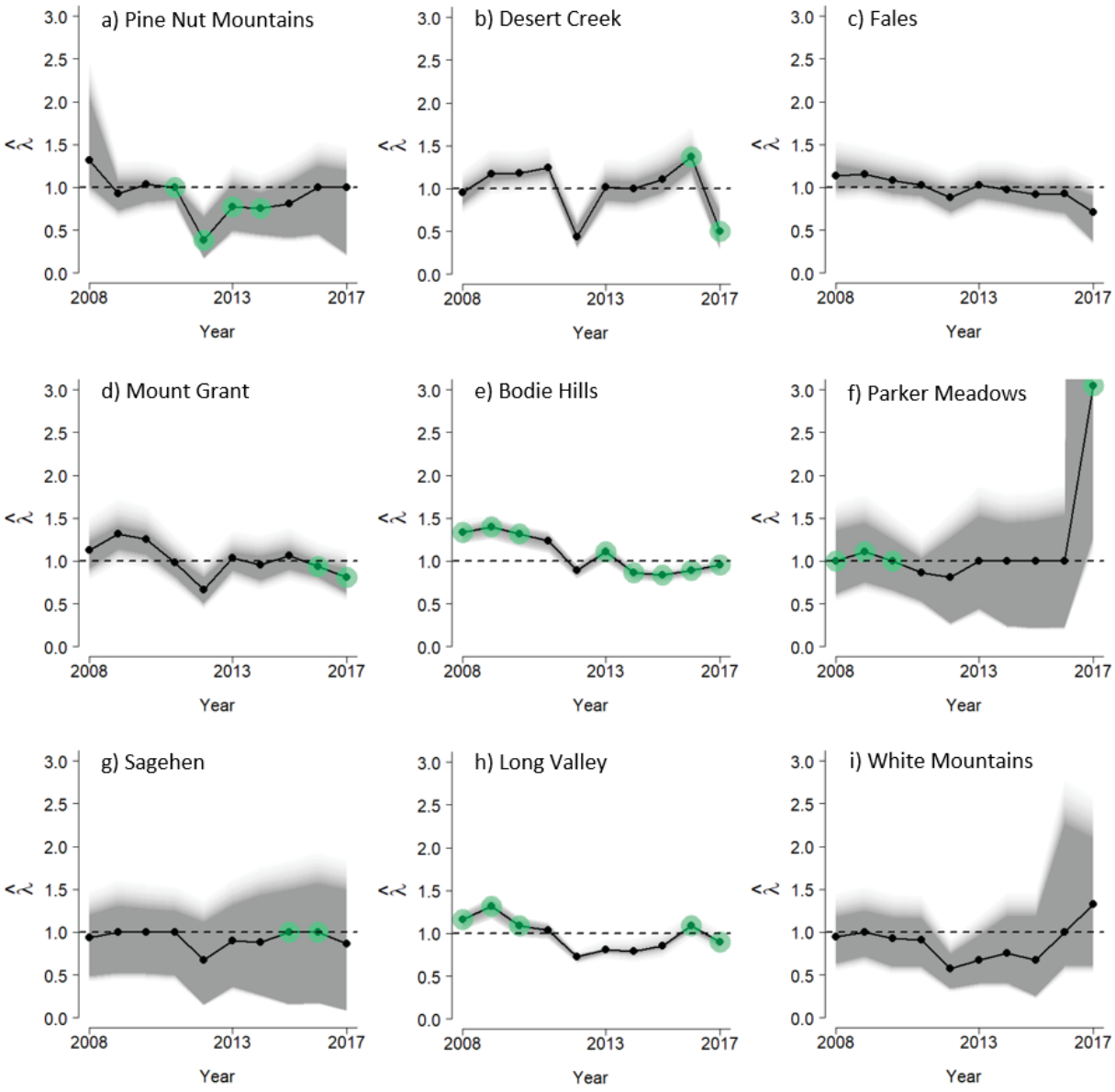

Figure 14. Median (solid lines) and sampled posterior predictions (grey lines) of $\hat{\lambda}$ (finite rate of annual change in $\hat{N}$) for greater sage-grouse (*Centrocercus urophasianus*) within the Bi-State Distinct Population Segment. Estimates were derived from an integrated population model that consists of lek count observations and demographic rates from telemetry data collected across all subpopulations. Green dots represent years of demographic rate estimates for each subpopulation.

Inferences for Population Management Units and Subpopulations

Pine Nut Subpopulation. We estimated a median $\hat{N}_{total}$ (following application of adjustment factors on $\hat{N}_{apparent}$) of 33 sage-grouse (95 percent CRI = 0–73) for the Pine Nut subpopulation as of spring 2018 (table 1; fig. 13*A*). Since 2008, we estimated average annual $\hat{\lambda}$ at 0.84 (95 percent CRI = 0.23–1.94), which was considerably lower than averaged $\hat{\lambda}$ across the Bi-State DPS for the same period (table 3; fig. 14*A*). Sage-grouse numbers were reduced by approximately 82.5 percent over the past 11 years, given the median prediction value. The 10-year extirpation probability was relatively high at 69.7 percent (table 1). Sparse lek counts for the Pine Nut subpopulation prior to 2008 did not yield sufficient data to calculate $\hat{N}$ and derive $\hat{\lambda}$ during the periods of 1995–2018 and 2001–18.

Several factors likely contribute to declining sage-grouse populations in the Pine Nuts during the last population cycle. First, although the Pine Nuts occur at relatively higher elevations, the site is also characterized by considerably warmer and drier soils compared to other areas within the Bi-State DPS. These soil regimes correlate with low resilience to disturbance and resistance to invasion by exotic plant communities (Chambers and others, 2014, 2017; Maestes and others, 2016). The Pine Nuts also endure an increased rain shadow effect from the Sierra Nevada mountain range compared to other subpopulations in the Bi-State DPS, and more closely align ecologically with environmental conditions experienced by sage-grouse populations in northeastern California and northwestern Nevada, than those further south in the Bi-State DPS. Collectively, these factors could exacerbate limitations on primary productivity by severe drought conditions beginning in 2012 during the last population cycle. Increased precipitation is associated with increased λ (Coates and others, 2018) by boosting primary productivity and slowing plant desiccation, which is important to provide habitat for nesting (Coates and others, 2018) and brood-rearing (Blomberg and others, 2014) sage-grouse during spring, summer, and fall months.

Second, sage-grouse occupy upper elevation sagebrush areas in the Pine Nut Mountains and rely on sporadic and temporally intermittent upland wet meadow springs that provide critical brood-rearing habitat (Coates and others, 2016a). Feral horses also heavily rely on these same types of habitats during similar times as sage-grouse (Perry and others, 2015; Kaweck and others, 2018) and can significantly impact the ecological functioning of these areas as brood-rearing habitat (Beever and Aldridge, 2011) through increased cover of bare ground (Boyd and others, 2017), soil compaction (Beever and Herrick, 2006), and exotic plant cover (Beever and others, 2008), and reduced vegetation height (Beever and Brussard, 2000). Notably, feral horse populations inhabiting the Pine Nut Mountains have increased substantially over the last sage-grouse population cycle and reached numbers at least 433 percent higher than those established as an Appropriate Management Level (Bureau of Land Management, 2018). Impacts of overly abundant feral horses on population growth of the Pine Nut subpopulation of sage-grouse warrants further investigation.

Lastly, the Pine Nuts experienced an abnormally large wildfire, known as the Bison fire, that burned 9,559 ha, including 4,559 ha within high priority sage-grouse habitat. Wildfires are known to have immediate adverse impacts to sage-grouse populations (Coates and others, 2016d). Although the Pine Nuts experienced some drought relief with pulses of late spring and summer precipitation in years since 2015, long-term impacts of wildfire have been shown to nullify any positive effects associated with precipitation (Coates and others, 2016d), which essentially mimics a continual drought effect.

Collectively, since 2012, these three stressors (drought, wildfire, and feral horses) likely limited important habitat for sage-grouse reproduction. Our telemetry data further indicate that many VHF- and GPS-marked sage-grouse made unusual long-distant movements out of the Pine Nuts between 2013 and 2015 (peak of drought) and established new home ranges within the Bodie Hills subpopulation (Coates and others, 2016a). The Pine Nut subpopulation represents approximately one percent of sage-grouse numbers within the Bi-State DPS (table 1), as a whole, so changes in $\hat{N}_{total}$ at this subpopulation has negligible impacts on average annual $\hat{\lambda}$ for the Bi-State DPS. However, local extirpation can be more meaningful to loss of occupied habitat and distribution within the Bi-State DPS (see "Seasonal and Life History Stage Habitat Mapping" section for percentage of habitat by each subpopulation). Furthermore, subpopulation losses may also reduce overall genetic diversity (Oyler-McCance and others, 2014) and gene flow for subpopulations that benefit from some level of connectivity.

Desert Creek/Fales Subpopulations. We estimated a median $\hat{N}_{total}$ (following application of adjustment factors on $\hat{N}_{apparent}$) of 447 sage-grouse (95 percent CRI = 218–750) for the Desert Creek and Fales combined subpopulations as of spring 2018 (table 1; figs. 13*B*, *C*). The 10-year extirpation probability was relatively low at 9.0 percent (table 1). Lek counts were only sufficient for estimation of λ across the long-term period for Fales, where a median annual $\hat{\lambda}$ of 0.99 (95 percent CRI = 0.68–1.42; table 3; figs. 14*B*, *C*) was estimated since 1995. This annual $\hat{\lambda}$ value indicated that $\hat{N}_{total}$ during 2018 was nearly equivalent to numbers 24 years prior. However, the combined Desert Creek and Fales subpopulation has been declining 4.5 percent annually over the past 18 years beginning in 2001 (table 3).

For the Desert Creek subpopulation alone, we estimated a median $\hat{N}_{total}$ (following application of adjustment factors on $\hat{N}_{apparent}$) of 325 sage-grouse (95 percent CRI = 163–542;) as of spring 2018 (table 1; fig. 13*B*). The 10-year extirpation probability was moderate at 23.4 percent (table 1). Estimates of median annual $\hat{\lambda}$ indicated approximate equivalent 6.2 percent rates of annual decline over mid- and short-term time periods beginning in 2001 and 2008, respectively (table 3; fig. 14*B*). In comparison to the nearest subpopulation to the south (that is, Mount Grant; fig. 1), sage-grouse at Desert Creek exhibit slightly lower demographic rates, resulting in lower estimates of recruitment. Sage-grouse are confined largely to drier and lower elevation environments in Desert Creek, where they are more vulnerable to common ravens (*Corvus corax*) associated with lower elevations and agricultural activities within sagebrush landscapes (O'Neil and others, 2018). Sage-grouse eggs are considered an important food source for ravens (Coates and Delehanty, 2010; Lockyer and others, 2013), and we documented sage-grouse nesting near the periphery of agriculture fields near Wellington, Nevada. Although we did not find evidence of variation in nest survival among subpopulations and constrained this parameter across the Bi-State DPS, further investigations into nest survival for this subpopulation would be beneficial. Ravens are also thought to consume relatively small birds (Boarman and Heinrich, 1999), which may pose an additional risk during brood rearing that may adversely impact chick survival rates.

For the Fales subpopulation alone, we estimated a median $\hat{N}_{total}$ (following application of adjustment factors on $\hat{N}_{apparent}$) of 121 sage-grouse (95 percent CRI = 54–208) as of spring of 2018 (table 1; fig. 13*C*). The 10-year extirpation probability was moderate, though higher than Desert Creek, at 38.4 percent (table 1). Sage-grouse populations declined most strongly at 3.5 percent annually during the short-term period of 2008–18 (table 3) that coincided with recent drought. The sharpest decline in abundance also occurred between 2017 and 2018 (fig. 13*C*), which could be attributed to a substantially lower adult (median; 59.5 percent) and yearling (median; 59.0 percent) survival than previous years (appendix 5). Fales recently experienced a substantial wildfire and, similar to the Pine Nut subpopulation, impacts of wildfire coupled with drought likely adversely impacted population demographic rates resulting in recent declines.

Mount Grant Subpopulation. We estimated a median $\hat{N}_{total}$ (following application of adjustment factors on $\hat{N}_{apparent}$) of 374 sage-grouse (95 percent CRI = 205–619) for the Mount Grant subpopulation as of spring 2008 (table 1; fig. 13*D*). The 10-year extirpation probability was moderate at 24.6 percent (table 1). Sparse lek counts did not yield sufficient data to calculate $\hat{N}$ and derive $\hat{\lambda}$ during the long and mid-term periods of 1995–2018 and 2001–18, respectively. Since 2008, the median annual $\hat{\lambda}$ was 0.99 (95 percent CRI = 0.55–1.54; table 3; fig. 14*D*) meaning the subpopulation growth rate was close to neutrality. Mount Grant might be buffered from drought effects affecting other subpopulations within the Bi-State DPS during the short-term period of 2008–18 because it is situated at higher and cooler elevations. These areas typically have higher productivity based on cooler and wetter soil profiles (Chambers and others, 2014) that likely contribute to relatively higher recruitment rates compared to other subpopulations. Sage-grouse at Mount Grant also occur in areas with seemingly fewer anthropogenic disturbances compared to other subpopulations. Also, we documented some movements of sage-grouse between Mount Grant and Bodie Hills subpopulations, and immigration from Bodie Hills could potentially buffer against population declines at Mount Grant during years of drought.

Bodie Hills Subpopulation. We estimated a median $\hat{N}_{total}$ (following application of adjustment factors on $\hat{N}_{apparent}$) of 1,521 sage-grouse (95 percent CRI = 1,181–1,941) for the Bodie Hills subpopulation as of spring 2008 (table 1; fig. 13*E*). Robust lek count data allowed estimation across all three time periods. Although this population experiences cycling (fig. 13*E*), all time periods of analysis demonstrate consistent population growth. Since 1995, average annual $\hat{\lambda}$ was 1.07 (95 percent CRI = 0.76–1.76; table 3; fig. 14*E*), meaning sage-grouse numbers as of 2018 were approximately four times higher than during the nadir 24 years ago. Population growth slowed somewhat, but remained positive, during the mid- and short-term periods of 2001–18 and 2008–18, respectively. Importantly, Bodie Hills represents nearly half (46.0 percent) of all sage-grouse within the Bi-State DPS and has a very low 10-year extirpation probability of 2.4 percent (table 1). Like Mount Grant, sage-grouse in Bodie Hills occur at relatively high elevations compared with other populations of the Bi-State DPS, and the Bodie Hills subpopulation receives higher amounts of annual precipitation compared to other subpopulations. These conditions likely act to help buffer the subpopulation against drought and subsequent population declines (Coates and others, 2018). For example, following the onset of severe drought in 2012, Bodie Hills was the only subpopulation that did not immediately decline but instead maintained relatively high numbers of sage-grouse for approximately 3 years into drought (fig. 13*E*). Similar

patterns of offsetting declines between Bodie Hills and other subpopulations in relation to reduced precipitation were observed. Additionally, telemetered sage-grouse from the Pine Nut subpopulation permanently moved to Bodie Hills during harsh drought conditions following 2012 (Coates and others, 2016a), possibly contributing to a lag in population decline during drought years. In addition, high elevation areas in Bodie Hills (like Mount Grant) are dominated by cool, moist soils that stimulate enhanced productivity and are correlated with high resilience to disturbance and resistance to invasion (Chambers and others, 2014). Thus, subpopulations inhabiting these types of environments are more likely to recover from large-scale disturbances, such as drought, faster than other subpopulations within the Bi-State DPS. As a result of these ecological conditions, Bodie Hills also consists of relatively large amounts of upland riparian springs and meadows that provide the greatest amount of late brood-rearing habitat in the Bi-State DPS (see "Seasonal and Life History Stage Mapping" section), which likely explains the highest recruitment rate among all subpopulations (appendix 5). Because the Bodie Hills subpopulation accounts for the bulk of population abundance across the entire Bi-State DPS (table 1), trends in its abundance substantially influence overall trends across the Bi-State DPS. It follows that any major disturbance to this subpopulation will likely have substantial impacts on population estimates for the entire Bi-State DPS.

South Mono Subpopulations. We estimated a median $\hat{N}_{total}$ (following application of adjustment factors on $\hat{N}_{apparent}$) of 885 sage-grouse (95 percent CRI = 1,181–1,941) for South Mono subpopulations combined as of spring 2018 (table 1; figs. 13*F–H*). Like Bodie Hills, the 10-year extirpation probability was low at 3.8 percent (table 1). The long-term period estimate of annual $\hat{\lambda}$ (median = 1.0; table 3; figs. 14*F–H*) predicted that median estimates of $\hat{N}_{total}$ for 2018 would be nearly identical to those during the nadir of 1995. However, sage-grouse have experienced annual declines of 1.8 and 3.9 percent since the nadirs of 2001 and 2008, respectively (table 3; figs. 14*F–H*).

The primary subpopulation in this region is Long Valley, which consists of 92.4 percent of the $\hat{N}_{total}$ across all South Mono subpopulations as of spring 2018 (table 1). Reflecting the trend for all South Mono subpopulations combined, the long-term period estimate of annual $\hat{\lambda}$ (median = 1.0; table 3; fig. 14*H*) indicate that sage-grouse numbers at Long Valley are nearly identical to those during the 1995 nadir. However, the subpopulation at Long Valley was historically the largest within the Bi-State DPS (Coates and others, 2018), but it has undergone substantial reductions in recent years that mirror trends across South Mono subpopulations combined (table 3). As of spring 2018, the Long Valley subpopulation now represents 24.8 percent of all sage-grouse within the Bi-State DPS (table 1). Because of its still large size, population changes at Long Valley have relatively large impacts on the overall Bi-State DPS trends. Substantial subpopulation declines over mid- and short-term periods for Long Valley (fig. 13*H*) may be related to drought effects on sage-grouse reproduction. For example, from 2008 to 2011 (that is, pre-drought), sage-grouse average recruitment was relatively high at approximately 0.43 for adults and 0.48 for yearlings, but was reduced to 0.27 for adults and 0.33 for yearlings following the onset of drought. Sage-grouse in Long Valley also encounter multiple hazards that potentially act as additive causes for recent population declines. First, our telemetry data indicate that sage-grouse broods were often located in large wet meadows and riparian habitat surrounding Lake Crowley and associated irrigated pastures. Sage-grouse are likely more vulnerable to predation due to a lack of overhead cover in the interior of meadows, which can become exacerbated as sage-grouse move further to the interior of meadows and pastures during periods of drought and concomitant changes to irrigation regimes (see "Objective 6. Effects of Precipitation and Managed Water Delivery on Brood Habitat" section). Second, Long Valley has an active, open landfill (Benton Crossing Landfill) located approximately 6.5 km from the largest lek in the population (that is, Lek 2), and 3.4 km from a historically large lek (that is, Lek 8), which likely provides resource subsidies for generalist predators, such as ravens (O'Neil and others, 2018). Finally, anthropogenic disturbances to sage-grouse are high at Long Valley compared to the other subpopulations of the Bi-State DPS. Although the effect of outdoor recreation pressure on sage-grouse has not been quantified, field crews have documented several nests less than 10 m from well-traveled roads and have documented domestic dogs and camp sites near active nests. Although we have no data on historical use of the area by people, we hypothesize that use of Long Valley for recreational activities, like visiting local hot springs and fishing, has increased during the study period.

We estimated a median $\hat{N}_{total}$ (following application of adjustment factors on $\hat{N}_{apparent}$) of 48 sage-grouse (95 percent CRI = 21–86) for the Parker Meadows subpopulation as of spring 2018 (table 1; fig. 13*F*), which accounts for approximately 1.4 percent of all sage-grouse across the Bi-State DPS. The 10-year extirpation probability was high at 64.3 percent (table 1). Sparse lek counts did not yield sufficient data to calculate $\hat{N}$ and derive $\hat{\lambda}$ during the long-term period of 1995–2018. For mid-term period, the estimated median annual $\hat{\lambda}$ of approximately 0.97 (table 3; fig. 14*F*) indicated 42.5 percent reduction in population numbers since 2001–18. Sage-grouse at Parker Meadows have exhibited lower recruitment through past years than other subpopulations (Coates and others, 2014b). The lower recruitment can be explained by the low rates of egg hatchability for adults, which likely stemmed from an observed high percentage of infertile eggs. Following identification of this problem, State and Federal agencies initiated a genetic rescue via translocation of males, females, and broods from the Bodie Hills subpopulation in 2017 that has continued through 2019 (translocation methodologies explained by Mathews and others, 2018). Following translocations, field crews documented large native broods (that is, broods from non-translocated females) in Parker Meadows, possibly indicating an increase in fertilization rates of eggs within nests. Accounting for this translocation effect in the IPM resulted in a 59.8 percent increase in population abundance over the short-term period (2008–18; table 3, fig. 14*F*). Furthermore, observed lek counts in 2018 were higher than pre-translocation lek counts and many translocated females have apparently joined the local population at Parker Meadows and reproduced successfully. Additionally, sage-grouse survival rate was much higher (median was 0.78 and 0.77 for adults and yearlings, respectively; appendix 5) before the onset of the drought (that is, 2008–11) than during years following the drought (that is, 2012–18; median was 0.63 and 0.64 for adults and yearlings, respectively; appendix 5). Although probability of subpopulation extirpation remains high, it may decrease following population gains from translocation and recent above-average precipitation, especially from novel brood-translocation techniques, which initially appear successful (Mathews and others, 2018).

We estimated a median $\hat{N}_{total}$ (following application of adjustment factors on $\hat{N}_{apparent}$) of 20 sage-grouse (95 percent CRI = 0–75) for the Sagehen subpopulation as of spring 2018 (table 1; fig. 13*G*). Sagehen has experienced increasingly strong population declines across all three time periods, beginning with an 8.4 percent median annual decline since 1995 and a 16.6 percent median annual decline since 2008 (table 3). These values equate to 86.7 and 83.7 percent reduction in abundance over the course of 24 and 11 years, respectively. Similar to Parker Meadows, average annual survival rates have declined following the onset of the 2012 drought—from approximately 0.72 and 0.73 to 0.61 and 0.61 for adults and yearlings, respectively (appendix 5).

White Mountains Subpopulation. We estimated a median $\hat{N}_{total}$ (following application of adjustment factors on $\hat{N}_{apparent}$) of 45 sage-grouse (95 percent CRI = 9–86) for the White Mountains subpopulation as of spring 2018 (table 1; fig. 13*I*). We estimated median annual $\hat{\lambda}$ at 0.85 (95 percent CRI = 0.34–1.96; table 3; fig. 14) over the past 11 years. Limitations in historic lek count data precluded estimated abundance across other nadir to nadir periods. Predicted abundances of 2018 should be interpreted with caution. Sage-grouse in the White Mountains were relatively understudied, largely because these sage-grouse reside at high elevations that are often inaccessible until mid-summer. The subpopulation represents the most southwestern, and potentially highest elevation occupancy of greater sage-grouse across the species range, representing a unique and potentially extreme study site. Thus, the predicted number of unknown leks is likely much higher than elsewhere in the DPS because of substantially less effort and success at locating leks within the White Mountains. Limitations in time-series data for known leks also resulted in omission of some leks to guard against erroneous trends. Thus, we suspect that the model underrepresented true abundance. We began monitoring of the White Mountains subpopulation in 2018, and data collection from 2019 and potentially in future years will help describe population parameters of this under-studied population. Notably, we discovered a new lek on the California side of the White Mountains in 2018 (that is, Iron Mountain lek).

Objective 2. Hierarchical Signal Analysis

When the signal evaluation process was applied to sage-grouse populations in the Bi-State DPS as of 2018, soft signals activated for two leks in the South Mono combined subpopulation (that is, Sagehen and Long Valley subpopulations) and one lek in Fales subpopulation (fig. 15, table 4). Soft signals did not activate for leks in the Pine Nut, Bodie Hills, Mount Grant, and White Mountain subpopulations. As of 2018, hard signals activated at one lek in the Bodie Hills subpopulation, two leks in the Mount Grant subpopulation, and one lek in the Long Valley subpopulation (fig. 15, table 4). Population decline was most severe for soft and hard signaling leks in the Long Valley subpopulation. Under our selected temporal threshold (that is, 3 out of 4 consecutive years of activated slow warnings or 2 out of 3 consecutive years of activated fast warnings), most (3 out of 4) hard signals activated at either large- or medium-sized leks (2008–18 average: lek size range = 10–26). Survey effort was consistent across all signaled leks, with the exception of those at Mount Grant that typically comprised a single aerial count per year. Hence, these signals could be confounded by variation in lek attendance and not actual changes in population abundance (Wann and others, 2019), which was not fully accounted for in modeled observation error.

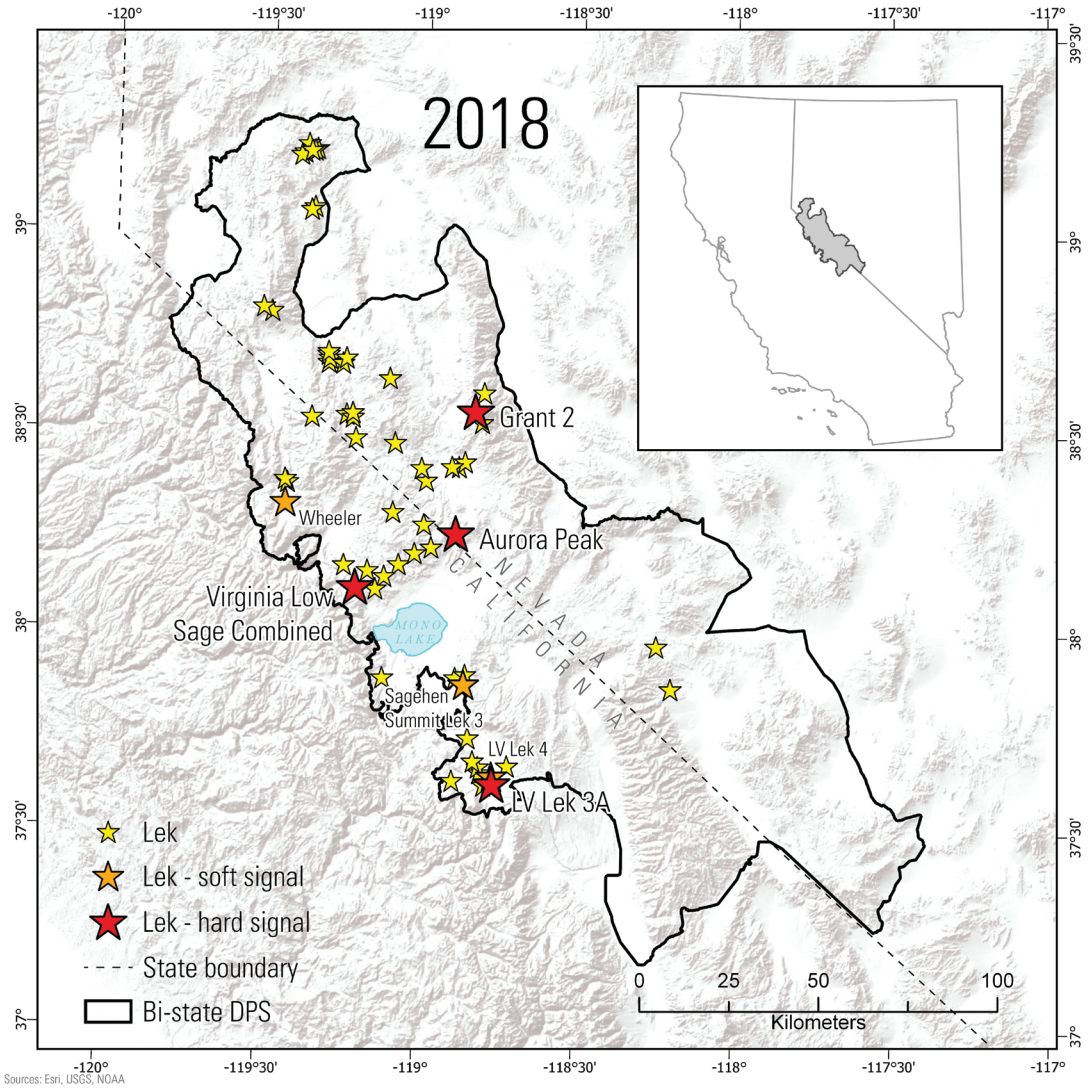

Figure 15. Results of population signals, which reflect evidence of lek level decline in $\hat{\lambda}$ and decoupling of $\hat{\lambda}$ from regional trend (all leks combined), for greater sage-grouse (*Centrocercus urophasianus*) leks within the Bi-State Distinct Population Segment during 2018.

Table 4. List of leks with population signals (soft and hard), which reflect evidence of lek level decline in $\hat{\lambda}$ and decoupling of $\hat{\lambda}$ from regional trend (all leks combined), for greater sage-grouse (*Centrocercus urophasianus*) leks within the Bi-State Distinct Population Segment during 2018.

[State-space model derived estimates of λ from 2015 to 2018 are provided for comparison]

Subpopulation	Lek	Signal	$\hat{\lambda}$
Fales	Wheeler	soft	0.83
Bodie Hills	Virginia/Little Sagebrush	hard	0.89
Mount Grant	Grant 2	hard	0.65
Mount Grant	Aurora Peak	hard	0.86
Sagehen	Sagehen Summit Lek 3	soft	0.61
Long Valley	LV Lek 3A	hard	0.67
Long Valley	LV Lek 4	soft	0.69

Objective 3. Seasonal and Life History Stage Habitat Mapping

Variable Screening

We considered 99 candidate predictors for spring, summer–fall, and winter resource RSFs, 116 candidate predictors for nest RSFs, and 96 candidate predictors for early and late brood RSFs. Nest RSFs had more candidate predictors due to the inclusion of the additional neighborhood size (radius = 75 m). Preliminary variable screening methods and model selection reduced the number of covariates included in any model to ≤ 19. Results of variable importance rankings from preliminary variable screening are available in appendix 6.

Summary of RSF Results by Season

Final RSF Models & Validation. The final RSF models of seasonal habitat selection based on telemetry locations included 15, 19, and 14 covariates for spring, summer–fall, and winter, respectively. Covariates largely explained sage-grouse habitat selection patterns in terms of selection for sagebrush vegetation communities with ample understory herbaceous cover, avoidance of coniferous tree and shrub cover (that is, pinyon-juniper), varying seasonal selection for landscape features indicating water and moisture availability (for example, perennial and intermittent streams, springs, water bodies), selection for intermediate topographic features (for example, typically moderate slopes, curvature, and topographic roughness), and avoidance of potential hazards associated with irrigation ditches or canals.

The results of the sensitivity analysis indicated that pinyon-juniper cover, topography characteristics, sagebrush height (which was correlated with sagebrush cover), and proximity to man-made ditches or canals had the strongest and most consistent influences on sage-grouse selection across seasons and life stages. Pinyon-juniper consistently had strong negative effects on selection (*d*HSI less than –0.60 across all seasons, life stages; fig. 16), while sagebrush height consistently had strong positive effects (*d*HSI greater than 0.35 across all seasons, life stages; fig. 16). Sage-grouse strongly avoided areas within 5 km of man-made ditches and canals (*d*HSI less than –0.25 across all seasons, life stages; fig. 16). However, this effect was based on NHD data where smaller irrigation ditches were not included (see "Objective 6. Effects of Precipitation and Managed Water Delivery on Brood Habitat" section), and thus likely represents avoidance of larger-scale diversions and agricultural operations. Topographic variables effects were more nuanced because they were non-linear effects in most models but had strong influence when included (fig. 16). In general, very high slope and roughness values were avoided, while greater curvature values were selected. Taken in combination, topographic characteristics generally indicate selection for relatively gentle slopes at intermediate elevations, where surface curvature tends toward upward concavity (Bolstad and Lillesand, 1992).

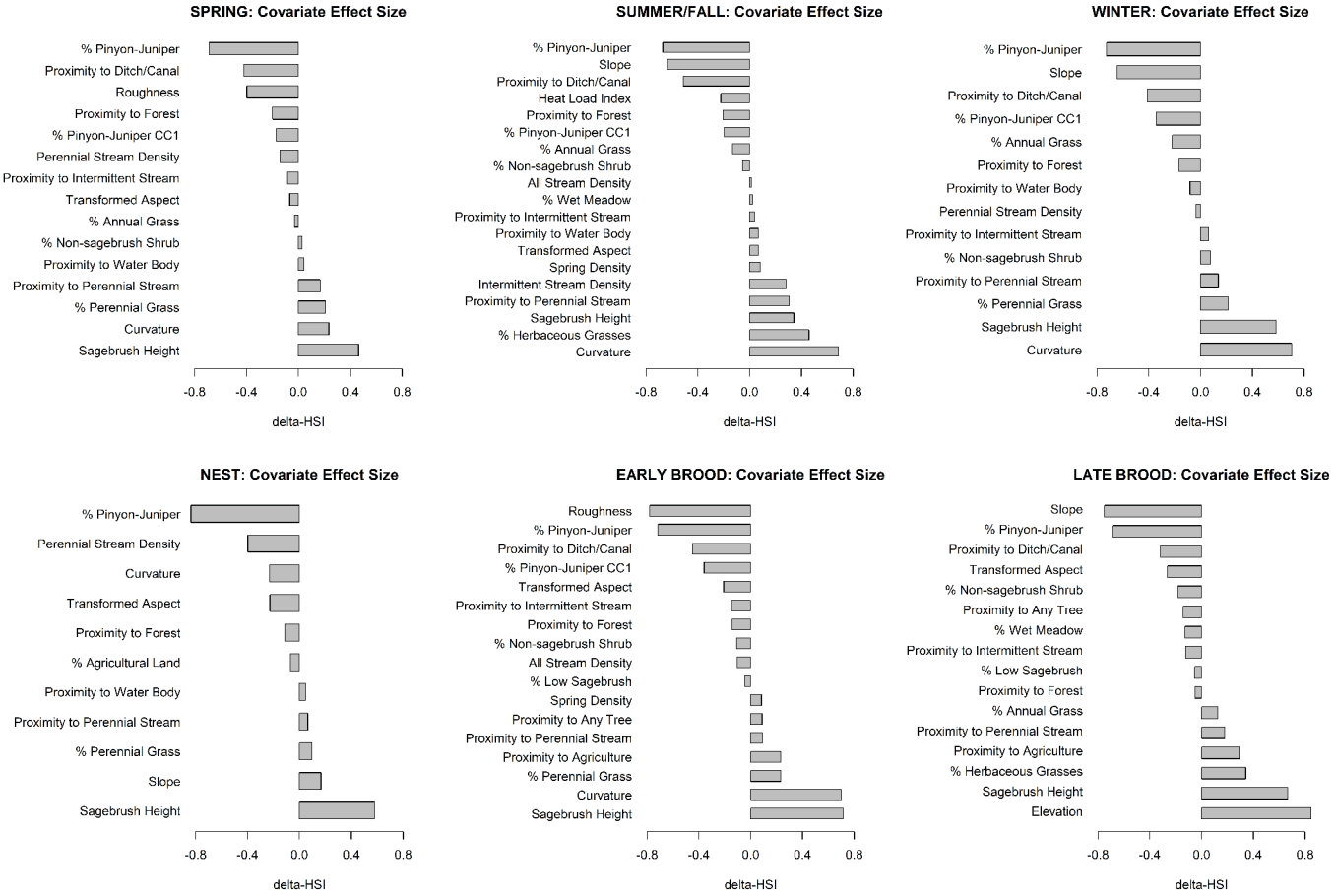

Figure 16. Sensitivity analysis of relative influence of covariates on habitat selection index of seasonal (spring, summer–fall, winter) and reproductive life stage specific (nest, early brood, late brood) resource selection functions of greater sage-grouse (*Centrocercus urophasianus*) within the Bi-State Distinct Population Segment.

We used RSF validation techniques (Johnson and others, 2006; Fieberg and others, 2018) to assess the final RSF model fit to the data for all seasons and life stages. Model fit was strong for each model, with Spearman's rank coefficient at least 0.95 and R^2 (observed versus predicted) at least 0.91, indicating consistent agreement between the number of locations predicted across 10 binned habitat classes of increasing RSF value and the number of actual locations observed in the data used to build the model (table 5).

Sagebrush Communities: Selection for sagebrush vegetation communities was primarily explained by sagebrush height. Sagebrush height was also highly correlated with other shrubland indicators, such as percent sagebrush, percent big sagebrush, and percent overall shrub cover. Sagebrush height was consistently the best predictor of sage-grouse habitat selection among these other correlated predictors; because of this, sagebrush height was retained for final models while the other correlated predictors were not. Sagebrush height had the most explanatory power at its coarsest measured spatial scale (neighborhood radius of 1,451 m), further suggesting that this metric serves as a broad indicator of sagebrush communities (structure and cover) for this analysis and within the entire Bi-State DPS (tables 4–6). Strong selection for greater sagebrush height occurred for all three seasons, with largest effect sizes observed in spring and winter (tables 4–6).

Other characteristics influencing selection for sagebrush vegetation communities included herbaceous grass cover (for example, percent perennial grass, percent annual grass, and overall percent herbaceous) and non-sagebrush shrub cover. We observed selection for greater proportions of perennial grass during spring and winter, and especially strong selection for overall percent herbaceous cover during summer–fall (tables 4–6). In contrast, all model selection coefficients indicated sage-grouse avoidance of greater proportions of annual grass cover across all seasons (tables 4–6). Models indicated a small influence of non-sagebrush shrub cover for all seasons, with positive selection observed in spring and winter (tables 4, 6), but negative selection (that is, avoidance) in summer–fall (table 5). Effect sizes were much smaller for non-sagebrush shrub cover compared to effect sizes describing selection for sagebrush height and herbaceous understory cover.

Pinyon-Juniper. Pinyon-juniper cover was strongly avoided across all seasons. Negative influences of pinyon-juniper included negative effects of overall percent pinyon-juniper, pinyon-juniper canopy cover class 1 (PJ-CC1; Gustafson and others, 2018), and negative associations with proximity to forest or proximity to a single tree. Overall percent pinyon-juniper was best characterized at a moderate spatial scale (radius of 439 m; tables 6–8), whereas PJ-CC1 had strongest negative effects at the finest spatial scale in spring and summer–fall (radius = 167 m; tables 6, 7) and the moderate spatial scale in winter (radius = 439 m; table 8).

Hydrologic. Stream densities and proximities (for example, perennial, intermittent, and combined) and other indicators of water availability (for example, springs, water bodies, wet meadows) were generally influential predictors of grouse habitat selection, although their effects varied among seasons. Selection for proximity and density of streams, water bodies, and springs was predictably greatest during the summer season when water availability was likely most limited. Grouse exhibited strong selection for greater intermittent stream density (radius = 439 m; table 7), proximity to perennial streams, and density of springs (radius = 439 m; table 7), while more moderate selection was observed for proportion of wet meadow habitat (radius = 439 m; table 7), proximity to water bodies, proximity to intermittent streams, and combined stream density (radius = 1,451 m; table 7). In contrast, grouse exhibited avoidance of greater perennial stream density (radius = 439 m; table 6) and areas near intermittent streams during spring, despite showing apparent selection of closer proximity to perennial streams and water bodies. During winter, areas near both intermittent and perennial streams were preferred, while relatively close to water bodies and greater perennial stream densities (radius = 439 m; table 8) were generally avoided. Sage-grouse avoided areas near irrigation ditches and canals across all seasons (tables 6–8).

Topography. Sage-grouse exhibited preference for intermediate curvature (radius = 439 and 1,451 m, respectively; tables 6, 7) with lower relative roughness (radius = 1,451 m; table 6) or slope (radius = 439, 167 m; tables 5 and 6 for summer–fall and winter, respectively) during all seasons, with reduced selection of southwest facing slopes during spring (transformed aspect, radius = 439 m; table 6).

Table 5. Resource Selection Function (RSF) validation statistics, including Spearman's rank coefficient, R^2, and the slope coefficient (β), between the number of greater sage-grouse (*Centrocercus urophasianus*) locations within the Bi-State Distinct Population Segment predicted across 10 binned habitat classes of increasing RSF value, and the number of actual locations observed in those classes within the data used to build the model.

[Validation statistics indicated strong agreement between predicted and observed numbers of locations across seasons and life stages]

Phenological season or life stage	Spearman's rank coefficient	R^2 (observed versus predicted)	β (observed versus predicted)
Spring	1.00	0.94	0.79
Summer–Fall	0.96	0.93	0.77
Winter	1.00	0.91	0.77
Nest	0.95	0.95	0.92
Early Brood	1.00	0.95	0.81
Late Brood	0.95	0.95	0.81

Table 6. Spring resource selection function (RSF) model coefficients (n = 17) and their best-ranked scale of measurement from final model of greater sage-grouse (*Centrocercus urophasianus*) habitat within the Bi-State Distinct Population Segment during the spring season.

[Model coefficients are ordered by absolute Z-value. For exponential decay distance metrics, a negative coefficient indicates reduced conditional selection at closer proximity]

Covariate	Scale	Estimate ($\hat{\beta}$)	SE ($\hat{\beta}$)	Z-value
Distance to Ditch	Exp. decay	–2.452	0.040	–61.075
Sagebrush Height	r = 1,451 m	0.669	0.012	56.031
Percent Perennial Grass	r = 1,451 m	0.429	0.010	44.825
Distance to Forest	Exp. decay	–1.199	0.035	–34.241
Roughness	r = 1,451 m	–0.806	0.025	–32.572
Percent Pinyon-Juniper	r = 439 m	–1.268	0.044	–28.545
Distance to Perennial Stream	Exp. decay	1.210	0.043	27.842
Curvature	r = 439 m	0.400	0.014	27.678
Perennial Stream Density	r = 439 m	–0.276	0.014	–19.258
Percent Pinyon-Juniper Cover Class 1	r = 167 m	–0.318	0.020	–16.276

Table 7. Summer resource selection function (RSF) model coefficients (n = 21) and their best-ranked scale of measurement from final model of greater sage-grouse (*Centrocercus urophasianus*) habitat within the Bi-State Distinct Population Segment during the summer–fall season.

[Model coefficients are ordered by absolute Z-value. For exponential decay distance metrics, a negative coefficient indicates reduced conditional selection at closer proximity]

Covariate	Scale	Estimate ($\hat{\beta}$)	SE ($\hat{\beta}$)	Z–value
Percent Herbaceous	r = 1,451 m	0.664	0.011	61.519
Intermittent Stream Density	r = 439 m	0.426	0.007	61.453
Distance to Ditch	Exp. decay	–2.530	0.048	–52.494
Curvature	r = 1,451 m	0.885	0.018	48.125
Spring Density	r = 439 m	0.163	0.004	41.465
Distance to Perennial Stream	Exp. decay	1.991	0.048	41.110
Slope	r = 439 m	–0.658	0.020	–32.202
Sagebrush Height	r = 1,451 m	0.387	0.014	27.085
Distance to Forest	Exp. decay	–0.921	0.037	–24.727
Percent Pinyon–Juniper	r = 439 m	–1.409	0.057	–24.634
Slope (quadratic)	r = 439 m	–0.352	0.018	–19.185
Heat Load Index	r = 167 m	–0.222	0.014	–15.596
Percent Annual Grass	r = 439 m	–0.160	0.011	–14.160
Percent Pinyon-Juniper Cover Class 1	r = 167 m	–0.289	0.023	–12.563
Percent Wet Meadow	r = 439 m	0.088	0.007	12.191
Curvature (quadratic)	r = 1,451 m	–0.056	0.006	–8.647
Distance to Water Body	Exp. decay	0.343	0.045	7.644
Transformed Aspect	r = 1,451 m	0.078	0.013	6.256
Non-sagebrush Shrub Cover	r = 439 m	–0.059	0.011	–5.615
Distance to Intermittent Stream	Exp. decay	0.167	0.040	4.176
All Stream Density	r = 1,451 m	0.018	0.011	1.606

Table 8. Winter resource selection function (RSF) model coefficients (n = 16) and their best-ranked scale of measurement from final model of greater sage-grouse (*Centrocercus urophasianus*) habitat within the Bi-State Distinct Population Segment during the winter season.

[Model coefficients are ordered by absolute Z-value. For exponential decay distance metrics, a negative coefficient indicates reduced conditional selection at closer proximity]

Covariate	Scale	Estimate ($\hat{\beta}$)	SE ($\hat{\beta}$)	Z–value
Sagebrush Height	r = 1,451 m	0.767	0.014	55.316
Curvature	r = 1,451 m	1.066	0.022	47.990
Slope	r = 167 m	–0.985	0.021	–47.502
Distance to Ditch	Exp. decay	–2.098	0.050	–41.615
Percent Perennial Grass	r = 1,451 m	0.349	0.011	30.693
Distance to Forest	Exp. decay	–0.935	0.043	–21.813
Percent Pinyon-Juniper Cover Class 1	r = 439 m	–0.564	0.026	–21.393
Percent Pinyon-Juniper	r = 439 m	–1.225	0.058	–21.243
Distance to Perennial Stream	Exp. decay	0.821	0.050	16.353
Percent Annual Grass	r = 167 m	–0.287	0.019	–14.983
Curvature (quadratic)	r = 1,451 m	–0.070	0.007	–10.491
Distance to Water Body	Exp. decay	–0.485	0.050	–9.643
Percent Non-Sagebrush Shrub	r = 167 m	0.105	0.013	8.392
Distance to Intermittent Stream	Exp. decay	0.325	0.040	8.085
Perennial Stream Density	r = 439 m	–0.061	0.016	–3.925
Slope (quadratic)	r = 167 m	0.064	0.017	3.833

While broad-scale aspect (radius = 1,451 m) was weakly influential during summer–fall, sage-grouse avoided areas with larger heat load (radius = 167 m; table 7). Topographic covariates for aspect and heat load were not influential predictors during winter. Topographic indices for slope and roughness were generally better predictors than elevation, which was too highly correlated with other topographic indices to be included together in the same models. However, selection patterns with respect to topography were generally consistent with sage-grouse use of intermediate elevations with moderate relative slope, roughness, and curvature.

Summary of RSF Results for Nesting and Brood-Rearing Life Stages

The final RSF models of nesting and brood-rearing habitat selection based on nest and brood locations included 11, 17, and 16 covariates for nesting, early brood-rearing, and late brood-rearing life stages, respectively. Selected covariates were largely consistent with covariates explaining seasonal habitat selection patterns, with some variation in scale of selection and across life stages.

Sagebrush Communities. As with seasonal habitat selection models, sagebrush height was the strongest predictor of sage-grouse nest site and brood habitat selection, with strongest predictive ability at the coarsest spatial scale (radius = 1,451 m; tables 9–11). Selection for greater sagebrush height was strong in terms of effect size for all life stages (tables 9–11). Similar to seasonal habitat selection patterns, nesting and early brood-rearing grouse selected greater perennial grass cover (radius = 439 and 1,451 m, respectively; tables 9, 10), while late brood-rearing grouse selected greater proportions of all herbaceous cover (radius = 1,451 m; table 11), including annual grass cover (radius = 439 m; table 9). Early and late broods exhibited some avoidance of other shrub cover (non-sagebrush shrub and little sagebrush), although effect sizes were considered near marginal (tables 10, 11).

Pinyon-Juniper. Avoidance of pinyon-juniper across life stages was altogether consistent with seasonal habitat selection patterns, with all nesting and brood-rearing grouse avoiding percent overall pinyon-juniper (radius = 439 and 1,451 m; tables 9–11), early brood-rearing grouse additionally avoiding PJ-CC1 (radius = 167 m; table 10), and all nesting and brood-rearing grouse avoiding closer proximity to forests (tables 9–11).

Table 9. Nest resource selection function (RSF) model coefficients (n = 11) and their best-ranked scale of measurement from final model of greater sage-grouse (*Centrocercus urophasianus*) nesting habitat within the Bi-State Distinct Population Segment based on nest locations.

[Model coefficients are ordered by absolute Z-value. For exponential decay distance metrics, a negative coefficient indicates reduced conditional selection at closer proximity]

Covariate	Scale	Estimate ($\hat{\beta}$)	SE ($\hat{\beta}$)	Z-value
Sagebrush Height	r = 1451 m	0.708	0.063	11.206
Percent Pinyon-Juniper	r = 439 m	–2.131	0.224	–9.531
Transformed Aspect	r = 439 m	–0.337	0.048	–6.987
Perennial Stream Density	r = 439 m	–0.580	0.109	–5.340
Curvature	r = 167 m	–0.282	0.059	–4.805
Slope	r = 1451 m	0.269	0.068	3.943
Distance to Forest	Exp. decay	–0.702	0.181	–3.874
Percent Perennial Grass	r = 439 m	0.157	0.066	2.374
Distance to Perennial Stream	Exp. decay	0.422	0.252	1.672
Percent Agriculture	r = 439 m	–0.624	0.385	–1.621
Distance to Water Body	Exp. decay	0.338	0.221	1.523

Table 10. Early brood resource selection function (RSF) model coefficients (n = 19) and their best-ranked scale of measurement from final model of greater sage-grouse (*Centrocercus urophasianus*) early brood-rearing habitat within the Bi-State Distinct Population Segment based on early brood locations.

[Model coefficients are ordered by absolute Z-value. For exponential decay distance metrics, a negative coefficient indicates reduced conditional selection at closer proximity]

Covariate	Scale	Estimate ($\hat{\beta}$)	SE ($\hat{\beta}$)	Z-value
Sagebrush Height	r = 1451 m	0.938	0.056	16.831
Distance to Ditch	Exp. decay	–2.402	0.155	–15.528
Curvature	r = 1451 m	0.960	0.079	12.224
Distance to Agricultural Field	Exp. decay	1.673	0.158	10.579
Percent Perennial Grass	r = 1451 m	0.388	0.045	8.540
Transformed Aspect	r = 439 m	–0.311	0.039	–7.909
Roughness	r = 167 m	–1.050	0.134	–7.822
Distance to Forest	Exp. decay	–0.839	0.140	–5.999
Distance to Intermittent Stream	Exp. decay	–0.843	0.147	–5.717
Percent Pinyon-Juniper	r = 439 m	–1.104	0.194	–5.702
Spring Density	r = 1451 m	0.156	0.028	5.608
Percent Pinyon-Juniper Cover Class 1	r = 167 m	–0.596	0.113	–5.286
Curvature (quadratic)	r = 1451 m	–0.148	0.033	–4.414
Distance to Perennial Stream	Exp. decay	0.560	0.184	3.044
Percent Non-sagebrush Shrub	r = 439 m	–0.150	0.051	–2.960
All Stream Density	r = 439 m	–0.189	0.068	–2.763
Distance to Tree	Exp. decay	0.455	0.172	2.636
Percent Little Sagebrush	r = 167 m	–0.062	0.038	–1.636
Roughness (quadratic)	r = 167 m	–0.288	0.188	–1.532

Table 11. Late brood resource selection function (RSF) model coefficients (n = 18) and their best-ranked scale of measurement from final model of greater sage-grouse (*Centrocercus urophasianus*) late brood-rearing habitat within the Bi-State Distinct Population Segment based on late brood locations.

[Model coefficients are ordered by absolute Z-value. For exponential decay distance metrics, a negative coefficient indicates reduced conditional selection at closer proximity]

Covariate	Scale	Estimate ($\hat{\beta}$)	SE ($\hat{\beta}$)	Z-value
Slope	r = 167 m	–1.243	0.073	–17.113
Elevation	r = 439 m	1.211	0.076	15.852
Sagebrush Height	r = 1451 m	0.770	0.055	14.083
Distance to Agricultural Field	Exp. decay	1.528	0.137	11.142
Percent Pinyon-Juniper	r = 1451 m	–1.267	0.121	–10.490
Transformed Aspect	r = 439 m	–0.304	0.031	–9.915
Distance to Ditch	Exp. decay	–1.456	0.149	–9.775
Percent Herbaceous	r = 1451 m	0.411	0.047	8.725
Distance to Perennial Stream	Exp. decay	0.861	0.114	7.550
Percent Annual Grass	r = 439 m	0.158	0.028	5.750
Percent Non-sagebrush shrub	r = 439 m	–0.198	0.035	–5.601
Distance to Intermittent Stream	Exp. decay	–0.527	0.100	–5.247
Distance to Tree	Exp. decay	–0.622	0.119	–5.206
Slope (quadratic)	r = 167 m	–0.360	0.076	–4.732
Percent Wet Meadow	r = 1451 m	–0.145	0.032	–4.485
Elevation (quadratic)	r = 439 m	–0.116	0.033	–3.499
Distance to Forest	Exp. decay	–0.218	0.097	–2.252
Percent Little Sagebrush	r = 167 m	–0.057	0.033	–1.753

Hydrologic. Nesting grouse avoided greater perennial stream densities (radius = 439 m; table 9), while exhibiting weak (that is, near marginal) selection for areas within close proximity to perennial streams and water bodies. Likewise, early brood-rearing grouse avoided greater stream density (r = 439 m; table 10) while selecting areas with greater spring density (radius = 1,451 m; table 10) near perennial streams but further away from intermittent streams (table 10). Late broods also selected near perennial streams but further from intermittent streams (table 11); intermittent streams may dry out early in the brood-rearing season, hence having little to offer in terms of water, cover, and forage availability. Late broods appeared to avoid areas with greater proportions of wet meadow, but this may have been confounded by land cover misclassification of wet meadow versus irrigated pasture habitat types; late broods strongly selected for areas closer to land cover classifications of agricultural pastures and croplands (table 11; see "Pastures and Cropland" section below). Similar to seasonal habitat selection patterns, early and late broods avoided areas near ditches and canals.

Topography. Nesting grouse apparently selected for greater slopes at coarse spatial scale (radius = 1,451 m; table 9), but less curvature at a finer spatial scale (radius = 167 m; table 9), while apparently avoiding steeper, south-facing slopes (transformed aspect, radius = 439 m; table 9). Early broods exhibited similar avoidance of steeper, south-facing slopes (radius = 439; table 10), but topographic patterns were otherwise explained by selection for intermediate curvature at coarse spatial scale (radius = 1,451 m; table 10) and avoidance of greater roughness at finer spatial scales (radius = 167 m; table 10). Late broods exhibited similar selection patterns, with greater slopes avoided at fine spatial scales (radius = 167 m; table 11), avoidance of steep south-facing slopes (radius = 167 m; table 11), and intermediate elevation strongly selected (radius = 439 m; table 11).

Pastures and Cropland. While seasonal habitat selection patterns were not influenced by proportion of or proximity to agricultural pasture or cropland, nesting and brood-rearing grouse had mixed selection patterns with respect to these landscape features. While nesting grouse exhibited marginal avoidance of greater proportion of agricultural land (radius = 439 m; table 9), both early and late broods exhibited selection for areas near agricultural land (tables 10, 11).

Objective 4. Spatially-Explicit Distributional Analysis

Long-Term Spatial Trends: 1995–2018

Sage-grouse DSAs at the 99 percent isopleth over 24 years and three population cycles in the Bi-State DPS were characterized by contractions for Fales, Long Valley, and Sagehen subpopulations and expansion in the Bodie Hills subpopulation (fig. 17). The net effect for these shifting DSAs was a loss of total area and corresponding volume over time with a high probability of occupation at any given time (tables 12, 13; figs. 18, 19), which corresponded to a median loss of 858 ha annually and 20,573 ha from 1995 to 2018 across the Bi-State DPS. Annual rates of area loss were most rapid in Long Valley and Sagehen (table 12, fig. 18), while annual rates of volume loss were most rapid in Fales and Long Valley (table 13, fig. 19). Evidence of respective increasing or decreasing rates was strong across all four measured subpopulations. Based on the non-overlapping 95-percent credible interval of the posterior probability distributions with zero (tables 12, 13), Bodie Hills was evidenced as increasing substantially in distributional area and volume through time, while all other subpopulations have experienced distributional losses. Across the Bi-State DPS, the population level trend estimate from the mixed model was negative (–0.05 [–0.31, 0.198]; table 12), which equates to 77 percent probability of contracting range for any given subpopulation.

Bodie Hills and Long Valley comprised all of the core DSA (50 percent isopleth) across the Bi-State DPS over the same time period (fig. 20), and similar patterns of opposing expansion and contraction between the two subpopulations were evident. Significant expansion of total area and volume in Bodie Hills was insufficient to offset concomitant losses in Long Valley (tables 14, 15; figs. 21, 22), which corresponded to a median loss of 88 ha annually across the Bi-State DPS.

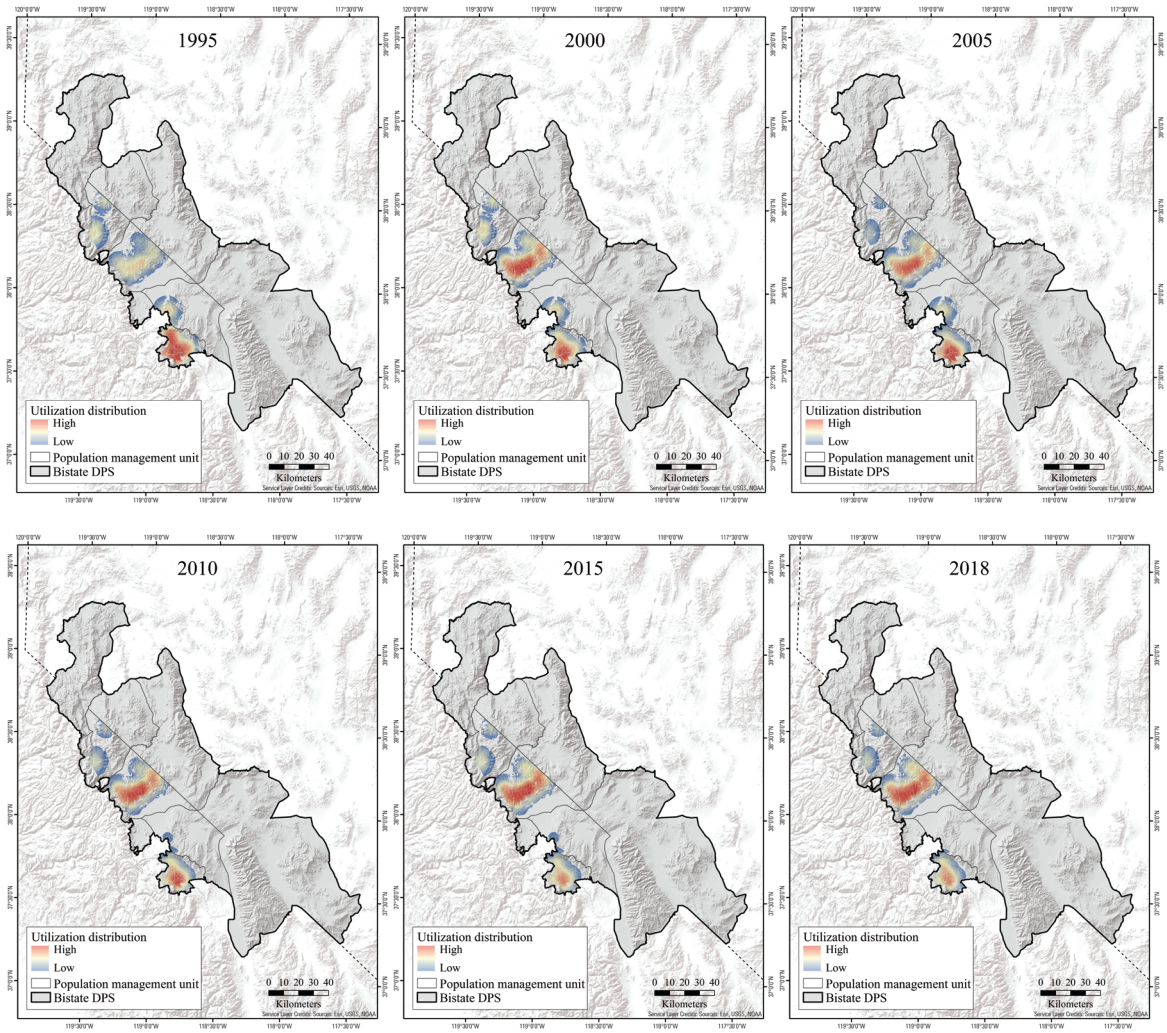

Figure 17. Long-term (1995–2018) changes in annual distributional area (DSA) at the 99 percent isopleth for greater sage-grouse (*Centrocercus urophasianus*) across the Fales, Bodie Hills, Long Valley, and Sagehen subpopulations in the Bi-State Distinct Population Segment. Only leks with IPM-derived estimates of abundance are used in DSA calculations. Warmer colors indicate larger DSA volume.

Table 12. Results from a linear mixed model of trends in annual distributional area (DSA) total area at the 99 percent isopleth across greater sage-grouse (*Centrocercus urophasianus*) subpopulations in the Bi-State Distinct Population Segment from 1995 to 2018.

[Only leks with IPM-derived estimates of abundance are used in DSA calculations. Net gain or loss (+/–95 percent credible interval) was projected from trend models, and the total net gain or loss was a derived parameter based on projected gains or losses by subpopulation. Parameters for βt are linear trend estimates, and P(|βt| > 0) indicates the probability estimate of an increase or decrease for a given subpopulation according to the trend estimate]

Subpopulation	Net gain/loss (ha)	βt (2.5th, 97.5th)	P(|βt| > 0)
Bodie	3,962 (1,945, 5,935)	0.085 (0.042, 0.126)	1.00
Fales	–5,360 (–8,294, –2,393)	–0.074 (–0.114, –0.033)	1.00
Long Valley	–3,272 (–4,449, –2,084)	–0.115 (–0.156, –0.073)	1.00
Sagehen	–15,877 (–22,102, –9,778)	–0.107 (–0.149, –0.066)	1.00
All subpopulations (net effect)	–20,573 (–27,853, –13,339)	–0.053 (–0.312, 0.198)	0.77

Table 13. Results from a generalized linear mixed model of trends in proportion of distributional area (DSA) volume at the 99 percent isopleth across greater sage-grouse (*Centrocercus urophasianus*) subpopulations in the Bi-State the Bi-State Distinct Population Segment from 1995 to 2018.

[Only leks with IPM-derived estimates of abundance are used in DSA calculations. Parameters for βt are linear trend estimates, and P(|βt| > 0) indicates the probability estimate of an increase or decrease for a given subpopulation according to the trend estimate]

Subpopulation	βt (2.5th, 97.5th)	P(|βt| > 0)
Bodie	0.061 (0.048, 0.074)	1.00
Fales	–0.029 (–0.058, –0.001)	0.98
Long Valley	–0.049 (–0.063, –0.036)	1.00
Sagehen	–0.101 (–0.137, –0.066)	1.00
All subpopulations (net effect)	–0.029 (–0.211, 0.146)	0.72

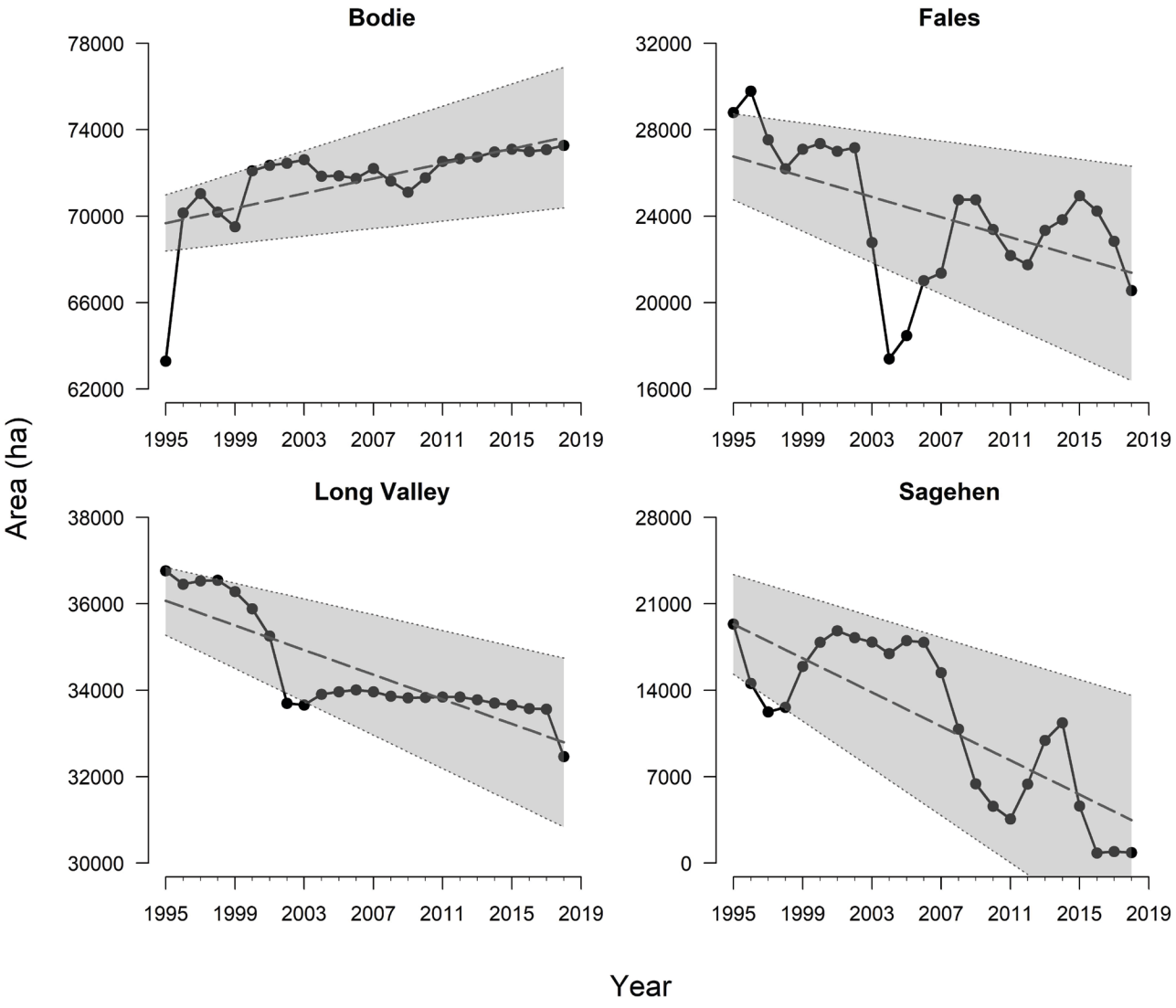

Figure 18. Time series of annual distributional area (DSA) estimates for total area at the 99 percent isopleth for subpopulations of greater sage-grouse (*Centrocercus urophasianus*) in the Bi-State Distinct Population Segment from 1995 to 2018. Only leks with IPM-derived estimates of abundance are used in DSA calculations.

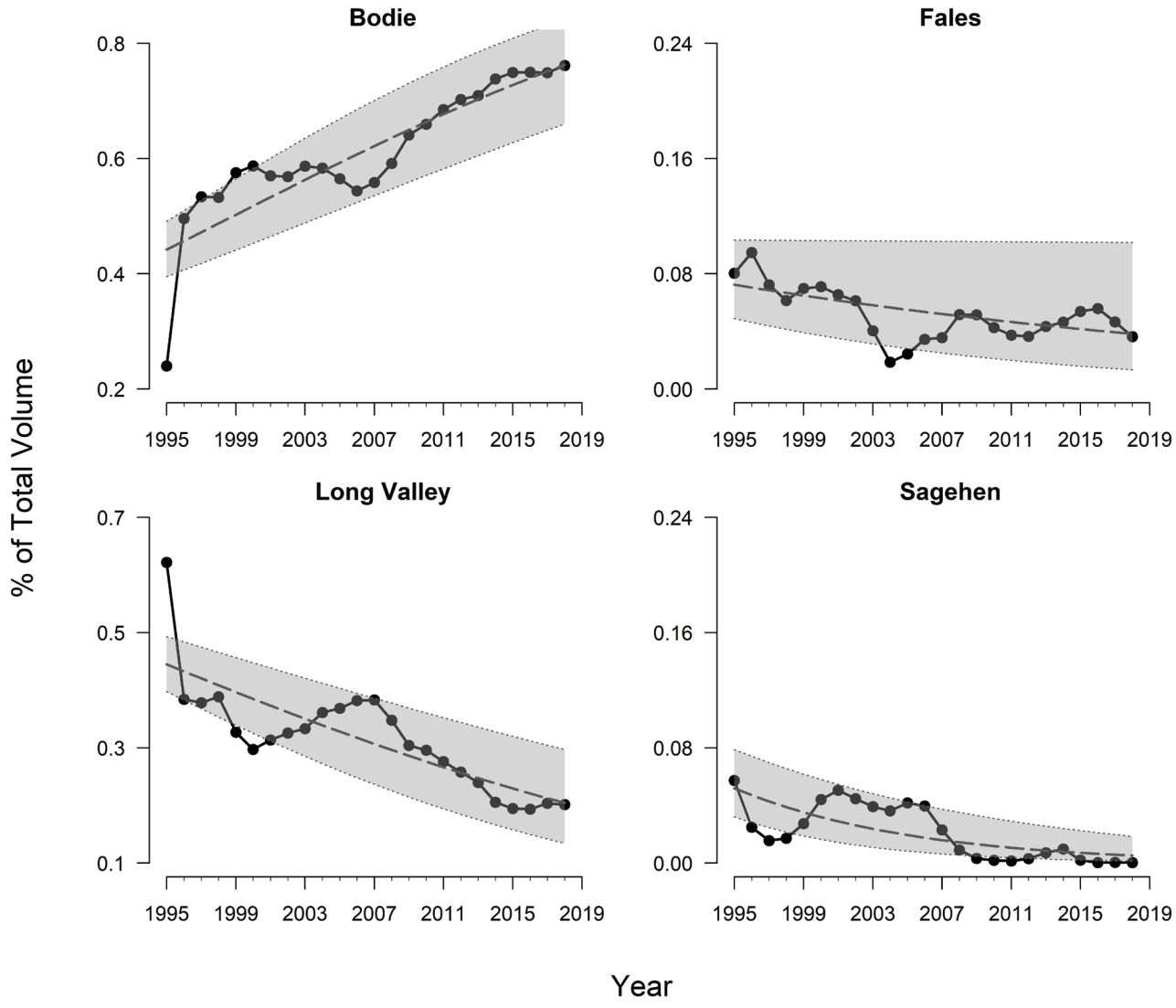

Figure 19. Time series of annual distributional area (DSA) estimates for proportional volume at the 99 percent isopleth for subpopulations of greater sage-grouse (*Centrocercus urophasianus*) in the Bi-State Distinct Population Segment from 1995 to 2018. Only leks with IPM-derived estimates of abundance are used in DSA calculations.

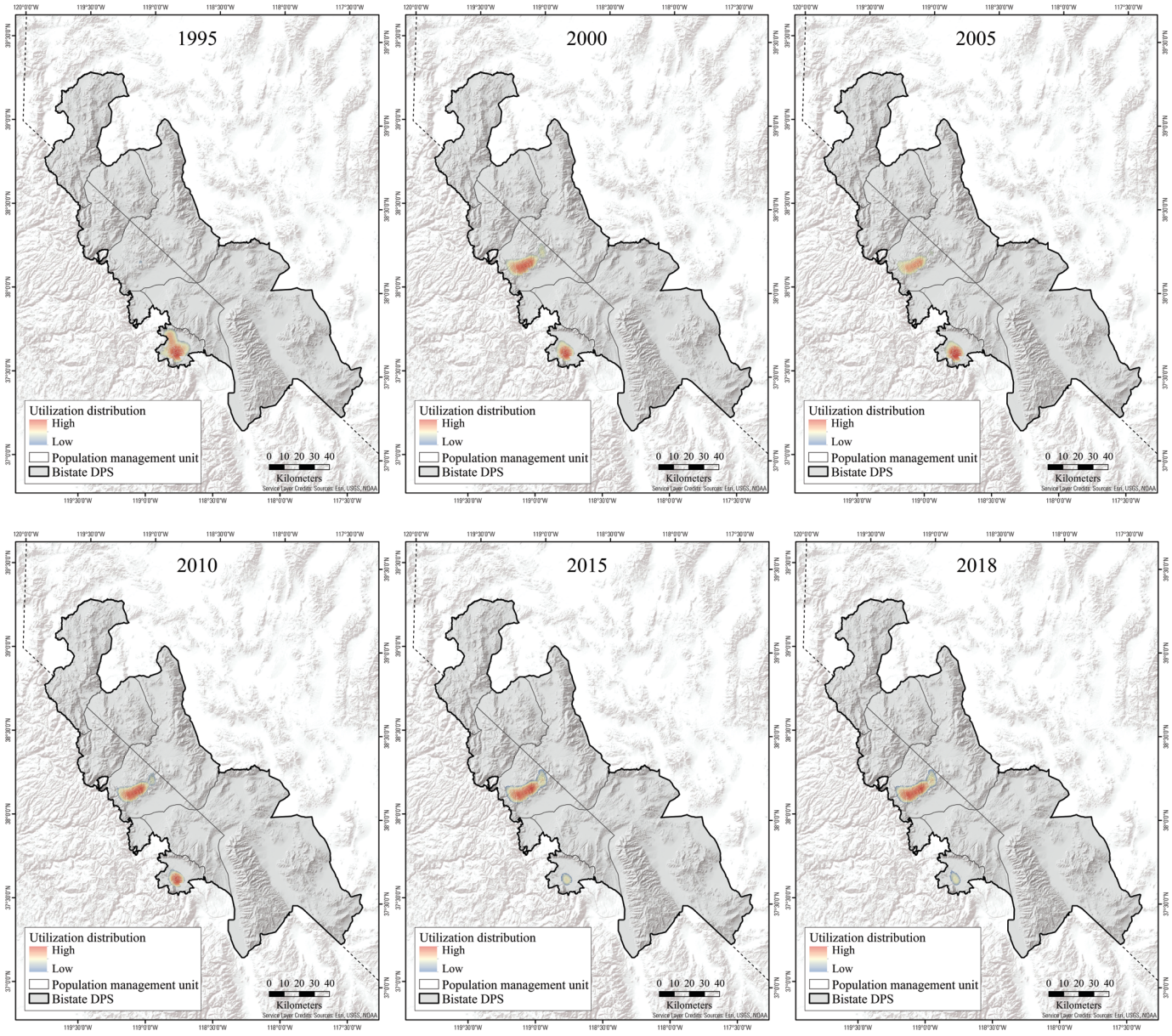

Figure 20. Long-term (1995–2018) changes in annual distributional area (DSA) at the 50 percent isopleth for greater sage-grouse (*Centrocercus urophasianus*) across the Fales, Bodie Hills, Long Valley, and Sagehen subpopulations in the Bi-State Distinct Population Segment. Only leks with IPM-derived estimates of abundance are used in DSA calculations. Warmer colors indicate larger DSA volume.

Table 14. Results from a linear mixed model of trends in DSA total area at the 50 percent isopleth across greater sage-grouse (*Centrocercus urophasianus*) subpopulations in the Bi-State Distinct Population Segment from 1995 to 2018.

[Only leks with IPM-derived estimates of abundance are used in DSA calculations. Net gain or loss (+/–95 percent credible interval) was projected from trend models, and the total net gain or loss was a derived parameter based on projected gains or losses by subpopulation. Parameters for βt are linear trend estimates, and P(|βt| > 0) indicates the probability estimate of an increase or decrease according to the trend estimate]

Subpopulation	Net gain/loss (ha)	βt (2.5th, 97.5th)	P(|βt| > 0)
Bodie	10,972 (6,170, 15,658)	0.088 (0.050, 0.126)	1.00
Long Valley	–13,063 (–8,979, –17,080)	–0.125 (–0.086, –0.163)	1.00
All subpopulations (net effect)	–2,110 (–8,297,4,098)	–0.026 (–22.01, 21.60)	0.52

Table 15. Results from a generalized linear mixed model of trends in proportion of annual distributional area (DSA) volume at the 50 percent isopleth across greater sage-grouse (*Centrocercus urophasianus*) subpopulations in the Bi-State Distinct Population Segment from 1995 to 2018.

[Only leks with IPM-derived estimates of abundance are used in DSA calculations. Parameters for βt are linear trend estimates, and P(|βt| > 0) indicates the probability estimate of an increase or decrease according to the trend estimate]

Subpopulation	βt (2.5th, 97.5th)	P(|βt| > 0)
Bodie	0.117 (0.073, 0.162)	1.00
Long Valley	–0.117 (–0.074, –0.161)	1.00
All subpopulations (net effect)	0.004 (–23.301, 23.262)	0.50

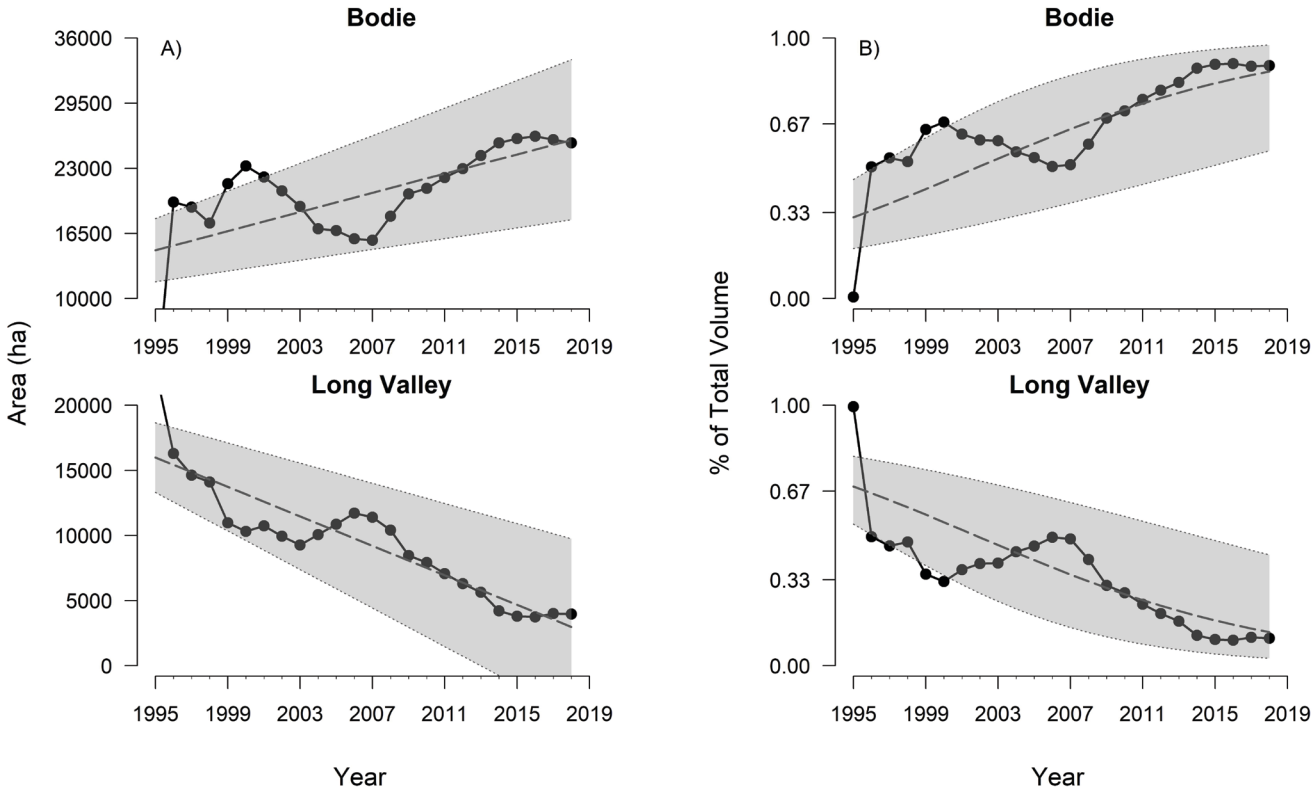

Figure 21. Time series of annual distributional area (DSA) estimates for total area (*A*) and proportional volume (*B*) at the 50 percent isopleth for subpopulations of greater sage-grouse (*Centrocercus urophasianus*) in the Bi-State Distinct Population Segment from 1995 to 2018. Only leks with IPM-derived estimates of abundance are used in DSA calculations.

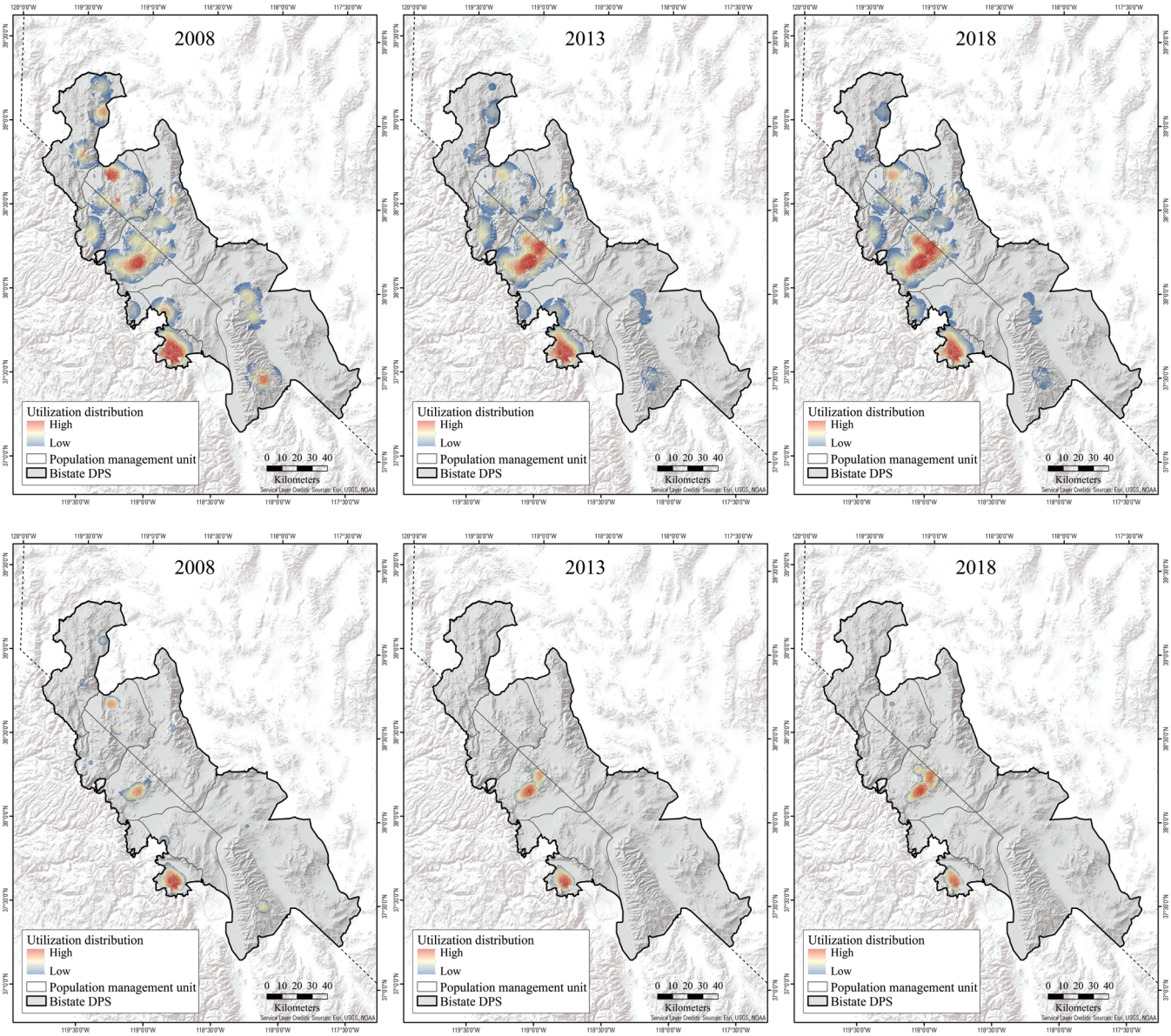

Figure 22. Short-term (2008–18) changes across one population cycle in annual distributional area (DSA) at the 99 (top row) and 50 (bottom row) percent isopleth for greater sage-grouse (*Centrocercus urophasianus*) across all subpopulations the Bi-State Distinct Population Segment. Average annual subpopulation abundance was used for active leks lacking sufficient counts for IPM estimation.

Short-Term Spatial Trends: 2008–18

Analyses of overall and core sage-grouse DSAs over 11 years and one population cycle in the Bi-State DPS revealed patterns similar to those described for the more restrictive long-term spatial trend analyses, but revealed more detailed patterns of contraction for subpopulations on the periphery on the Bi-State DPS range (fig. 22). DSAs at the 99 percent isopleth were characterized by contractions of total area at Desert Creek, Long Valley, Mount Grant, Pine Nuts, Sagehen, and White Mountains subpopulations, and expansion in the Bodie Hills, Fales, and Parker Meadows subpopulations (table 16; fig. 23). Patterns for DSA volume were similar, with the exception of evidence for reductions in volume at Parker Meadows and Fales (table 17; fig. 24). Similar to the long-term analyses, the net effect for these shifting DSAs over 11 years was a loss of total area and volume over time now represented by all subpopulations (tables 16, 17; figs. 23, 24), which corresponded to a median loss of 2,312 ha annually and 55,492 ha from 2008 to 2018 across the Bi-State DPS. Evidence of respective increasing or decreasing rates exceeded 80 percent for all subpopulations except Mount Grant for total area (table 16), and Fales and Mount Grant for volume (table 17). Across the Bi-State DPS, we found evidence of range contraction, although the 95-percent credible interval overlapped zero (–0.07 [–0.19, 0.07]; table 16).

Table 16. Results from a generalized linear mixed model of trends in annual distributional (DSA) total area at the 99 percent isopleth across greater sage-grouse (*Centrocercus urophasianus*) subpopulations in the Bi-State Distinct Population Segment from 2008 to 2018.

[Average annual subpopulation abundance was used for active leks lacking sufficient counts for IPM estimation. Parameters for βt are linear trend estimates, and P(|βt| > 0) indicates the probability estimate of an increase or decrease for a given subpopulation according to the trend estimate]

Subpopulation	Net gain/loss (ha)	βt (2.5th, 97.5th)	P(|βt| > 0)
Bodie	2,989 (247, 5,994)	0.152 (0.013, 0.304)	0.99
Desert Creek	–1,316 (–3,662, 781)	–0.072 (–0.200, 0.043)	0.89
Fales	712 (–479, 2,092)	0.069 (–0.047, 0.204)	0.87
Long Valley	–81 (–186, 11)	–0.103 (–0.237, 0.015)	0.96
Mount Grant	–331 (–1,391, 648)	–0.038 (–0.158, 0.074)	0.75
Parker Meadows	1,185 (–794, 3,493)	0.069 (–0.046, 0.202)	0.87
Pine Nuts	–28,099 (–39,678, –16,407)	–0.206 (–0.291, –0.120)	1.00
Sagehen	–8,077 (–11,454, –4,681)	–0.203 (–0.288, –0.118)	1.00
White Mountain	–22,514 (–30,289, –14,871)	–0.246 (–0.331, –0.162)	1.00
All subpopulations (net effect)	–55,492 (–70,815, –40,2062)	–0.065 (–0.193, 0.070)	0.85

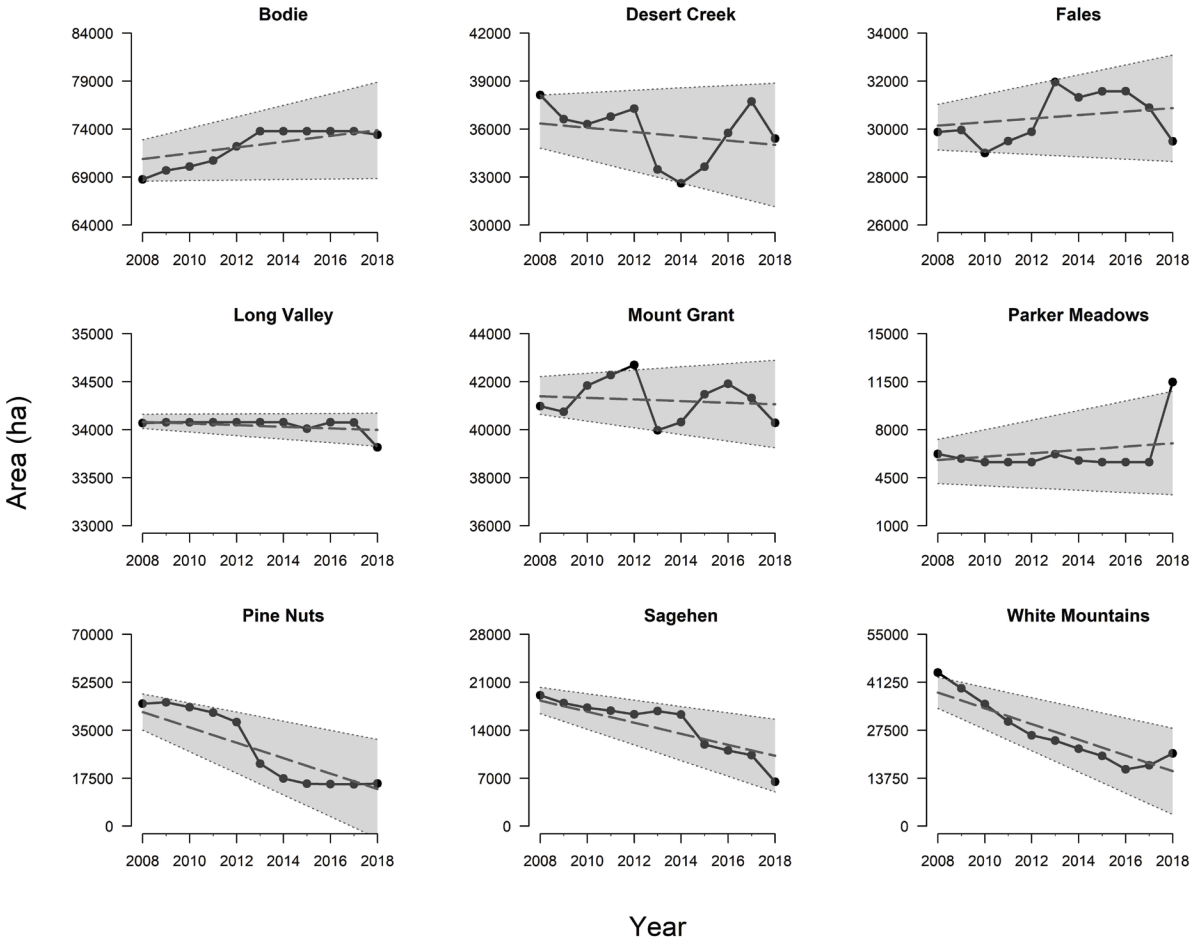

Figure 23. Time series of annual distributional area (DSA) estimates for total area at the 99 percent isopleth for subpopulations of greater sage-grouse (*Centrocercus urophasianus*) in the Bi-State Distinct Population Segment from 2008 to 2018. Average annual subpopulation abundance was used for active leks lacking sufficient counts for IPM estimation.

Table 17. Results from a generalized linear mixed model of trends in proportion of annual distributional area (DSA) volume at the 99 percent isopleth across greater sage-grouse (*Centrocercus urophasianus*) subpopulations in the Bi-State Distinct Population Segment from 2008 to 2018.

[Average annual subpopulation abundance was used for active leks lacking sufficient counts for IPM estimation. Parameters for βt are linear trend estimates, and P(|βt| > 0) indicates the probability estimate of an increase or decrease for a given subpopulation according to the trend estimate]

Subpopulation	βt (2.5th, 97.5th)	P(|βt| > 0)	Subpopulation	βt (2.5th, 97.5th)	P(|βt| > 0)
Bodie	0.128 (0.106, 0.150)	1.00	Parker Meadows	–0.089 (–0.222, 0.025)	0.94
Desert Creek	–0.043 (–0.085, –0.002)	0.98	Pine Nuts	–0.293 (–0.367, –0.226)	1.00
Fales	–0.010 (–0.062, 0.039)	0.66	Sagehen	–0.228 (–0.317, –0.150)	1.00
Long Valley	–0.060 (–0.084, –0.037)	1.00	White Mountains	–0.314 (–0.399, –0.238)	1.00
Mount Grant	0.004 (–0.035, 0.040)	0.58	All subpopulations (net effect)	–0.101 (–0.234, 0.029)	0.95

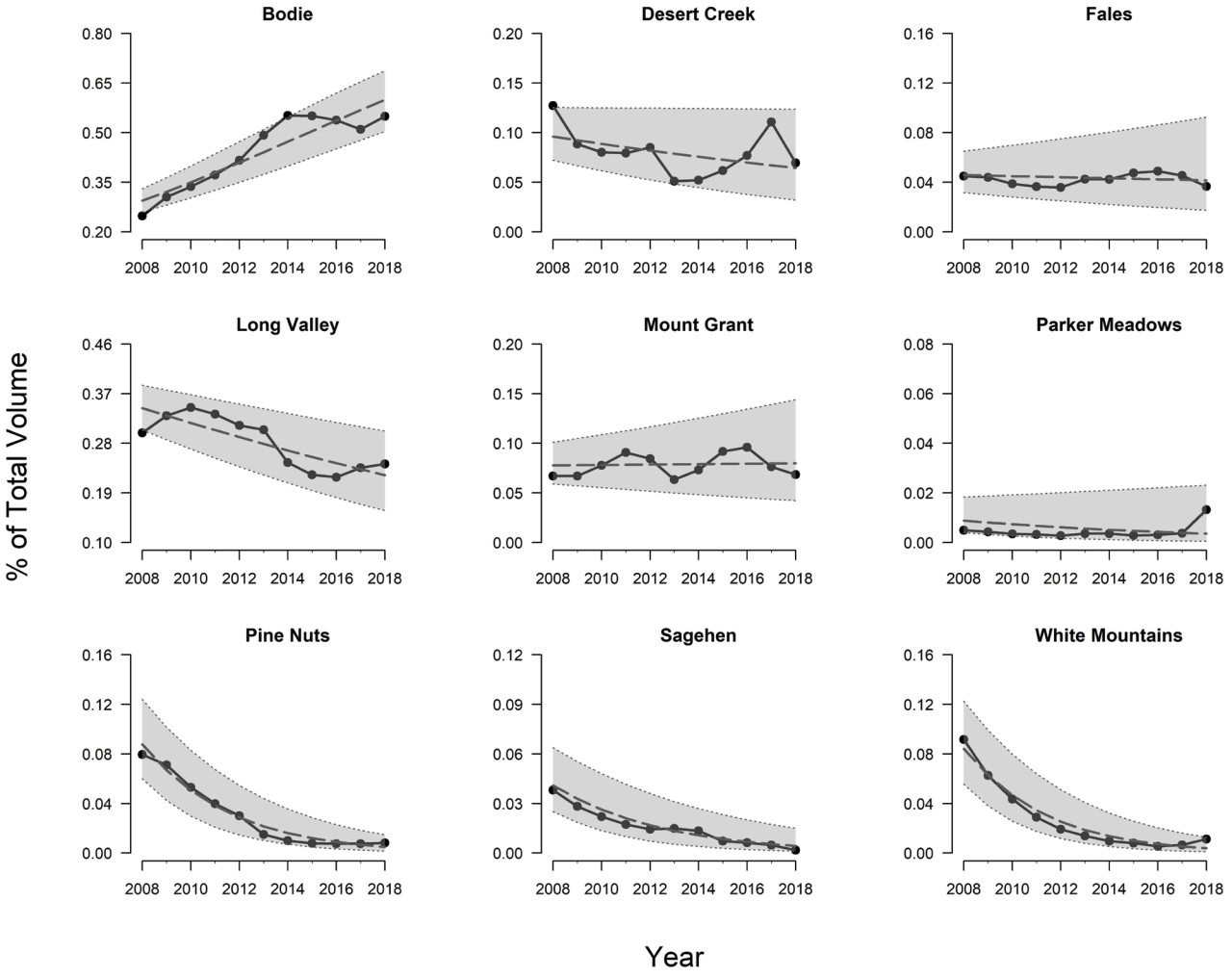

Figure 24. Time series of annual distributional area (DSA) estimates for proportional volume at the 99 percent isopleth for subpopulations of greater sage-grouse (*Centrocercus urophasianus*) in the Bi-State Distinct Population Segment from 2008 to 2018. Average annual subpopulation abundance was used for active leks lacking sufficient counts for IPM estimation.

Loss of core DSAs across all subpopulations was more evident, whereby core DSAs existing in peripheral subpopulations of Pine Nuts, Desert Creek, Fales, Sagehen, and White Mountains during 2008 became functionally absent as of 2018 (figs. 22, 25, 26). With the exception of Bodie Hills, all subpopulations showed strong evidence of contracted total area and volume of core DSAs since 2008 (tables 18, 19). Declines were notably precipitous at Pine Nuts, Fales, Sagehen, and White Mountains (figs. 25, 26). Across the Bi-State DPS, we found strong evidence for core DSA decrease in total area and volume ($P(|\beta t| > 0)$) greater than or equal to 0.95; tables 18, 19).

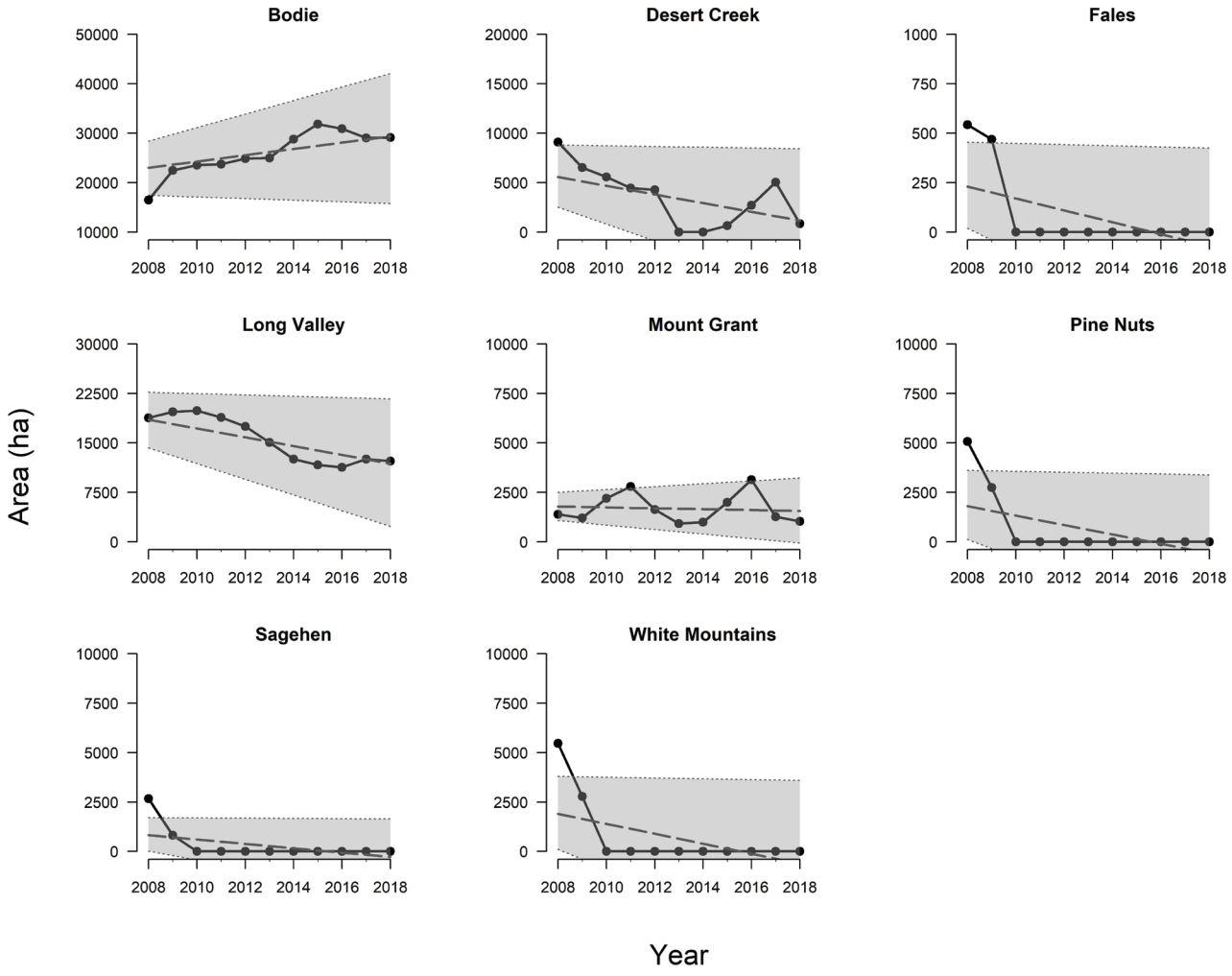

Figure 25. Time series of annual distributional area (DSA) estimates for total area at the 50 percent isopleth for subpopulations of greater sage-grouse (*Centrocercus urophasianus*) in the Bi-State Distinct Population Segment from 2008 to 2018. Average annual subpopulation abundance was used for active leks lacking sufficient counts for IPM estimation. Parker Meadows did not contribute to any measurable DSA.

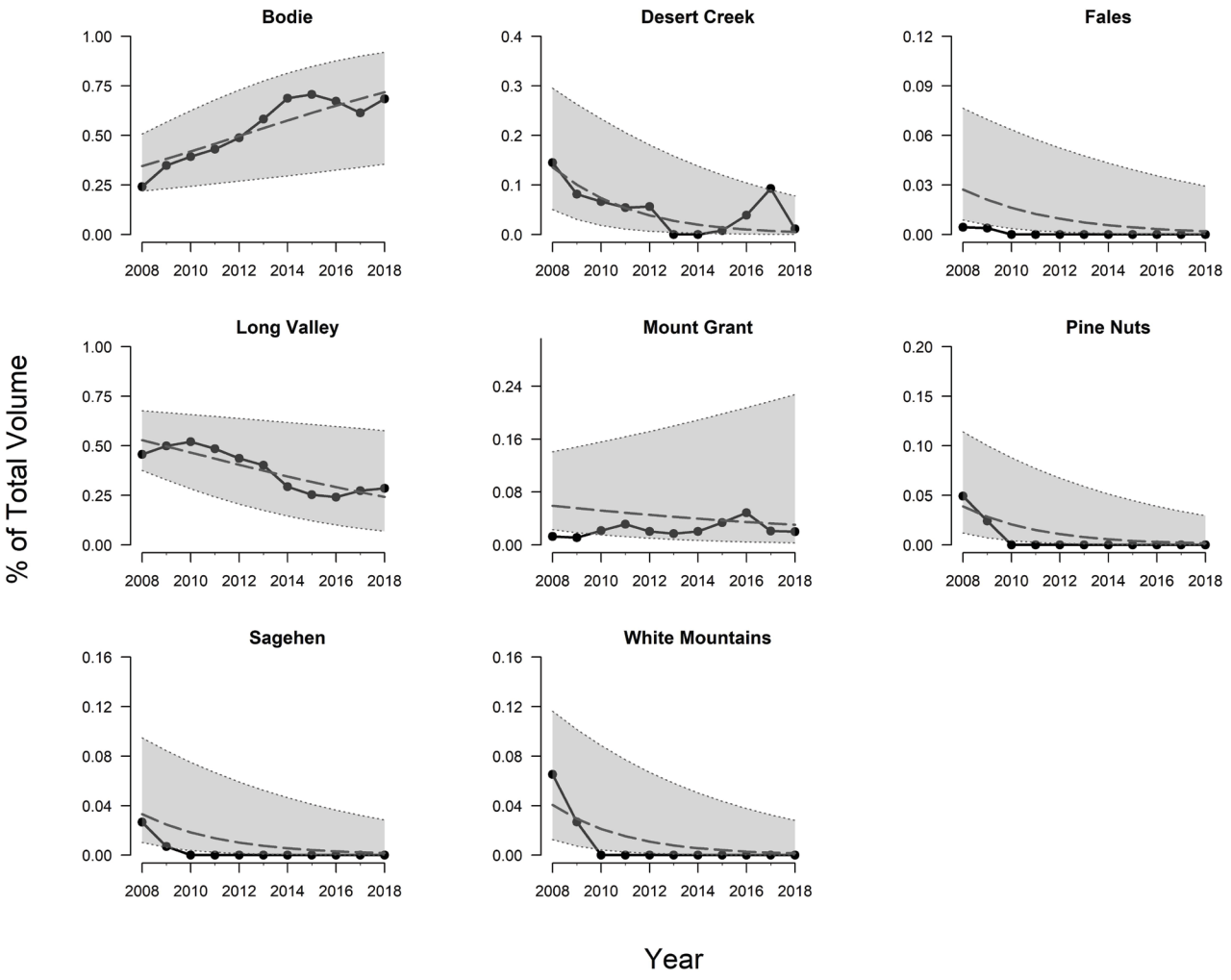

Figure 26. Time series of annual distributional area (DSA) estimates for proportional volume at the 50 percent isopleth for subpopulations of greater sage-grouse (*Centrocercus urophasianus*) in the Bi-State Distinct Population Segment from 2008 to 2018. Average annual subpopulation abundance was used for active leks lacking sufficient counts for IPM estimation. Parker Meadows did not contribute to any measurable DSA.

Table 18. Results from a generalized linear mixed model of trends in proportion of annual distributional (DSA) total area at the 50 percent isopleth across greater sage-grouse (*Centrocercus urophasianus*) subpopulations in the Bi-State Distinct Population Segment from 2008 to 2018.

[Average annual subpopulation abundance was used for active leks lacking sufficient counts for IPM estimation. Parameters for βt are linear trend estimates, and P(|βt| > 0) indicates the probability estimate of an increase or decrease for a given subpopulation according to the trend estimate]

Subpopulation	Net gain/loss (ha)	βt (2.5th, 97.5th)	P(|βt| > 0)
Bodie	5,134 (–2,600, 13,105)	0.114 (–0.058, 0.292)	0.92
Desert Creek	–3,791 (–8,210, 118)	–0.127 (–0.275, –0.004)	0.99
Fales	–156 (–319, –8)	–0.104 (–0.214, –0.006)	0.99
Long Valley	–5,860 (–11,495, –546)	–0.167 (–0.327, –0.016)	1.00
Mount Grant	–234 (–1,135, 676)	–0.031 (–0.151, 0.090)	0.70
Pine Nuts	–2,053 (–4,537, –32)	–0.124 (–0.273, –0.002)	0.99
Sagehen	–946 (–2,145, 13)	–0.116 (–0.262, 0.002)	0.98
White Mountain	–2,147 (–4,792, 31)	–0.121 (–0.271, –0.002)	0.99
All subpopulations (net effect)	–10,159 (–20,758, –831)	–0.081 (–0.218, 0.024)	0.95

Table 19. Results from a generalized linear mixed model of trends in proportion of annual distributional area (DSA) volume at the 50 percent isopleth across greater sage-grouse (*Centrocercus urophasianus*) subpopulations in the Bi-State Distinct Population Segment from 2008 to 2018.

[Average annual subpopulation abundance was used for active leks lacking sufficient counts for IPM estimation. Parameters for βt are linear trend estimates, and P(|βt| > 0) indicates the probability estimate of an increase or decrease for a given subpopulation according to the trend estimate. Parker Meadows did not contribute to any measurable DSA]

Subpopulation	βt (2.5th, 97.5th)	P(|βt| > 0)
Bodie	0.159 (0.072, 0.240)	1.00
Desert Creek	–0.341 (–0.527, –0.156)	1.00
Fales	–0.148 (–0.271, –0.031)	1.00
Long Valley	–0.124 (–0.208, –0.044)	1.00
Mount Grant	–0.066 (–0.211, 0.060)	0.86
Pine Nuts	–0.319 (–0.524, –0.144)	1.00
Sagehen	–0.291 (–0.489, –0.124)	1.00
White Mountains	–0.327 (–0.536, –0.148)	1.00
All subpopulations (net effect)	–0.182 (–0.376, –0.004)	0.98

Objective 5. Region-Wide Habitat Indices of Selected and Occupied Habitats for Conservation Planning

We created spatially explicit maps depicting habitat selection using the parameter estimates from each seasonal or reproductive model to create predictions based on underlying environmental conditions (that is, GIS layers) associated with each parameter estimate. There were some areas in the northwestern portion of the Bi-State DPS where predictions could not be made owing to insufficient spatial coverage of the National Land Cover Database shrubland products (available at https://www.mrlc.gov/data/type/shrubland).

Across phenological seasons, highly selected habitat was more consistently located in the Bodie Hills and Long Valley subpopulations (fig. 27). Selected habitat across all categories was most widely distributed during fall and winter (greater than 0.55 million hectares), particularly across the southeastern portion of the Bi-State DPS, and was more restricted during summer–fall (greater than 0.98 million hectares). Across reproductive seasons, selected habitat across all categories was more widely distributed during nesting (greater than 0.49 million hectares) compared to early (greater than 0.26 million hectares) and brood-rearing (greater than 0.18 million hectares). Late brood rearing habitat was located primarily near Desert Creek/Fales, Bodie Hills, and Long Valley. The distribution of selected habitats within reproductive seasons was more restricted compared to phenological seasons (fig. 28). Nesting overlapped spring habitat by 58.6 percent, early brood rearing overlapped spring and summer–fall habitat by 43.4 percent, and late brood rearing overlapped summer–fall by 40.4 percent (fig. 29).

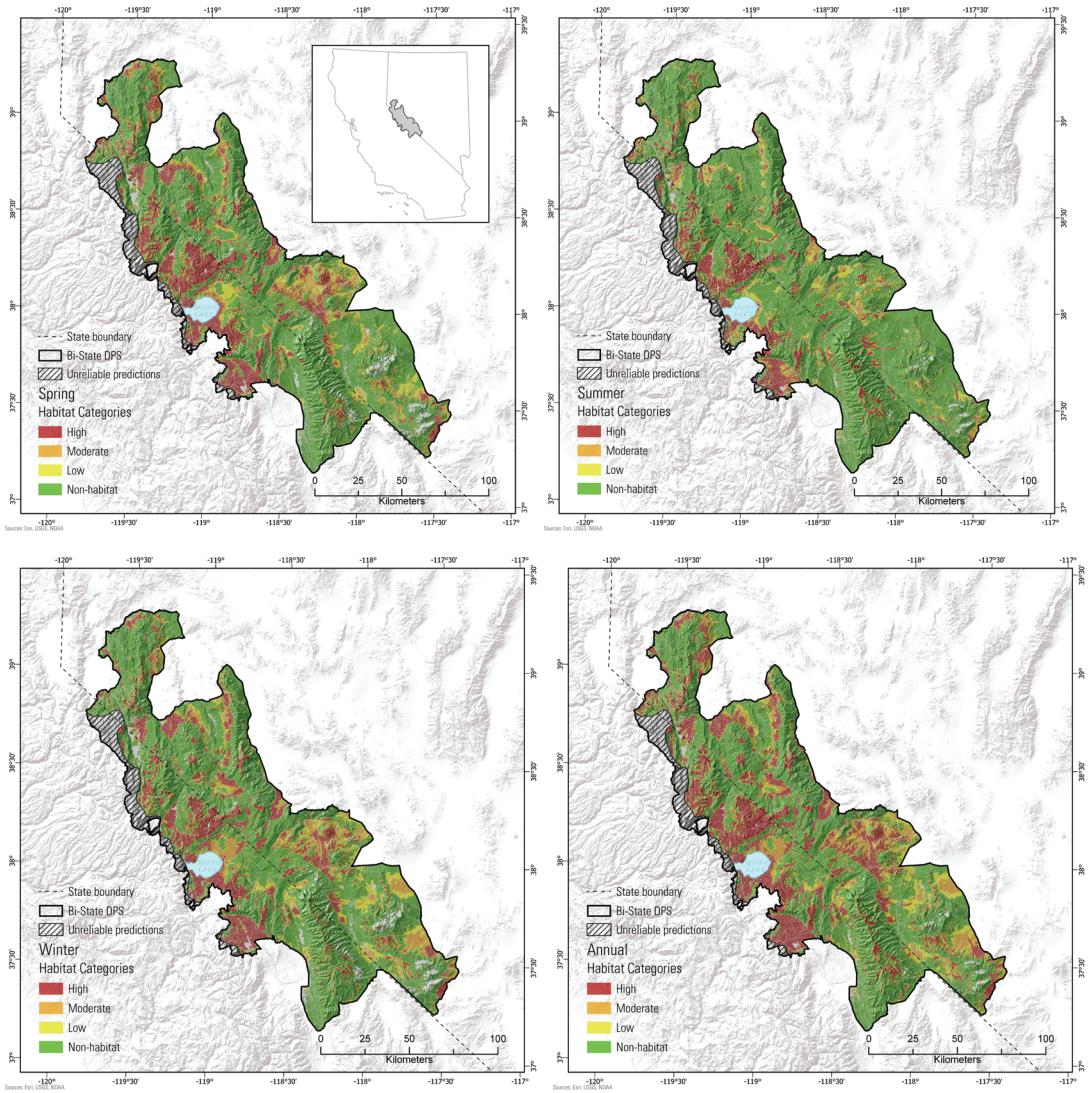

Figure 27. Habitat selection categories (high, moderate, low, and non-habitat) for all radio-marked greater sage-grouse (*Centrocercus urophasianus*) in the Bi-State Distinct Population Segment (DPS) regardless of sex or reproductive status during spring, summer–fall, and winter.

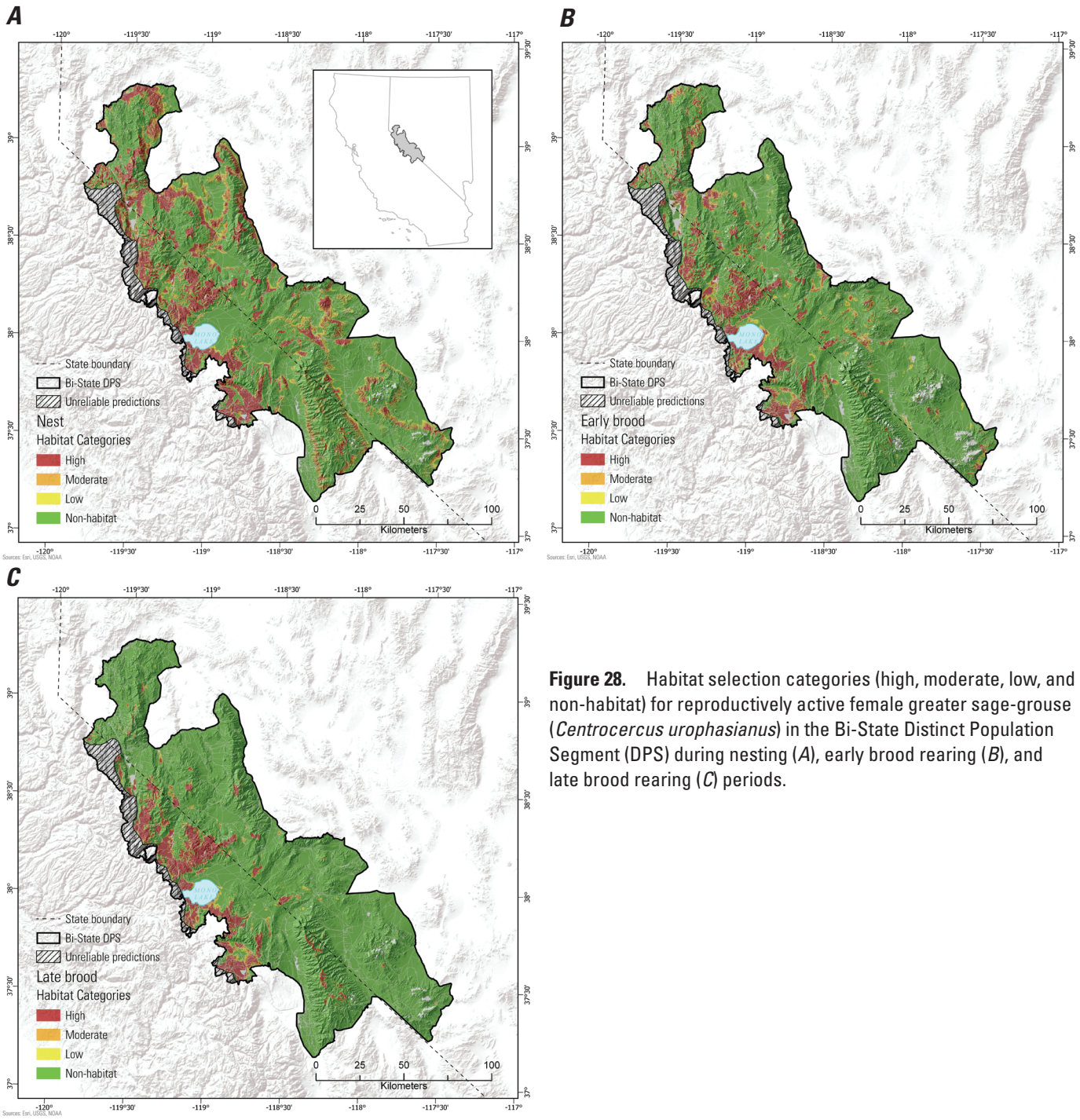

Figure 28. Habitat selection categories (high, moderate, low, and non-habitat) for reproductively active female greater sage-grouse (*Centrocercus urophasianus*) in the Bi-State Distinct Population Segment (DPS) during nesting (*A*), early brood rearing (*B*), and late brood rearing (*C*) periods.

Selected habitat across annual, phenological, and reproductive seasons was relatively evenly distributed across all subpopulations (less than 20 percent), with the notable exception of late brood-rearing habitat in Bodie Hills (31 percent) and all phenological (28–39 percent) and nesting (27 percent) in White Mountains (table 20). When intersected with the generalized DSA (fig. 30) to create categories of occupied habitat, patterns reversed whereby White Mountains represented less than 10 percent of all occupied habitats, while Bodie Hills represented 25–28 percent of occupied habitat. Disproportionate use defined by ratios of occupied to selected habitat greater than 1.0 was most evident for Bodie Hills, Desert Creek, Fales, Long Valley, and Parker Meadows, while under-utilization of available habitat defined by ratios of occupied to selected habitat less than 1.0 were most evident for Sagehen and White Mountains (table 20). Patterns were similar across reproductive life stages where White Mountains, Sagehen, and Parker Meadow represented only 2–7 percent of occupied habitat, whereas Bodie Hills represented 25 percent of occupied habitat across all reproductive seasons.

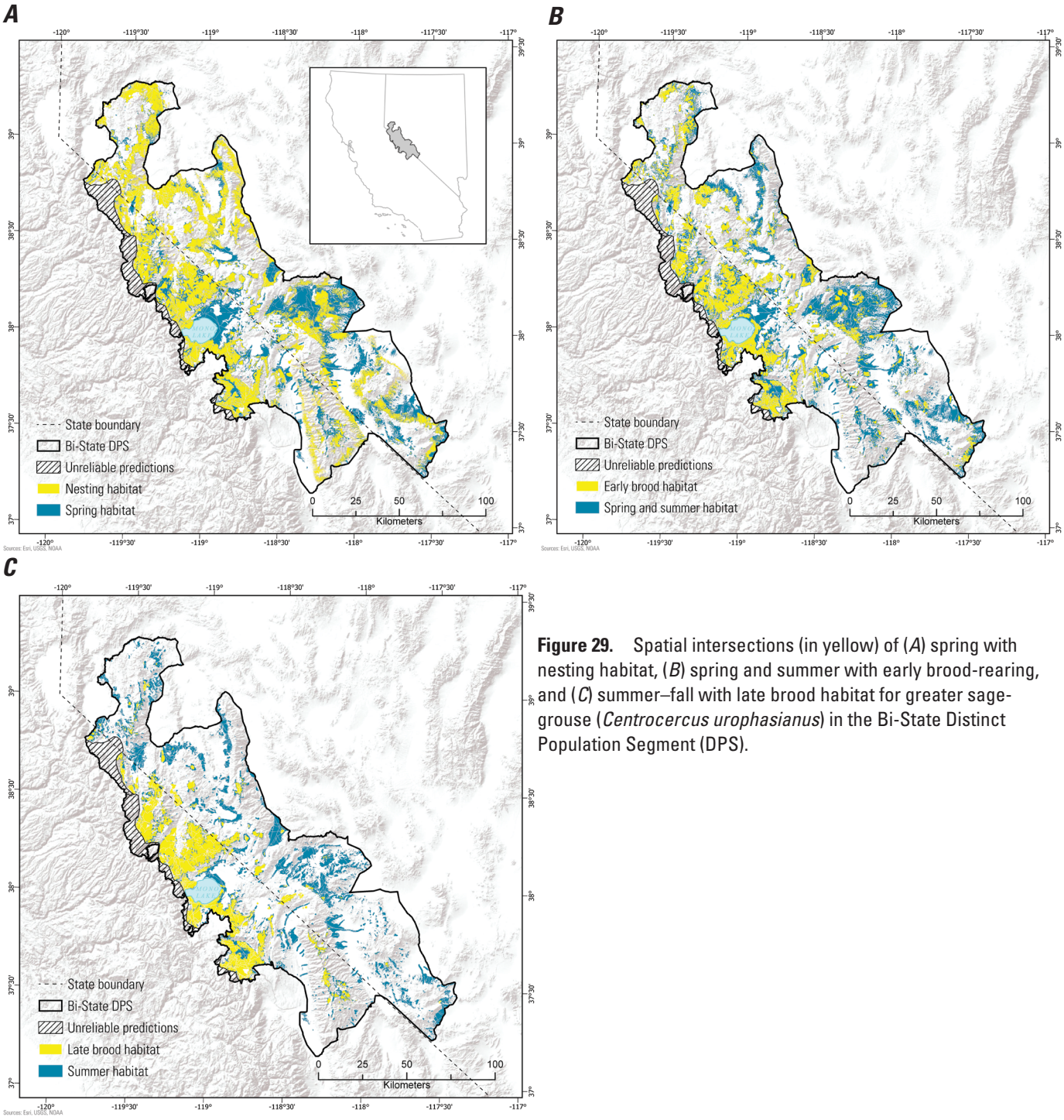

Figure 29. Spatial intersections (in yellow) of (*A*) spring with nesting habitat, (*B*) spring and summer with early brood-rearing, and (*C*) summer–fall with late brood habitat for greater sage-grouse (*Centrocercus urophasianus*) in the Bi-State Distinct Population Segment (DPS).

Disproportionate use was most evident for Bodie Hills, Desert Creek, Fales, Long Valley, and Parker Meadows, while large expanses of under-utilized available habitat were evident for White Mountains. Within the nesting and early-brood rearing life stages, Bodie Hills comprised the most occupied nesting habitat; disproportionate use was most evident for Bodie Hills, Long Valley, Desert Creek, and Fales; and underutilization was most evident for White Mountains. Patterns were similar during the late-brood rearing life stage, except for low percentages (that is, less than 5 percent) of occupied habitat for Pine Nuts, Desert Creek, Mount Grant, Parker Meadows, Sagehen, and White Mountains, and strongest evidence for under-utilization for Pine Nuts and White Mountains.

Table 20. Percent of all modeled selected habitat and habitats likely to be occupied by existing greater sage-grouse (*Centrocercus urophasianus*) populations within subpopulations of the Bi-State Distinct Population Segment by phenological and reproductive life stage seasons.

[SH, selected habitat; OH, occupied habitat; OH/SH, ratio of selected to occupied habitat; E, early; L, late; Repro, all reproductive life stages]

Subpopulation	Type	Phenological				Life-Stage			
		Spring	Summer	Winter	Annual	Nest	E-brood	L-brood	Repro
Bodie Hills	SH	14.4	15.9	12.6	12.1	11.4	19.8	30.6	12.6
Bodie Hills	OH	26.2	27.5	25.0	24.6	22.7	31.0	38.8	24.7
Bodie Hills	OH/SH	1.8	1.7	2.0	2.0	2.0	1.6	1.3	2.0
Desert Creek	SH	6.7	6.2	6.5	6.2	9.1	8.9	3.9	8.2
Desert Creek	OH	11.0	9.6	10.9	10.7	14.1	11.9	5.0	13.0
Desert Creek	OH/SH	1.6	1.5	1.7	1.7	1.5	1.3	1.3	1.6
Fales	SH	5.5	7.1	4.1	5.1	6.6	8.0	15.4	7.3
Fales	OH	9.7	10.0	7.9	9.4	10.6	10.6	15.3	11.2
Fales	OH/SH	1.8	1.4	1.9	1.9	1.6	1.3	1.0	1.5
Long Valley	SH	5.7	8.2	5.7	5.1	6.5	8.7	14.2	6.1
Long Valley	OH	11.5	14.5	13.1	11.5	12.1	13.3	17.4	11.5
Long Valley	OH/SH	2.0	1.8	2.3	2.3	1.9	1.5	1.2	1.9
Mount Grant	SH	12.9	12.9	13.5	12.8	14.8	10.8	6.2	14.0
Mount Grant	OH	11.7	10.6	14.7	13.7	10.9	8.2	4.9	10.4
Mount Grant	OH/SH	0.9	0.8	1.1	1.1	0.7	0.8	0.8	0.7
Parker Meadows	SH	2.1	2.7	1.9	1.8	2.4	3.6	5.5	2.2
Parker Meadows	OH	3.0	3.2	3.0	2.8	3.0	3.8	5.0	2.9
Parker Meadows	OH/SH	1.4	1.2	1.6	1.6	1.3	1.1	0.9	1.3
Pine Nut	SH	10.4	10.4	7.9	9.7	16.4	13.9	4.4	15.0
Pine Nut	OH	11.0	8.5	9.4	11.1	14.4	9.6	1.5	13.4
Pine Nut	OH/SH	1.1	0.8	1.2	1.1	0.9	0.7	0.3	0.9
Sagehen	SH	8.7	8.8	8.7	8.6	6.0	10.8	12.4	7.1
Sagehen	OH	6.5	6.7	6.7	6.1	5.5	7.6	9.1	5.7
Sagehen	OH/SH	0.7	0.8	0.8	0.7	0.9	0.7	0.7	0.8
White Mountains	SH	33.7	27.9	39.1	38.7	26.8	15.5	7.5	27.6
White Mountains	OH	9.5	9.5	9.3	10.3	6.9	4.0	3.1	7.1
White Mountains	OH/SH	0.3	0.3	0.2	0.3	0.3	0.3	0.4	0.3

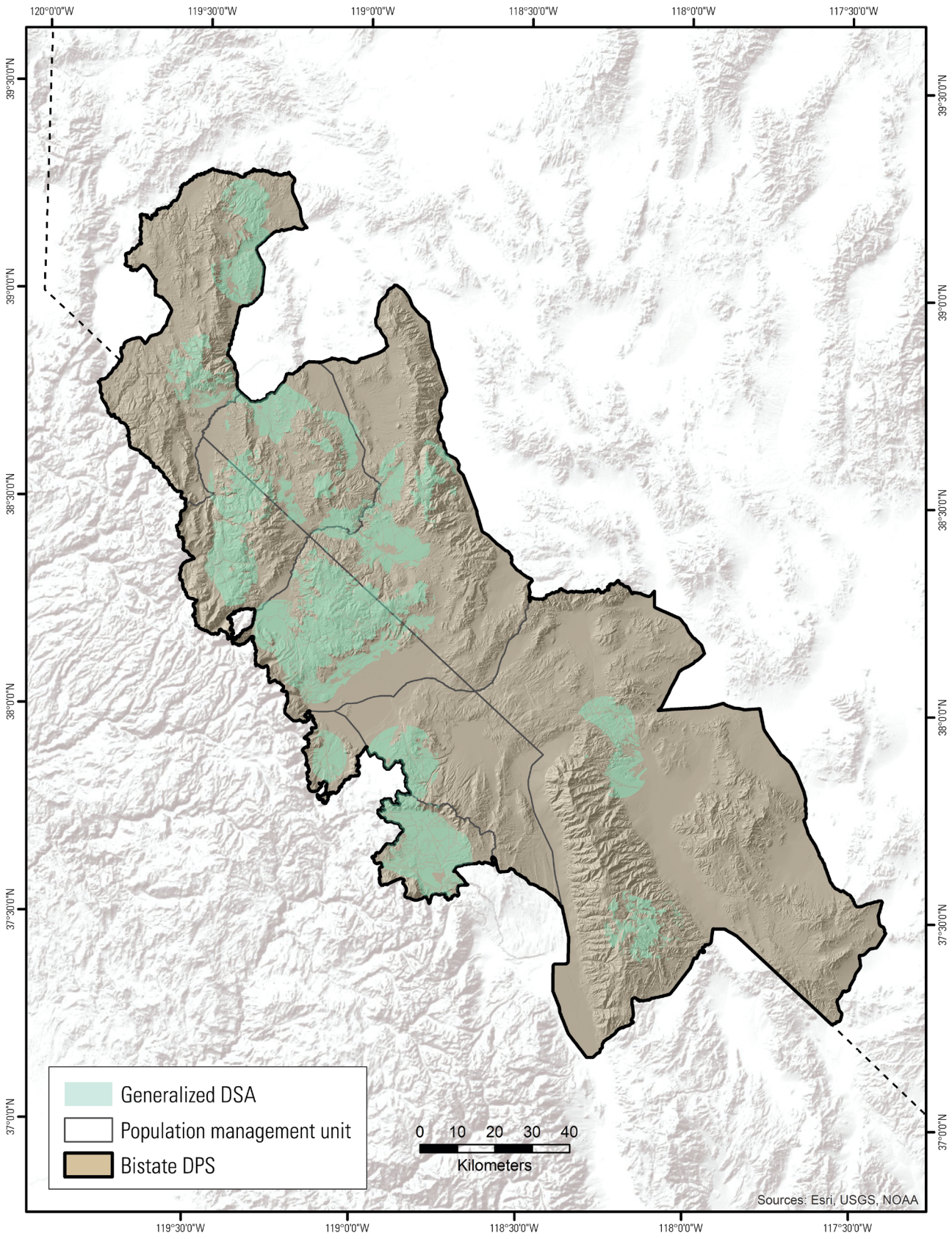

Figure 30. Average annual distributional area (DSA) at the 99 percent isopleth during one population cycle (2008–2018) for greater sage-grouse (*Centrocercus urophasianus*) across all subpopulations in the Bi-State Distinct Population Segment.

Objective 6. Effects of Precipitation and Managed Water Delivery on Brood Habitat

We used 939 locations from 65 broods to inform the analysis of all mesic resources in Long Valley. In step 1 of the model selection process, NDVI within 1,000 m of the mesic edge (NDVI.1000) was the best predictor scale for greenness with a model weight (w) of 0.751 and was carried forward to step 2 (table 21). In step 2, the best model comprised an interaction between distance to mesic resource edge (MESIC.DIST) and ordinal day (DAY), with an additive effect of NDVI.1000 (w = 0.956). A model with interactions of both MESIC.DIST and NDVI.1000 with DAY also provided weight (w = 0.043), and because we were interested in potential temporal effects, we moved both top models on to step 3 to reassess the NDVI scale. When we reassessed the NDVI scale in step 3 using the top 2 models from step 2, the top model contained interactions of both MESIC.DIST and NDVI within 30 m (NDVI.30) with DAY (w = 0.559), while the top model from step 2 dropped to the second most supported model (w = 0.166). The third ranked model comprised interactions of both MESIC.DIST and NDVI.100 with DAY (w = 0.166). For simplicity, we do not discuss the second and third ranked models, but the patterns were very similar to the top model. No other models were within 4.95 ΔAICc units of the top model.

For all mesic resources in Long Valley prior to approximately day 180 (June 29), sage-grouse broods selected generally for habitat within approximately 4 km of the mesic resources (fig. 31*A*). However, after day 180, broods moved to the edges of mesic resources, and then moved further into mesic resources as the season progressed (fig. 31*A*). Additionally, early in the season, broods selected for areas with low late-summer NDVI and selected for a peak of ~0.3 NDVI at day 180 and greater than 0.3 NDVI later in the season (fig. 31*B*). We therefore consider the end of June to be an approximate average cutoff between early brood-rearing and late brood-rearing seasons.

The Convict Creek mesic area analysis used a subset of 620 brood locations representing 66 percent of all locations form the entire study area. The best model included average NDVI within 100 m of the pasture edge in a three-way interaction including MESIC.DIST, average NDVI within 100 m of the pasture edge, and brood rearing period (early versus late; w = 0.438; table 22). The second- and third-ranked models were also supported and included three-way interactions with average NDVI throughout the entire pasture (CON.NDVI; w = 0.296) and proportion of the pasture with greater than 0.3 NDVI (w = 0.248). No other models were within 6 ΔAICc units of the top model.

Overall, there was a marked difference in the use of the pasture between seasons. During early brood-rearing, broods generally selected for habitat outside the pasture but within approximately 4,000 m (fig. 32*A*). The condition of the pasture did not affect habitat use during early brood-rearing. During late brood-rearing, broods generally selected for the edge of the pasture within approximately 1,000 m (fig. 32*B*). When the pasture edge was dry (indicated by lower average NDVI values), broods tended to move further inside the pasture away from the edge. When the pasture edge was greener, broods tended to use the upland side of the edge and even expanded further away from the edge.

Across the study period, water deliveries to Diversion 26 and 27 contributed more to greenness of Convict Creek compared to unmanaged deliveries (fig. 33). Mountain precipitation during winter still had evidence of relative importance (approximately 60 percent of Diversion 27 importance), while local precipitation as rain during spring and summer had minimal impact on greenness. Segmented regression analyses indicated that greenness, measured by either the proportional area within 100 m of the edge with NDVI greater than 0.3 or the average NDVI within 100 m of the edge, reached an approximate asymptote after deliveries exceeded approximately 2,900 acre-feet from Diversions 26 and 27 (fig. 34). We stress that we have no information regarding how timing, location, or pulses of water delivery from these irrigation ditches influences greenness.

We quantified spatial transitions of brooding sage-grouse into both managed and unmanaged mesic resources as greenness changed over time. Generally, the upland-mesic resource interface, or edge, provides cover from shrubs on the upland side while also providing food in the form of green vegetation within the meadow in close proximity (Trueblood, 1954; Casazza and others, 2011). However, during dry years, edges support less green vegetation, causing females with broods to move further from the edge into the meadow interior where there is less concealment cover. These movements may also incur subsequent increased energetic demands and mortality risk through decreased body condition and susceptibility to predation. Lastly, our findings help independently corroborate a NDVI value of 0.3 recently proposed as a threshold for stimulating productive conditions in mesic habitat types (Donnelly and others, 2016, 2018).

Table 21. Three-step model selection describing models of all mesic resources available to brooding greater sage-grouse (*Centrocercus urophasianus*) in the Long Valley subpopulation within the South Mono Population Management Unit of the Bi-State Distinct Population Segment between 2003 and 2018.

[Step 3 describes final models. All models included year and individual bird as random effects. Additive effects were fit with thin plate regression splines with maximum knots set to 5. Interactive effects were fit using tensor product smooths of cubic regression splines. Number of knots was estimated with maximum likelihood. **Abbreviations**: edf, estimated degrees of freedom of regression splines (f) in the generalized additive mixed model; logLik, log-liklihood; AICc, bias-corrected Akaike's information criterion; Weight, probability the model is the best in the set given the other models in the set. See text for description of model steps and covariates]

Model	edf	logLik	AICc	ΔAICc	Weight
Step 1					
f(NDVI.1000)	4.9	–638.66	1,287.10	0.00	0.751
f(NDVI.400)	4.7	–640.24	1,290.00	2.84	0.182
f(NDVI.30)	4.8	–641.33	1,292.30	5.12	0.058
f(NDVI.100)	4.0	–643.91	1,295.80	8.72	0.010
null	1.0	–650.87	1,303.70	16.60	0.000
Step 2					
f(MESIC.DIST × DAY) + f(NDVI.1000)	19.4	–572.89	1,184.70	0.00	0.956
f(MESIC.DIST × DAY) + f(NDVI.1000 × DAY)	20.8	–574.63	1,190.90	6.22	0.043
f(MESIC.DIST × DAY)	15.3	–583.60	1,197.90	13.19	0.001
f(MESIC.DIST) + f(NDVI.1000 × DAY)	16.5	–609.12	1,251.20	66.58	0.000
f(MESIC.DIST × NDVI.1000)	11.4	–618.06	1,258.90	74.19	0.000
f(MESIC.DIST) + f(NDVI.1000)	5.9	–627.02	1,265.80	81.18	0.000
f(MESIC.DIST × NEAR.MESIC.NDVI)	13.0	–622.33	1,270.60	85.94	0.000
f(NDVI.1000 × DAY)	12.6	–624.43	1,274.20	89.50	0.000
f(MESIC.DIST)	5.0	–632.30	1,274.60	89.90	0.000
f(MESIC.DIST × SA.NDVI)	11.4	–630.09	1,283.10	98.42	0.000
f(NDVI.1000)	4.9	–638.66	1,287.10	102.46	0.000
Step 3					
f(MESIC.DIST × DAY) + f(NDVI.30 × DAY)	20.6	–570.45	1,182.20	0.00	0.559
f(MESIC.DIST × DAY) + f(NDVI.1000)	19.4	–572.89	1,184.70	2.42	0.166
f(MESIC.DIST × DAY) + f(NDVI.100 × DAY)	20.7	–571.62	1,184.70	2.44	0.166
f(MESIC.DIST × DAY) + f(NDVI.30)	18.1	–575.43	1,187.20	4.95	0.047
f(MESIC.DIST × DAY) + f(NDVI.400)	18.7	–575.53	1,188.50	6.27	0.024
f(MESIC.DIST × DAY) + f(NDVI.100)	17.0	–576.45	1,188.90	6.67	0.020
f(MESIC.DIST × DAY) + f(NDVI.400 × DAY)	22.2	–572.98	1,190.40	8.15	0.009
f(MESIC.DIST × DAY) + f(NDVI.1000 × DAY)	20.8	–574.63	1,190.90	8.64	0.007

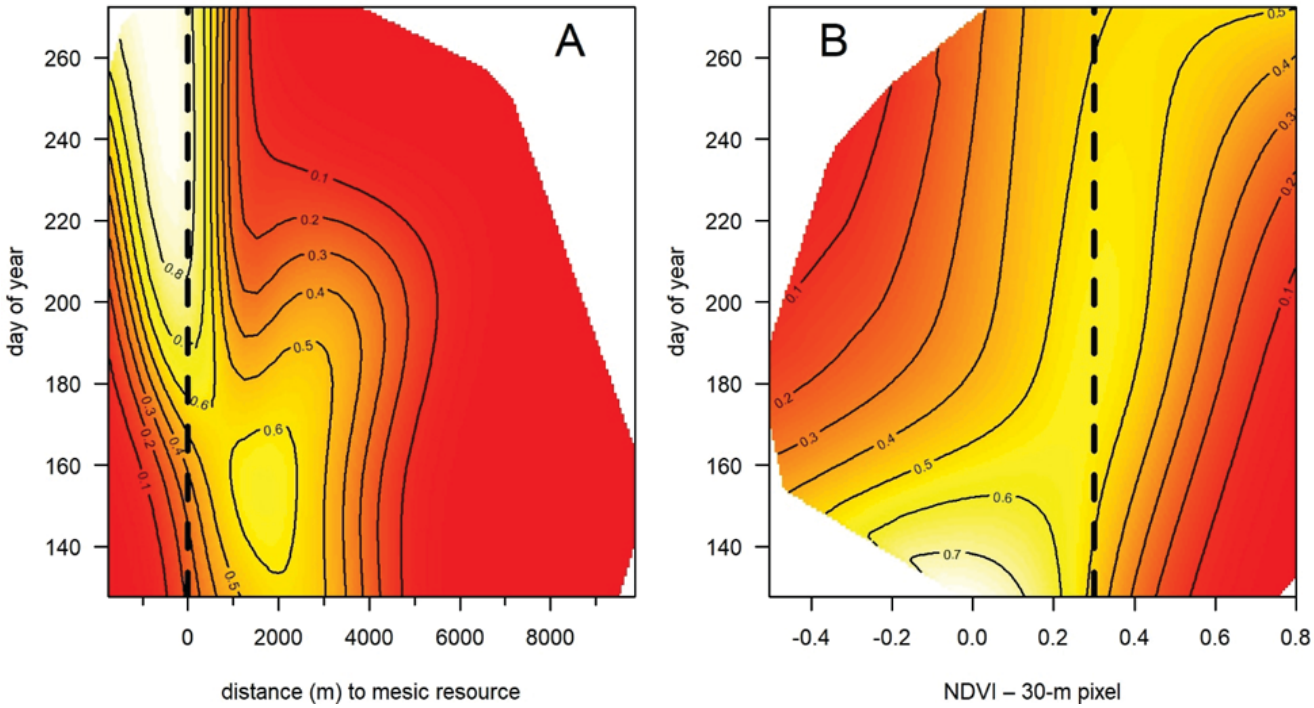

Figure 31. Relative selection probability surface describing the best model of greater sage-grouse (*Centrocercus urophasianus*) brood habitat for the Long Valley subpopulation within the South Mono Population Management Unit of the Bi-State Distinct Population Segment between 2003 and 2018. *A*, Interaction between distance to major mesic resource and ordinal day of year. Vertical dashed line represents a distance of 0 meters (m; that is, edge) with negative values (or to the left) represent probability of selection inside the mesic resource, and positive values (or to the right) represent probability of selection of adjacent upland cover at increasing distances away from the mesic resource edge. *B*, Interaction between normalized difference vegetation index (NDVI) at the 30 m pixel scale and ordinal day of year. Vertical dashed line represents NDVI = 0.3. Contours represent relative probability of selection, with lighter and darker colors representing higher and lower probabilities of selection, respectively.

Table 22. Three-step model selection describing models of all mesic resources available to brooding greater sage-grouse (*Centrocercus urophasianus*) in the Long Valley subpopulation within the South Mono Population Management Unit of the Bi-State Distinct Population Segment between 2003 and 2018.

[Step 3 describes final models. All models included year and individual bird as random effects. Additive effects were fit with thin plate regression splines with maximum knots set to 5. Interactive effects were fit using tensor product smooths of cubic regression splines. Number of knots was estimated with maximum likelihood. **Abbreviations**: edf, estimated degrees of freedom of regression splines (f) in the generalized additive mixed model; logLik, log-liklihood; AICc, bias-corrected Akaike's information criterion; Weight, probability the model is the best in the set given the other models in the set. See text for description of model steps and covariates]

Model	edf	logLik	AICc	ΔAICc	Weight
f(MESIC.DIST × CON.NDVI.100 × SEASON)	59.1	–304.00	727.50	0.00	0.438
f(MESIC.DIST × CON.NDVI × SEASON)	59.4	–304.16	728.30	0.79	0.296
f(MESIC.DIST × CON.NDVI.P3 × SEASON)	60.0	–303.73	728.60	1.13	0.248
f(MESIC.DIST × CON.NDVI.P3.100 × SEASON)	63.5	–302.71	733.80	6.36	0.018
f(MESIC.DIST × SA.NDVI × SEASON)	60.3	–310.50	742.90	15.41	0.000
f(MESIC.DIST)	43.1	–331.33	749.60	22.10	0.000
f(MESIC.DIST × SEASON)	47.5	–327.06	749.80	22.32	0.000
f(MESIC.DIST × CON.NDVI.P3)	51.2	–323.53	750.20	22.75	0.000
f(MESIC.DIST × CON.NDVI.100)	47.5	–328.15	752.10	24.57	0.000
f(MESIC.DIST × CON.NDVI.P3.100)	51.4	–326.69	757.00	29.52	0.000
f(MESIC.DIST × CON.NDVI)	52.5	–327.18	760.40	32.89	0.000
f(MESIC.DIST × SA.NDVI)	53.6	–327.59	763.40	35.94	0.000
null	38.6	–351.62	781.00	53.48	0.000

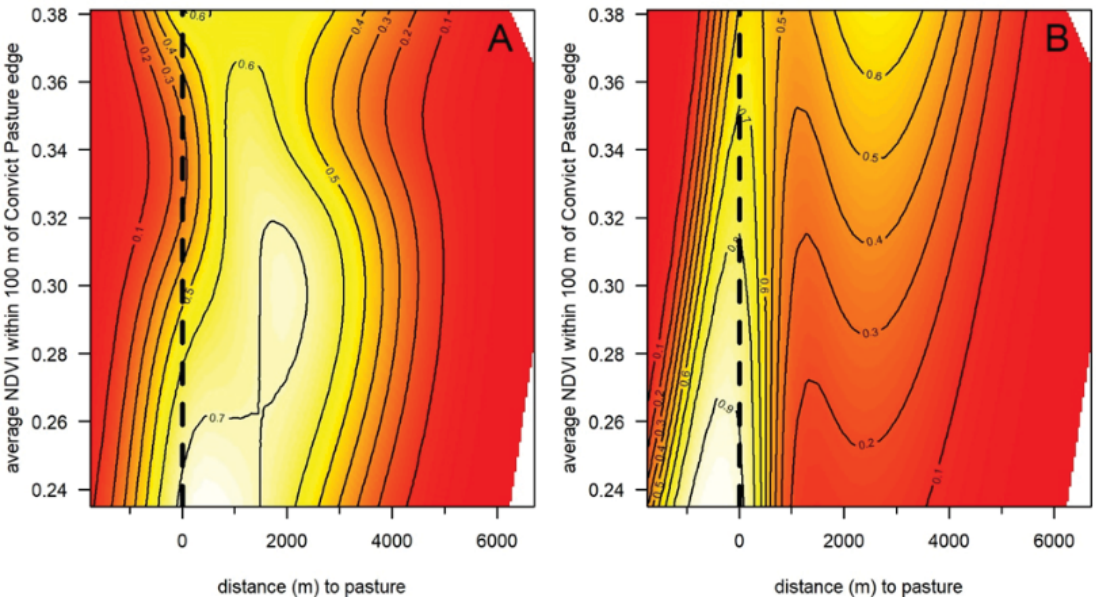

Figure 32. Relative selection probability surface from best model of greater sage-grouse (*Centrocercus urophasianus*) brood habitat near the Convict Creek pasture used by the Long Valley subpopulation within the South Mono Population Management Unit of the Bi-State Distinct Population Segment between 2003 and 2018. Surfaces represent interactions between distance to the pasture and average NDVI within 100 m of the pasture edge during (*A*) early brood-rearing and (*B*) late brood-rearing seasons. Vertical dashed line denotes a distance of 0 m (that is, edge), where negative values (or to the left) represent probability of selection inside the mesic resource, and positive values (or to the right) represent probability of selection of adjacent upland cover at increasing distances away from the mesic resource edge. Contours represent relative probability of selection with lighter and darker colors representing higher and lower probabilities of selection, respectively.

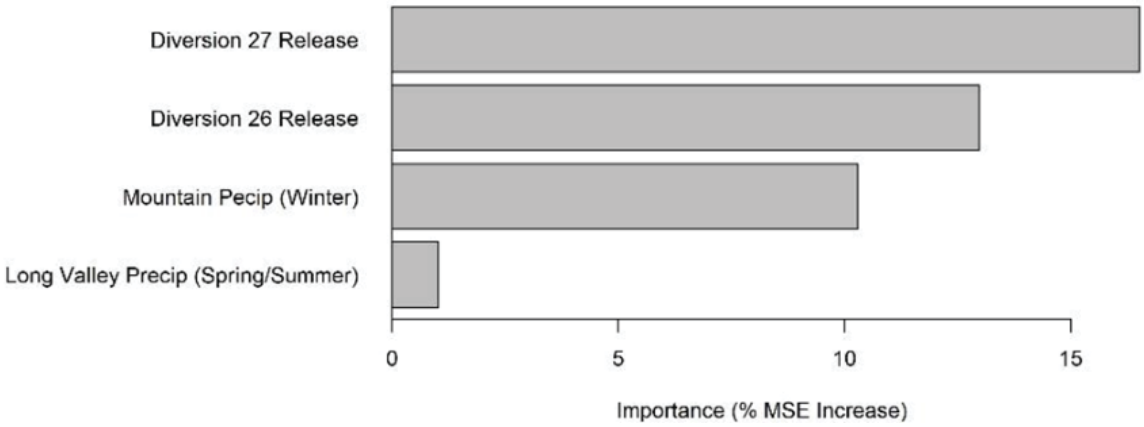

Figure 33. Relative importance of managed and unmanaged water delivery on greenness associated with Convict Creek Pasture used by the Long Valley subpopulation of greater sage-grouse (*Centrocercus urophasianus*) within the South Mono Population Management Unit of the Bi-State Distinct Population Segment.

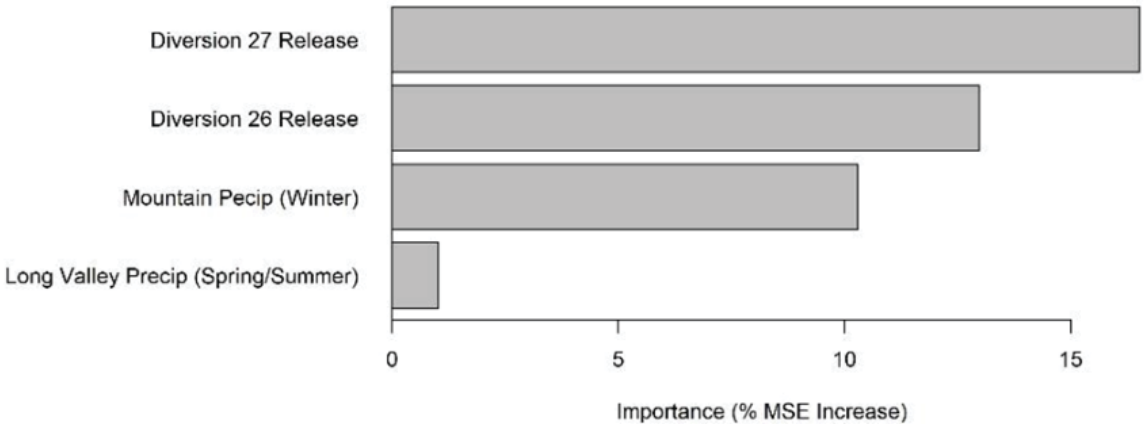

Figure 34. Segmented regression analyses showing relationships between acre-feet releases from Diversion 26 and 27 and Normalized Difference Vegetation Index (NDVI) values within 100 meters of Convict Creek pasture edge used by the Long Valley subpopulation within the South Mono Population Management Unit of the Bi-State Distinct Population Segment.

Summary

We completed an updated assessment of population trends for the Bi-State DPS, as well as for representative populations in Great Basin, across comparative years of nadir in abundance over three periods of short-, mid-, and long-term population cycling. Across all three periods, models did not predict long-term declines in abundance. Although we found substantial declines in recent years, with abundance roughly halved since its 24-year peak during 2012, our models estimated more individuals (approximately 140 percent greater) currently within the Bi-State DPS than a quarter of a century ago. We also found Bi-State DPS has decoupled in trend from other subpopulations within the Great Basin where long-term declines were evidenced. Two hypotheses for these differences in long-term changes in population abundance between the two regions are (1) increase in large-scale impacts of wildfire and invasive grasses within the Great Basin (Coates and others, 2016d) and (2) effectiveness of numerous conservation actions (for example, conifer removal) recently carried out within the Bi-State DPS (Duvall and others, 2017). These hypotheses are not mutually exclusive. However, while the Bi-State, as a whole, has increased in abundance, we found substantial evidence of range contraction. All peripheral populations and one core population (that is, Long Valley) have declined substantially in distributional area and volume, while Bodie Hills has increased substantially over time.

Within the Bi-State DPS substantial variability in abundance existed among subpopulations and nested subpopulations. The majority of the Bi-State DPS was comprised of sage-grouse in Bodie Hills (1,521 sage-grouse using median estimate, 46.0 percent of the overall Bi-State DPS population), which experienced consistent population growth across all three cycles (7, 3, and 6 percent annual increases since 1995, 2001, and 2008) and experienced growth in distributional area and volume. In contrast, the remaining smaller, and in some cases, peripheral subpopulations experienced consistent decline in abundance and distribution across all three cycles. These declines, however, appeared to have negligible impacts on the overall population trend for the Bi-State DPS, largely because of increases at Bodie Hills and shifting of sage-grouse over time between two source populations Long Valley to Bodie Hills. Bodie Hills seems to be less susceptible to effects of long-term drought and responds much more dramatically to pulses of high precipitation that stimulate primary productivity, such as those that occurred prior to 2012. These extreme "boom periods" provide a buffer against long-term declines during periods of drought and contribute to neutrality or slight growth across population cycles for the Bi-State DPS and Bodie Hills (figs. 11 and 13, respectively). Moreover, data from GPS-marked sage-grouse indicate exodus of individuals from the Pine Nut subpopulation, and to a lesser extent, Desert Creek and Fales subpopulations during periods of drought. Further investigation into metapopulation source-sink dynamics is warranted. Perhaps most striking was the dramatic reduction in relative subpopulation abundance for the Long Valley subpopulation in comparison to previous analyses (Coates and others, 2014b, 2018; Matthews and others, 2018). We found this population declined substantially in numbers and distributional area over time. Long Valley was previously estimated to comprise greater than 40 percent of the Bi-State DPS (Coates and others, 2018) but now only comprises approximately 25 percent and has been declining at approximately 4 percent annually since the last period of nadir in 2008. The onset of prolonged drought in 2012 combined with reductions in available managed water during the critical brood-rearing life stage is likely adversely impacting this subpopulation. In addition, Long Valley may be disproportionately impacted by human disturbance and expanding raven populations.

We also conducted an extensive habitat mapping exercise across important phenological and reproductive life stage seasons, which have not been published previously for the Bi-State DPS. Spatial intersections of phenological and life stage maps (fig. 19) could help to identify areas critical to population growth within PMUs and across the Bi-State DPS. In addition, spatial intersections of the generalized DSA (fig. 30), which identifies areas of sage-grouse occupancy with habitat-selection based mapping products (figs. 27, 28), could help further identify occupied habitats where conservation actions and protections may be warranted. These DSA-based intersections can also be updated annually with survey data describing lek distribution and associated IPM-based estimates of abundance, thus facilitating tracking of dynamic habitat occupancy patterns.

Lastly, the Bi-State can be characterized by fragmented subpopulations, largely as a result of conifer expansion into sagebrush ecosystems. Although declines in smaller peripheral populations may have minor contributions to overall population rate of change, extirpation of these populations may impact sage-grouse distribution and connectivity. That is, extirpation of small periphery subpopulations appear to have disproportionate impacts on overall occupied habitat, when compared to their influence on overall population growth trends for the Bi-State DPS.

References Cited

Aldridge, C.L., Saher, D.J., Childers, T.M., Stahlnecker, K.E., and Bowen, Z.H., 2012, Crucial nesting habitat for Gunnison sage-grouse—A spatially explicit hierarchical approach: The Journal of Wildlife Management, v. 76, no. 2, p. 391–406, https://doi.org/10.1002/jwmg.268.

Ammann, G.A., 1944, Determining the age of pinnated and sharp-tailed grouse: The Journal of Wildlife Management, v. 8, no. 2, p. 170–171, https://doi.org/10.2307/3796451.

Arnold, T.W., 2010, Uninformative parameters and model selection using Akaike's information criterion: The Journal of Wildlife Management, v. 74, no. 6, p. 1175–1178, https://doi.org/10.1111/j.1937-2817.2010.tb01236.x.

Atamian, M.T., and Sedinger, J.S., 2010a, Balanced sex ratio at hatch in a greater sage-grouse (*Centrocercus urophasianus*) population: The Auk, v. 127, no. 1, p. 16–22, https://doi.org/10.1525/auk.2009.09136.

Atamian, M.T., Sedinger, J.S., Heaton, J.S., and Blomberg, E.J., 2010b, Landscape-level assessment of brood rearing habitat for greater sage-grouse in Nevada: The Journal of Wildlife Management, v. 74, no. 7, p. 1533–1543, https://doi.org/10.1111/j.1937-2817.2010.tb01281.x.

Austin, J.E., O'Neil, S.T., and Warren, J.M., 2017, Habitat selection by postbreeding female diving ducks—Influence of habitat attributes and conspecifics: Journal of Avian Biology, v. 48, no. 2, p. 295–308, https://doi.org/10.1111/jav.01063.

Baddeley, A., Rubak, E., and Turner, R., 2016, Spatial point patterns—Methodology and applications with R: Boca Raton, London, New York, CRC Press, Taylor & Francis Group, 810 p.

Baruch-Mordo, S., Evans, J.S., Severson, J.P., Naugle, D.E., Maestas, J.D., Kiesecker, J.M., Falkowski, M.J., Hagen, C.A., and Reese, K.P., 2013, Saving sage-grouse from the trees—A proactive solution to reducing a key threat to a candidate species: Biological Conservation, v. 167, p. 233–241, https://doi.org/10.1016/j.biocon.2013.08.017.

Bates, D., Mächler, M., Bolker, B., and Walker, S., 2015, Fitting linear mixed-effects models using lme4: Journal of Statistical Software, v. 67, no. 1, p. 1–48, https://doi.org/10.18637/jss.v067.i01.

Baumgardt, J.A., Reese, K.P., Connelly, J.W., and Garton, E.O., 2017, Visibility bias for sage-grouse lek counts: Wildlife Society Bulletin, v. 41, no. 3, p. 461–470, https://doi.org/10.1002/wsb.800.

Beever, E.A., and Brussard, P.F., 2000, Examining ecological consequences of feral horse grazing using exclosures: Western North American Naturalist, v. 60, no. 3, p. 236–254.

Beever, E.A., and Herrick, J.E., 2006, Effects of feral horses in Great Basin landscapes on soils and ants—Direct and indirect mechanisms: Journal of Arid Environments, v. 66, no. 1, p. 96–112, https://doi.org/10.1016/j.jaridenv.2005.11.006.

Beever, E.A., Tausch, R.J., and Thogmartin, W.E., 2008, Multi-scale responses of vegetation to removal of horse grazing from Great Basin (USA) mountain ranges: Plant Ecology, v. 196, no. 2, p. 163–184, https://doi.org/10.1007/s11258-007-9342-5.

Beever, E.A., and Aldridge, C.L., 2011, Influences of free-roaming equids on sagebrush ecosystems, with a focus on greater sage-grouse, chap. 14 *of* Knick, S.T., and Connelly, J.W., eds., Greater sage-grouse—Ecology and conservation of a landscape species and its habitats: Berkeley, Calif., University of California Press, p. 272–290, https://doi.org/10.1525/california/9780520267114.003.0015.

Bi-State Action Plan, 2012, Bi-state action plan—Past, present, and future actions for conservation of the greater sage-grouse Bi-state distinct population segment: Prepared by the Bi-State Technical Advisory Committee, Nevada and California; Prepared for the Bi-State Executive Oversight Committee for Conservation of Greater Sage-Grouse, 108 p., available at http://sagebrusheco.nv.gov/uploadedFiles/sagebrusheconvgov/content/Archive/Bi-StateActionPlan2012.pdf.

Bi-State Local Planning Group, 2004, Greater sage-grouse conservation plan for the Bi-state plan area of Nevada and eastern California—First edition: 193 p., accessed March 4, 2014, at http://www.ndow.org/uploadedFiles/ndoworg/Content/Nevada_Wildlife/Sage_Grouse/Bi-State-Plan.pdf.

Bi-State Technical Advisory Committee, 2019, 2012–2018 Bi-state accomplishment report: 53 p., accessed July 2019 at https://www.bistatesagegrouse.com/general/page/2012-2018-bi-state-accomplishment-report.

Bivand, R., Pebesma, E.J., and Gómez-Rubio, V., 2013, Applied spatial data analysis with R 2nd ed.: New York, N.Y., Springer-Verlag, 405 p, https://doi.org/10.1007/978-1-4614-7618-4.

Blomberg, E.J., Sedinger, J.S., Atamian, M.T., and Nonne, D.V., 2012, Characteristics of climate and landscape disturbance influence the dynamics of greater sage grouse populations: Ecosphere, v. 3, no. 6, p. 1–20, https://doi.org/10.1890/ES11-00304.1.

Blomberg, E.J., Sedinger, J.S., Gibson, D., Coates, P.S., and Casazza, M.L., 2014, Carryover effects and climatic conditions influence the postfledging survival of greater sage-grouse: Ecology and Evolution, v. 4, no. 23, p. 4488–4499, https://doi.org/10.1002%2Fece3.1139.

Boarman, W.I., and Heinrich, B., 1999, Common raven (*Corvus corax*), *in* Poole, A.F., and Gill, F.B., eds., The Birds of North America, No. 476, The Birds of North America, Inc: Philadelphia, Pa., p. 1–31, https://birdsna.org/Species-Account/bna/home.

Bolker, B.M., Brooks, M.E., Clark, C.J., Geange, S.W., Poulsen, J.R., Stevens, M.H.H., and White, J.-S.S., 2009, Generalized linear mixed models—A practical guide for ecology and evolution: Trends in Ecology & Evolution, v. 24, no. 3, p. 127–135, https://doi.org/10.1016/j.tree.2008.10.008.

Bolstad, P.V., and Lillesand, T.M., 1992, Improved classification of forest vegetation in northern Wisconsin through a rule-based combination of soils, terrain, and Landsat Thematic Mapper data: Forest Science, v. 38, p. 5–20.

Boyce, M.S., and McDonald, L.L., 1999, Relating populations to habitats using resource selection functions: Trends in Ecology & Evolution, v. 14, no. 7, p. 268–272, https://doi.org/10.1016/S0169-5347(99)01593-1.

Boyd, C.S., Davies, K.W., and Collins, G.H., 2017, Impacts of feral horse use on herbaceous riparian vegetation within a sagebrush steppe ecosystem: Rangeland Ecology and Management, v. 70, no. 4, p. 411–417, https://doi.org/10.1016/j.rama.2017.02.001.

Braun, C.E., Britt, T., and Wallestad, R.O., 1977, Guidelines for maintenance of sage grouse habitats: Wildlife Society Bulletin, v. 5, no. 3, p. 99–106, https://www.jstor.org/stable/3781451.

Braun, C.E., Budeau, D.A., and Schroeder, M.A., 2015, Fall population structure of sage-grouse in Colorado and Oregon: Oregon Department of Fish and Wildlife, Wildlife Technical Report 005–2015, 70 p., https://www.dfw.state.or.us/wildlife/research/docs/Fall_Popn_Structure_Sage-grouse_v3182015.pdf.

Brooks, M.L., D'Antonio, C.M., Richardson, D.M., Grace, J.B., Keeley, J.E., DiTomaso, J.M., Hobbs, R.J., Pellant, M., and Pyke, D., 2004, Effects of invasive alien plants on fire regimes: Bioscience, v. 54, no. 7, p. 677–688, https://doi.org/10.1641/0006-3568(2004)054[0677:EOIAPO]2.0.CO;2.

Bureau of Land Management, 2015, Notice of availability of the record of decision and approved resource management plan amendments for the Great Basin region greater sage-grouse sub-regions of Idaho and southwestern Montana; Nevada and northeastern California; Oregon; and Utah: Federal Register, v. 80, p. 57633–57635, https://www.govinfo.gov/content/pkg/FR-2015-09-24/pdf/2015-24213.pdf.

Bureau of Land Management, 2018, Herd area and herd management statistics as of March 1, 2018: accessed December 1, 2018, at https://www.blm.gov/programs/wild-horse-and-burro/about-the-program/program-data.

Burnham, K.P., and Anderson, D.R., 2002, Model selection and multimodel inference 2nd ed.: New York, Springer, 488 p.

Calenge, C., 2006, The package "adehabitat" for the R software—A tool for the analysis of space and habitat use by animals: Ecological Modelling, v. 197, no. 3–4, p. 516–519, https://doi.org/10.1016/j.ecolmodel.2006.03.017.

Casazza, M.L., Coates, P.S., and Overton, C.T., 2011, Linking habitat selection to brood success in greater sage-grouse, *in* Sandercock, B.K., Martin, K., and Segelbacher, G., eds., Ecology, conservation, and management of Grouse—Studies in Avian Biology v. 39: Berkeley, Calif., University of California Press, p. 151–167.

Caswell, H., 2001, Matrix population models—Construction, analysis, and interpretation 2nd ed.: Sunderland, Mass., Sinauer Associates.

Chambers, J.C., Bradley, B.A., Brown, C.S., D'Antonio, C., Germino, M.J., Grace, J.B., Hardegree, S.P., Miller, R.F., and Pyke, D.A., 2014, Resilience to stress and disturbance, and resistance to *Bromus tectorum L.* invasion in cold desert shrublands of western North America: Ecosystems (New York, N.Y.), v. 17, no. 2, p. 360–375, https://doi.org/10.1007/s10021-013-9725-5.

Chambers, J.C., Beck, J.L., Bradford, J.B., Bybee, J., Campbell, S., Carlson, J., Christensen, T.J., Clause, K.J., Collins, G., Crist, M.R., Dinkins, J.B., Doherty, K.E., Edwards, F., Espinosa, S., Griffin, K.A., Griffin, P., Haas, J.R., Hanser, S.E., Havlina, D.W., Henke, K.F., Hennig, J.D., Joyce, L.A., Kilkenny, F.M., Kulpa, S.M., Kurth, L.L., Maestas, J.D., Manning, M., Mayer, K.E., Mealor, B.A., McCarthy, C., Pellant, M., Perea, M.A., Prentice, K.L., Pyke, D.A., Wiechman, L.A., and Wuenschel, A., 2017, Science framework for conservation and restoration of the sagebrush biome—Linking the Department of the Interior's integrated rangeland fire management strategy to long-term strategic conservation actions: U.S Department of Agriculture, Forest Service, Rocky Mountain Research Station, General Technical Report RMRS-GTR-360, Fort Collins, Colo., 213 p., https://www.fs.usda.gov/treesearch/pubs/53983.

Coates, P.S., and Delehanty, D.J., 2010, Nest predation of greater sage-grouse in relation to microhabitat factors and predators: The Journal of Wildlife Management, v. 74, no. 2, p. 240–248, https://doi.org/10.2193/2009-047.

Coates, P.S., Casazza, M.L., Blomberg, E.J., Gardner, S.C., Espinosa, S.P., Yee, J.L., Wiechman, L., and Halstead, B.J., 2013, Evaluating greater sage-grouse seasonal space use relative to leks—Implications for surface use designations in sagebrush ecosystems: The Journal of Wildlife Management, v. 77, no. 8, p. 1598–1609, https://doi.org/10.1002/jwmg.618.

Coates, P.S., Casazza, M.L., Brussee, B.E., Ricca, M.A., Gustafson, K.B., Overton, C.T., Sanchez-Chopitea, E., Kroger, T., Mauch, K., Niell, L., Howe, K., Gardner, S., Espinosa, S., and Delehanty, D.J., 2014a, Spatially explicit modeling of greater sage-grouse (*Centrocercus urophasianus*) habitat in Nevada and northeastern California—A decision-support tool for management: U.S. Geological Survey Open-File Report 2014–1163, 83 p., accessed September 20, 2017, at https://doi.org/10.3133/ofr20141163.

Coates, P.S., Halstead, B.J., Blomberg, E.J., Brussee, B., Howe, K.B., Wiechman, L., Tebbenkamp, J., Reese, K.P., Gardner, S.C., and Casazza, M.L., 2014b, A hierarchical integrated population model for greater sage-grouse (*Centrocercus urophasianus*) in the Bi-state distinct population segment, California and Nevada: U.S. Geological Survey Open-File Report 2014–1165, 34 p., accessed September 20, 2017, at https://doi.org/10.3133/ofr20141165.

Coates, P.S., Andrle, K.M., Ziegler, P.T., and Casazza, M.L., 2016a, Monitoring and research on the bi-state distinct population segment of greater sage-grouse (Centrocercus urophasianus) in the Pine Nut Mountains, California and Nevada—Study progress report, 2011–15: U.S. Geological Survey Open-File Report 2015–1222, accessed December 1, 2017, at https://doi.org/10.3133/ofr20151222.

Coates, P.S., Brussee, B.E., Howe, K.B., Gustafson, K.B., Casazza, M.L., and Delehanty, D.J., 2016b, Landscape characteristics and livestock presence influence common ravens—Relevance to greater sage-grouse conservation: Ecosphere, v. 7, no. 2, https://doi.org/10.1002/ecs2.1203.

Coates, P.S., Casazza, M.L., Brussee, B.E., Ricca, M.A., Gustafson, K.B., Sanchez-Chopitea, E., Mauch, K., Niell, L., Gardner, S., Espinosa, S., and Delehanty, D.J., 2016c, Spatially explicit modeling of annual and seasonal habitat for greater sage-grouse (*Centrocercus urophasianus*) in Nevada and northeastern California—An updated decision-support tool for management: U.S. Geological Survey Open-File Report 2016–1080, accessed December 1, 2017, at https://doi.org/10.3133/ofr20161080.

Coates, P.S., Ricca, M.A., Prochazka, B.G., Brooks, M.L., Doherty, K.E., Kroger, T., Blomberg, E.J., Hagen, C.A., and Casazza, M.L., 2016d, Wildfire, climate, and invasive grass interactions negatively impact an indicator species by reshaping sagebrush ecosystems: Proceedings of the National Academy of Sciences of the United States of America, v. 113, no. 45, p. 12745–12750, https://doi.org/10.1073/pnas.1606898113.

Coates, P.S., Casazza, M.L., Ricca, M.A., Brussee, B.E., Blomberg, E.J., Gustafson, K.B., Overton, C.T., Davis, D.M., Niell, L.E., Espinosa, S.P. and Gardner, S.C., 2016e, Integrating spatially explicit indices of abundance and habitat quality: an applied example for greater sage-grouse management: Journal of Applied Ecology, v. 53, no. 1, p. 83–95.

Coates, P.S., Prochazka, B.G., Ricca, M.A., Wann, G.T., Aldridge, C.L., Hanser, S.E., Doherty, K.E., O'Donnell, M.S., Edmunds, D.R., and Espinosa, S.P., 2017a, Hierarchical population monitoring of greater sage-grouse (*Centrocercus urophasianus*) in Nevada and California—Identifying populations for management at the appropriate spatial scale: U.S. Geological Survey Open-File Report 2017–1089, 49 p., https://doi.org/10.3133/ofr20171089.

Coates, P.S., Prochazka, B.G., Ricca, M.A., Gustafson, K.B., Ziegler, P., and Casazza, M.L., 2017b, Pinyon and juniper encroachment into sagebrush ecosystems impacts distribution and survival of greater sage-grouse: Rangeland Ecology and Management, v. 70, no. 1, p. 25–38, https://doi.org/10.1016/j.rama.2016.09.001.

Coates, P.S., Prochazka, B.G., Ricca, M.A., Halstead, B.J., Casazza, M.L., Blomberg, E.J., Brussee, B.E., Wiechman, L., Tebbenkamp, J., Gardner, S.C., and Reese, K.P., 2018, The relative importance of intrinsic and extrinsic drivers to population growth vary among local populations of greater sage-grouse—An integrated population modeling approach: The Auk, v. 135, no. 2, p. 240–261, https://doi.org/10.1642/AUK-17-137.1.

Coates, P.S., Wann, G.T., Gillette, G.L., Ricca, M.A., Prochazka, B.G., Severson, J.P., Andrle, K.M., Espinosa, S.P., Casazza, M.L., and Delehanty, D.L., 2019, Estimating sightability of greater sage-grouse at leks using an aerial infrared system and *N*-mixture models: Wildlife Biology, v. 2019, no. 1, https://doi.org/10.2981/wlb.00552.

Connelly, J.W., Reese, K.P., and Schroeder, M.A., 2003, Monitoring of greater sage-grouse habitats and populations—College of Natural Resources Experiment Station Bulletin 80: Moscow, Idaho, University of Idaho, https://doi.org/10.5962/bhl.title.153828.

Connelly, J.W., Knick, S.T., Schroeder, M.A., and Stiver, S.J., 2004, Conservation assessment of greater sage-grouse and sagebrush habitats: Western Association of Fish and Wildlife Agencies, Unpublished Report, Cheyenne, Wyo.

Dahlgren, D.K., Guttery, M.R., Messmer, T.A., Caudill, D., Dwayne Elmore, R., Chi, R., and Koons, D.N., 2016, Evaluating vital rate contributions to greater sage-grouse population dynamics to inform conservation: Ecosphere, v. 7, no. 3, https://doi.org/10.1002/ecs2.1249.

Daly, C., Halbleib, M., Smith, J.I., Gibson, W.P., Doggett, M.K., Taylor, G.H., Curtis, J., and Pasteris, P.P., 2008, Physiographically sensitive mapping of climatological temperature and precipitation across the conterminous United States: International Journal of Climatology, v. 28, no. 15, p. 2031–2064, https://doi.org/10.1002/joc.1688.

Dennis, B., and Taper, M.L., 1994, Density dependence in time series observations of natural populations—Estimation and testing: Ecological Monographs, v. 64, no. 2, p. 205–224, https://doi.org/10.2307/2937041.

Didan, K., 2015, MOD13Q1—MODIS/Terra Vegetation Indices 16-day L3 Global 250m SIN Grid, v006: distributed by NASA EOSDIS Land Processes DAAC, https://lpdaac.usgs.gov/products/mod13q1v006/.

Doherty, K.E., Tack, J.D., Evans, J.S. and Naugle, D.E., 2010, Mapping breeding densities of greater sage-grouse—A tool for range-wide conservation planning: Bureau of Land Management Completion Report. Interagency Agreement Number #L10PG00911. Bureau of Land Management, Washington, D.C., USA.

Doherty, K.E., Evans, J.S., Coates, P.S., Juliusson, L.M., and Fedy, B.C., 2016, Importance of regional variation in conservation planning—A rangewide example of the greater sage-grouse: Ecosphere, v. 7, no. 10, https://doi.org/10.1002/ecs2.1462.

Donnelly, J.P., Naugle, D.E., Hagen, C.A., and Maestas, J.D., 2016, Public lands and private waters—Scarce mesic resources structure land tenure and sage-grouse distributions: Ecosphere, v. 7, no. 1, https://doi.org/10.1002/ecs2.1208.

Donnelly, J.P., Allred, B.W., Perret, D., Silverman, N.L., Tack, J.D., Dreitz, V.J., Maestas, J.D., and Naugle, D.E., 2018, Seasonal drought in North America's sagebrush biome structures dynamic mesic resources for sage-grouse: Ecology and Evolution, v. 8, no. 24, p. 12492–12505, https://doi.org/10.1002/ece3.4614.

Dormann, C.F., Elith, J., Bacher, S., Buchmann, C., Carl, G., Carré, G., García Marquéz, J.R., Gruber, B., Lafourcade, B., Leitão, P.J., Münkemüller, T., McClean, C., Osborne, P.E., Reineking, B., Schröder, B., Skidmore, A.K., Zurell, D., and Lautenbach, S., 2013, Collinearity—A review of methods to deal with it and a simulation study evaluating their performance: Ecography, v. 36, no. 1, p. 27–46, https://doi.org/10.1111/j.1600-0587.2012.07348.x.

Drut, M.S., Crawford, J.A., and Gregg, M.A., 1994, Brood habitat use by sage grouse in Oregon: Great Basin Naturalist, v. 54, o. 2, p. 170–176, https://pdfs.semanticscholar.org/2c0a/35ca54cb72e43470095193b5b0a46492aa71.pdf.

Dudko, J.E., Coates, P.S., and Delehanty, D.J., 2018, Movements of female sage grouse *Centrocercus urophasianus* during incubation recess—IBIS: International Journal of Avian Science, v. 161, no. 1, p. 222–229, https://doi.org/10.1111/ibi.12670.

Duvall, A.L., Metcalf, A.L., and Coates, P.S., 2017, Conserving the greater sage-grouse—A social-ecological systems case study from the California–Nevada region: Rangeland Ecology and Management, v. 70, no. 1, p. 129–140, https://doi.org/10.1016/j.rama.2016.08.001.

Dwyer, J.L., Roy, D.P., Sauer, B., Jenkerson, C.B., Zhang, H.K., and Lymburner, L., 2018, Analysis ready data—Enabling analysis of the Landsat archive: Remote Sensing, v. 10, no. 9, https://doi.org/10.3390/rs10091363.

Elliott-Fisk, D.L., 1991, Geomorphology, chap. 2 *of* Hall, C.A., Jr., ed., Natural history of the White-Inyo Range, Eastern California: Berkeley, University of California Press, p. 28–42, http://ark.cdlib.org/ark:/13030/ft3t1nb2pn/.

Evans, J.S., and Oakleaf, J., 2012, Geomorphometry & gradient metrics toolbox (ArcGIS 10.0): accessed on March 1, 2019, at https://www.arcgis.com/home/item.html?id=63ffcecf3b2a45bf99a84cdaedefaccf.

Fedy, B.C., and Doherty, K.E., 2011, Population cycles are highly correlated over long time series and large spatial scales in two unrelated species—Greater sage-grouse and cottontail rabbits: Oecologia, v. 165, no. 4, p. 915–924. https://doi.org/10.1007/s00442-010-1768-0.

Ferrari, S., and Cribari-Neto, F., 2004, Beta regression for modelling rates and proportions: Journal of Applied Statistics, v. 31, no. 7, p. 799–815, https://doi.org/10.1080/0266476042000214501.

Fieberg, J.R., Forester, J.D., Street, G.M., Johnson, D.H., ArchMiller, A.A., and Matthiopoulos, J., 2018, Used-habitat calibration plots—A new procedure for validating species distribution, resource selection, and step-selection models: Ecography, v. 41, no. 5, p. 737–752, https://doi.org/10.1111/ecog.03123.

Fremgen, A.L., Hansen, C.P., Rumble, M.A., Gamo, R.S., and Millspaugh, J.J., 2016, Male greater sage-grouse detectability on leks: The Journal of Wildlife Management, v. 80, no. 2, p. 266–274, https://doi.org/10.1002/jwmg.1001.

Garton, E.O., Connelly, J.W., Horne, J.S., Hagen, C.A., Moser, A., and Schroeder, M., 2011, Greater sage-grouse population dynamics and probability of persistence, chap. 15 *of* Knick, S.T., and Connelly, J.W., eds., Greater sage-grouse—Ecology and conservation of a landscape species and its habitats—Studies in Avian Biology, no. 38: Berkeley, California, University of California Press, p. 292–382, https://doi.org/10.1525/california/9780520267114.003.0016.

Garton, E.O., Wells, A.G., Baumgardt, J.A., and Connelly, J.W., 2015, Greater sage-grouse population dynamics and probability of persistence—Final report to Pew Charitable Trusts: 90 p., https://www.pewtrusts.org/-/media/assets/2015/04/garton-et-al-2015-greater-sagegrouse-population-dynamics-and-persistence-31815.pdf.

Gelman, A., Carlin, J.B., Stern, H.S., and Rubin, D.B., 2014, Bayesian data analysis 2nd ed.: Chapman and Hall, 690 p.

Gessler, P.E., Moore, I.D., McKenzie, N.J., and Ryan, P.J., 1995, Soil-landscape modelling and spatial prediction of soil attributes: International Journal of Geographical Information Systems, v. 9, no. 4, p. 421–432, https://doi.org/10.1080/02693799508902047.

Gibson, D., Blomberg, E.J., Atamian, M.T., and Sedinger, J.S., 2017, Weather, habitat composition, and female behavior interact to modify offspring survival in greater sage-grouse: Ecological Applications, v. 27, no. 1, p. 168–181, https://doi.org/10.1002/eap.1427.

Gillies, C.S., Hebblewhite, M., Nielsen, S.E., Krawchuk, M.A., Aldridge, C.L., Frair, J.L., Saher, D.J., Stevens, C.E., and Jerde, C.L., 2006, Application of random effects to the study of resource selection by animals: Journal of Animal Ecology, v. 75, no. 4, p. 887–898, https://doi.org/10.1111/j.1365-2656.2006.01106.x.

Gitzen, R.A., Millspaugh, J.J., and Kernohan, B.J., 2006, Bandwidth selection for fixed-kernel analysis of animal utilization distributions: The Journal of Wildlife Management, v. 70, no. 5, p. 1334–1344, https://doi.org/10.2193/0022-541X(2006)70[1334:BSFFAO]2.0.CO;2.

Grace, J.B., and Bollen, K.A., 2005, Interpreting the results from multiple regression and structural equation models: Bulletin of the Ecological Society of America, v. 86, no. 4, p. 283–295, https://doi.org/10.1890/0012-9623(2005)86[283:ITRFMR]2.0.CO;2.

Green, A.W., Aldridge, C.L., and O'Donnell, M.S., 2017, Investigating impacts of oil and gas development on greater sage-grouse: The Journal of Wildlife Management, v. 81, no. 1, p. 46–57, https://doi.org/10.1002/jwmg.21179.

Gustafson, K.B., Coates, P.S., Roth, C.L., Chenaille, M.P., Ricca, M.A., Sanchez-Chopitea, E., and Casazza, M.L., 2018, Using object-based image analysis to conduct high-resolution conifer extraction at regional spatial scales: International Journal of Applied Earth Observation and Geoinformation, v. 73, p. 148–155, https://doi.org/10.1016/j.jag.2018.06.002.

Halstead, B.J., Wylie, G.D., Coates, P.S., Valcarcel, P., and Casazza, M.L., 2012, Bayesian shared frailty models for regional inference about wildlife survival: Animal Conservation, v. 15, no. 2, p. 117–124, https://doi.org/10.1111/j.1469-1795.2011.00495.x.

Hooten, M.B., and Hobbs, N.T., 2015, A guide to Bayesian model selection for ecologists: Ecological Monographs, v. 85, no. 1, p. 3–28, https://doi.org/10.1890/14-0661.1.

Johnson, C.J., Nielsen, S.E., Merrill, E.H., McDonald, T.L., and Boyce, M.S., 2006, Resource selection functions based on use–availability data—Theoretical motivation and evaluation methods: The Journal of Wildlife Management, v. 70, no. 2, p. 347–357, https://doi.org/10.2193/0022-541X(2006)70[347:RSFBOU]2.0.CO;2.

Kaweck, M.M., Severson, J.P., and Launchbaugh, K.L., 2018, Impacts of wild horses, cattle, and wildlife on riparian areas in Idaho: Rangelands, v. 40, no. 2, p. 45–52, https://doi.org/10.1016/j.rala.2018.03.001.

Kéry, M., and Schaub, M., 2012, Bayesian population analysis using WinBUGS—A hierarchical perspective: San Diego, Calif., Academic Press, 554 p.

Knick, S.T., Hanser, S.E., and Preston, K.L., 2013, Modeling ecological minimum requirements for distribution of greater sage-grouse leks—Implications for population connectivity across their western range, U.S.A: Ecology and Evolution, v. 3, no. 6, p. 1539–1551, https://doi.org/10.1002/ece3.557.

Liaw, A., and Wiener, M., 2002, Classification and regression by randomForest: R News, v. 2–3, p. 18–22, http://cogns.northwestern.edu/cbmg/LiawAndWiener2002.pdf.

Lockyer, Z.B., Coates, P.S., Casazza, M.L., Espinosa, S., and Delehanty, D.J., 2013, Greater sage-grouse nest predators in the Virginia Mountains of northwestern Nevada: Journal of Fish and Wildlife Management, v. 4, no. 2, p. 242–255, https://doi.org/10.3996/122012-JFWM-110R1.

Maestas, J.D., Campbell, S.B., Chambers, J.C., Pellant, M., and Miller, R.F., 2016, Tapping soil survey information for rapid assessment of sagebrush ecosystem resilience and resistance: Rangelands, v. 38, no. 3, p. 120–128, https://doi.org/10.1016/j.rala.2016.02.002.

Manly, B.F., McDonald, L.L., Thomas, D.L., McDonald, L., and Erickson, W.P., 2002, Resource selection by animals—Statistical design and analysis for field studies: London, Chapman, and Hall, 222 p.

Mathews, S.R., Coates, P.S., Prochazka, B.G., Ricca, M.A., Meyerpeter, M.B., Espinosa, S.P., Lisius, S., Gardner, S.C., and Delehanty, D.J., 2018, An integrated population model for greater sage-grouse (*Centrocercus urophasianus*) in the bi-state distinct population segment, California and Nevada, 2003–17: U.S. Geological Survey Open-File Report 2018–1177, 89 p., accessed March 1, 2019, at https://doi.org/10.3133/ofr20181177.

Mensing, S., Smith, J., Burkle Norman, K., and Allan, M., 2008, Extended drought in the Great Basin of western North America in the last two millennia reconstructed from pollen records: Quaternary International, v. 188, no. 1, p. 79–89, https://doi.org/10.1016/j.quaint.2007.06.009.

McCune, B., and Keon, D., 2002, Equations for potential annual direct incident radiation and heat load: Journal of Vegetation Science, v. 13, no. 4, p. 603–606, https://doi.org/10.1111/j.1654-1103.2002.tb02087.x.

McDonald, T.L., 2013, The point process use-availability or presence-only likelihood and comments on analysis: Journal of Animal Ecology, v. 82, no. 6, p. 1174–1182, https://doi.org/10.1111/1365-2656.12132.

Monroe, A.P., Aldridge, C.L., Assal, T.J., Veblen, K.E., Pyke, D.A., and Casazza, M.L., 2017, Patterns in greater sage-grouse population dynamics correspond with public grazing records at broad scales: Ecological Applications, v. 27, no. 4, p. 1096–1107, https://doi.org/10.1002/eap.1512.

Monroe, A.P., Wann, G.T., Aldridge, C.L., and Coates, P.S., 2019, The importance of simulation assumptions when evaluating detectability in population models: Ecosphere, v. 10, no. 7, https://doi.org/10.1002/ecs2.2791.

Muggeo, V.M.R., 2008, Segmented: an R package to fit regression models with broken-line relationships: R News, v. 8, no. 1, p. 20–25.

Nevada Governor's Sage-Grouse Conservation Team, 2004, Greater sage-grouse conservation plan for Nevada and eastern California: accessed March 1, 2019, at http://www.ndow.org/wild/conservation/sg/plan.

Northrup, J.M., Hooten, M.B., Anderson, C.R., Jr., and Wittemyer, G., 2013, Practical guidance on characterizing availability in resource selection functions under a use–availability design: Ecology, v. 94, no. 7, p. 1456–1463, https://doi.org/10.1890/12-1688.1.

O'Donnell, M.S., Edmunds, D.R., Aldridge, C.L., Heinrichs, J.A., Coates, P.S., Prochazka, B.G., and Hanser, S.E., 2019, Designing multi-scale hierarchical monitoring frameworks for wildlife to support management—A sage-grouse case study: Ecosphere, v. 10, no. 9, https://doi.org/10.1002/ecs2.2872.

O'Neil, S.T., Coates, P.S., Brussee, B.E., Jackson, P.J., Howe, K.B., Moser, A.M., Foster, L.J., and Delehanty, D.J., 2018, Broad-scale occurrence of a subsidized avian predator—Reducing impacts of ravens on sage-grouse and other sensitive prey: Journal of Applied Ecology, v. 55, no. 6, p. 2641–2652, https://doi.org/10.1111/1365-2664.13249.

Oyler-McCance, S.J., Taylor, S.E., and Quinn, T.W., 2005, A multilocus population genetic survey of the greater sage-grouse across their range: Molecular Ecology, v. 14, no. 5, p. 1293–1310, https://doi.org/10.1111/j.1365-294X.2005.02491.x.

Oyler-McCance, S.J., Casazza, M.L., Fike, J.A., and Coates, P.S., 2014, Hierarchical spatial genetic structure in a distinct population segment of greater sage-grouse: Conservation Genetics, v. 15, no. 6, p. 1299–1311, https://doi.org/10.1007/s10592-014-0618-8.

Pagano, A.M., and Arnold, T.W., 2009, Estimating detection probabilities of waterfowl broods from ground-based surveys: The Journal of Wildlife Management, v. 73, no. 5, p. 686–694, https://doi.org/10.2193/2007-524.

Patterson, R.L., 1952, The sage grouse in Wyoming: Denver, Colo., Sage Books, 341 p.

Perry, N.D., Morey, P., and San Miguel, G., 2015, Dominance of a natural water source by feral horses: The Southwestern Naturalist, v. 60, no. 4, p. 390–393, https://doi.org/10.1894/0038-4909-60.4.390.

Pettorelli, N., Ryan, S., Mueller, T., Bunnefeld, N., Jędrzejewska, B., Lima, M., and Kausrud, K., 2011, The normalized difference vegetation index (NDVI)—Unforeseen successes in animal ecology: Climate Research, v. 46, no. 1, p. 15–27, https://doi.org/10.3354/cr00936.

Plummer, M.T., 2003, JAGS—A program for analysis of Bayesian graphical models using Gibbs sampling: Vienna, Austria, Proceedings of the 3rd International Workshop on Distributed Statistical Computing (DSC 2003), March 20–22, 2003, v. 124, p. 10, http://www.r-project.org/conferences/DSC-2003/.

Plummer, M., 2016, Package 'rjags'—The comprehensive R archive network: accessed January 1, 2017, at http://cran.r-project.org/.

Prochazka, B.G., Coates, P.S., Ricca, M.A., Casazza, M.L., Gustafson, K.B., and Hull, J.M., 2017, Encounters with pinyon-juniper influence riskier movements in greater sage-grouse across the Great Basin: Rangeland Ecology and Management, v. 70, no. 1, p. 39–49, https://doi.org/10.1016/j.rama.2016.07.004.

R-Core Team, 2018, The R project for statistical computing: Vienna, Austria, R Foundation for Statistical Computing, accessed February 2, 2018, at http://www.R-project.org/.

Ricca, M.A., Coates, P.S., Gustafson, K.B., Brussee, B.E., Chambers, J.C., Espinosa, S.P., Gardner, S.C., Lisius, S., Ziegler, P., Delehanty, D.J., and Casazza, M.L., 2018, A conservation planning tool for greater sage-grouse using indices of species distribution, resilience, and resistance: Ecological Applications, v. 28, no. 4, p. 878–896, https://doi.org/10.1002/eap.1690.

Ricker, W.E., 1954, Stock and recruitment: Journal of the Fisheries Research Board of Canada, v. 11, no. 5, p. 559–623, https://doi.org/10.1139/f54-039.

Riley, S.J., DeGloria, S.D., and Elliot, R., 1999, A terrain ruggedness index that quantifies topographic heterogeneity: Intermountain Journal of Sciences, v. 5, no. 1–4, p. 23–27, https://download.osgeo.org/qgis/doc/reference-docs/Terrain_Ruggedness_Index.pdf.

Roberts, D.W., and Cooper, S.V., 1989, Concepts and techniques of vegetation mapping, *in* Proceedings—Land classifications based on vegetation—Applications for resource management: USDA Forest Service INT-GTR-257, Ogden, Utah, p. 90–96.

Row, J.R., and Fedy, B.C., 2017, Spatial and temporal variation in the range-wide cyclic dynamics of greater sage-grouse: Oecologia, v. 185, no. 4, p. 687–698, https://doi.org/10.1007/s00442-017-3970-9.

Rowland, M.W., Wisdom, M.J., Suring, L.H., and Meinke, C.W., 2006, Greater sage-grouse as an umbrella species for sagebrush-associated vertebrates: Biological Conservation, v. 129, no. 3, p. 323–335, https://doi.org/10.1016/j.biocon.2005.10.048.

Runge, C.A., Withey, J.C., Naugle, D.E., Fargione, J.E., Helmstedt, K.J., Larsen, A.E., Martinuzzi, S., and Tack, J.D., 2019, Single species conservation as an umbrella for management of landscape threats: PLoS One, v. 14, no. 1, p. e0209619, https://doi.org/10.1371/journal.pone.0209619.

Sage and Columbian Sharp-Tailed Grouse Technical Committee, 2008, Greater sage-grouse population trends—An analysis of lek count databases 1965–2007: Cheyenne, Wyo., Western Association of Fish and Wildlife Agencies.

Schaub, M., and Abadi, F., 2011, Integrated population models—A novel analysis framework for deeper insights into population dynamics: Journal of Ornithology, v. 152, no. S1, p. 227–237, https://doi.org/10.1007/s10336-010-0632-7.

Schroeder, M.A., Aldridge, C.L., Apa, A.D., Bohne, J.R., Braun, C.E., Bunnell, S.D., Connelly, J.W., Deibert, P.A., Gardner, S.C., Hilliard, M.A., Kobriger, G.D., McAdam, S.M., McCarthy, C.W., McCarthy, J.J., Mitchell, D.L., Rickerson, E.V., and Stiver, S.J., 2004, Distribution of sage-grouse in North America: The Condor, v. 106, no. 2, p. 363–376, https://doi.org/10.1093/condor/106.2.363.

Seager, R., Ting, M., Held, I., Kushnir, Y., Lu, J., Vecchi, G., Huang, H.-P., Harnik, N., Leetmaa, A., Lau, N.-C., Li, C., Velez, J., and Naik, N., 2007, Model projections of an imminent transition to a more arid climate in southwestern North America: Science, v. 316, no. 5828, p. 1181–1184, https://doi.org/10.1126/science.1139601.

Severson, J.P., Hagen, C.A., Maestas, J.D., Naugle, D.E., Forbes, J.T., and Reese, K.P., 2017, Effects of conifer expansion on greater sage-grouse nesting habitat selection: The Journal of Wildlife Management, v. 81, no. 1, p. 86–95, https://doi.org/10.1002/jwmg.21183.

Severson, J.P., Coates, P.S., Prochazka, B.P., Ricca, M.A., Casazza, M.L., and Delehanty, D.J., 2019, Global positioning system tracking devices can decrease greater sage-grouse survival: The Condor—Ornithological Applications, v. 121, no. 3, https://doi.org/10.1093/condor/duz032.

Snyder, K., Huntington, J., Wehan, B., Morton, C., and Stringham, T., 2019, Comparison of landsat and land-based phenology camera normalized difference vegetation index (NDVI) for dominant plant communities in the Great Basin: Sensors (Basel), v. 19, no. 5, p. 1139, https://doi.org/10.3390/s19051139.

Taylor, R.L., Walker, B.L., Naugle, D.E., and Mills, L.S., 2012, Managing multiple vital rates to maximize greater sage-grouse population growth: The Journal of Wildlife Management, v. 76, no. 2, p. 336–347, https://doi.org/10.1002/jwmg.267.

Trueblood, R.W., 1954, The effect of grass reseeding in sagebrush lands on sage grouse populations: All Graduate Theses and Dissertations, Utah State University, Logan. 77 p., https://digitalcommons.usu.edu/etd/4717.

U.S. Fish and Wildlife Service, 2013, Endangered and threatened wildlife and plants; withdrawal of proposed rule to list the bi-state distinct population segment of greater sage-grouse and designate critical habitat: Federal Register, v. 80, no. 78, p. 22827–22866, https://www.govinfo.gov/content/pkg/FR-2015-04-23/pdf/2015-09417.pdf.

U.S. Fish and Wildlife Service, 2015, Endangered and threatened wildlife and plants; 12-Month finding on a petition to list greater sage-grouse *(Centrocercus urophasianus*) as an endangered or threatened species: Federal Register, v. 80, no. 191, p. 59857–59942, https://www.govinfo.gov/content/pkg/FR-2015-10-02/pdf/2015-24292.pdf.

U.S. Fish and Wildlife Service, 2019, Endangered and threatened wildlife and plants; Threatened status for the bi-state distinct population segment of greater sage-grouse and designation of critical habitat: Federal Register, v. 84, no. 71, p. 14909–14910, https://www.govinfo.gov/content/pkg/FR-2019-04-12/pdf/2019-07252.pdf.

U.S. Geological Survey, 2009, National elevation dataset (NED): https://catalog.data.gov/dataset/usgs-national-elevation-dataset-ned.

U.S. Geological Survey, 2014, National hydrography dataset: https://nhd.usgs.gov.

Wakkinen, W.L., Reese, K.P., Connelly, J.W., and Fischer, R.A., 1992, An improved spotlighting technique for capturing sage grouse: Wildlife Society Bulletin, v. 20, no. 4, p. 425–426.

Walters, C.J., 1986, Adaptive management of renewable resources: New York, McGraw Hill, http://pure.iiasa.ac.at/2752.

Wann, G.T., Coates, P.S., Prochazka, B.G., Severson, J.P., Monroe, A.P., and Aldridge, C.L., 2019, Assessing lek attendance of male greater sage-grouse using fine resolution GPS data—Implications for population monitoring of lek mating grouse: Population Ecology, v. 61, no. 2, p. 183–197, https://doi.org/10.1002/1438-390X.1019.

Watanabe, S., 2010, Asymptotic equivalence of Bayes cross validation and widely applicable information criterion in singular learning theory: Journal of Machine Learning Research, v. 11, p. 3571–3594, http://www.jmlr.org/papers/volume11/watanabe10a/watanabe10a.pdf.

Watanabe, S., 2013, A widely applicable Bayesian information criterion: Journal of Machine Learning Research, v. 14, p. 867–897, http://www.jmlr.org/papers/volume14/watanabe13a/watanabe13a.pdf.

Wood, S., 2019, Package ‘mgcv’—Mixed GAM computation vehicle with automatic smoothness estimation—R package version 1.8-28: The R Project for Statistical Computing web page, accessed February 2, 2012, at cran.r-project.org/web/packages/mgcv/mgcv.pdf.

Worton, B.J., 1989, Kernel methods for estimating the utilization distribution in home-range studies: Ecology, v. 70, no. 1, p. 164–168, https://doi.org/10.2307/1938423.

Xian, G., Homer, C., Rigge, M., Shi, H., and Meyer, D., 2015, Characterization of shrubland ecosystem components as continuous fields in the northwest United States: Remote Sensing of Environment, v. 168, p. 286–300, https://doi.org/10.1016/j.rse.2015.07.014.

Appendix 1. Demographic Subcomponent Models for IPM

Adult and yearling survival was estimated using frailty models (Halstead and others, 2012) which assumed constant hazard using discrete monthly intervals created from alive-dead encounter histories. Individuals with unknown fates following the last known fate were right censored (for example, alive or status unknown), which was considered a random process. Sage-grouse identified as yearlings (that is, first year after hatch year) were graduated to the adult age class if they remained alive up to the month of March of the subsequent year of capture. Each encounter interval allowed estimation of unit hazard (*UH*) using a Bernoulli process. An example of model structure with nested random effects took the form:

$$\begin{aligned} IUH_{ahijk} &= \exp\left(\beta_{age,a} + \alpha_i + \gamma_j + \zeta_{ij}\right) \\ \beta_{age,a} &\sim Uniform\left(-20, 0\right) \\ \alpha_i &\sim Normal\left(0, \sigma_\alpha^2\right) \\ \gamma_j &\sim Normal\left(0, \sigma_\gamma^2\right) \\ \zeta_{ij} &\sim Normal\left(0, \sigma_\zeta^2\right) \end{aligned} \quad (1\text{–}1)$$

where *IUH* was a function of random effect for subpopulation α_i, a random effect for year γ_j, a random effect for subpopulation and year ζ_{ij}, each of which were assumed to arise from Normal distributions with mean zero, and variances σ_α^2, σ_γ^2, and σ_ζ^2, respectively. Separate hazard ratios were estimated for each age class ($\beta_{age,a}$), and the same vague prior specified for each. The hazard ratio represented the ratio of hazard rates (in this case, monthly risk of mortality) between the two age classes. Subscripts *a*, *h*, *k*, *i*, and *j* reference age, sage-grouse, month, subpopulation, and year. Following the modeling process, we derived the annual (*an*) survival parameter (*s*) as the following:

$$s_{an,aij} = e^{-CH_{aij}} \quad (1\text{–}2)$$

$$CH_{aij} = \sum_{j=1}^{T=12} UH_{aij} \quad (1\text{–}3)$$

where *CH* represented the cumulative hazard ($T = 12$ months represented annual survival). Inferences of survival models were made from VHF-marked sage-grouse owing to reduced survival probabilities of GPS-marked sage-grouse (Severson and others, 2019).

We did not estimate parameters for nest propensity based on telemetry data because data were too sparse. Thus, we used estimates from Taylor and others (2012) of 0.96 (95-percent confidence interval [CI] = 0.94–0.97) and 0.89 (95-percent CI = 0.87–0.91) as informative priors for adults and yearlings, respectively. We considered these values reliable because of the large number of studies used in the analysis (Taylor and others, 2012). However, we used priors that were slightly wider as a more conservative approach (adults = Beta [97,5] and yearlings = Beta [90,12]) and assumed these proportions to be constant among subpopulation and years.

We developed a log-linear model for clutch size of first (*cl1*) and second (*cl2*) nests using nest encounter data. We assumed clutch size arose from a Poisson distribution which took the form:

$$\begin{aligned} y_{cl,achj} &\sim Poisson\left(\mu_{cl,caj}\right) \\ \log\left(\mu_{cl,caj}\right) &= \beta_{clutch,c} * x_{cl,achj} + \beta_{age,a} + \gamma_j \\ \beta_{clutch,cl} &\sim Normal\left(0, 100\right) \\ \beta_{age,a} &\sim Normal\left(0, 100\right) \\ \gamma_j &\sim Normal\left(0, \sigma_\gamma^2\right) \end{aligned} \quad (1\text{–}4)$$

Thus, the log expected count of clutch size μ_{cl} at clutch *c* and year *j* was considered a linear function of the fixed effects for clutch, $\beta_{clutch,c}$ and age, $\beta_{age,a}$, with a random effect of year, γ_j, that was assumed to arise from a Normal distribution with mean zero, and variance σ_γ^2. Priors for the fixed effects were non-informative.

Survival parameters of first (*ns1*) and second (*ns2*) nests were derived using frailty models as expressed in equation 1–1. We modeled nest survival at discrete daily intervals ($T = 38$) to estimate cumulative survival during the laying and incubation phases. A random effect for individual hen was added to the likelihood to account for individuals with multiple nests within or across seasons. We also fit fixed effects for nest attempt and female age. Separate analyses did not support the inclusion of random effects in the nest survival models (Coates and others, 2018), so estimates by site and year are not reported.

Egg hatchability (*h*) was modeled from successful nests as arising from a Binomial distribution (logit-link function) that took the following form:

$$\begin{aligned} y_{h,ahij} &\sim Binomial\left(p_{h,aij}, n_{h,ahij}\right) \\ \text{logit}\left(p_{h,aij}\right) &= \beta_{age,a} + a_i + \gamma_j + \zeta_{ij} \\ \beta_{age,a} &\sim Normal\left(0,100\right) \\ \alpha_i &\sim Normal\left(0,\sigma_\alpha^2\right) \\ \gamma_j &\sim Normal\left(0,\sigma_\gamma^2\right) \\ \zeta_{ij} &\sim Normal\left(0,\sigma_\zeta^2\right) \end{aligned} \tag{1–5}$$

where $y_{h,aij}$ represents the number of hatched eggs (successes) out of the initial number (that is, number of trials; $n_{h,aij}$) of eggs in a clutch, at subpopulation *i* and year *j*. The logit-link ($p_{h,aij}$) is a linear function of random subpopulation effects a_i, random year effects γ_j, as well as subpopulation and year effects combined ζ_{ij}; all were assumed to arise from normal distributions with mean zero and variances σ_α^2, σ_γ^2, and σ_ζ^2, respectively. The fixed effect for each age class, $\beta_{age,a}$ was assigned a vague prior.

Parameters were derived for the probability of second nest attempt (*np2*) directly from data collected in the Bi-State DPS. Second-nest propensity data were modeled as arising from a Binomial distribution as follows:

$$\begin{aligned} y_{np,aij} &\sim Binomial\left(P_{np2,aij}, n_{np2,aij}\right) \\ logit\left(P_{np2,aij}\right) &= \beta_{age,a} + a_i + \gamma_j + \zeta_{ij} \\ \beta_{age,a} &\sim Normal\left(0,100\right) \\ \alpha_i &\sim Normal\left(0,\sigma_\alpha^2\right) \\ \gamma_j &\sim Normal\left(0,\sigma_\gamma^2\right) \\ \zeta_{ij} &\sim Normal\left(0,\sigma_\zeta^2\right) \end{aligned} \tag{1–6}$$

where the number of unsuccessful nests at each subpopulation in each year were denoted by $n_{np2,aij}$. In this model, $y_{np2,aij}$ represents the number of renests and logit($p_{np2,aij}$) is a linear function of random subpopulation effects a_i, random year effects γ_j, as well as random subpopulation and year effects combined ζ_{ij}, each of which were assumed to arise from Normal distributions with mean zero, and variances σ_α^2, σ_γ^2, σ_ζ^2, respectively. The influences of age on *np2* were measured as fixed effects with magnitude $\beta_{age,a}$, which were derived separately for each age class.

Chick survival (*cs*) probabilities were derived from two brood counts with time interval lengths that varied across the 16-year study period. However, the number of days elapsed from nest hatch to brood count varied by study year (2003–05, 50 days; 2007–09, 35 days; 2010–11, 28 days; 2012–18, 50 days). Therefore, we used an adjustment in estimating survival probabilities depending on the year of study. We modeled chick survival based on brood count data as arising from a Binomial distribution where the initial brood size was scored as the number of trials, and chicks that survived to days *d* were scored as successes and took the following form:

$$y_{cs,abi} \sim Binomial\left(p_{cs,abid}, n_{cs,abi}\right)$$

where *d* on the binomial probability *p* is $d = d(j)$ and represents one of three survival periods depending on the year *j* of data collection (d = 28, 35, or 50). For a 35-day interval, the probability of survival is modeled by this logistic relationship:

$$\begin{aligned} \text{logit}\left(p_{cs,abi,35}\right) &= \beta_{age,a} + \beta_{dd} * x_{dd,abi} + a_i \\ \beta_{age,a} &\sim Normal\left(0,100\right) \\ \beta_{dd} &\sim Normal\left(0,100\right) \\ \alpha_i &\sim Normal\left(0,\sigma_\alpha^2\right) \end{aligned} \tag{1–7}$$

In this model, $y_{cs,abi}$ represents the number of chicks that survived for each brood, *b*, at subpopulation *i*. The logit($p_{cs,abi,35}$) is a linear function of random subpopulation effects a_i. The influence of age and density dependence on chick survival were measured as fixed effects with magnitude $\beta_{age,a}$ and β_{dd}, where the the density dependent variable was the natural log of abundance with a 1-year lag. We assumed a constant hazard function, and consistent with this assumption, the probabilities of survival for the other intervals are related as follows:

$$p_{cs,abid} = \begin{Bmatrix} \left(p_{cs,abi,35}\right)^{28/35}, & t = 28 \\ p_{cs,abi,35}, & t = 35 \\ \left(p_{cs,abi,35}\right)^{50/35}, & t = 50 \end{Bmatrix} \tag{1–9}$$

Juvenile sage-grouse (*js*; post-fledging, greater than 35 days and less than 1 year old) were not radio-marked and tracked in the Bi-State DPS. However, we derived a posterior distribution of juvenile survival rates (*js*) during this period by using an informative prior of 0.75 (95-percent CI = 0.67–0.82) reported in Taylor and others (2012) in the form of Beta (100,34).

References Cited

Coates, P.S., Prochazka, B.G., Ricca, M.A., Halstead, B.J., Casazza, M.L., Blomberg, E.J., Brussee, B.E., Wiechman, L., Tebbenkamp, J., Gardner, S.C., and Reese, K.P., 2018, The relative importance of intrinsic and extrinsic drivers to population growth vary among local populations of greater sage-grouse—An integrated population modeling approach: The Auk, v. 135, no. 2, p. 240–261, https://doi.org/10.1642/AUK-17-137.1.

Halstead, B.J., Wylie, G.D., Coates, P.S., Valcarcel, P., and Casazza, M.L., 2012, Bayesian shared frailty models for regional inference about wildlife survival: Animal Conservation, v. 15, no. 2, p. 117–124, https://doi.org/10.1111/j.1469-1795.2011.00495.x.

Severson, J.P., Coates, P.S., Prochazka, B.P., Ricca, M.A., Casazza, M.L., and Delehanty, D.J., 2019, Global positioning system tracking devices can decrease greater sage-grouse survival: The Condor—Ornithological Applications, v. 121, no. 3, https://doi.org/10.1093/condor/duz032.

Taylor, R.L., Walker, B.L., Naugle, D.E., and Mills, L.S., 2012, Managing multiple vital rates to maximize greater sage-grouse population growth: The Journal of Wildlife Management, v. 76, no. 2, p. 336–347, https://doi.org/10.1002/jwmg.267.

Appendix 2. State-Space Model Formulation for Hierarchical Signal Analysis

Posterior parameter distributions were generated for each lek, subpopulations (hereafter, nested scale), and entire Bi-State (hereafter, region) using a nested design, which took the form:

$$N_{l,t+1} = N_{l,t} \times \lambda_{l,t} \quad (2\text{–}1)$$

$$\lambda_{l,t} \sim \text{Normal}\left(\eta_{l,t}, \sigma_l^2\right)\text{T}(0,) \quad (2\text{–}2)$$

$$y_{l,t} \sim \text{Poisson}\left(N_{l,t}\right) \quad (2\text{–}3)$$

$$N_{l,t} \sim \text{Normal}\left(y_{l,t'}, 100\right)\text{T}(0,) \quad (2\text{–}4)$$

$$\sigma_l^2 \sim \text{Uniform}(0,5) \quad (2\text{–}5)$$

$$\eta_{l,t} \sim \text{Normal}\left(\eta_{c,t}, \sigma_{c,t}^2\right)\text{T}(0,) \quad (2\text{–}6)$$

$$\sigma_{c,t}^2 \sim \text{Uniform}(0,5) \quad (2\text{–}7)$$

$$\eta_{c,t} \sim \text{Normal}\left(\eta_{r,t}, \sigma_{r,t}^2\right)\text{T}(0,) \quad (2\text{–}8)$$

$$\sigma_{r,t}^2 \sim \text{Uniform}(0,5) \quad (2\text{–}9)$$

$$\eta_{r,t} \sim \text{Normal}\left(\eta_{p,t}, \sigma_{p,t}^2\right)\text{T}(0,) \quad (2\text{–}10)$$

$$\sigma_{p,t}^2 \sim \text{Uniform}(0,5) \quad (2\text{–}11)$$

$$\eta_{p,t} \sim \text{Normal}\left(\eta_{\hat{p}}, \sigma_{\hat{p}}^2\right)\text{T}(0,) \quad (2\text{–}12)$$

$$\eta_{\hat{p}} \sim Normal(1,10)\text{T}(0,) \quad (2\text{–}13)$$

$$\sigma_{\hat{p}}^2 \sim \text{Uniform}(0,5) \quad (2\text{–}14)$$

Here, the state process (eqs. 2–1 and 2–2) was modeled while accounting for observation error (eq. 2–3). Equation 2–3 mapped the true state of the process onto the observed data ($y_{l,t}$), which in this case were individual maximum counts (y) at a given lek (l) and year (t). The errors in the counts were modeled using a Poisson distribution with a mean equal to the variance. Use of a Poisson error structure, as specified in equation 2–3, assumed that observation error increased as the true number of birds present on the lek increased, which was a reasonable assumption for counts of sage-grouse at leks (Coates and others, 2019). Priors for the initial ($t = 1$) population size of each lek were specified using a normal distribution with mean equal to the first observed count ($y_{l,1}$) and variance of 100 (eq. 2–4). Equations 2–5 through 2–14 describe the state process in greater detail via the specification of spatiotemporally nested random effects, priors, and their hyperparameters. The random effects structure was chosen based on the structure of the data and derived parameters of interest. As such, random effects consisted of a hierarchical nesting of lek within year ($\eta_{l,t}$), which was distributed normally about sub-population within year ($\eta_{c,t}$; eq. 2–6), which was distributed normally about region within year ($\eta_{r,t}$; eq. 2–8), which was distributed normally about superpopulation within year ($\eta_{p,t}$; eq. 2–10), which was distributed normally about the long-term superpopulation growth rate ($\eta_{\bar{p}}$; eq. 2–12). The T(,) construct was added to the right side of normally distributed stochastic nodes, and the lower truncation value set to 0. This censored illogical values for N and λ while avoiding the specification of informative priors.

We carried out the following steps to determine values for decoupling and destabilization. We first used state-space models with nested random effects to derive posterior distributions (PD) of $\hat{\lambda}$ for each lek (that is, smallest spatial scale; point) and the region (that is, largest spatial scale; polygon) from 2000 to 2018. In the next step, we developed a method for describing the relationship between two PD of $\hat{\lambda}$, calculated at spatiotemporally nested scales (for example, a 2002 comparison for a leks or subpopulation to the Bi-State DPS), using a the log odds ratio (LOR) of the two PDs. Comparisons of PDs were only made within the same year and between leks or subpopulations and the Bi-State DPS. The steps required to derive the LOR for the lek were as follows.

The density of the PD of $\hat{\lambda}$ for the lek ($\rho\hat{\lambda}_l$) and the density of the PD of $\hat{\lambda}$ for the climatic region ($\rho\hat{\lambda}_r$) were plotted together along with a vertical line at 1.0 (that is, demarcating stability) and a vertical line at the median of the PD of $\hat{\lambda}$ of the climatic region ($\tilde{X}_r$), effectively slicing the $\rho\lambda_l$ into n (n = 1–4) distinct polygons (fig. 1). Those four polygons were described in terms of the relationship of the $\rho\hat{\lambda}_l$ to the overlapping elements in the plot (that is, $\rho\lambda_r$, 1, $\tilde{X}_r$), namely: (1) decoupled with the region and decreasing (DD); (2) coupled with the region, decreasing, and less than the median of the region PD (CDL); (3) coupled, decreasing, and greater than the median of the region PD (CDG); and (4) stable or increasing (S).

Once isolated and identified, the n polygons that made up the $\rho\hat{\lambda}_l$ were measured separately, in terms of area under the curve (AUC), using the 'overlap' function from the "overlapping" package (Pastore, 2018) in R (R Core Team, 2018). Polygons that were entirely missing received an AUC value of 0.

Because a LOR calculation requires two values (that is, numerator and denominator), we needed to reduce the number of polygons (AUC values) to two, which we accomplished by grouping polygons into the following categories: (1) evidence of decrease (EOD) and (2) evidence against decrease (EAD). For our purposes, the DD AUC was the only area that warranted management consideration because it corresponded to the proportion of the $\rho\hat{\lambda}_l$ that was below stability ($\hat{\lambda}$ = 1) and decoupled downward from the climatic region to which it was spatially nested. In other words, the DD AUC was the only proportion of the $\rho\hat{\lambda}_l$ that provided evidence of a decreasing population not being associated with larger scale events (that is, the same process performed at larger scales would be used to capture those phenomena). Therefore, the DD AUC was assigned to the EOD category. The CDL and CDG AUC were similar to the DD AUC in that they were below stability ($\hat{\lambda}$ = 1), but unlike the DD AUC, they were trending with or outperforming the climatic region to which they were nested. For that reason, when calculating the LOR, we combined the CDL and CDG AUC with the S AUC and treated all three areas as probabilistic evidence against management action (EAD). As such, the LOR formula took the form:

$$ln\left(\frac{EOD}{EAD}\right) = ln\left(\frac{AUC(DD)}{AUC(CDL)+AUC(CDG)+AUC(S)}\right) \quad (2\text{–}20)$$

We used the following steps to determine thresholds for decoupling and destabilization. For the next step, we developed a method that would identify, based on LOR values, whether leks were declining slowly or precipitously, which would then signal the need for possible management action. We did this using an iterative process in program R, which is described as follows.

We created two, identical, 100-element long vectors of threshold values that spanned, at equal intervals, the 2.5th to 97.5th percentiles of LOR values calculated using the methods in step 2. However, we used the much larger database of leks and neighborhood clusters (that is, groups of leks primarily closed to immigration or emigration, and similar to subpopulations defined for the Bi-State DPS) in Nevada and California spanning 2000–15 that was compiled for the Coates and others (2017) original hierarchical signal analysis. We referred to these vectors as the slow-threshold and fast-threshold vectors, where the first element in both vectors corresponded to the minimum slow and fast threshold values, respectively. Likewise, the 100th element from each vector corresponded to the maximum slow and fast threshold values, respectively.

We iterated through every possible combination (n = 10,000) of slow and fast-threshold values (T_s and T_f) by choosing one T_s and one T_f value at every iteration of the simulation analysis. We compared the LOR value (calculated in step 2) for every lek and year combination r to the T_s and one T_f values selected in iteration i. If the LOR value for that lek in that year was at least T_s it received a value of 1, otherwise it received a value of 0. Likewise, if the LOR value for that lek in that year was at least T_f it received a value of 1, otherwise it received a value of 0. The binary indicators for T_s and T_f were kept separate, so that a lek in a given year could possess the following T_s/T_f codes: 0/0, 1/0, 0/1, 1/1.

When a lek had a T_s binary indicator of 1 in three out of four consecutive years, regardless of T_f values over the same time frame, that lek would 'signal' and begin to receive simulated management action. When a lek had a T_f binary indicator of 1 in two out of three consecutive years, regardless of T_s values over the same time frame, that lek would 'signal' and begin to receive simulated management action. The term management action represented an 'improvement' in population growth for the subject lek. The word improvement is placed in quotes because the simulation analysis guarded against overambitious management action in the final step of the simulation, where a comparison of observed and 'improved' growth rates took place (described in detail below). That aside, once a lek signaled, its observed $\hat{\lambda}$ value for that year would be replaced with a $\hat{\lambda}$ value sampled from a distribution of $\hat{\lambda}$ values formed from the pool of leks that did not signal in the same year. To simulate a non-linear relationship between management action and population performance through time, the percentile of the distribution that was sampled would increase every year (fig. 2–1). In the first year following a signal, the offending lek's $\hat{\lambda}$ value would represent the 10th percentile of all non-signaled leks in that same year. Seven years later the observed $\hat{\lambda}$ value would be replaced with the ~57th percentile of all non-signaled leks in that year based on simulations. By sampling from leks that did not signal within the same year, population growth was maximized. In other words, management simulations improve over those with a chosen arbitrary value (for example, $\hat{\lambda} = 1$; stability), which could underperform or outperform observed values, from all leks, during the same time frame. That said, the percentile of the distribution sampled is a subjective choice and changing those values could change the results of the simulation (that is, optimal T_s/T_f value combination chosen). For that reason, we decided to pick a conservative vector of values so that the implementation of this framework would not fail to identify the lowest performing leks, in terms of population growth, that when managed in real-time would contribute to the stability of the population as a whole.

All simulated management action would take place one year after the signal event. For example, if a lek signaled in 2007, the first signs of management action would be detected in 2008. Furthermore, once a lek signaled, it would remain in the signaled state and continue to receive management action for the remainder of the time series. As such, a lek that signaled in 2007 would receive management action from 2008 to 2015 (that is, eight years). This does not imply that active management occur every year of that time frame. It is possible that management action taking place in 2008 could perpetuate through to 2015—a one-time management action with carry-over effects.

At the end of each iteration, an evaluation process took place, wherein we compared a weighted-average of $\hat{\lambda}$ from the original, observed dataset and the improved (simulated management) dataset. Likewise, the same comparison was made between the improved dataset and a value of 1.0 (that is, stability). To account for variability in population sizes across leks, the $\hat{\lambda}$ values were first transformed to intrinsic growth rates ($\hat{r}$), and a weighted-average (based on lek size) was calculated. The weighted-average intrinsic growth rate was then exponentiated to convert it back to $\hat{\lambda}$. An important aside: during the simulated management portion, the observed abundance values were updated to reflect/match the "improved" $\hat{\lambda}$ value. Using the weighted-average observed and improved λ values, a percent improvement was calculated. Using the weighted-average improved and stability values, an optimization index was calculated:

$$1 - \left| \hat{\mu}\hat{\lambda}_{improved} - 1 \right| \tag{2–21}$$

This index places $\hat{\mu}\hat{\lambda}_{improved}$ values, which are the overall averaged $\hat{\lambda}$ across entire population, near 1 at the very top and ranks absolute distances from 1 successively lower and lower (figs. 2–1*A*, *D*). For example, management scenarios that resulted in $\hat{\mu}\hat{\lambda}_{improved}$ values of 1.1 and 0.9 would be ranked equally in terms of their optimization index. The rationale for this type of index was that a management scenario that did not result in population stability was inadequate, while a management scenario that unrealistically improved population growth was too aggressive. In addition to the percent improvement over observed calculation and optimization index, we also kept track of the number of leks that signaled during every iteration of the simulation (figs. 2–1*B*, *E*). When multiple iterations produced $\hat{\mu}\hat{\lambda}_{improved}$ values very near 1, we chose the T_s/T_f combination that resulted in the fewest number of signaled (that is, fewest resources required to reach the objective). We refer to the T_s/T_f pair with the highest $\hat{\mu}\hat{\lambda}_{improved}$ value and fewest number of signals as the optimal combinatorial threshold pair.

Because we cannot assume that management actions will be 100 percent effective, we ran an additional analysis under different efficiency rates. Specifically, we repeated all 10,000 iterations (that is, T_s/T_f combinatorial pairs) under the assumption of management efficacy rates equaling 10 percent, 20 percent, 30 percent, …, 90 percent, and 100 percent. We accomplished this by taking a random subset of the leks that signaled and reinstating their observed λ values instead of the improved λ values. For example, under the 40 percent management efficacy scenario, 60 percent of the signaled leks would not receive an improved λ value. This simulation represented management efforts that failed (for example, a sagebrush planting that did not take), and as such resulted in lower percent improvements in the population as a whole (figs. 2–1*C*, *F*). For the final step, we contrasted LORs for leks and sub-populations against the optimal combinatorial pair (under a 50% management efficacy scenario). Optimal LOR T_s (50% management efficacy) was 0.004000005 and optimal LOR T_f (50% management efficacy) was 0.4557269.

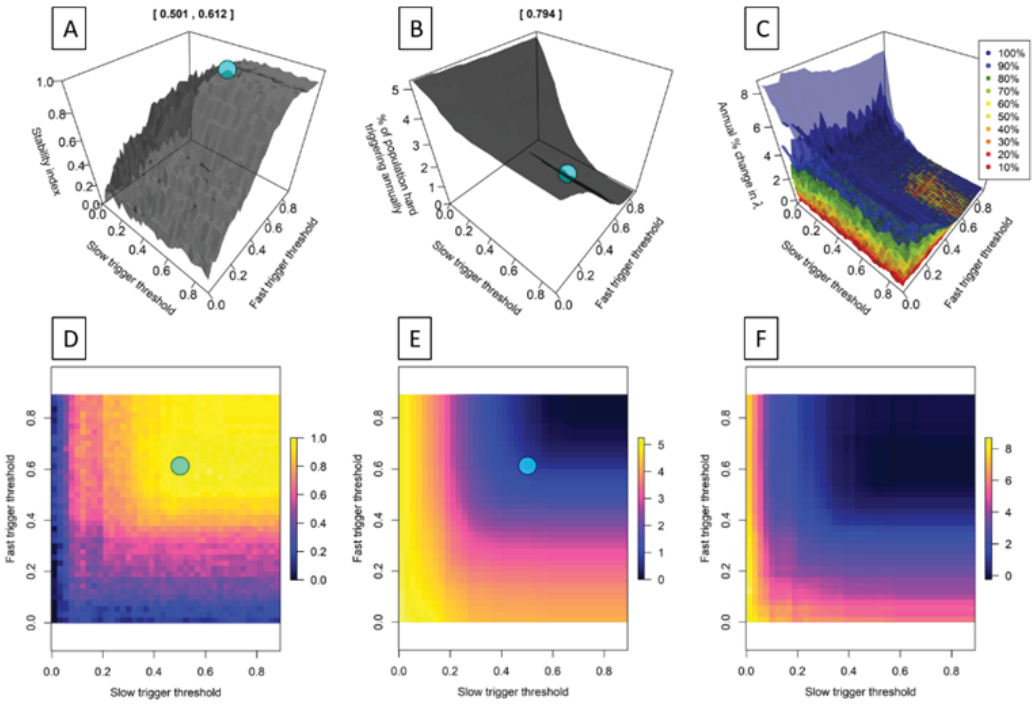

Figure 2–1. The lek threshold optimization process are depicted in panels *A*–*C*. Panels *D*–*F* represent their two-dimensional complements. Panels *A* and *D* represent the optimal slow-fast threshold combination, assuming 50 percent management efficacy, is highlighted by the cyan circle, and their values are presented at the top of panel *A*. Panels *B* and *E* represent the percentage of leks requiring management, assuming 50 percent management efficacy, are highlighted by the cyan circle, and the value presented at the top of panel *B*. Panel *C* represents the annual percent change in λ under varying management efficacy scenarios. Panel *F* represents the annual percent change in λ under a 100 percent management efficacy scenario.

References Cited

Coates, P.S., Prochazka, B.G., Ricca, M.A., Wann, G.T., Aldridge, C.L., Hanser, S.E., Doherty, K.E., O'Donnell, M.S., Edmunds, D.R., and Espinosa, S.P., 2017, Hierarchical population monitoring of greater sage-grouse (*Centrocercus urophasianus*) in Nevada and California—Identifying populations for management at the appropriate spatial scale: U.S. Geological Survey Open-File Report 2017–1089, 49 p., https://doi.org/10.3133/ofr20171089.

Coates, P.S., Wann, G.T., Gillette, G.L., Ricca, M.A., Prochazka, B.G., Severson, J.P., Andrle, K.M., Espinosa, S.P., Casazza, M.L., and Delehanty, D.L., 2019, Estimating sightability of greater sage-grouse at leks using an aerial infrared system and *N*-mixture models: Wildlife Biology, v. 2019, no. 1, https://doi.org/10.2981/wlb.00552.

Pastore, M., 2018, Overlapping—A R package for estimating overlapping in empirical distributions: accessed March 1, 2017, at http://cran.r-project.org/.

R-Core Team, 2018, The R project for statistical computing: Vienna, Austria, R Foundation for Statistical Computing, accessed February 2, 2018, at http://www.R-project.org/.

Appendix 3. List of Environmental Covariates for Resource Selection Models

Table 3–1. All spatial variables, metrics, scales, and sources of data considered in the analyses of greater sage-grouse (*Centrocercus urophasianus*) nest selection and survival in the Bi-State Distinct Population Segment, 2009–17.

[m, meter; % = percent. **Metric legend**: 1, for each scale, mean value of a continuous percent cover for that vegetation type; 2, for each scale, proportion of pixels classified as dominant cover type. For each cover type, pixel was classified as either dominant (1) or not (0); 3, for each scale, mean value of a continuous variable; 4, transformed distances to linear or point features using exponential decay function; 5, density of linear features (that is, length/area), quantified in km × km-2; 6, Density of point features (that is, count/area), quantified in n × km-2; 7, 10-year cumulative value (that is, time-dependent); if area burned in last 10 years, pixel value = 1, 0 otherwise; 7, Normalized Differentiated Vegetation Index (NDVI) is a spatiotemporal variable, measured at 16-day intervals. We created average NDVI variables for each life stage and year, averaging across 16-day intervals corresponding to each life stage (that is, for nesting, we averaged 16-day intervals falling between March and June; for broods, we averaged 16-day intervals falling between July and October; for winter, we averaged 16-day intervals falling between November and February; Coates and others, 2016)]

Type	Metric	Scales (m)	Sources
Vegetation and land cover			
Bare ground	1	75, 167.9, 439.5, 1,451.7	Xian and others, 2015
Litter cover	1	75, 167.9, 439.5, 1,451.7	Xian and others, 2015
Annual grass cover	1	75, 167.9, 439.5, 1,451.7	Xian and others, 2015
Herbaceous canopy cover	1	75, 167.9, 439.5, 1,451.7	Xian and others, 2015
Big sagebrush	1	75, 167.9, 439.5, 1,451.7	Xian and others, 2015
Little sagebrush	1	75, 167.9, 439.5, 1,451.7	Xian and others, 2015
Total sagebrush cover	1	75, 167.9, 439.5, 1,451.7	Xian and others, 2015
Non-sagebrush shrub canopy cover	1	75, 167.9, 439.5, 1,451.7	Xian and others, 2015
Total shrub cover	1	75, 167.9, 439.5, 1,451.7	Xian and others, 2015
Sagebrush shrub heights	3	75, 167.9, 439.5, 1,451.7	Xian and others, 2015
Non-sagebrush shrub heights	3	75, 167.9, 439.5, 1,451.7	Xian and others, 2015
Forests	1	75, 167.9, 439.5, 1,451.7	LANDFIRE, 2014; Homer and others, 2015
Distance to forest	4	Exponential decay	LANDFIRE, 2014; Homer and others, 2015
Cropland	2	75, 167.9, 439.5, 1,451.7	LANDFIRE, 2014; Homer and others, 2015
Distance to cropland	4	Exponential decay	LANDFIRE, 2014; Homer and others, 2015
Wet meadows	2	75, 167.9, 439.5, 1,451.7	LANDFIRE, 2014; Homer and others, 2015
Distance to wet meadow	4	Exponential decay	LANDFIRE, 2014; Homer and others, 2015
Pinyon-juniper canopy cover	1	75, 167.9, 439.5, 1,451.7	Gustafson and others, 2018
Pinyon-juniper cover class 1 canopy cover	1	75, 167.9, 439.5, 1,451.7	Gustafson and others, 2018
Distance to pinyon-juniper cover class 1	4	Exponential decay	Gustafson and others, 2018
Distance to pinyon-juniper cover class 2	4	Exponential decay	Gustafson and others, 2018
Distance to nearest Pinyon-juniper tree	4	Exponential decay	Gustafson and others, 2018
Normalized Differentiated Vegetation Index (NDVI)	3, 7	250, 439.5, 1451.9	NASA LP DAAC, 2017
Topography			
Elevation	3	75, 167.9, 439.5, 1,451.7	U.S. Geological Survey, 2009
Ruggedness	3	75, 167.9, 439.5, 1,451.7	U.S. Geological Survey, 2009; Evans and others, 2014
Slope	3	75, 167.9, 439.5, 1,451.7	U.S. Geological Survey, 2009; Evans and others, 2014
Curvature	3	75, 167.9, 439.5, 1,451.7	U.S. Geological Survey, 2009; Evans and others, 2014
Heat Load Index	3	75, 167.9, 439.5, 1,451.7	U.S. Geological Survey, 2009; Evans and others, 2014
Compound Topographic Index	3	75, 167.9, 439.5, 1,451.7	U.S. Geological Survey, 2009; Evans and others, 2014
Transformed aspect	3	75, 167.9, 439.5, 1,451.7	U.S. Geological Survey, 2009; Evans and others, 2014

Table 3–1. All spatial variables, metrics, scales, and sources of data considered in the analyses of greater sage-grouse (*Centrocercus urophasianus*) nest selection and survival in the Bi-State Distinct Population Segment, 2009–17.—Continued

[m, meter; % = percent. **Metric legend**: 1, for each scale, mean value of a continuous percent cover for that vegetation type; 2, for each scale, proportion of pixels classified as dominant cover type. For each cover type, pixel was classified as either dominant (1) or not (0); 3, for each scale, mean value of a continuous variable; 4, transformed distances to linear or point features using exponential decay function; 5, density of linear features (that is, length/area), quantified in km × km-2; 6, Density of point features (that is, count/area), quantified in n × km-2; 7, 10-year cumulative value (that is, time-dependent); if area burned in last 10 years, pixel value = 1, 0 otherwise; 7, Normalized Differentiated Vegetation Index (NDVI) is a spatiotemporal variable, measured at 16-day intervals. We created average NDVI variables for each life stage and year, averaging across 16-day intervals corresponding to each life stage (that is, for nesting, we averaged 16-day intervals falling between March and June; for broods, we averaged 16-day intervals falling between July and October; for winter, we averaged 16-day intervals falling between November and February; Coates and others, 2016)]

Type	Metric	Scales (m)	Sources
		Water & Streams	
Distance to waterbody	4	Exponential decay	U.S. Geological Survey, 2014
Stream Density	5	75, 167.9, 439.5, 1,451.7	U.S. Geological Survey, 2014
Distance to Stream	4	Exponential decay	U.S. Geological Survey, 2014
Perennial Stream Density	5	75, 167.9, 439.5, 1,451.7	U.S. Geological Survey, 2014
Distance to Perennial Stream	4	Exponential decay	U.S. Geological Survey, 2014
Intermittent Stream Density	5	75, 167.9, 439.5, 1,451.7	U.S. Geological Survey, 2014
Distance to Intermittent Stream	4	Exponential decay	U.S. Geological Survey, 2014
Spring density	5	75, 167.9, 439.5, 1,451.7	U.S. Geological Survey, 2014
Distance to spring	4	Exponential decay	U.S. Geological Survey, 2014
Ditches and canals density	6	75, 167.9, 439.5, 1,451.7	U.S. Geological Survey, 2014
Distance to ditches and canals	4	Exponential decay	U.S. Geological Survey, 2014
Well density	6	75, 167.9, 439.5, 1,451.7	U.S. Geological Survey, 2014
Distance to wells	4	Exponential decay	U.S. Geological Survey, 2014

References Cited

Coates, P.S., Casazza, M.L., Brussee, B.E., Ricca, M.A., Gustafson, K.B., Sanchez-Chopitea, E., Mauch, K., Niell, L., Gardner, S., Espinosa, S., and Delehanty, D.J., 2016, Spatially explicit modeling of annual and seasonal habitat for greater sage-grouse (*Centrocercus urophasianus*) in Nevada and northeastern California—An updated decision-support tool for management: U.S. Geological Survey Open-File Report 2016–1080, accessed December 1, 2017, https://doi.org/10.3133/ofr20161080.

Evans, J.S., Oakleaf, J, Cushman, S.A., and Theobald, D., 2014, An ArcGIS Toolbox for Surface Gradient and Geomorphometric Modeling, version 2.0-0.

Gustafson, K.B., Coates, P.S., Roth, C.L., Chenaille, M.P., Ricca, M.A., Sanchez-Chopitea, E., and Casazza, M.L., 2018, Using object-based image analysis to conduct high-resolution conifer extraction at regional spatial scales: International Journal of Applied Earth Observation and Geoinformation, v. 73, p. 148–155, https://doi.org/10.1016/j.jag.2018.06.002.

Homer, C.G., Dewitz, J., Yang, L., Jin, S., Danielson, P., Xian, P., Coulston, J., Herold, N., Wickham, J., and Megown, K., 2015, Completion of the 2011 national land cover database for the conterminous United States—Representing a decade of land cover change information: Bethesda, Md., Photogrammetric Engineering and Remote Sensing, American Society for Photogrammertry and Remose Sensing, v. 81, p. 345–353, https://cfpub.epa.gov/si/si_public_record_report.cfm?Lab=NERL&dirEntryId=309950.

LANDFIRE, 2014, Existing vegetation type layer: LANDFIRE 1.4.0, available at https://www.landfire.gov.

NASA LP DAAC, 2017, Vegetation indices 16-day L3 Global 250m: MOD13Q1, version 5: available at https://lpdaac.usgs.gov/products/mod13q1v006/.

U.S. Geological Survey, 2009, National elevation dataset (NED): https://catalog.data.gov/dataset/usgs-national-elevation-dataset-ned.

U.S. Geological Survey, 2014, National hydrography dataset: https://nhd.usgs.gov.

Xian, G., Homer, C., Rigge, M., Shi, H., and Meyer, D., 2015, Characterization of shrubland ecosystem components as continuous fields in the northwest United States: Remote Sensing of Environment, v. 168, p. 286–300, https://doi.org/10.1016/j.rse.2015.07.014.

Appendix 4. Preliminary Correlated Candidate Predictor Analysis for Seasonal and Life History Stage Mapping

Potential correlated candidate predictors included multiple characterizations of specific landscape features. For example, percent conifer cover class 1 was measured across 3 different spatial extents in relation to telemetry relocation (that is, via a circular moving windows of radius = 167 m, 439 m, and 1,451 m, respectively), in addition to a covariate that represented distance to conifer cover class 1. While investigating multiple characterizations helps to identify appropriate functional relationships between sage-grouse habitat selection and landscape features, such investigations can also complicate conventional resource selection function (RSF) analysis by inducing collinear variables into RSFs, leading to models that may have redundant parameters, and may be difficult to interpret. For these reasons, we developed an iterative variable selection procedure that explores the performance of each candidate habitat predictor within a multivariate RSF framework while preventing models from including any pair or set of strongly correlated variables.

We initially identified a suite of candidate predictors for seasonal RSF and brood life stage mapping. However, we added an additional scale of a 75 m radius for within the nest RSF analysis, which increased the candidate predictor variables. The purpose of this extent was to represent the most immediate vegetation around nesting sage-grouse and included finer resolution characterization of nest cover that might influence nest predation rates. For nesting RSFs, we initially identified another suite of candidate predictors. Variable screening was performed within a loop of length $M = 2{,}500$ for seasonal and brood models, and $M = 5{,}000$ for nest models. The length of the procedure was set to be longer for nest models due to a larger number of candidate variables to select from and a smaller overall dataset (that is, number of nests versus number of locations) which reduced processing time.

For each iteration within the loop, we performed the following analyses, where $\mathbf{X}$ denotes the matrix of all candidate landscape predictors and j indexes the current iteration in 1:M:

1. We computed the correlation matrix of $\mathbf{X}$ and then used it to randomly generate a new matrix ($\mathbf{X}_{sub}$) of uncorrelated predictors (that is, all $|r| < 0.5$). This was done by first randomly selecting any predictor x_1 from $\mathbf{X}$ and then randomly adding additional predictors x_i to $\mathbf{X}_{sub}$ under the condition that $\text{corr}(x_i, [x_{1-i,\ldots,} x_{k-i}]) < 0.5$.

2. From $\mathbf{X}_{sub}$, we randomly selected 3–6 model predictors to include in a model fit for iteration j (current matrix = $\mathbf{X}_j$). This was done to reduce the influence of potential model misspecification by omitting important predictors while avoiding overfitting from including too many predictors.

3. From each individual bird or brood included in the dataset, we randomly selected 2 used locations, and 2×10 random locations to include in a generalized linear model (GLM), where the response variable was a binary variable indicating a used (y = 1) versus random (y = 0) location. To further allow for computation of model validation statistics for each sub-model, each of these subsets was assigned to either a testing or training dataset, where the probability of being assigned to the testing data was $p = 0.2$.

4. We fit a GLM relating the current set of predictors in the training dataset, $\mathbf{X}_{j,train}$, to the binary response variable Y_{train}. The GLM was akin to a logistic regression model, where $Y \sim Bernoulli(p)$ and the model was fit using the binomial family and a logit link function.

5. We stored the results of the model fit in (4), namely the β coefficient estimate for each predictor included in the model for iteration j, and the Akaike's information criterion (AIC; Burnham and Anderson, 2002) value of that model. We performed resource selection function (RSF) validation of the model using the testing data held out in step (3), and stored Spearman's rank correlation, R^2 (that is, observed versus predicted), and the slope coefficient (Fieberg and others, 2018; Johnson and others, 2006). We calculated variable importance for each predictor k in model j as following:

   a. For each predictor k, we computed the AIC and RSF validation statistics of a new model *without* that predictor

   b. We calculated the difference (dAIC) between AIC(model j without predictor k) and AIC(model j), where a positive value indicated improvement in model fit when k was included (Laforge and others, 2015), and stored this result. Similarly, we calculated the difference between Spearman's rank, R^2, and the slope coefficient of the base sub-model (model j) versus the sub-model without predictor k, such that a positive value again indicated a better model fit with variable k.

6. At the conclusion of the loop, we averaged across all dAIC scores and RSF validation scores for all possible predictors and ranked correlated predictors by their average dAIC across all models that included them.

References Cited

Burnham, K.P., and Anderson, D.R., 2002, Model selection and multimodel inference 2nd ed.: New York, Springer, 488 p.

Fieberg, J.R., Forester, J.D., Street, G.M., Johnson, D.H., ArchMiller, A.A., and Matthiopoulos, J., 2018, Used-habitat calibration plots—A new procedure for validating species distribution, resource selection, and step-selection models: Ecography, v. 41, no. 5, p. 737–752, https://doi.org/10.1111/ecog.03123.

Johnson, C.J., Nielsen, S.E., Merrill, E.H., McDonald, T.L., and Boyce, M.S., 2006, Resource selection functions based on use–availability data—Theoretical motivation and evaluation methods: The Journal of Wildlife Management, v. 70, no. 2, p. 347–357, https://doi.org/10.2193/0022-541X(2006)70[347:RSFBOU]2.0.CO;2.

Laforge, M.P., Vander Wal, E., Brook, R.K., Bayne, E.M., and McLoughlin, P.D., 2015, Process-focussed, multi-grain resource selection functions: Ecological Modelling, v. 305, p. 10–21, https://doi.org/10.1016/j.ecolmodel.2015.03.003.

Appendix 5. Sampled Estimates of Posterior Probability Distributions of Demographic Rates From IPM

Table 5–1. Parameter estimates (median, 50 percent; lower credible interval, 2.5 percent and upper credible interval, 97.5 percent) sampled from the posterior distribution for models density dependence and random effects for greater sage-grouse within the Bi-State Distinct Population Segment between 2008 and 2018.

[Subpopulations: BH, Bodie Hills; FA, Fales; DC, Desert Creek; LV, Long Valley; MG, Mount Grant; PM. Parker Meadows; PN, Pine Nut; SA, Sagehen; WM, White Mountains; —, values indicate overall estimates for respective fixed effect]

Life stage	Density dependence	Random effect	Sub-population	Year	Age	Percentile		
						50.0	2.5	97.5
Chick survival	lag Gompertz	Subpopulation	BH	—	Adult	0.35	0.29	0.44
Chick survival	lag Gompertz	Subpopulation	FA	—	Adult	0.35	0.24	0.51
Chick survival	lag Gompertz	Subpopulation	DC	—	Adult	0.35	0.27	0.46
Chick survival	lag Gompertz	Subpopulation	LV	—	Adult	0.33	0.27	0.42
Chick survival	lag Gompertz	Subpopulation	MG	—	Adult	0.37	0.30	0.49
Chick survival	lag Gompertz	Subpopulation	PM	—	Adult	0.37	0.26	0.52
Chick survival	lag Gompertz	Subpopulation	PN	—	Adult	0.35	0.23	0.48
Chick survival	lag Gompertz	Subpopulation	SA	—	Adult	0.39	0.28	0.53
Chick survival	lag Gompertz	Subpopulation	WM	—	Adult	0.40	0.28	0.57
Chick survival	lag Gompertz	Subpopulation	BH	—	Yearling	0.39	0.32	0.49
Chick survival	lag Gompertz	Subpopulation	FA	—	Yearling	0.39	0.26	0.55
Chick survival	lag Gompertz	Subpopulation	DC	—	Yearling	0.39	0.29	0.51
Chick survival	lag Gompertz	Subpopulation	LV	—	Yearling	0.37	0.29	0.47
Chick survival	lag Gompertz	Subpopulation	MG	—	Yearling	0.41	0.32	0.53
Chick survival	lag Gompertz	Subpopulation	PM	—	Yearling	0.41	0.28	0.57
Chick survival	lag Gompertz	Subpopulation	PN	—	Yearling	0.39	0.24	0.52
Chick survival	lag Gompertz	Subpopulation	SA	—	Yearling	0.43	0.30	0.58
Chick survival	lag Gompertz	Subpopulation	WM	—	Yearling	0.44	0.30	0.62
Clutch size (first)	—	Year	BS	2008	Adult	7.38	6.63	8.43
Clutch size (first)	—	Year	BS	2009	Adult	7.56	6.72	8.68
Clutch size (first)	—	Year	BS	2010	Adult	7.40	6.63	8.42
Clutch size (first)	—	Year	BS	2011	Adult	6.72	5.79	7.53
Clutch size (first)	—	Year	BS	2012	Adult	6.71	5.41	7.85
Clutch size (first)	—	Year	BS	2013	Adult	6.85	5.78	7.91
Clutch size (first)	—	Year	BS	2014	Adult	6.82	5.31	8.09
Clutch size (first)	—	Year	BS	2015	Adult	6.57	5.23	7.50
Clutch size (first)	—	Year	BS	2016	Adult	6.90	6.20	7.61
Clutch size (first)	—	Year	BS	2017	Adult	6.59	5.86	7.29
Clutch size (first)	—	Year	BS	2018	Adult	6.78	6.07	7.45
Clutch size (first)	—	Year	BS	2008	Yearling	6.89	5.94	8.18
Clutch size (first)	—	Year	BS	2009	Yearling	7.06	6.09	8.30
Clutch size (first)	—	Year	BS	2010	Yearling	6.91	6.01	8.13
Clutch size (first)	—	Year	BS	2011	Yearling	6.27	5.33	7.20
Clutch size (first)	—	Year	BS	2012	Yearling	6.25	5.01	7.42
Clutch size (first)	—	Year	BS	2013	Yearling	6.37	5.32	7.56
Clutch size (first)	—	Year	BS	2014	Yearling	6.33	4.94	7.68

Table 5–1. Parameter estimates (median, 50 percent; lower credible interval, 2.5 percent and upper credible interval, 97.5 percent) sampled from the posterior distribution for models density dependence and random effects for greater sage-grouse within the Bi-State Distinct Population Segment between 2008 and 2018.—Continued

[Subpopulations: BH, Bodie Hills; FA, Fales; DC, Desert Creek; LV, Long Valley; MG, Mount Grant; PM. Parker Meadows; PN, Pine Nut; SA, Sagehen; WM, White Mountains; —, values indicate overall estimates for respective fixed effect]

Life stage	Density dependence	Random effect	Sub-population	Year	Age	Percentile		
						50.0	2.5	97.5
Clutch size (first)	—	Year	BS	2015	Yearling	6.11	4.87	7.13
Clutch size (first)	—	Year	BS	2016	Yearling	6.45	5.65	7.27
Clutch size (first)	—	Year	BS	2017	Yearling	6.16	5.42	6.91
Clutch size (first)	—	Year	BS	2018	Yearling	6.32	5.64	7.07
Clutch size (second)	—	Year	BS	2008	Adult	6.96	5.82	8.25
Clutch size (second)	—	Year	BS	2009	Adult	7.13	5.91	8.69
Clutch size (second)	—	Year	BS	2010	Adult	6.99	5.91	8.21
Clutch size (second)	—	Year	BS	2011	Adult	6.30	5.17	7.52
Clutch size (second)	—	Year	BS	2012	Adult	6.30	4.84	7.76
Clutch size (second)	—	Year	BS	2013	Adult	6.43	5.13	7.87
Clutch size (second)	—	Year	BS	2014	Adult	6.40	4.78	7.90
Clutch size (second)	—	Year	BS	2015	Adult	6.16	4.69	7.59
Clutch size (second)	—	Year	BS	2016	Adult	6.49	5.43	7.69
Clutch size (second)	—	Year	BS	2017	Adult	6.20	5.07	7.46
Clutch size (second)	—	Year	BS	2018	Adult	6.38	5.27	7.62
Clutch size (second)	—	Year	BS	2008	Yearling	6.49	5.30	8.00
Clutch size (second)	—	Year	BS	2009	Yearling	6.65	5.40	8.26
Clutch size (second)	—	Year	BS	2010	Yearling	6.52	5.35	7.92
Clutch size (second)	—	Year	BS	2011	Yearling	5.89	4.79	7.18
Clutch size (second)	—	Year	BS	2012	Yearling	5.88	4.50	7.31
Clutch size (second)	—	Year	BS	2013	Yearling	6.00	4.73	7.53
Clutch size (second)	—	Year	BS	2014	Yearling	5.96	4.46	7.54
Clutch size (second)	—	Year	BS	2015	Yearling	5.73	4.35	7.24
Clutch size (second)	—	Year	BS	2016	Yearling	6.06	4.98	7.34
Clutch size (second)	—	Year	BS	2017	Yearling	5.79	4.72	7.04
Clutch size (second)	—	Year	BS	2018	Yearling	5.94	4.89	7.19
Fecundity	—	—	BH	2008	Adult	0.47	0.35	0.63
Fecundity	—	—	BH	2009	Adult	0.49	0.35	0.68
Fecundity	—	—	BH	2010	Adult	0.54	0.40	0.70
Fecundity	—	—	BH	2011	Adult	0.47	0.33	0.63
Fecundity	—	—	BH	2012	Adult	0.37	0.22	0.60
Fecundity	—	—	BH	2013	Adult	0.37	0.22	0.59
Fecundity	—	—	BH	2014	Adult	0.26	0.07	0.41
Fecundity	—	—	BH	2015	Adult	0.31	0.20	0.46
Fecundity	—	—	BH	2016	Adult	0.33	0.25	0.44
Fecundity	—	—	BH	2017	Adult	0.32	0.23	0.43
Fecundity	—	—	BH	2018	Adult	0.30	0.23	0.40
Fecundity	—	—	FA	2008	Adult	0.36	0.14	0.72
Fecundity	—	—	FA	2009	Adult	0.35	0.14	0.63
Fecundity	—	—	FA	2010	Adult	0.33	0.11	0.61

Table 5–1. Parameter estimates (median, 50 percent; lower credible interval, 2.5 percent and upper credible interval, 97.5 percent) sampled from the posterior distribution for models density dependence and random effects for greater sage-grouse within the Bi-State Distinct Population Segment between 2008 and 2018.—Continued

[Subpopulations: BH, Bodie Hills; FA, Fales; DC, Desert Creek; LV, Long Valley; MG, Mount Grant; PM. Parker Meadows; PN, Pine Nut; SA, Sagehen; WM, White Mountains; —, values indicate overall estimates for respective fixed effect]

Life stage	Density dependence	Random effect	Sub-population	Year	Age	Percentile		
						50.0	2.5	97.5
Fecundity	—	—	FA	2011	Adult	0.30	0.11	0.55
Fecundity	—	—	FA	2012	Adult	0.28	0.10	0.54
Fecundity	—	—	FA	2013	Adult	0.29	0.11	0.54
Fecundity	—	—	FA	2014	Adult	0.28	0.07	0.55
Fecundity	—	—	FA	2015	Adult	0.27	0.07	0.52
Fecundity	—	—	FA	2016	Adult	0.28	0.07	0.53
Fecundity	—	—	FA	2017	Adult	0.27	0.07	0.52
Fecundity	—	—	FA	2018	Adult	0.29	0.10	0.56
Fecundity	—	—	DC	2008	Adult	0.33	0.13	0.59
Fecundity	—	—	DC	2009	Adult	0.37	0.19	0.65
Fecundity	—	—	DC	2010	Adult	0.40	0.20	0.63
Fecundity	—	—	DC	2011	Adult	0.40	0.20	0.63
Fecundity	—	—	DC	2012	Adult	0.25	0.06	0.45
Fecundity	—	—	DC	2013	Adult	0.30	0.15	0.55
Fecundity	—	—	DC	2014	Adult	0.34	0.13	0.62
Fecundity	—	—	DC	2015	Adult	0.36	0.18	0.63
Fecundity	—	—	DC	2016	Adult	0.44	0.28	0.64
Fecundity	—	—	DC	2017	Adult	0.34	0.23	0.48
Fecundity	—	—	DC	2018	Adult	0.26	0.18	0.38
Fecundity	—	—	LV	2008	Adult	0.48	0.36	0.63
Fecundity	—	—	LV	2009	Adult	0.43	0.31	0.61
Fecundity	—	—	LV	2010	Adult	0.39	0.28	0.52
Fecundity	—	—	LV	2011	Adult	0.44	0.31	0.59
Fecundity	—	—	LV	2012	Adult	0.25	0.09	0.45
Fecundity	—	—	LV	2013	Adult	0.25	0.06	0.44
Fecundity	—	—	LV	2014	Adult	0.26	0.07	0.46
Fecundity	—	—	LV	2015	Adult	0.26	0.08	0.43
Fecundity	—	—	LV	2016	Adult	0.28	0.21	0.38
Fecundity	—	—	LV	2017	Adult	0.32	0.23	0.43
Fecundity	—	—	LV	2018	Adult	0.29	0.22	0.39
Fecundity	—	—	MG	2008	Adult	0.38	0.15	0.71
Fecundity	—	—	MG	2009	Adult	0.42	0.23	0.75
Fecundity	—	—	MG	2010	Adult	0.41	0.17	0.72
Fecundity	—	—	MG	2011	Adult	0.30	0.08	0.55
Fecundity	—	—	MG	2012	Adult	0.23	0.04	0.43
Fecundity	—	—	MG	2013	Adult	0.29	0.17	0.51
Fecundity	—	—	MG	2014	Adult	0.31	0.09	0.59
Fecundity	—	—	MG	2015	Adult	0.31	0.11	0.57
Fecundity	—	—	MG	2016	Adult	0.30	0.20	0.47
Fecundity	—	—	MG	2017	Adult	0.29	0.20	0.45

Table 5–1. Parameter estimates (median, 50 percent; lower credible interval, 2.5 percent and upper credible interval, 97.5 percent) sampled from the posterior distribution for models density dependence and random effects for greater sage-grouse within the Bi-State Distinct Population Segment between 2008 and 2018.—Continued

[Subpopulations: BH, Bodie Hills; FA, Fales; DC, Desert Creek; LV, Long Valley; MG, Mount Grant; PM. Parker Meadows; PN, Pine Nut; SA, Sagehen; WM, White Mountains; —, values indicate overall estimates for respective fixed effect]

Life stage	Density dependence	Random effect	Sub-population	Year	Age	Percentile		
						50.0	2.5	97.5
Fecundity	—	—	MG	2018	Adult	0.32	0.23	0.48
Fecundity	—	—	PM	2008	Adult	0.30	0.08	0.61
Fecundity	—	—	PM	2009	Adult	0.35	0.20	0.58
Fecundity	—	—	PM	2010	Adult	0.18	0.08	0.34
Fecundity	—	—	PM	2011	Adult	0.06	0.01	0.20
Fecundity	—	—	PM	2012	Adult	0.26	0.05	0.57
Fecundity	—	—	PM	2013	Adult	0.29	0.07	0.63
Fecundity	—	—	PM	2014	Adult	0.27	0.04	0.59
Fecundity	—	—	PM	2015	Adult	0.28	0.06	0.60
Fecundity	—	—	PM	2016	Adult	0.31	0.07	0.65
Fecundity	—	—	PM	2017	Adult	0.32	0.18	0.61
Fecundity	—	—	PM	2018	Adult	0.35	0.21	0.67
Fecundity	—	—	PN	2008	Adult	0.40	0.13	1.28
Fecundity	—	—	PN	2009	Adult	0.28	0.09	0.52
Fecundity	—	—	PN	2010	Adult	0.28	0.11	0.51
Fecundity	—	—	PN	2011	Adult	0.26	0.14	0.45
Fecundity	—	—	PN	2012	Adult	0.22	0.13	0.34
Fecundity	—	—	PN	2013	Adult	0.26	0.15	0.40
Fecundity	—	—	PN	2014	Adult	0.25	0.11	0.45
Fecundity	—	—	PN	2015	Adult	0.28	0.09	0.59
Fecundity	—	—	PN	2016	Adult	0.31	0.11	0.63
Fecundity	—	—	PN	2017	Adult	0.31	0.11	0.68
Fecundity	—	—	PN	2018	Adult	0.32	0.12	0.69
Fecundity	—	—	SA	2008	Adult	0.34	0.10	0.68
Fecundity	—	—	SA	2009	Adult	0.35	0.10	0.68
Fecundity	—	—	SA	2010	Adult	0.34	0.08	0.67
Fecundity	—	—	SA	2011	Adult	0.32	0.08	0.64
Fecundity	—	—	SA	2012	Adult	0.29	0.07	0.58
Fecundity	—	—	SA	2013	Adult	0.31	0.09	0.63
Fecundity	—	—	SA	2014	Adult	0.31	0.07	0.65
Fecundity	—	—	SA	2015	Adult	0.33	0.18	0.58
Fecundity	—	—	SA	2016	Adult	0.50	0.30	0.82
Fecundity	—	—	SA	2017	Adult	0.34	0.11	0.69
Fecundity	—	—	SA	2018	Adult	0.35	0.12	0.71
Fecundity	—	—	WM	2008	Adult	0.31	0.06	0.65
Fecundity	—	—	WM	2009	Adult	0.31	0.06	0.65
Fecundity	—	—	WM	2010	Adult	0.29	0.04	0.62
Fecundity	—	—	WM	2011	Adult	0.27	0.05	0.59
Fecundity	—	—	WM	2012	Adult	0.25	0.04	0.53
Fecundity	—	—	WM	2013	Adult	0.27	0.05	0.55

Table 5–1. Parameter estimates (median, 50 percent; lower credible interval, 2.5 percent and upper credible interval, 97.5 percent) sampled from the posterior distribution for models density dependence and random effects for greater sage-grouse within the Bi-State Distinct Population Segment between 2008 and 2018.—Continued

[Subpopulations: BH, Bodie Hills; FA, Fales; DC, Desert Creek; LV, Long Valley; MG, Mount Grant; PM. Parker Meadows; PN, Pine Nut; SA, Sagehen; WM, White Mountains; —, values indicate overall estimates for respective fixed effect]

Life stage	Density dependence	Random effect	Sub-population	Year	Age	Percentile		
						50.0	2.5	97.5
Fecundity	—	—	WM	2014	Adult	0.28	0.04	0.62
Fecundity	—	—	WM	2015	Adult	0.30	0.05	0.64
Fecundity	—	—	WM	2016	Adult	0.37	0.08	0.77
Fecundity	—	—	WM	2017	Adult	0.37	0.10	0.82
Fecundity	—	—	WM	2018	Adult	0.41	0.19	0.79
Fecundity	—	—	BH	2008	Yearling	0.52	0.34	0.75
Fecundity	—	—	BH	2009	Yearling	0.54	0.36	0.78
Fecundity	—	—	BH	2010	Yearling	0.58	0.39	0.81
Fecundity	—	—	BH	2011	Yearling	0.50	0.34	0.70
Fecundity	—	—	BH	2012	Yearling	0.42	0.25	0.67
Fecundity	—	—	BH	2013	Yearling	0.42	0.26	0.65
Fecundity	—	—	BH	2014	Yearling	0.31	0.09	0.50
Fecundity	—	—	BH	2015	Yearling	0.35	0.22	0.53
Fecundity	—	—	BH	2016	Yearling	0.39	0.26	0.56
Fecundity	—	—	BH	2017	Yearling	0.37	0.25	0.52
Fecundity	—	—	BH	2018	Yearling	0.37	0.25	0.52
Fecundity	—	—	FA	2008	Yearling	0.42	0.16	0.79
Fecundity	—	—	FA	2009	Yearling	0.41	0.16	0.72
Fecundity	—	—	FA	2010	Yearling	0.39	0.12	0.69
Fecundity	—	—	FA	2011	Yearling	0.35	0.12	0.61
Fecundity	—	—	FA	2012	Yearling	0.33	0.11	0.59
Fecundity	—	—	FA	2013	Yearling	0.34	0.12	0.60
Fecundity	—	—	FA	2014	Yearling	0.33	0.09	0.60
Fecundity	—	—	FA	2015	Yearling	0.32	0.10	0.56
Fecundity	—	—	FA	2016	Yearling	0.34	0.09	0.59
Fecundity	—	—	FA	2017	Yearling	0.32	0.09	0.58
Fecundity	—	—	FA	2018	Yearling	0.35	0.12	0.63
Fecundity	—	—	DC	2008	Yearling	0.38	0.14	0.69
Fecundity	—	—	DC	2009	Yearling	0.43	0.21	0.74
Fecundity	—	—	DC	2010	Yearling	0.45	0.22	0.75
Fecundity	—	—	DC	2011	Yearling	0.44	0.23	0.72
Fecundity	—	—	DC	2012	Yearling	0.29	0.07	0.52
Fecundity	—	—	DC	2013	Yearling	0.36	0.17	0.63
Fecundity	—	—	DC	2014	Yearling	0.39	0.14	0.71
Fecundity	—	—	DC	2015	Yearling	0.41	0.21	0.71
Fecundity	—	—	DC	2016	Yearling	0.47	0.28	0.73
Fecundity	—	—	DC	2017	Yearling	0.38	0.24	0.57
Fecundity	—	—	DC	2018	Yearling	0.32	0.20	0.49
Fecundity	—	—	LV	2008	Yearling	0.51	0.33	0.75
Fecundity	—	—	LV	2009	Yearling	0.48	0.31	0.69

Table 5–1. Parameter estimates (median, 50 percent; lower credible interval, 2.5 percent and upper credible interval, 97.5 percent) sampled from the posterior distribution for models density dependence and random effects for greater sage-grouse within the Bi-State Distinct Population Segment between 2008 and 2018.—Continued

[Subpopulations: BH, Bodie Hills; FA, Fales; DC, Desert Creek; LV, Long Valley; MG, Mount Grant; PM. Parker Meadows; PN, Pine Nut; SA, Sagehen; WM, White Mountains; —, values indicate overall estimates for respective fixed effect]

Life stage	Density dependence	Random effect	Sub-population	Year	Age	Percentile		
						50.0	2.5	97.5
Fecundity	—	—	LV	2010	Yearling	0.43	0.28	0.61
Fecundity	—	—	LV	2011	Yearling	0.48	0.31	0.67
Fecundity	—	—	LV	2012	Yearling	0.30	0.11	0.51
Fecundity	—	—	LV	2013	Yearling	0.30	0.08	0.51
Fecundity	—	—	LV	2014	Yearling	0.30	0.10	0.53
Fecundity	—	—	LV	2015	Yearling	0.31	0.10	0.49
Fecundity	—	—	LV	2016	Yearling	0.35	0.23	0.50
Fecundity	—	—	LV	2017	Yearling	0.37	0.24	0.52
Fecundity	—	—	LV	2018	Yearling	0.35	0.23	0.49
Fecundity	—	—	MG	2008	Yearling	0.44	0.18	0.78
Fecundity	—	—	MG	2009	Yearling	0.49	0.25	0.82
Fecundity	—	—	MG	2010	Yearling	0.47	0.20	0.80
Fecundity	—	—	MG	2011	Yearling	0.35	0.10	0.60
Fecundity	—	—	MG	2012	Yearling	0.28	0.05	0.51
Fecundity	—	—	MG	2013	Yearling	0.34	0.20	0.57
Fecundity	—	—	MG	2014	Yearling	0.37	0.12	0.67
Fecundity	—	—	MG	2015	Yearling	0.36	0.12	0.63
Fecundity	—	—	MG	2016	Yearling	0.35	0.21	0.53
Fecundity	—	—	MG	2017	Yearling	0.35	0.24	0.53
Fecundity	—	—	MG	2018	Yearling	0.40	0.27	0.57
Fecundity	—	—	PM	2008	Yearling	0.36	0.09	0.69
Fecundity	—	—	PM	2009	Yearling	0.43	0.24	0.71
Fecundity	—	—	PM	2010	Yearling	0.22	0.09	0.42
Fecundity	—	—	PM	2011	Yearling	0.08	0.01	0.24
Fecundity	—	—	PM	2012	Yearling	0.32	0.07	0.63
Fecundity	—	—	PM	2013	Yearling	0.34	0.09	0.70
Fecundity	—	—	PM	2014	Yearling	0.32	0.05	0.67
Fecundity	—	—	PM	2015	Yearling	0.33	0.08	0.67
Fecundity	—	—	PM	2016	Yearling	0.37	0.09	0.72
Fecundity	—	—	PM	2017	Yearling	0.38	0.21	0.68
Fecundity	—	—	PM	2018	Yearling	0.42	0.24	0.73
Fecundity	—	—	PN	2008	Yearling	0.47	0.17	1.33
Fecundity	—	—	PN	2009	Yearling	0.33	0.11	0.61
Fecundity	—	—	PN	2010	Yearling	0.33	0.13	0.60
Fecundity	—	—	PN	2011	Yearling	0.31	0.16	0.52
Fecundity	—	—	PN	2012	Yearling	0.28	0.15	0.45
Fecundity	—	—	PN	2013	Yearling	0.32	0.17	0.50
Fecundity	—	—	PN	2014	Yearling	0.28	0.12	0.51
Fecundity	—	—	PN	2015	Yearling	0.33	0.11	0.65
Fecundity	—	—	PN	2016	Yearling	0.37	0.13	0.70

Table 5–1. Parameter estimates (median, 50 percent; lower credible interval, 2.5 percent and upper credible interval, 97.5 percent) sampled from the posterior distribution for models density dependence and random effects for greater sage-grouse within the Bi-State Distinct Population Segment between 2008 and 2018.—Continued

[Subpopulations: BH, Bodie Hills; FA, Fales; DC, Desert Creek; LV, Long Valley; MG, Mount Grant; PM. Parker Meadows; PN, Pine Nut; SA, Sagehen; WM, White Mountains; —, values indicate overall estimates for respective fixed effect]

Life stage	Density dependence	Random effect	Sub-population	Year	Age	Percentile		
						50.0	2.5	97.5
Fecundity	—	—	PN	2017	Yearling	0.36	0.13	0.74
Fecundity	—	—	PN	2018	Yearling	0.37	0.13	0.74
Fecundity	—	—	SA	2008	Yearling	0.39	0.12	0.79
Fecundity	—	—	SA	2009	Yearling	0.41	0.12	0.77
Fecundity	—	—	SA	2010	Yearling	0.39	0.10	0.76
Fecundity	—	—	SA	2011	Yearling	0.36	0.10	0.69
Fecundity	—	—	SA	2012	Yearling	0.34	0.08	0.63
Fecundity	—	—	SA	2013	Yearling	0.37	0.11	0.71
Fecundity	—	—	SA	2014	Yearling	0.35	0.08	0.72
Fecundity	—	—	SA	2015	Yearling	0.39	0.21	0.66
Fecundity	—	—	SA	2016	Yearling	0.55	0.31	0.91
Fecundity	—	—	SA	2017	Yearling	0.40	0.13	0.74
Fecundity	—	—	SA	2018	Yearling	0.41	0.15	0.78
Fecundity	—	—	WM	2008	Yearling	0.36	0.08	0.72
Fecundity	—	—	WM	2009	Yearling	0.37	0.08	0.72
Fecundity	—	—	WM	2010	Yearling	0.34	0.05	0.71
Fecundity	—	—	WM	2011	Yearling	0.31	0.05	0.65
Fecundity	—	—	WM	2012	Yearling	0.29	0.05	0.59
Fecundity	—	—	WM	2013	Yearling	0.32	0.06	0.63
Fecundity	—	—	WM	2014	Yearling	0.33	0.04	0.69
Fecundity	—	—	WM	2015	Yearling	0.35	0.06	0.70
Fecundity	—	—	WM	2016	Yearling	0.42	0.09	0.84
Fecundity	—	—	WM	2017	Yearling	0.43	0.12	0.86
Fecundity	—	—	WM	2018	Yearling	0.45	0.22	0.86
Hatchability	—	Subpopulation × Year	BH	2008	Adult	0.94	0.86	0.98
Hatchability	—	Subpopulation × Year	BH	2009	Adult	0.94	0.86	0.98
Hatchability	—	Subpopulation × Year	BH	2010	Adult	0.86	0.73	0.94
Hatchability	—	Subpopulation × Year	BH	2011	Adult	0.95	0.78	0.99
Hatchability	—	Subpopulation × Year	BH	2012	Adult	0.93	0.66	0.99
Hatchability	—	Subpopulation × Year	BH	2013	Adult	0.94	0.68	1.00
Hatchability	—	Subpopulation × Year	BH	2014	Adult	0.83	0.20	0.99
Hatchability	—	Subpopulation × Year	BH	2015	Adult	0.80	0.67	0.91
Hatchability	—	Subpopulation × Year	BH	2016	Adult	0.96	0.91	0.99
Hatchability	—	Subpopulation × Year	BH	2017	Adult	0.89	0.80	0.94
Hatchability	—	Subpopulation × Year	BH	2018	Adult	0.89	0.83	0.94
Hatchability	—	Subpopulation × Year	FA	2008	Adult	0.91	0.35	1.00
Hatchability	—	Subpopulation × Year	FA	2009	Adult	0.90	0.35	1.00
Hatchability	—	Subpopulation × Year	FA	2010	Adult	0.84	0.26	0.99
Hatchability	—	Subpopulation × Year	FA	2011	Adult	0.86	0.30	0.99
Hatchability	—	Subpopulation × Year	FA	2012	Adult	0.88	0.28	0.99

Table 5–1. Parameter estimates (median, 50 percent; lower credible interval, 2.5 percent and upper credible interval, 97.5 percent) sampled from the posterior distribution for models density dependence and random effects for greater sage-grouse within the Bi-State Distinct Population Segment between 2008 and 2018.—Continued

[Subpopulations: BH, Bodie Hills; FA, Fales; DC, Desert Creek; LV, Long Valley; MG, Mount Grant; PM. Parker Meadows; PN, Pine Nut; SA, Sagehen; WM, White Mountains; —, values indicate overall estimates for respective fixed effect]

Life stage	Density dependence	Random effect	Sub-population	Year	Age	Percentile		
						50.0	2.5	97.5
Hatchability	—	Subpopulation × Year	FA	2013	Adult	0.89	0.31	0.99
Hatchability	—	Subpopulation × Year	FA	2014	Adult	0.85	0.20	0.99
Hatchability	—	Subpopulation × Year	FA	2015	Adult	0.86	0.21	0.99
Hatchability	—	Subpopulation × Year	FA	2016	Adult	0.85	0.20	0.99
Hatchability	—	Subpopulation × Year	FA	2017	Adult	0.86	0.22	0.99
Hatchability	—	Subpopulation × Year	FA	2018	Adult	0.87	0.29	0.99
Hatchability	—	Subpopulation × Year	DC	2008	Adult	0.89	0.33	0.99
Hatchability	—	Subpopulation × Year	DC	2009	Adult	0.91	0.50	0.99
Hatchability	—	Subpopulation × Year	DC	2010	Adult	0.88	0.48	0.99
Hatchability	—	Subpopulation × Year	DC	2011	Adult	0.91	0.58	0.99
Hatchability	—	Subpopulation × Year	DC	2012	Adult	0.82	0.18	0.99
Hatchability	—	Subpopulation × Year	DC	2013	Adult	0.90	0.46	0.99
Hatchability	—	Subpopulation × Year	DC	2014	Adult	0.87	0.33	0.99
Hatchability	—	Subpopulation × Year	DC	2015	Adult	0.91	0.55	0.99
Hatchability	—	Subpopulation × Year	DC	2016	Adult	0.88	0.79	0.94
Hatchability	—	Subpopulation × Year	DC	2017	Adult	0.90	0.78	0.97
Hatchability	—	Subpopulation × Year	DC	2018	Adult	0.86	0.70	0.95
Hatchability	—	Subpopulation × Year	LV	2008	Adult	0.98	0.94	1.00
Hatchability	—	Subpopulation × Year	LV	2009	Adult	0.95	0.90	0.98
Hatchability	—	Subpopulation × Year	LV	2010	Adult	0.81	0.67	0.90
Hatchability	—	Subpopulation × Year	LV	2011	Adult	0.97	0.88	1.00
Hatchability	—	Subpopulation × Year	LV	2012	Adult	0.90	0.32	0.99
Hatchability	—	Subpopulation × Year	LV	2013	Adult	0.89	0.19	0.99
Hatchability	—	Subpopulation × Year	LV	2014	Adult	0.85	0.23	0.99
Hatchability	—	Subpopulation × Year	LV	2015	Adult	0.87	0.26	0.99
Hatchability	—	Subpopulation × Year	LV	2016	Adult	0.91	0.80	0.97
Hatchability	—	Subpopulation × Year	LV	2017	Adult	0.93	0.86	0.98
Hatchability	—	Subpopulation × Year	LV	2018	Adult	0.91	0.82	0.96
Hatchability	—	Subpopulation × Year	MG	2008	Adult	0.89	0.34	0.99
Hatchability	—	Subpopulation × Year	MG	2009	Adult	0.91	0.54	0.99
Hatchability	—	Subpopulation × Year	MG	2010	Adult	0.86	0.38	0.99
Hatchability	—	Subpopulation × Year	MG	2011	Adult	0.81	0.21	0.99
Hatchability	—	Subpopulation × Year	MG	2012	Adult	0.72	0.11	0.98
Hatchability	—	Subpopulation × Year	MG	2013	Adult	0.78	0.56	0.92
Hatchability	—	Subpopulation × Year	MG	2014	Adult	0.83	0.27	0.99
Hatchability	—	Subpopulation × Year	MG	2015	Adult	0.86	0.30	0.99
Hatchability	—	Subpopulation × Year	MG	2016	Adult	0.77	0.60	0.90
Hatchability	—	Subpopulation × Year	MG	2017	Adult	0.85	0.74	0.92
Hatchability	—	Subpopulation × Year	MG	2018	Adult	0.93	0.84	0.97
Hatchability	—	Subpopulation × Year	PM	2008	Adult	0.83	0.22	0.99

Table 5–1. Parameter estimates (median, 50 percent; lower credible interval, 2.5 percent and upper credible interval, 97.5 percent) sampled from the posterior distribution for models density dependence and random effects for greater sage-grouse within the Bi-State Distinct Population Segment between 2008 and 2018.—Continued

[Subpopulations: BH, Bodie Hills; FA, Fales; DC, Desert Creek; LV, Long Valley; MG, Mount Grant; PM. Parker Meadows; PN, Pine Nut; SA, Sagehen; WM, White Mountains; —, values indicate overall estimates for respective fixed effect]

Life stage	Density dependence	Random effect	Sub-population	Year	Age	Percentile		
						50.0	2.5	97.5
Hatchability	—	Subpopulation × Year	PM	2009	Adult	0.92	0.79	0.98
Hatchability	—	Subpopulation × Year	PM	2010	Adult	0.45	0.25	0.65
Hatchability	—	Subpopulation × Year	PM	2011	Adult	0.16	0.03	0.43
Hatchability	—	Subpopulation × Year	PM	2012	Adult	0.76	0.16	0.98
Hatchability	—	Subpopulation × Year	PM	2013	Adult	0.80	0.19	0.99
Hatchability	—	Subpopulation × Year	PM	2014	Adult	0.72	0.11	0.98
Hatchability	—	Subpopulation × Year	PM	2015	Adult	0.77	0.16	0.98
Hatchability	—	Subpopulation × Year	PM	2016	Adult	0.78	0.18	0.99
Hatchability	—	Subpopulation × Year	PM	2017	Adult	0.81	0.61	0.94
Hatchability	—	Subpopulation × Year	PM	2018	Adult	0.89	0.69	0.98
Hatchability	—	Subpopulation × Year	PN	2008	Adult	0.94	0.56	1.00
Hatchability	—	Subpopulation × Year	PN	2009	Adult	0.88	0.26	0.99
Hatchability	—	Subpopulation × Year	PN	2010	Adult	0.86	0.33	0.99
Hatchability	—	Subpopulation × Year	PN	2011	Adult	0.90	0.72	0.97
Hatchability	—	Subpopulation × Year	PN	2012	Adult	0.90	0.76	0.97
Hatchability	—	Subpopulation × Year	PN	2013	Adult	0.96	0.86	1.00
Hatchability	—	Subpopulation × Year	PN	2014	Adult	0.61	0.38	0.83
Hatchability	—	Subpopulation × Year	PN	2015	Adult	0.87	0.28	0.99
Hatchability	—	Subpopulation × Year	PN	2016	Adult	0.88	0.32	0.99
Hatchability	—	Subpopulation × Year	PN	2017	Adult	0.89	0.36	0.99
Hatchability	—	Subpopulation × Year	PN	2018	Adult	0.89	0.33	0.99
Hatchability	—	Subpopulation × Year	SA	2008	Adult	0.89	0.27	0.99
Hatchability	—	Subpopulation × Year	SA	2009	Adult	0.88	0.23	0.99
Hatchability	—	Subpopulation × Year	SA	2010	Adult	0.82	0.20	0.99
Hatchability	—	Subpopulation × Year	SA	2011	Adult	0.83	0.21	0.99
Hatchability	—	Subpopulation × Year	SA	2012	Adult	0.83	0.19	0.99
Hatchability	—	Subpopulation × Year	SA	2013	Adult	0.87	0.25	0.99
Hatchability	—	Subpopulation × Year	SA	2014	Adult	0.80	0.16	0.99
Hatchability	—	Subpopulation × Year	SA	2015	Adult	0.91	0.59	0.99
Hatchability	—	Subpopulation × Year	SA	2016	Adult	0.85	0.64	0.95
Hatchability	—	Subpopulation × Year	SA	2017	Adult	0.86	0.27	0.99
Hatchability	—	Subpopulation × Year	SA	2018	Adult	0.87	0.30	0.99
Hatchability	—	Subpopulation × Year	WM	2008	Adult	0.82	0.15	0.99
Hatchability	—	Subpopulation × Year	WM	2009	Adult	0.81	0.14	0.99
Hatchability	—	Subpopulation × Year	WM	2010	Adult	0.70	0.10	0.98
Hatchability	—	Subpopulation × Year	WM	2011	Adult	0.74	0.12	0.98
Hatchability	—	Subpopulation × Year	WM	2012	Adult	0.73	0.09	0.99
Hatchability	—	Subpopulation × Year	WM	2013	Adult	0.77	0.13	0.99
Hatchability	—	Subpopulation × Year	WM	2014	Adult	0.71	0.08	0.98
Hatchability	—	Subpopulation × Year	WM	2015	Adult	0.76	0.12	0.99

Table 5–1. Parameter estimates (median, 50 percent; lower credible interval, 2.5 percent and upper credible interval, 97.5 percent) sampled from the posterior distribution for models density dependence and random effects for greater sage-grouse within the Bi-State Distinct Population Segment between 2008 and 2018.—Continued

[Subpopulations: BH, Bodie Hills; FA, Fales; DC, Desert Creek; LV, Long Valley; MG, Mount Grant; PM. Parker Meadows; PN, Pine Nut; SA, Sagehen; WM, White Mountains; —, values indicate overall estimates for respective fixed effect]

Life stage	Density dependence	Random effect	Sub-population	Year	Age	Percentile		
						50.0	2.5	97.5
Hatchability	—	Subpopulation × Year	WM	2016	Adult	0.82	0.17	0.99
Hatchability	—	Subpopulation × Year	WM	2017	Adult	0.83	0.22	0.99
Hatchability	—	Subpopulation × Year	WM	2018	Adult	0.75	0.45	0.92
Hatchability	—	Subpopulation × Year	BH	2008	Yearling	0.95	0.86	0.98
Hatchability	—	Subpopulation × Year	BH	2009	Yearling	0.94	0.87	0.98
Hatchability	—	Subpopulation × Year	BH	2010	Yearling	0.87	0.73	0.95
Hatchability	—	Subpopulation × Year	BH	2011	Yearling	0.95	0.78	1.00
Hatchability	—	Subpopulation × Year	BH	2012	Yearling	0.93	0.67	0.99
Hatchability	—	Subpopulation × Year	BH	2013	Yearling	0.94	0.69	1.00
Hatchability	—	Subpopulation × Year	BH	2014	Yearling	0.84	0.22	0.99
Hatchability	—	Subpopulation × Year	BH	2015	Yearling	0.82	0.67	0.92
Hatchability	—	Subpopulation × Year	BH	2016	Yearling	0.97	0.91	0.99
Hatchability	—	Subpopulation × Year	BH	2017	Yearling	0.90	0.82	0.95
Hatchability	—	Subpopulation × Year	BH	2018	Yearling	0.90	0.84	0.94
Hatchability	—	Subpopulation × Year	FA	2008	Yearling	0.92	0.36	1.00
Hatchability	—	Subpopulation × Year	FA	2009	Yearling	0.90	0.36	1.00
Hatchability	—	Subpopulation × Year	FA	2010	Yearling	0.85	0.28	0.99
Hatchability	—	Subpopulation × Year	FA	2011	Yearling	0.87	0.31	0.99
Hatchability	—	Subpopulation × Year	FA	2012	Yearling	0.89	0.30	0.99
Hatchability	—	Subpopulation × Year	FA	2013	Yearling	0.90	0.32	1.00
Hatchability	—	Subpopulation × Year	FA	2014	Yearling	0.86	0.20	0.99
Hatchability	—	Subpopulation × Year	FA	2015	Yearling	0.87	0.24	0.99
Hatchability	—	Subpopulation × Year	FA	2016	Yearling	0.87	0.21	0.99
Hatchability	—	Subpopulation × Year	FA	2017	Yearling	0.87	0.24	0.99
Hatchability	—	Subpopulation × Year	FA	2018	Yearling	0.88	0.31	0.99
Hatchability	—	Subpopulation × Year	DC	2008	Yearling	0.90	0.33	0.99
Hatchability	—	Subpopulation × Year	DC	2009	Yearling	0.92	0.51	0.99
Hatchability	—	Subpopulation × Year	DC	2010	Yearling	0.89	0.50	0.99
Hatchability	—	Subpopulation × Year	DC	2011	Yearling	0.92	0.60	0.99
Hatchability	—	Subpopulation × Year	DC	2012	Yearling	0.83	0.19	0.99
Hatchability	—	Subpopulation × Year	DC	2013	Yearling	0.91	0.49	0.99
Hatchability	—	Subpopulation × Year	DC	2014	Yearling	0.88	0.34	0.99
Hatchability	—	Subpopulation × Year	DC	2015	Yearling	0.91	0.57	0.99
Hatchability	—	Subpopulation × Year	DC	2016	Yearling	0.89	0.78	0.95
Hatchability	—	Subpopulation × Year	DC	2017	Yearling	0.91	0.77	0.97
Hatchability	—	Subpopulation × Year	DC	2018	Yearling	0.87	0.70	0.95
Hatchability	—	Subpopulation × Year	LV	2008	Yearling	0.98	0.94	1.00
Hatchability	—	Subpopulation × Year	LV	2009	Yearling	0.96	0.90	0.99
Hatchability	—	Subpopulation × Year	LV	2010	Yearling	0.82	0.67	0.91
Hatchability	—	Subpopulation × Year	LV	2011	Yearling	0.97	0.89	1.00

Table 5–1. Parameter estimates (median, 50 percent; lower credible interval, 2.5 percent and upper credible interval, 97.5 percent) sampled from the posterior distribution for models density dependence and random effects for greater sage-grouse within the Bi-State Distinct Population Segment between 2008 and 2018.—Continued

[Subpopulations: BH, Bodie Hills; FA, Fales; DC, Desert Creek; LV, Long Valley; MG, Mount Grant; PM. Parker Meadows; PN, Pine Nut; SA, Sagehen; WM, White Mountains; —, values indicate overall estimates for respective fixed effect]

Life stage	Density dependence	Random effect	Sub-population	Year	Age	Percentile		
						50.0	2.5	97.5
Hatchability	—	Subpopulation × Year	LV	2012	Yearling	0.90	0.33	0.99
Hatchability	—	Subpopulation × Year	LV	2013	Yearling	0.90	0.20	0.99
Hatchability	—	Subpopulation × Year	LV	2014	Yearling	0.86	0.25	0.99
Hatchability	—	Subpopulation × Year	LV	2015	Yearling	0.88	0.28	0.99
Hatchability	—	Subpopulation × Year	LV	2016	Yearling	0.91	0.81	0.97
Hatchability	—	Subpopulation × Year	LV	2017	Yearling	0.94	0.86	0.98
Hatchability	—	Subpopulation × Year	LV	2018	Yearling	0.91	0.84	0.96
Hatchability	—	Subpopulation × Year	MG	2008	Yearling	0.90	0.35	0.99
Hatchability	—	Subpopulation × Year	MG	2009	Yearling	0.91	0.55	0.99
Hatchability	—	Subpopulation × Year	MG	2010	Yearling	0.87	0.39	0.99
Hatchability	—	Subpopulation × Year	MG	2011	Yearling	0.82	0.22	0.99
Hatchability	—	Subpopulation × Year	MG	2012	Yearling	0.74	0.11	0.99
Hatchability	—	Subpopulation × Year	MG	2013	Yearling	0.80	0.56	0.93
Hatchability	—	Subpopulation × Year	MG	2014	Yearling	0.84	0.27	0.99
Hatchability	—	Subpopulation × Year	MG	2015	Yearling	0.87	0.31	0.99
Hatchability	—	Subpopulation × Year	MG	2016	Yearling	0.78	0.60	0.91
Hatchability	—	Subpopulation × Year	MG	2017	Yearling	0.86	0.75	0.93
Hatchability	—	Subpopulation × Year	MG	2018	Yearling	0.93	0.84	0.97
Hatchability	—	Subpopulation × Year	PM	2008	Yearling	0.83	0.24	0.99
Hatchability	—	Subpopulation × Year	PM	2009	Yearling	0.92	0.80	0.98
Hatchability	—	Subpopulation × Year	PM	2010	Yearling	0.46	0.25	0.69
Hatchability	—	Subpopulation × Year	PM	2011	Yearling	0.17	0.03	0.44
Hatchability	—	Subpopulation × Year	PM	2012	Yearling	0.77	0.17	0.98
Hatchability	—	Subpopulation × Year	PM	2013	Yearling	0.81	0.20	0.99
Hatchability	—	Subpopulation × Year	PM	2014	Yearling	0.73	0.11	0.98
Hatchability	—	Subpopulation × Year	PM	2015	Yearling	0.78	0.17	0.99
Hatchability	—	Subpopulation × Year	PM	2016	Yearling	0.79	0.19	0.99
Hatchability	—	Subpopulation × Year	PM	2017	Yearling	0.82	0.61	0.95
Hatchability	—	Subpopulation × Year	PM	2018	Yearling	0.90	0.70	0.98
Hatchability	—	Subpopulation × Year	PN	2008	Yearling	0.94	0.58	1.00
Hatchability	—	Subpopulation × Year	PN	2009	Yearling	0.89	0.30	0.99
Hatchability	—	Subpopulation × Year	PN	2010	Yearling	0.87	0.35	0.99
Hatchability	—	Subpopulation × Year	PN	2011	Yearling	0.90	0.74	0.98
Hatchability	—	Subpopulation × Year	PN	2012	Yearling	0.90	0.77	0.97
Hatchability	—	Subpopulation × Year	PN	2013	Yearling	0.97	0.86	1.00
Hatchability	—	Subpopulation × Year	PN	2014	Yearling	0.63	0.37	0.85
Hatchability	—	Subpopulation × Year	PN	2015	Yearling	0.87	0.30	0.99
Hatchability	—	Subpopulation × Year	PN	2016	Yearling	0.88	0.32	0.99
Hatchability	—	Subpopulation × Year	PN	2017	Yearling	0.90	0.38	0.99
Hatchability	—	Subpopulation × Year	PN	2018	Yearling	0.90	0.34	0.99

Table 5–1. Parameter estimates (median, 50 percent; lower credible interval, 2.5 percent and upper credible interval, 97.5 percent) sampled from the posterior distribution for models density dependence and random effects for greater sage-grouse within the Bi-State Distinct Population Segment between 2008 and 2018.—Continued

[Subpopulations: BH, Bodie Hills; FA, Fales; DC, Desert Creek; LV, Long Valley; MG, Mount Grant; PM. Parker Meadows; PN, Pine Nut; SA, Sagehen; WM, White Mountains; —, values indicate overall estimates for respective fixed effect]

Life stage	Density dependence	Random effect	Sub-population	Year	Age	Percentile		
						50.0	2.5	97.5
Hatchability	—	Subpopulation × Year	SA	2008	Yearling	0.90	0.29	1.00
Hatchability	—	Subpopulation × Year	SA	2009	Yearling	0.89	0.26	0.99
Hatchability	—	Subpopulation × Year	SA	2010	Yearling	0.82	0.21	0.99
Hatchability	—	Subpopulation × Year	SA	2011	Yearling	0.84	0.24	0.99
Hatchability	—	Subpopulation × Year	SA	2012	Yearling	0.85	0.20	0.99
Hatchability	—	Subpopulation × Year	SA	2013	Yearling	0.87	0.25	0.99
Hatchability	—	Subpopulation × Year	SA	2014	Yearling	0.81	0.17	0.99
Hatchability	—	Subpopulation × Year	SA	2015	Yearling	0.92	0.60	0.99
Hatchability	—	Subpopulation × Year	SA	2016	Yearling	0.85	0.66	0.95
Hatchability	—	Subpopulation × Year	SA	2017	Yearling	0.87	0.28	0.99
Hatchability	—	Subpopulation × Year	SA	2018	Yearling	0.88	0.32	0.99
Hatchability	—	Subpopulation × Year	WM	2008	Yearling	0.83	0.16	0.99
Hatchability	—	Subpopulation × Year	WM	2009	Yearling	0.82	0.16	0.99
Hatchability	—	Subpopulation × Year	WM	2010	Yearling	0.71	0.11	0.98
Hatchability	—	Subpopulation × Year	WM	2011	Yearling	0.75	0.12	0.99
Hatchability	—	Subpopulation × Year	WM	2012	Yearling	0.75	0.10	0.99
Hatchability	—	Subpopulation × Year	WM	2013	Yearling	0.78	0.14	0.99
Hatchability	—	Subpopulation × Year	WM	2014	Yearling	0.73	0.09	0.99
Hatchability	—	Subpopulation × Year	WM	2015	Yearling	0.78	0.13	0.99
Hatchability	—	Subpopulation × Year	WM	2016	Yearling	0.83	0.18	0.99
Hatchability	—	Subpopulation × Year	WM	2017	Yearling	0.84	0.24	0.99
Hatchability	—	Subpopulation × Year	WM	2018	Yearling	0.76	0.48	0.93
Nest propensity (first)	—	—	—	—	Adult	0.95	0.90	0.98
Nest propensity (first)	—	—	—	—	Yearling	0.88	0.81	0.94
Nest propensity (second)	—	Subpopulation × Year	BH	2008	Adult	0.37	0.13	0.64
Nest propensity (second)	—	Subpopulation × Year	BH	2009	Adult	0.35	0.06	0.73
Nest propensity (second)	—	Subpopulation × Year	BH	2010	Adult	0.80	0.51	0.95
Nest propensity (second)	—	Subpopulation × Year	BH	2011	Adult	0.67	0.37	0.89
Nest propensity (second)	—	Subpopulation × Year	BH	2012	Adult	0.40	0.00	0.98
Nest propensity (second)	—	Subpopulation × Year	BH	2013	Adult	0.37	0.00	0.98
Nest propensity (second)	—	Subpopulation × Year	BH	2014	Adult	0.08	0.00	0.47
Nest propensity (second)	—	Subpopulation × Year	BH	2015	Adult	0.43	0.08	0.89
Nest propensity (second)	—	Subpopulation × Year	BH	2016	Adult	0.13	0.01	0.43
Nest propensity (second)	—	Subpopulation × Year	BH	2017	Adult	0.21	0.05	0.49
Nest propensity (second)	—	Subpopulation × Year	BH	2018	Adult	0.08	0.01	0.28
Nest propensity (second)	—	Subpopulation × Year	FA	2008	Adult	0.31	0.00	0.98
Nest propensity (second)	—	Subpopulation × Year	FA	2009	Adult	0.21	0.00	0.97
Nest propensity (second)	—	Subpopulation × Year	FA	2010	Adult	0.33	0.00	0.98
Nest propensity (second)	—	Subpopulation × Year	FA	2011	Adult	0.36	0.00	0.99
Nest propensity (second)	—	Subpopulation × Year	FA	2012	Adult	0.18	0.00	0.97

Table 5–1. Parameter estimates (median, 50 percent; lower credible interval, 2.5 percent and upper credible interval, 97.5 percent) sampled from the posterior distribution for models density dependence and random effects for greater sage-grouse within the Bi-State Distinct Population Segment between 2008 and 2018.—Continued

[Subpopulations: BH, Bodie Hills; FA, Fales; DC, Desert Creek; LV, Long Valley; MG, Mount Grant; PM. Parker Meadows; PN, Pine Nut; SA, Sagehen; WM, White Mountains; —, values indicate overall estimates for respective fixed effect]

Life stage	Density dependence	Random effect	Sub-population	Year	Age	Percentile		
						50.0	2.5	97.5
Nest propensity (second)	—	Subpopulation × Year	FA	2013	Adult	0.18	0.00	0.97
Nest propensity (second)	—	Subpopulation × Year	FA	2014	Adult	0.21	0.00	0.97
Nest propensity (second)	—	Subpopulation × Year	FA	2015	Adult	0.21	0.00	0.97
Nest propensity (second)	—	Subpopulation × Year	FA	2016	Adult	0.21	0.00	0.97
Nest propensity (second)	—	Subpopulation × Year	FA	2017	Adult	0.16	0.00	0.97
Nest propensity (second)	—	Subpopulation × Year	FA	2018	Adult	0.16	0.00	0.97
Nest propensity (second)	—	Subpopulation × Year	DC	2008	Adult	0.27	0.00	0.98
Nest propensity (second)	—	Subpopulation × Year	DC	2009	Adult	0.32	0.00	0.98
Nest propensity (second)	—	Subpopulation × Year	DC	2010	Adult	0.55	0.01	0.99
Nest propensity (second)	—	Subpopulation × Year	DC	2011	Adult	0.72	0.01	0.99
Nest propensity (second)	—	Subpopulation × Year	DC	2012	Adult	0.14	0.00	0.90
Nest propensity (second)	—	Subpopulation × Year	DC	2013	Adult	0.28	0.00	0.97
Nest propensity (second)	—	Subpopulation × Year	DC	2014	Adult	0.34	0.00	0.98
Nest propensity (second)	—	Subpopulation × Year	DC	2015	Adult	0.48	0.01	0.98
Nest propensity (second)	—	Subpopulation × Year	DC	2016	Adult	0.65	0.25	0.92
Nest propensity (second)	—	Subpopulation × Year	DC	2017	Adult	0.33	0.11	0.62
Nest propensity (second)	—	Subpopulation × Year	DC	2018	Adult	0.06	0.00	0.39
Nest propensity (second)	—	Subpopulation × Year	LV	2008	Adult	0.63	0.34	0.88
Nest propensity (second)	—	Subpopulation × Year	LV	2009	Adult	0.47	0.08	0.83
Nest propensity (second)	—	Subpopulation × Year	LV	2010	Adult	0.68	0.40	0.89
Nest propensity (second)	—	Subpopulation × Year	LV	2011	Adult	0.87	0.46	1.00
Nest propensity (second)	—	Subpopulation × Year	LV	2012	Adult	0.15	0.00	0.92
Nest propensity (second)	—	Subpopulation × Year	LV	2013	Adult	0.13	0.00	0.91
Nest propensity (second)	—	Subpopulation × Year	LV	2014	Adult	0.19	0.00	0.94
Nest propensity (second)	—	Subpopulation × Year	LV	2015	Adult	0.16	0.00	0.92
Nest propensity (second)	—	Subpopulation × Year	LV	2016	Adult	0.05	0.00	0.29
Nest propensity (second)	—	Subpopulation × Year	LV	2017	Adult	0.21	0.04	0.50
Nest propensity (second)	—	Subpopulation × Year	LV	2018	Adult	0.11	0.02	0.30
Nest propensity (second)	—	Subpopulation × Year	MG	2008	Adult	0.24	0.00	0.96
Nest propensity (second)	—	Subpopulation × Year	MG	2009	Adult	0.30	0.00	0.97
Nest propensity (second)	—	Subpopulation × Year	MG	2010	Adult	0.42	0.00	0.99
Nest propensity (second)	—	Subpopulation × Year	MG	2011	Adult	0.26	0.00	0.97
Nest propensity (second)	—	Subpopulation × Year	MG	2012	Adult	0.09	0.00	0.85
Nest propensity (second)	—	Subpopulation × Year	MG	2013	Adult	0.16	0.00	0.96
Nest propensity (second)	—	Subpopulation × Year	MG	2014	Adult	0.21	0.00	0.97
Nest propensity (second)	—	Subpopulation × Year	MG	2015	Adult	0.20	0.00	0.96
Nest propensity (second)	—	Subpopulation × Year	MG	2016	Adult	0.20	0.02	0.65
Nest propensity (second)	—	Subpopulation × Year	MG	2017	Adult	0.09	0.00	0.64
Nest propensity (second)	—	Subpopulation × Year	MG	2018	Adult	0.06	0.00	0.47
Nest propensity (second)	—	Subpopulation × Year	PM	2008	Adult	0.12	0.00	0.80

Table 5–1. Parameter estimates (median, 50 percent; lower credible interval, 2.5 percent and upper credible interval, 97.5 percent) sampled from the posterior distribution for models density dependence and random effects for greater sage-grouse within the Bi-State Distinct Population Segment between 2008 and 2018.—Continued

[Subpopulations: BH, Bodie Hills; FA, Fales; DC, Desert Creek; LV, Long Valley; MG, Mount Grant; PM. Parker Meadows; PN, Pine Nut; SA, Sagehen; WM, White Mountains; —, values indicate overall estimates for respective fixed effect]

Life stage	Density dependence	Random effect	Sub-population	Year	Age	Percentile		
						50.0	2.5	97.5
Nest propensity (second)	—	Subpopulation × Year	PM	2009	Adult	0.06	0.00	0.46
Nest propensity (second)	—	Subpopulation × Year	PM	2010	Adult	0.09	0.00	0.65
Nest propensity (second)	—	Subpopulation × Year	PM	2011	Adult	0.24	0.00	0.97
Nest propensity (second)	—	Subpopulation × Year	PM	2012	Adult	0.09	0.00	0.95
Nest propensity (second)	—	Subpopulation × Year	PM	2013	Adult	0.11	0.00	0.93
Nest propensity (second)	—	Subpopulation × Year	PM	2014	Adult	0.12	0.00	0.93
Nest propensity (second)	—	Subpopulation × Year	PM	2015	Adult	0.14	0.00	0.94
Nest propensity (second)	—	Subpopulation × Year	PM	2016	Adult	0.15	0.00	0.93
Nest propensity (second)	—	Subpopulation × Year	PM	2017	Adult	0.12	0.00	0.93
Nest propensity (second)	—	Subpopulation × Year	PM	2018	Adult	0.09	0.00	0.92
Nest propensity (second)	—	Subpopulation × Year	PN	2008	Adult	0.54	0.00	0.99
Nest propensity (second)	—	Subpopulation × Year	PN	2009	Adult	0.14	0.00	0.91
Nest propensity (second)	—	Subpopulation × Year	PN	2010	Adult	0.31	0.00	0.97
Nest propensity (second)	—	Subpopulation × Year	PN	2011	Adult	0.17	0.00	0.83
Nest propensity (second)	—	Subpopulation × Year	PN	2012	Adult	0.03	0.00	0.23
Nest propensity (second)	—	Subpopulation × Year	PN	2013	Adult	0.05	0.00	0.38
Nest propensity (second)	—	Subpopulation × Year	PN	2014	Adult	0.50	0.09	0.93
Nest propensity (second)	—	Subpopulation × Year	PN	2015	Adult	0.18	0.00	0.95
Nest propensity (second)	—	Subpopulation × Year	PN	2016	Adult	0.17	0.00	0.95
Nest propensity (second)	—	Subpopulation × Year	PN	2017	Adult	0.16	0.00	0.94
Nest propensity (second)	—	Subpopulation × Year	PN	2018	Adult	0.13	0.00	0.93
Nest propensity (second)	—	Subpopulation × Year	SA	2008	Adult	0.31	0.00	0.97
Nest propensity (second)	—	Subpopulation × Year	SA	2009	Adult	0.25	0.00	0.97
Nest propensity (second)	—	Subpopulation × Year	SA	2010	Adult	0.36	0.00	0.98
Nest propensity (second)	—	Subpopulation × Year	SA	2011	Adult	0.38	0.00	0.99
Nest propensity (second)	—	Subpopulation × Year	SA	2012	Adult	0.17	0.00	0.96
Nest propensity (second)	—	Subpopulation × Year	SA	2013	Adult	0.20	0.00	0.97
Nest propensity (second)	—	Subpopulation × Year	SA	2014	Adult	0.24	0.00	0.97
Nest propensity (second)	—	Subpopulation × Year	SA	2015	Adult	0.16	0.00	0.83
Nest propensity (second)	—	Subpopulation × Year	SA	2016	Adult	0.80	0.28	0.99
Nest propensity (second)	—	Subpopulation × Year	SA	2017	Adult	0.23	0.00	0.96
Nest propensity (second)	—	Subpopulation × Year	SA	2018	Adult	0.20	0.00	0.97
Nest propensity (second)	—	Subpopulation × Year	WM	2008	Adult	0.27	0.00	0.98
Nest propensity (second)	—	Subpopulation × Year	WM	2009	Adult	0.24	0.00	0.97
Nest propensity (second)	—	Subpopulation × Year	WM	2010	Adult	0.35	0.00	0.99
Nest propensity (second)	—	Subpopulation × Year	WM	2011	Adult	0.37	0.00	0.99
Nest propensity (second)	—	Subpopulation × Year	WM	2012	Adult	0.16	0.00	0.97
Nest propensity (second)	—	Subpopulation × Year	WM	2013	Adult	0.17	0.00	0.96
Nest propensity (second)	—	Subpopulation × Year	WM	2014	Adult	0.24	0.00	0.98
Nest propensity (second)	—	Subpopulation × Year	WM	2015	Adult	0.24	0.00	0.98

Table 5–1. Parameter estimates (median, 50 percent; lower credible interval, 2.5 percent and upper credible interval, 97.5 percent) sampled from the posterior distribution for models density dependence and random effects for greater sage-grouse within the Bi-State Distinct Population Segment between 2008 and 2018.—Continued

[Subpopulations: BH, Bodie Hills; FA, Fales; DC, Desert Creek; LV, Long Valley; MG, Mount Grant; PM. Parker Meadows; PN, Pine Nut; SA, Sagehen; WM, White Mountains; —, values indicate overall estimates for respective fixed effect]

Life stage	Density dependence	Random effect	Sub-population	Year	Age	Percentile		
						50.0	2.5	97.5
Nest propensity (second)	—	Subpopulation × Year	WM	2016	Adult	0.30	0.00	0.97
Nest propensity (second)	—	Subpopulation × Year	WM	2017	Adult	0.29	0.00	0.98
Nest propensity (second)	—	Subpopulation × Year	WM	2018	Adult	0.53	0.04	0.99
Nest propensity (second)	—	Subpopulation × Year	BH	2008	Yearling	0.22	0.05	0.57
Nest propensity (second)	—	Subpopulation × Year	BH	2009	Yearling	0.21	0.02	0.62
Nest propensity (second)	—	Subpopulation × Year	BH	2010	Yearling	0.66	0.24	0.93
Nest propensity (second)	—	Subpopulation × Year	BH	2011	Yearling	0.50	0.15	0.85
Nest propensity (second)	—	Subpopulation × Year	BH	2012	Yearling	0.25	0.00	0.97
Nest propensity (second)	—	Subpopulation × Year	BH	2013	Yearling	0.22	0.00	0.96
Nest propensity (second)	—	Subpopulation × Year	BH	2014	Yearling	0.04	0.00	0.36
Nest propensity (second)	—	Subpopulation × Year	BH	2015	Yearling	0.27	0.03	0.83
Nest propensity (second)	—	Subpopulation × Year	BH	2016	Yearling	0.07	0.01	0.34
Nest propensity (second)	—	Subpopulation × Year	BH	2017	Yearling	0.11	0.02	0.37
Nest propensity (second)	—	Subpopulation × Year	BH	2018	Yearling	0.04	0.00	0.19
Nest propensity (second)	—	Subpopulation × Year	FA	2008	Yearling	0.18	0.00	0.96
Nest propensity (second)	—	Subpopulation × Year	FA	2009	Yearling	0.12	0.00	0.95
Nest propensity (second)	—	Subpopulation × Year	FA	2010	Yearling	0.19	0.00	0.97
Nest propensity (second)	—	Subpopulation × Year	FA	2011	Yearling	0.22	0.00	0.97
Nest propensity (second)	—	Subpopulation × Year	FA	2012	Yearling	0.10	0.00	0.95
Nest propensity (second)	—	Subpopulation × Year	FA	2013	Yearling	0.10	0.00	0.94
Nest propensity (second)	—	Subpopulation × Year	FA	2014	Yearling	0.12	0.00	0.95
Nest propensity (second)	—	Subpopulation × Year	FA	2015	Yearling	0.11	0.00	0.93
Nest propensity (second)	—	Subpopulation × Year	FA	2016	Yearling	0.12	0.00	0.95
Nest propensity (second)	—	Subpopulation × Year	FA	2017	Yearling	0.09	0.00	0.94
Nest propensity (second)	—	Subpopulation × Year	FA	2018	Yearling	0.08	0.00	0.95
Nest propensity (second)	—	Subpopulation × Year	DC	2008	Yearling	0.15	0.00	0.96
Nest propensity (second)	—	Subpopulation × Year	DC	2009	Yearling	0.18	0.00	0.96
Nest propensity (second)	—	Subpopulation × Year	DC	2010	Yearling	0.38	0.00	0.99
Nest propensity (second)	—	Subpopulation × Year	DC	2011	Yearling	0.55	0.01	0.99
Nest propensity (second)	—	Subpopulation × Year	DC	2012	Yearling	0.07	0.00	0.83
Nest propensity (second)	—	Subpopulation × Year	DC	2013	Yearling	0.15	0.00	0.95
Nest propensity (second)	—	Subpopulation × Year	DC	2014	Yearling	0.20	0.00	0.96
Nest propensity (second)	—	Subpopulation × Year	DC	2015	Yearling	0.31	0.00	0.97
Nest propensity (second)	—	Subpopulation × Year	DC	2016	Yearling	0.49	0.10	0.89
Nest propensity (second)	—	Subpopulation × Year	DC	2017	Yearling	0.19	0.04	0.54
Nest propensity (second)	—	Subpopulation × Year	DC	2018	Yearling	0.03	0.00	0.28
Nest propensity (second)	—	Subpopulation × Year	LV	2008	Yearling	0.46	0.13	0.83
Nest propensity (second)	—	Subpopulation × Year	LV	2009	Yearling	0.30	0.04	0.72
Nest propensity (second)	—	Subpopulation × Year	LV	2010	Yearling	0.52	0.18	0.83
Nest propensity (second)	—	Subpopulation × Year	LV	2011	Yearling	0.77	0.25	0.99

Table 5–1. Parameter estimates (median, 50 percent; lower credible interval, 2.5 percent and upper credible interval, 97.5 percent) sampled from the posterior distribution for models density dependence and random effects for greater sage-grouse within the Bi-State Distinct Population Segment between 2008 and 2018.—Continued

[Subpopulations: BH, Bodie Hills; FA, Fales; DC, Desert Creek; LV, Long Valley; MG, Mount Grant; PM. Parker Meadows; PN, Pine Nut; SA, Sagehen; WM, White Mountains; —, values indicate overall estimates for respective fixed effect]

Life stage	Density dependence	Random effect	Sub-population	Year	Age	Percentile		
						50.0	2.5	97.5
Nest propensity (second)	—	Subpopulation × Year	LV	2012	Yearling	0.08	0.00	0.87
Nest propensity (second)	—	Subpopulation × Year	LV	2013	Yearling	0.07	0.00	0.84
Nest propensity (second)	—	Subpopulation × Year	LV	2014	Yearling	0.11	0.00	0.89
Nest propensity (second)	—	Subpopulation × Year	LV	2015	Yearling	0.09	0.00	0.83
Nest propensity (second)	—	Subpopulation × Year	LV	2016	Yearling	0.02	0.00	0.22
Nest propensity (second)	—	Subpopulation × Year	LV	2017	Yearling	0.11	0.02	0.44
Nest propensity (second)	—	Subpopulation × Year	LV	2018	Yearling	0.06	0.01	0.23
Nest propensity (second)	—	Subpopulation × Year	MG	2008	Yearling	0.13	0.00	0.94
Nest propensity (second)	—	Subpopulation × Year	MG	2009	Yearling	0.17	0.00	0.95
Nest propensity (second)	—	Subpopulation × Year	MG	2010	Yearling	0.27	0.00	0.98
Nest propensity (second)	—	Subpopulation × Year	MG	2011	Yearling	0.14	0.00	0.94
Nest propensity (second)	—	Subpopulation × Year	MG	2012	Yearling	0.04	0.00	0.76
Nest propensity (second)	—	Subpopulation × Year	MG	2013	Yearling	0.09	0.00	0.93
Nest propensity (second)	—	Subpopulation × Year	MG	2014	Yearling	0.11	0.00	0.94
Nest propensity (second)	—	Subpopulation × Year	MG	2015	Yearling	0.11	0.00	0.93
Nest propensity (second)	—	Subpopulation × Year	MG	2016	Yearling	0.11	0.01	0.52
Nest propensity (second)	—	Subpopulation × Year	MG	2017	Yearling	0.05	0.00	0.52
Nest propensity (second)	—	Subpopulation × Year	MG	2018	Yearling	0.03	0.00	0.33
Nest propensity (second)	—	Subpopulation × Year	PM	2008	Yearling	0.06	0.00	0.66
Nest propensity (second)	—	Subpopulation × Year	PM	2009	Yearling	0.03	0.00	0.31
Nest propensity (second)	—	Subpopulation × Year	PM	2010	Yearling	0.05	0.00	0.53
Nest propensity (second)	—	Subpopulation × Year	PM	2011	Yearling	0.13	0.00	0.94
Nest propensity (second)	—	Subpopulation × Year	PM	2012	Yearling	0.04	0.00	0.90
Nest propensity (second)	—	Subpopulation × Year	PM	2013	Yearling	0.06	0.00	0.87
Nest propensity (second)	—	Subpopulation × Year	PM	2014	Yearling	0.07	0.00	0.88
Nest propensity (second)	—	Subpopulation × Year	PM	2015	Yearling	0.07	0.00	0.89
Nest propensity (second)	—	Subpopulation × Year	PM	2016	Yearling	0.08	0.00	0.88
Nest propensity (second)	—	Subpopulation × Year	PM	2017	Yearling	0.06	0.00	0.89
Nest propensity (second)	—	Subpopulation × Year	PM	2018	Yearling	0.05	0.00	0.87
Nest propensity (second)	—	Subpopulation × Year	PN	2008	Yearling	0.36	0.00	0.98
Nest propensity (second)	—	Subpopulation × Year	PN	2009	Yearling	0.07	0.00	0.84
Nest propensity (second)	—	Subpopulation × Year	PN	2010	Yearling	0.18	0.00	0.95
Nest propensity (second)	—	Subpopulation × Year	PN	2011	Yearling	0.09	0.00	0.72
Nest propensity (second)	—	Subpopulation × Year	PN	2012	Yearling	0.01	0.00	0.13
Nest propensity (second)	—	Subpopulation × Year	PN	2013	Yearling	0.02	0.00	0.28
Nest propensity (second)	—	Subpopulation × Year	PN	2014	Yearling	0.33	0.04	0.87
Nest propensity (second)	—	Subpopulation × Year	PN	2015	Yearling	0.09	0.00	0.91
Nest propensity (second)	—	Subpopulation × Year	PN	2016	Yearling	0.09	0.00	0.90
Nest propensity (second)	—	Subpopulation × Year	PN	2017	Yearling	0.08	0.00	0.88
Nest propensity (second)	—	Subpopulation × Year	PN	2018	Yearling	0.06	0.00	0.87

Table 5–1. Parameter estimates (median, 50 percent; lower credible interval, 2.5 percent and upper credible interval, 97.5 percent) sampled from the posterior distribution for models density dependence and random effects for greater sage-grouse within the Bi-State Distinct Population Segment between 2008 and 2018.—Continued

[Subpopulations: BH, Bodie Hills; FA, Fales; DC, Desert Creek; LV, Long Valley; MG, Mount Grant; PM. Parker Meadows; PN, Pine Nut; SA, Sagehen; WM, White Mountains; —, values indicate overall estimates for respective fixed effect]

Life stage	Density dependence	Random effect	Sub-population	Year	Age	Percentile		
						50.0	2.5	97.5
Nest propensity (second)	—	Subpopulation × Year	SA	2008	Yearling	0.17	0.00	0.96
Nest propensity (second)	—	Subpopulation × Year	SA	2009	Yearling	0.14	0.00	0.95
Nest propensity (second)	—	Subpopulation × Year	SA	2010	Yearling	0.22	0.00	0.97
Nest propensity (second)	—	Subpopulation × Year	SA	2011	Yearling	0.24	0.00	0.97
Nest propensity (second)	—	Subpopulation × Year	SA	2012	Yearling	0.09	0.00	0.93
Nest propensity (second)	—	Subpopulation × Year	SA	2013	Yearling	0.11	0.00	0.94
Nest propensity (second)	—	Subpopulation × Year	SA	2014	Yearling	0.14	0.00	0.94
Nest propensity (second)	—	Subpopulation × Year	SA	2015	Yearling	0.09	0.00	0.73
Nest propensity (second)	—	Subpopulation × Year	SA	2016	Yearling	0.67	0.12	0.99
Nest propensity (second)	—	Subpopulation × Year	SA	2017	Yearling	0.13	0.00	0.94
Nest propensity (second)	—	Subpopulation × Year	SA	2018	Yearling	0.11	0.00	0.94
Nest propensity (second)	—	Subpopulation × Year	WM	2008	Yearling	0.16	0.00	0.97
Nest propensity (second)	—	Subpopulation × Year	WM	2009	Yearling	0.13	0.00	0.96
Nest propensity (second)	—	Subpopulation × Year	WM	2010	Yearling	0.21	0.00	0.98
Nest propensity (second)	—	Subpopulation × Year	WM	2011	Yearling	0.22	0.00	0.98
Nest propensity (second)	—	Subpopulation × Year	WM	2012	Yearling	0.08	0.00	0.94
Nest propensity (second)	—	Subpopulation × Year	WM	2013	Yearling	0.09	0.00	0.92
Nest propensity (second)	—	Subpopulation × Year	WM	2014	Yearling	0.13	0.00	0.96
Nest propensity (second)	—	Subpopulation × Year	WM	2015	Yearling	0.13	0.00	0.96
Nest propensity (second)	—	Subpopulation × Year	WM	2016	Yearling	0.17	0.00	0.95
Nest propensity (second)	—	Subpopulation × Year	WM	2017	Yearling	0.17	0.00	0.97
Nest propensity (second)	—	Subpopulation × Year	WM	2018	Yearling	0.35	0.02	0.98
Survival	—	Subpopulation × Year	BH	2008	Adult	0.82	0.67	0.93
Survival	—	Subpopulation × Year	BH	2009	Adult	0.86	0.74	0.94
Survival	—	Subpopulation × Year	BH	2010	Adult	0.76	0.63	0.88
Survival	—	Subpopulation × Year	BH	2011	Adult	0.77	0.61	0.90
Survival	—	Subpopulation × Year	BH	2012	Adult	0.53	0.34	0.69
Survival	—	Subpopulation × Year	BH	2013	Adult	0.73	0.55	0.86
Survival	—	Subpopulation × Year	BH	2014	Adult	0.62	0.45	0.78
Survival	—	Subpopulation × Year	BH	2015	Adult	0.55	0.41	0.69
Survival	—	Subpopulation × Year	BH	2016	Adult	0.59	0.43	0.73
Survival	—	Subpopulation × Year	BH	2017	Adult	0.62	0.50	0.74
Survival	—	Subpopulation × Year	BH	2018	Adult	0.59	0.41	0.74
Survival	—	Subpopulation × Year	FA	2008	Adult	0.77	0.51	0.92
Survival	—	Subpopulation × Year	FA	2009	Adult	0.81	0.55	0.94
Survival	—	Subpopulation × Year	FA	2010	Adult	0.76	0.48	0.91
Survival	—	Subpopulation × Year	FA	2011	Adult	0.74	0.48	0.91
Survival	—	Subpopulation × Year	FA	2012	Adult	0.58	0.29	0.84
Survival	—	Subpopulation × Year	FA	2013	Adult	0.71	0.46	0.89
Survival	—	Subpopulation × Year	FA	2014	Adult	0.69	0.42	0.89

Table 5–1. Parameter estimates (median, 50 percent; lower credible interval, 2.5 percent and upper credible interval, 97.5 percent) sampled from the posterior distribution for models density dependence and random effects for greater sage-grouse within the Bi-State Distinct Population Segment between 2008 and 2018.—Continued

[Subpopulations: BH, Bodie Hills; FA, Fales; DC, Desert Creek; LV, Long Valley; MG, Mount Grant; PM. Parker Meadows; PN, Pine Nut; SA, Sagehen; WM, White Mountains; —, values indicate overall estimates for respective fixed effect]

Life stage	Density dependence	Random effect	Sub-population	Year	Age	Percentile		
						50.0	2.5	97.5
Survival	—	Subpopulation × Year	FA	2015	Adult	0.67	0.39	0.88
Survival	—	Subpopulation × Year	FA	2016	Adult	0.69	0.38	0.89
Survival	—	Subpopulation × Year	FA	2017	Adult	0.51	0.16	0.78
Survival	—	Subpopulation × Year	FA	2018	Adult	0.67	0.31	0.89
Survival	—	Subpopulation × Year	DC	2008	Adult	0.68	0.38	0.88
Survival	—	Subpopulation × Year	DC	2009	Adult	0.79	0.53	0.93
Survival	—	Subpopulation × Year	DC	2010	Adult	0.77	0.53	0.91
Survival	—	Subpopulation × Year	DC	2011	Adult	0.79	0.60	0.93
Survival	—	Subpopulation × Year	DC	2012	Adult	0.27	0.06	0.54
Survival	—	Subpopulation × Year	DC	2013	Adult	0.69	0.41	0.88
Survival	—	Subpopulation × Year	DC	2014	Adult	0.65	0.37	0.86
Survival	—	Subpopulation × Year	DC	2015	Adult	0.69	0.44	0.88
Survival	—	Subpopulation × Year	DC	2016	Adult	0.79	0.58	0.93
Survival	—	Subpopulation × Year	DC	2017	Adult	0.28	0.05	0.63
Survival	—	Subpopulation × Year	DC	2018	Adult	0.66	0.28	0.88
Survival	—	Subpopulation × Year	LV	2008	Adult	0.70	0.55	0.82
Survival	—	Subpopulation × Year	LV	2009	Adult	0.84	0.70	0.92
Survival	—	Subpopulation × Year	LV	2010	Adult	0.70	0.57	0.82
Survival	—	Subpopulation × Year	LV	2011	Adult	0.62	0.47	0.78
Survival	—	Subpopulation × Year	LV	2012	Adult	0.48	0.30	0.65
Survival	—	Subpopulation × Year	LV	2013	Adult	0.57	0.38	0.77
Survival	—	Subpopulation × Year	LV	2014	Adult	0.56	0.35	0.76
Survival	—	Subpopulation × Year	LV	2015	Adult	0.63	0.44	0.80
Survival	—	Subpopulation × Year	LV	2016	Adult	0.79	0.65	0.91
Survival	—	Subpopulation × Year	LV	2017	Adult	0.57	0.42	0.70
Survival	—	Subpopulation × Year	LV	2018	Adult	0.66	0.45	0.83
Survival	—	Subpopulation × Year	MG	2008	Adult	0.76	0.48	0.92
Survival	—	Subpopulation × Year	MG	2009	Adult	0.83	0.61	0.94
Survival	—	Subpopulation × Year	MG	2010	Adult	0.78	0.55	0.92
Survival	—	Subpopulation × Year	MG	2011	Adult	0.72	0.43	0.90
Survival	—	Subpopulation × Year	MG	2012	Adult	0.54	0.30	0.79
Survival	—	Subpopulation × Year	MG	2013	Adult	0.72	0.53	0.86
Survival	—	Subpopulation × Year	MG	2014	Adult	0.63	0.39	0.82
Survival	—	Subpopulation × Year	MG	2015	Adult	0.74	0.52	0.91
Survival	—	Subpopulation × Year	MG	2016	Adult	0.70	0.52	0.85
Survival	—	Subpopulation × Year	MG	2017	Adult	0.58	0.39	0.76
Survival	—	Subpopulation × Year	MG	2018	Adult	0.67	0.44	0.83
Survival	—	Subpopulation × Year	PM	2008	Adult	0.76	0.49	0.91
Survival	—	Subpopulation × Year	PM	2009	Adult	0.80	0.55	0.92
Survival	—	Subpopulation × Year	PM	2010	Adult	0.78	0.54	0.92

Table 5–1. Parameter estimates (median, 50 percent; lower credible interval, 2.5 percent and upper credible interval, 97.5 percent) sampled from the posterior distribution for models density dependence and random effects for greater sage-grouse within the Bi-State Distinct Population Segment between 2008 and 2018.—Continued

[Subpopulations: BH, Bodie Hills; FA, Fales; DC, Desert Creek; LV, Long Valley; MG, Mount Grant; PM. Parker Meadows; PN, Pine Nut; SA, Sagehen; WM, White Mountains; —, values indicate overall estimates for respective fixed effect]

Life stage	Density dependence	Random effect	Sub-population	Year	Age	Percentile		
						50.0	2.5	97.5
Survival	—	Subpopulation × Year	PM	2011	Adult	0.76	0.50	0.92
Survival	—	Subpopulation × Year	PM	2012	Adult	0.53	0.19	0.82
Survival	—	Subpopulation × Year	PM	2013	Adult	0.69	0.36	0.89
Survival	—	Subpopulation × Year	PM	2014	Adult	0.66	0.31	0.87
Survival	—	Subpopulation × Year	PM	2015	Adult	0.67	0.31	0.88
Survival	—	Subpopulation × Year	PM	2016	Adult	0.71	0.39	0.90
Survival	—	Subpopulation × Year	PM	2017	Adult	0.45	0.19	0.68
Survival	—	Subpopulation × Year	PM	2018	Adult	0.72	0.44	0.90
Survival	—	Subpopulation × Year	PN	2008	Adult	0.78	0.55	0.93
Survival	—	Subpopulation × Year	PN	2009	Adult	0.74	0.34	0.92
Survival	—	Subpopulation × Year	PN	2010	Adult	0.75	0.48	0.91
Survival	—	Subpopulation × Year	PN	2011	Adult	0.78	0.60	0.90
Survival	—	Subpopulation × Year	PN	2012	Adult	0.46	0.26	0.70
Survival	—	Subpopulation × Year	PN	2013	Adult	0.68	0.49	0.85
Survival	—	Subpopulation × Year	PN	2014	Adult	0.68	0.46	0.85
Survival	—	Subpopulation × Year	PN	2015	Adult	0.69	0.43	0.87
Survival	—	Subpopulation × Year	PN	2016	Adult	0.71	0.37	0.90
Survival	—	Subpopulation × Year	PN	2017	Adult	0.58	0.22	0.84
Survival	—	Subpopulation × Year	PN	2018	Adult	0.66	0.31	0.88
Survival	—	Subpopulation × Year	SA	2008	Adult	0.70	0.33	0.89
Survival	—	Subpopulation × Year	SA	2009	Adult	0.77	0.36	0.92
Survival	—	Subpopulation × Year	SA	2010	Adult	0.72	0.33	0.90
Survival	—	Subpopulation × Year	SA	2011	Adult	0.71	0.35	0.90
Survival	—	Subpopulation × Year	SA	2012	Adult	0.46	0.09	0.78
Survival	—	Subpopulation × Year	SA	2013	Adult	0.65	0.27	0.87
Survival	—	Subpopulation × Year	SA	2014	Adult	0.66	0.34	0.88
Survival	—	Subpopulation × Year	SA	2015	Adult	0.64	0.36	0.84
Survival	—	Subpopulation × Year	SA	2016	Adult	0.65	0.36	0.84
Survival	—	Subpopulation × Year	SA	2017	Adult	0.53	0.16	0.82
Survival	—	Subpopulation × Year	SA	2018	Adult	0.65	0.27	0.88
Survival	—	Subpopulation × Year	WM	2008	Adult	0.71	0.37	0.90
Survival	—	Subpopulation × Year	WM	2009	Adult	0.78	0.40	0.93
Survival	—	Subpopulation × Year	WM	2010	Adult	0.71	0.36	0.90
Survival	—	Subpopulation × Year	WM	2011	Adult	0.70	0.34	0.89
Survival	—	Subpopulation × Year	WM	2012	Adult	0.44	0.12	0.74
Survival	—	Subpopulation × Year	WM	2013	Adult	0.62	0.25	0.84
Survival	—	Subpopulation × Year	WM	2014	Adult	0.62	0.26	0.85
Survival	—	Subpopulation × Year	WM	2015	Adult	0.62	0.25	0.85
Survival	—	Subpopulation × Year	WM	2016	Adult	0.70	0.39	0.90
Survival	—	Subpopulation × Year	WM	2017	Adult	0.60	0.29	0.85

Table 5–1. Parameter estimates (median, 50 percent; lower credible interval, 2.5 percent and upper credible interval, 97.5 percent) sampled from the posterior distribution for models density dependence and random effects for greater sage-grouse within the Bi-State Distinct Population Segment between 2008 and 2018.—Continued

[Subpopulations: BH, Bodie Hills; FA, Fales; DC, Desert Creek; LV, Long Valley; MG, Mount Grant; PM. Parker Meadows; PN, Pine Nut; SA, Sagehen; WM, White Mountains; —, values indicate overall estimates for respective fixed effect]

Life stage	Density dependence	Random effect	Sub-population	Year	Age	Percentile		
						50.0	2.5	97.5
Survival	—	Subpopulation × Year	WM	2018	Adult	0.64	0.38	0.83
Survival	—	Subpopulation × Year	BH	2008	Juvenile	0.76	0.69	0.83
Survival	—	Subpopulation × Year	BH	2009	Juvenile	0.76	0.69	0.83
Survival	—	Subpopulation × Year	BH	2010	Juvenile	0.76	0.69	0.82
Survival	—	Subpopulation × Year	BH	2011	Juvenile	0.75	0.68	0.82
Survival	—	Subpopulation × Year	BH	2012	Juvenile	0.75	0.68	0.82
Survival	—	Subpopulation × Year	BH	2013	Juvenile	0.75	0.67	0.82
Survival	—	Subpopulation × Year	BH	2014	Juvenile	0.75	0.67	0.82
Survival	—	Subpopulation × Year	BH	2015	Juvenile	0.74	0.66	0.81
Survival	—	Subpopulation × Year	BH	2016	Juvenile	0.74	0.66	0.81
Survival	—	Subpopulation × Year	BH	2017	Juvenile	0.75	0.68	0.82
Survival	—	Subpopulation × Year	BH	2018	Juvenile	0.75	0.67	0.82
Survival	—	Subpopulation × Year	FA	2008	Juvenile	0.75	0.67	0.82
Survival	—	Subpopulation × Year	FA	2009	Juvenile	0.75	0.67	0.81
Survival	—	Subpopulation × Year	FA	2010	Juvenile	0.75	0.67	0.82
Survival	—	Subpopulation × Year	FA	2011	Juvenile	0.75	0.67	0.82
Survival	—	Subpopulation × Year	FA	2012	Juvenile	0.75	0.67	0.82
Survival	—	Subpopulation × Year	FA	2013	Juvenile	0.75	0.67	0.82
Survival	—	Subpopulation × Year	FA	2014	Juvenile	0.75	0.67	0.82
Survival	—	Subpopulation × Year	FA	2015	Juvenile	0.75	0.67	0.82
Survival	—	Subpopulation × Year	FA	2016	Juvenile	0.75	0.67	0.82
Survival	—	Subpopulation × Year	FA	2017	Juvenile	0.74	0.67	0.81
Survival	—	Subpopulation × Year	FA	2018	Juvenile	0.75	0.67	0.82
Survival	—	Subpopulation × Year	DC	2008	Juvenile	0.75	0.66	0.81
Survival	—	Subpopulation × Year	DC	2009	Juvenile	0.75	0.67	0.82
Survival	—	Subpopulation × Year	DC	2010	Juvenile	0.75	0.67	0.82
Survival	—	Subpopulation × Year	DC	2011	Juvenile	0.75	0.68	0.82
Survival	—	Subpopulation × Year	DC	2012	Juvenile	0.74	0.66	0.81
Survival	—	Subpopulation × Year	DC	2013	Juvenile	0.75	0.67	0.82
Survival	—	Subpopulation × Year	DC	2014	Juvenile	0.75	0.67	0.81
Survival	—	Subpopulation × Year	DC	2015	Juvenile	0.75	0.68	0.82
Survival	—	Subpopulation × Year	DC	2016	Juvenile	0.76	0.68	0.83
Survival	—	Subpopulation × Year	DC	2017	Juvenile	0.74	0.66	0.81
Survival	—	Subpopulation × Year	DC	2018	Juvenile	0.75	0.67	0.82
Survival	—	Subpopulation × Year	LV	2008	Juvenile	0.75	0.68	0.82
Survival	—	Subpopulation × Year	LV	2009	Juvenile	0.77	0.70	0.83
Survival	—	Subpopulation × Year	LV	2010	Juvenile	0.75	0.68	0.82
Survival	—	Subpopulation × Year	LV	2011	Juvenile	0.74	0.67	0.81
Survival	—	Subpopulation × Year	LV	2012	Juvenile	0.75	0.67	0.82
Survival	—	Subpopulation × Year	LV	2013	Juvenile	0.74	0.67	0.81

Table 5–1. Parameter estimates (median, 50 percent; lower credible interval, 2.5 percent and upper credible interval, 97.5 percent) sampled from the posterior distribution for models density dependence and random effects for greater sage-grouse within the Bi-State Distinct Population Segment between 2008 and 2018.—Continued

[Subpopulations: BH, Bodie Hills; FA, Fales; DC, Desert Creek; LV, Long Valley; MG, Mount Grant; PM. Parker Meadows; PN, Pine Nut; SA, Sagehen; WM, White Mountains; —, values indicate overall estimates for respective fixed effect]

Life stage	Density dependence	Random effect	Sub-population	Year	Age	Percentile		
						50.0	2.5	97.5
Survival	—	Subpopulation × Year	LV	2014	Juvenile	0.75	0.67	0.81
Survival	—	Subpopulation × Year	LV	2015	Juvenile	0.74	0.66	0.81
Survival	—	Subpopulation × Year	LV	2016	Juvenile	0.75	0.67	0.82
Survival	—	Subpopulation × Year	LV	2017	Juvenile	0.75	0.68	0.82
Survival	—	Subpopulation × Year	LV	2018	Juvenile	0.75	0.67	0.82
Survival	—	Subpopulation × Year	MG	2008	Juvenile	0.75	0.67	0.82
Survival	—	Subpopulation × Year	MG	2009	Juvenile	0.75	0.67	0.82
Survival	—	Subpopulation × Year	MG	2010	Juvenile	0.75	0.67	0.82
Survival	—	Subpopulation × Year	MG	2011	Juvenile	0.75	0.67	0.81
Survival	—	Subpopulation × Year	MG	2012	Juvenile	0.74	0.66	0.82
Survival	—	Subpopulation × Year	MG	2013	Juvenile	0.75	0.67	0.82
Survival	—	Subpopulation × Year	MG	2014	Juvenile	0.75	0.67	0.82
Survival	—	Subpopulation × Year	MG	2015	Juvenile	0.75	0.67	0.81
Survival	—	Subpopulation × Year	MG	2016	Juvenile	0.75	0.67	0.82
Survival	—	Subpopulation × Year	MG	2017	Juvenile	0.74	0.67	0.81
Survival	—	Subpopulation × Year	MG	2018	Juvenile	0.75	0.67	0.81
Survival	—	Subpopulation × Year	PM	2008	Juvenile	0.75	0.67	0.82
Survival	—	Subpopulation × Year	PM	2009	Juvenile	0.75	0.67	0.82
Survival	—	Subpopulation × Year	PM	2010	Juvenile	0.75	0.67	0.81
Survival	—	Subpopulation × Year	PM	2011	Juvenile	0.75	0.67	0.81
Survival	—	Subpopulation × Year	PM	2012	Juvenile	0.75	0.67	0.81
Survival	—	Subpopulation × Year	PM	2013	Juvenile	0.75	0.67	0.82
Survival	—	Subpopulation × Year	PM	2014	Juvenile	0.75	0.67	0.82
Survival	—	Subpopulation × Year	PM	2015	Juvenile	0.75	0.67	0.82
Survival	—	Subpopulation × Year	PM	2016	Juvenile	0.75	0.67	0.82
Survival	—	Subpopulation × Year	PM	2017	Juvenile	0.75	0.67	0.82
Survival	—	Subpopulation × Year	PM	2018	Juvenile	0.75	0.67	0.81
Survival	—	Subpopulation × Year	PN	2008	Juvenile	0.75	0.68	0.82
Survival	—	Subpopulation × Year	PN	2009	Juvenile	0.75	0.67	0.81
Survival	—	Subpopulation × Year	PN	2010	Juvenile	0.75	0.67	0.82
Survival	—	Subpopulation × Year	PN	2011	Juvenile	0.75	0.67	0.82
Survival	—	Subpopulation × Year	PN	2012	Juvenile	0.74	0.66	0.81
Survival	—	Subpopulation × Year	PN	2013	Juvenile	0.75	0.67	0.82
Survival	—	Subpopulation × Year	PN	2014	Juvenile	0.75	0.67	0.82
Survival	—	Subpopulation × Year	PN	2015	Juvenile	0.75	0.67	0.82
Survival	—	Subpopulation × Year	PN	2016	Juvenile	0.75	0.67	0.82
Survival	—	Subpopulation × Year	PN	2017	Juvenile	0.75	0.67	0.82
Survival	—	Subpopulation × Year	PN	2018	Juvenile	0.75	0.67	0.82
Survival	—	Subpopulation × Year	SA	2008	Juvenile	0.75	0.67	0.82
Survival	—	Subpopulation × Year	SA	2009	Juvenile	0.75	0.67	0.81

Table 5–1. Parameter estimates (median, 50 percent; lower credible interval, 2.5 percent and upper credible interval, 97.5 percent) sampled from the posterior distribution for models density dependence and random effects for greater sage-grouse within the Bi-State Distinct Population Segment between 2008 and 2018.—Continued

[Subpopulations: BH, Bodie Hills; FA, Fales; DC, Desert Creek; LV, Long Valley; MG, Mount Grant; PM. Parker Meadows; PN, Pine Nut; SA, Sagehen; WM, White Mountains; —, values indicate overall estimates for respective fixed effect]

Life stage	Density dependence	Random effect	Sub-population	Year	Age	Percentile		
						50.0	2.5	97.5
Survival	—	Subpopulation × Year	SA	2010	Juvenile	0.75	0.67	0.82
Survival	—	Subpopulation × Year	SA	2011	Juvenile	0.75	0.67	0.82
Survival	—	Subpopulation × Year	SA	2012	Juvenile	0.75	0.67	0.81
Survival	—	Subpopulation × Year	SA	2013	Juvenile	0.75	0.67	0.81
Survival	—	Subpopulation × Year	SA	2014	Juvenile	0.75	0.67	0.82
Survival	—	Subpopulation × Year	SA	2015	Juvenile	0.75	0.67	0.81
Survival	—	Subpopulation × Year	SA	2016	Juvenile	0.75	0.67	0.81
Survival	—	Subpopulation × Year	SA	2017	Juvenile	0.75	0.67	0.82
Survival	—	Subpopulation × Year	SA	2018	Juvenile	0.75	0.67	0.81
Survival	—	Subpopulation × Year	WM	2008	Juvenile	0.75	0.67	0.81
Survival	—	Subpopulation × Year	WM	2009	Juvenile	0.75	0.67	0.81
Survival	—	Subpopulation × Year	WM	2010	Juvenile	0.75	0.67	0.82
Survival	—	Subpopulation × Year	WM	2011	Juvenile	0.75	0.67	0.82
Survival	—	Subpopulation × Year	WM	2012	Juvenile	0.75	0.67	0.82
Survival	—	Subpopulation × Year	WM	2013	Juvenile	0.75	0.67	0.81
Survival	—	Subpopulation × Year	WM	2014	Juvenile	0.75	0.67	0.82
Survival	—	Subpopulation × Year	WM	2015	Juvenile	0.75	0.67	0.82
Survival	—	Subpopulation × Year	WM	2016	Juvenile	0.75	0.67	0.82
Survival	—	Subpopulation × Year	WM	2017	Juvenile	0.75	0.67	0.82
Survival	—	Subpopulation × Year	WM	2018	Juvenile	0.75	0.67	0.82
Survival	—	Subpopulation × Year	BH	2008	Yearling	0.83	0.67	0.93
Survival	—	Subpopulation × Year	BH	2009	Yearling	0.86	0.73	0.95
Survival	—	Subpopulation × Year	BH	2010	Yearling	0.77	0.61	0.89
Survival	—	Subpopulation × Year	BH	2011	Yearling	0.77	0.61	0.90
Survival	—	Subpopulation × Year	BH	2012	Yearling	0.53	0.34	0.71
Survival	—	Subpopulation × Year	BH	2013	Yearling	0.73	0.54	0.88
Survival	—	Subpopulation × Year	BH	2014	Yearling	0.62	0.43	0.81
Survival	—	Subpopulation × Year	BH	2015	Yearling	0.56	0.38	0.73
Survival	—	Subpopulation × Year	BH	2016	Yearling	0.59	0.41	0.74
Survival	—	Subpopulation × Year	BH	2017	Yearling	0.63	0.49	0.76
Survival	—	Subpopulation × Year	BH	2018	Yearling	0.59	0.42	0.75
Survival	—	Subpopulation × Year	FA	2008	Yearling	0.77	0.48	0.93
Survival	—	Subpopulation × Year	FA	2009	Yearling	0.81	0.53	0.94
Survival	—	Subpopulation × Year	FA	2010	Yearling	0.76	0.47	0.92
Survival	—	Subpopulation × Year	FA	2011	Yearling	0.74	0.47	0.92
Survival	—	Subpopulation × Year	FA	2012	Yearling	0.59	0.28	0.85
Survival	—	Subpopulation × Year	FA	2013	Yearling	0.72	0.44	0.90
Survival	—	Subpopulation × Year	FA	2014	Yearling	0.70	0.40	0.89
Survival	—	Subpopulation × Year	FA	2015	Yearling	0.68	0.37	0.89
Survival	—	Subpopulation × Year	FA	2016	Yearling	0.70	0.37	0.89

Table 5–1. Parameter estimates (median, 50 percent; lower credible interval, 2.5 percent and upper credible interval, 97.5 percent) sampled from the posterior distribution for models density dependence and random effects for greater sage-grouse within the Bi-State Distinct Population Segment between 2008 and 2018.—Continued

[Subpopulations: BH, Bodie Hills; FA, Fales; DC, Desert Creek; LV, Long Valley; MG, Mount Grant; PM. Parker Meadows; PN, Pine Nut; SA, Sagehen; WM, White Mountains; —, values indicate overall estimates for respective fixed effect]

Life stage	Density dependence	Random effect	Sub-population	Year	Age	Percentile		
						50.0	2.5	97.5
Survival	—	Subpopulation × Year	FA	2017	Yearling	0.51	0.15	0.81
Survival	—	Subpopulation × Year	FA	2018	Yearling	0.68	0.32	0.89
Survival	—	Subpopulation × Year	DC	2008	Yearling	0.68	0.36	0.89
Survival	—	Subpopulation × Year	DC	2009	Yearling	0.80	0.52	0.93
Survival	—	Subpopulation × Year	DC	2010	Yearling	0.77	0.52	0.92
Survival	—	Subpopulation × Year	DC	2011	Yearling	0.80	0.59	0.93
Survival	—	Subpopulation × Year	DC	2012	Yearling	0.27	0.06	0.58
Survival	—	Subpopulation × Year	DC	2013	Yearling	0.70	0.41	0.89
Survival	—	Subpopulation × Year	DC	2014	Yearling	0.66	0.38	0.87
Survival	—	Subpopulation × Year	DC	2015	Yearling	0.70	0.43	0.89
Survival	—	Subpopulation × Year	DC	2016	Yearling	0.79	0.58	0.93
Survival	—	Subpopulation × Year	DC	2017	Yearling	0.28	0.05	0.65
Survival	—	Subpopulation × Year	DC	2018	Yearling	0.67	0.29	0.88
Survival	—	Subpopulation × Year	LV	2008	Yearling	0.70	0.52	0.84
Survival	—	Subpopulation × Year	LV	2009	Yearling	0.84	0.70	0.93
Survival	—	Subpopulation × Year	LV	2010	Yearling	0.70	0.54	0.83
Survival	—	Subpopulation × Year	LV	2011	Yearling	0.63	0.44	0.80
Survival	—	Subpopulation × Year	LV	2012	Yearling	0.48	0.30	0.68
Survival	—	Subpopulation × Year	LV	2013	Yearling	0.58	0.36	0.79
Survival	—	Subpopulation × Year	LV	2014	Yearling	0.57	0.34	0.79
Survival	—	Subpopulation × Year	LV	2015	Yearling	0.63	0.43	0.81
Survival	—	Subpopulation × Year	LV	2016	Yearling	0.80	0.63	0.92
Survival	—	Subpopulation × Year	LV	2017	Yearling	0.57	0.39	0.73
Survival	—	Subpopulation × Year	LV	2018	Yearling	0.67	0.45	0.83
Survival	—	Subpopulation × Year	MG	2008	Yearling	0.76	0.47	0.92
Survival	—	Subpopulation × Year	MG	2009	Yearling	0.83	0.60	0.94
Survival	—	Subpopulation × Year	MG	2010	Yearling	0.79	0.55	0.93
Survival	—	Subpopulation × Year	MG	2011	Yearling	0.73	0.41	0.90
Survival	—	Subpopulation × Year	MG	2012	Yearling	0.54	0.29	0.80
Survival	—	Subpopulation × Year	MG	2013	Yearling	0.73	0.51	0.87
Survival	—	Subpopulation × Year	MG	2014	Yearling	0.63	0.37	0.83
Survival	—	Subpopulation × Year	MG	2015	Yearling	0.74	0.51	0.91
Survival	—	Subpopulation × Year	MG	2016	Yearling	0.71	0.49	0.86
Survival	—	Subpopulation × Year	MG	2017	Yearling	0.59	0.36	0.77
Survival	—	Subpopulation × Year	MG	2018	Yearling	0.68	0.46	0.83
Survival	—	Subpopulation × Year	PM	2008	Yearling	0.76	0.49	0.92
Survival	—	Subpopulation × Year	PM	2009	Yearling	0.80	0.54	0.93
Survival	—	Subpopulation × Year	PM	2010	Yearling	0.78	0.54	0.92
Survival	—	Subpopulation × Year	PM	2011	Yearling	0.77	0.49	0.92
Survival	—	Subpopulation × Year	PM	2012	Yearling	0.54	0.18	0.82

Table 5–1. Parameter estimates (median, 50 percent; lower credible interval, 2.5 percent and upper credible interval, 97.5 percent) sampled from the posterior distribution for models density dependence and random effects for greater sage-grouse within the Bi-State Distinct Population Segment between 2008 and 2018.—Continued

[Subpopulations: BH, Bodie Hills; FA, Fales; DC, Desert Creek; LV, Long Valley; MG, Mount Grant; PM. Parker Meadows; PN, Pine Nut; SA, Sagehen; WM, White Mountains; —, values indicate overall estimates for respective fixed effect]

Life stage	Density dependence	Random effect	Sub-population	Year	Age	Percentile		
						50.0	2.5	97.5
Survival	—	Subpopulation × Year	PM	2013	Yearling	0.70	0.34	0.90
Survival	—	Subpopulation × Year	PM	2014	Yearling	0.66	0.31	0.88
Survival	—	Subpopulation × Year	PM	2015	Yearling	0.67	0.30	0.89
Survival	—	Subpopulation × Year	PM	2016	Yearling	0.72	0.38	0.91
Survival	—	Subpopulation × Year	PM	2017	Yearling	0.45	0.19	0.70
Survival	—	Subpopulation × Year	PM	2018	Yearling	0.73	0.44	0.90
Survival	—	Subpopulation × Year	PN	2008	Yearling	0.79	0.52	0.93
Survival	—	Subpopulation × Year	PN	2009	Yearling	0.75	0.31	0.93
Survival	—	Subpopulation × Year	PN	2010	Yearling	0.76	0.46	0.91
Survival	—	Subpopulation × Year	PN	2011	Yearling	0.78	0.60	0.91
Survival	—	Subpopulation × Year	PN	2012	Yearling	0.47	0.23	0.72
Survival	—	Subpopulation × Year	PN	2013	Yearling	0.69	0.46	0.86
Survival	—	Subpopulation × Year	PN	2014	Yearling	0.69	0.44	0.86
Survival	—	Subpopulation × Year	PN	2015	Yearling	0.69	0.41	0.88
Survival	—	Subpopulation × Year	PN	2016	Yearling	0.71	0.37	0.90
Survival	—	Subpopulation × Year	PN	2017	Yearling	0.59	0.22	0.85
Survival	—	Subpopulation × Year	PN	2018	Yearling	0.66	0.30	0.89
Survival	—	Subpopulation × Year	SA	2008	Yearling	0.70	0.31	0.90
Survival	—	Subpopulation × Year	SA	2009	Yearling	0.77	0.36	0.93
Survival	—	Subpopulation × Year	SA	2010	Yearling	0.72	0.33	0.91
Survival	—	Subpopulation × Year	SA	2011	Yearling	0.71	0.33	0.91
Survival	—	Subpopulation × Year	SA	2012	Yearling	0.47	0.09	0.79
Survival	—	Subpopulation × Year	SA	2013	Yearling	0.66	0.26	0.88
Survival	—	Subpopulation × Year	SA	2014	Yearling	0.67	0.32	0.88
Survival	—	Subpopulation × Year	SA	2015	Yearling	0.64	0.35	0.85
Survival	—	Subpopulation × Year	SA	2016	Yearling	0.66	0.34	0.86
Survival	—	Subpopulation × Year	SA	2017	Yearling	0.54	0.15	0.83
Survival	—	Subpopulation × Year	SA	2018	Yearling	0.65	0.28	0.87
Survival	—	Subpopulation × Year	WM	2008	Yearling	0.72	0.36	0.91
Survival	—	Subpopulation × Year	WM	2009	Yearling	0.78	0.38	0.93
Survival	—	Subpopulation × Year	WM	2010	Yearling	0.72	0.34	0.90
Survival	—	Subpopulation × Year	WM	2011	Yearling	0.70	0.35	0.90
Survival	—	Subpopulation × Year	WM	2012	Yearling	0.45	0.11	0.74
Survival	—	Subpopulation × Year	WM	2013	Yearling	0.62	0.23	0.85
Survival	—	Subpopulation × Year	WM	2014	Yearling	0.63	0.25	0.85
Survival	—	Subpopulation × Year	WM	2015	Yearling	0.62	0.24	0.86
Survival	—	Subpopulation × Year	WM	2016	Yearling	0.71	0.39	0.90
Survival	—	Subpopulation × Year	WM	2017	Yearling	0.61	0.28	0.86
Survival	—	Subpopulation × Year	WM	2018	Yearling	0.65	0.39	0.8

Appendix 6. Tables of Variable Importance from Preliminary Variable Screening for Seasonal and Life-Stage Habitat Selection Models

Table 6–1. Rankings of variable importance from preliminary variable screening, including change in AIC (ΔAIC), change in Spearman's rank coefficient (ΔSpearman's), and change in R^2 (ΔR^2) of observed versus predicted numbers of locations for sage-grouse spring telemetry locations.

[Variable importance was determined by repeatedly refitting GLM's with logit link and binomial family to response variable data indicating used vs. random locations. Each candidate covariate was tested in models with and without that covariate, in the presence of as many as 5 other covariates; no covariates were allowed to exist in the same model if they had a correlation coefficient of at least 0.5 with the other covariate or covariates]

Covariate	ΔAIC	ΔSpearman's	ΔR^2
All PJ (r = 439)	659.4850	0.2029	0.0394
All PJ (r = 167)	603.4354	0.2288	0.0442
All PJ (r = 1,451)	543.2425	0.2084	0.0173
PJ-CC1 (r = 439)	476.2039	0.1992	0.0089
Sage height (r = 1,451)	432.7922	0.1592	0.0355
PJ-CC1 (r = 167)	429.8950	0.2043	0.0366
PJ-CC1 (r = 1,451)	428.4031	0.1417	–0.0041
Sage height (r = 439)	357.7398	0.1832	0.0480
Sage height (r = 167)	335.1678	0.1308	0.0142
% Big sagebrush (r = 1,451)	300.1991	0.1107	–0.0064
Roughness (r = 1,451)	267.1151	0.1355	0.0209
Slope (r = 167)	251.6971	0.1464	0.0250
% Big sagebrush (r = 439)	250.6275	0.1813	0.0532
Slope (r = 439)	245.7490	0.1000	0.0030
Roughness (r = 167)	243.5540	0.1655	0.0498
Distance to perennial stream	239.2089	0.1267	0.0147
% Bare ground (r = 1,451)	235.2331	0.0988	–0.0196
% Sagebrush (r = 1,451)	220.7999	0.1240	–0.0290
Elevation (r = 167)	220.2745	0.0651	–0.0215
Roughness (r = 439)	219.2009	0.1788	0.0273
% Big sagebrush (r = 167)	210.1398	0.0628	0.0265
Elevation (r = 439)	199.5817	0.0420	–0.0262
Slope (r = 1,451)	189.4991	0.1156	0.0329
Distance to water body	177.3838	0.1958	0.0587
Elevation (r = 1,451)	176.5560	0.0417	–0.0198
% Sagebrush (r = 439)	172.8323	0.1491	0.0215
% Sagebrush (r = 167)	168.9240	0.0884	0.0157
% Bare ground (r = 167)	158.5579	0.2092	0.0615
% Bare ground (r = 439)	134.5758	0.0606	–0.0387
Distance to all streams	125.7165	0.0901	0.0084
Transformed aspect (r = 1,451)	106.6515	0.0936	0.0018
Shrub Height (r = 1,451)	103.8116	0.1277	0.0035
Transformed aspect (r = 439)	96.0041	0.1297	0.0233
Transformed aspect (r = 167)	93.6274	0.1160	0.0274
Compound topographic index (r = 1,451)	87.5587	0.0897	0.0201
% Perennial grass (r = 1,451)	83.0866	0.1264	0.0179
% Herbaceous (r = 1,451)	81.1832	0.1050	0.0045
Curvature (r = 1,451)	79.9775	0.1066	0.0086
Compound topographic index (r = 439)	74.6251	0.1810	0.0077
Compound topographic index (r = 167)	71.3899	0.0954	0.0124
Distance to ditch	65.9445	0.0410	0.0195
% Herbaceous (r = 439)	59.9396	0.0733	0.0187
% Perennial grass (r = 439)	55.7044	0.1156	0.0164
% Shrub Cover (r = 1,451)	54.0952	0.0220	–0.0296
Distance to forest	50.8655	0.0141	0.0113
NDVI	49.4992	0.0622	–0.0001
Heat load index (r = 1,451)	47.6946	0.0735	0.0060
% Perennial grass (r = 167)	47.2069	0.1024	0.0081
% Little sagebrush (r = 1,451)	46.7342	0.0856	–0.0048
% Non-sagebrush shrub (r = 167)	44.4592	0.0661	0.0205
% Little sagebrush (r = 167)	44.2800	0.1067	0.0163
% Herbaceous (r = 167)	41.1381	0.0831	–0.0042
% Non-sagebrush shrub (r = 439)	41.1211	0.0636	0.0153
NDVI (r = 439)	39.1854	0.0343	–0.0293
Distance to PJ-CC2	37.6068	0.0824	0.0158
% Shrub cover (r = 439)	36.8860	0.0610	0.0145
Shrub height (r = 439)	34.9795	0.0627	–0.0068
% Shrub cover (r = 167)	32.7615	–0.0068	–0.0008
Distance to PJ-CC1	32.4152	0.0964	0.0088
Heat load index (r = 439)	30.7628	0.0621	–0.0166
% Non-sagebrush shrub (r = 1,451)	30.5397	0.0293	0.0017
Distance to tree	29.2592	0.1004	0.0084
Curvature (r = 439)	28.9050	0.0550	0.0160
Distance to intermittent stream	28.2076	0.0998	0.0172
Shrub height (r = 167)	26.9695	0.0462	0.0187
Distance to wet meadow	26.5678	–0.0338	–0.0152

Table 6–1. Rankings of variable importance from preliminary variable screening, including change in AIC (ΔAIC), change in Spearman's rank coefficient (ΔSpearman's), and change in R^2 (ΔR^2) of observed versus predicted numbers of locations for sage-grouse spring telemetry locations.—Continued

[Variable importance was determined by repeatedly refitting GLM's with logit link and binomial family to response variable data indicating used vs. random locations. Each candidate covariate was tested in models with and without that covariate, in the presence of as many as 5 other covariates; no covariates were allowed to exist in the same model if they had a correlation coefficient of at least 0.5 with the other covariate or covariates]

Covariate	ΔAIC	ΔSpearman's	ΔR^2
% Little sagebrush (r = 439)	25.5447	0.0378	–0.0378
NDVI (r = 1,451)	24.1435	0.0020	–0.0427
Heat load index (r = 167)	23.2107	0.0682	–0.0012
Well density (r = 1,451)	20.5674	0.0189	0.0032
% Agricultural land (r = 1,451)	18.3970	0.0199	0.0029
Spring density (r = 1,451)	12.3948	0.0603	0.0100
Ditch density (r = 1,451)	11.3180	0.0233	–0.0009
Ditch density (r = 439)	10.0975	0.0140	0.0006
Perennial stream density (r = 439)	9.4825	0.0168	0.0116
All stream density (r = 1,451)	9.0036	0.0682	0.0199
Perennial stream density (r = 1,451)	7.5531	0.0473	0.0119
All stream density (r = 439)	7.5230	0.0122	0.0110
Perennial stream density (r = 167)	7.1823	0.0270	0.0064
Distance to agricultural land	6.6349	0.0038	0.0039
All stream density (r = 167)	6.5178	0.0195	0.0065
% Wet meadow (r = 1,451)	4.7391	0.0382	0.0094
Curvature (r = 167)	4.2946	0.0100	0.0064
% Annual grass (r = 1,451)	4.0307	0.0134	0.0189
Ditch density (r = 167)	3.2133	0.0041	–0.0016
% Annual grass (r = 439)	2.7214	–0.0003	0.0036
% Annual grass (r = 167)	2.4375	0.0144	0.0045
Intermittent stream density (r = 1,451)	2.3027	0.0182	0.0041
% Agricultural land (r = 439)	2.0997	0.0003	0.0028
% Wet meadow (r = 439)	1.0537	0.0113	0.0043
% Wet meadow (r = 167)	0.9084	0.0010	0.0031
Well density (r = 439)	0.8931	0.0011	0.0001
% Agricultural land (r = 167)	0.7518	0.0031	0.0013
Distance to well	0.3093	–0.0070	–0.0031
Spring density (r = 439)	–0.0013	–0.0001	0.0021
Spring density (r = 167)	–0.1532	–0.0003	–0.0005
Intermittent stream density (r = 439)	–0.2211	0.0058	–0.0020
Intermittent stream density (r = 167)	–0.8576	–0.0015	0.0001
Well density (r = 167)	–1.4867	0.0021	0.0006

Table 6–2. Rankings of variable importance from preliminary variable screening, including change in AIC (ΔAIC), change in Spearman's rank coefficient (ΔSpearman's), and change in R^2 (ΔR^2) of observed versus predicted numbers of locations for sage-grouse summer\fall telemetry locations.

[Variable importance was determined by repeatedly refitting GLM's with logit link and binomial family to response variable data indicating used vs. random locations. Each candidate covariate was tested in models with and without that covariate, in the presence of as many as 5 other covariates; no covariates were allowed to exist in the same model if they had a correlation coefficient of at least 0.5 with the other covariate or covariates]

Covariate	ΔAIC	ΔSpearman's	ΔR^2
Distance to perennial stream	529.2461	0.1799	0.0388
Distance to all streams	520.9965	0.1455	0.0635
All PJ (r = 439)	502.5178	0.1601	0.0187
All PJ (r = 167)	488.2565	0.1676	0.0174
% PJ-CC1 (r = 167)	439.5359	0.1704	0.0461
% PJ-CC1 (r = 439)	436.3210	0.0976	0.0078
All PJ (r = 1,451)	408.5535	0.1739	0.0226
% PJ-CC1 (r = 1,451)	387.2671	0.2051	–0.0262
Elevation (r = 439)	382.9204	0.1152	–0.0835
Elevation (r = 1,451)	369.1957	0.0943	–0.0831
Elevation (r = 167)	359.7502	0.0574	–0.0768
Slope (r = 439)	328.1367	0.0948	0.0218
% Bare ground (r = 1,451)	310.8374	0.1556	–0.0208
% Herbaceous (r = 1,451)	297.6050	0.1125	0.0394
Roughness (r = 439)	282.8105	0.1047	0.0321
% Perennial grass (r = 1,451)	280.4824	0.2172	0.0165
% Herbaceous (r = 439)	251.6325	0.1497	0.0558
% Herbaceous (r = 167)	250.9424	0.1442	0.0535
Roughness (r = 1,451)	229.7835	0.1605	0.0577
Slope (r = 167)	228.8035	0.1256	0.0292
% Bare ground (r = 439)	223.2682	0.3077	0.0618
Roughness (r = 167)	222.4944	0.0997	0.0210
% Bare ground (r = 167)	218.0113	0.1400	0.0350
Distance to water body	209.8439	0.1519	0.0343
% Perennial grass (r = 167)	207.5372	0.1958	0.0529
% Perennial grass (r = 439)	190.7774	0.1220	0.0266
Compound topographic index (r = 167)	141.2706	0.1138	0.0383
% Sagebrush (r = 1,451)	135.6409	0.0567	0.0047
Sagebrush height (r = 1,451)	126.9410	0.1126	0.0592
% Annual grass (r = 439)	124.2325	0.0123	0.0236
Slope (r = 1,451)	122.8048	0.0106	–0.0079
% Big sagebrush (r = 1,451)	120.7209	0.0874	0.0367
Distance to forest	118.7641	0.0289	0.0290
% Wet meadow (r = 1,451)	116.6342	0.0564	0.0013
Sagebrush height (r = 439)	109.9506	0.1056	0.0500
Compound topographic index (r = 1,451)	108.6883	0.0194	–0.0010
Compound topographic index (r = 439)	105.2025	0.0479	0.0153
Sagebrush height (r = 167	105.1597	0.0643	0.0252
Transformed aspect (r = 1,451)	104.7673	0.1151	0.0215
All stream density (r = 1,451)	103.9057	0.1551	0.0236
Transformed aspect (r = 439)	103.0485	0.0675	0.0493
Spring density (r = 1,451)	97.1057	0.0636	0.0074
% Sagebrush (r = 167)	95.6760	0.0809	0.0031
% Annual grass (r = 1,451)	94.6655	–0.0295	0.0198
% Annual grass (r = 167)	92.0964	0.0136	0.0269
Ditch density (r = 439)	90.4766	0.0224	–0.0017
% Big sagebrush (r = 439)	90.4636	0.1200	0.0444
% Wet meadow (r = 439)	86.5795	0.0365	0.0130
Transformed aspect (r = 167)	82.9371	0.1089	0.0518
Perennial stream density (r = 1,451)	82.8327	0.0916	0.0103
% Sagebrush (r = 439)	80.6475	0.0300	0.0181
% Big sagebrush (r = 167)	79.0057	0.1144	0.0625
Distance to ditch	76.0511	0.0373	0.0171
Ditch density (r = 1,451)	73.9668	0.0113	–0.0057
Ditch density (r = 167)	65.7882	0.0238	–0.0001
% Shrub cover (r = 1,451)	64.5340	0.0688	–0.0075
NDVI (r = 439)	63.0804	0.0300	0.0097
Curvature (r = 1,451)	59.3366	0.1048	0.0168
% Wet meadow (r = 167)	58.8860	0.0276	0.0112
Spring density (r = 439)	57.3095	0.0298	0.0112
% Little sagebrush (r = 1,451)	55.1726	0.1615	0.0073
Shrub height (r = 1,451)	49.9906	0.0105	–0.0588
% Sagebrush (r = 167)	47.4370	–0.0044	–0.0128
% Little sagebrush (r = 439)	46.9864	0.1286	0.0094
% Agricultural land (r = 439)	44.2656	0.0136	0.0016
NDVI (r = 1,451)	38.5950	0.1075	0.0196
Distance to PJ-CC1	37.0679	0.0527	0.0079
Intermittent stream density (r = 439)	36.5946	0.0391	0.0137
Shrub height (r = 167)	35.6161	0.1229	0.0279
Distance to PJ-CC2	34.1464	0.0686	0.0067
Distance to tree	33.4392	0.0566	–0.0134
Heat load index (r = 1,451)	33.2358	0.0653	0.0041
Shrub height (r = 439)	32.3593	0.0435	–0.0039
Intermittent stream density (r = 167)	30.6814	0.0221	0.0035

Table 6–2. Rankings of variable importance from preliminary variable screening, including change in AIC (ΔAIC), change in Spearman's rank coefficient (ΔSpearman's), and change in R^2 (ΔR^2) of observed versus predicted numbers of locations for sage-grouse summer\fall telemetry locations. —Continued

[Variable importance was determined by repeatedly refitting GLM's with logit link and binomial family to response variable data indicating used vs. random locations. Each candidate covariate was tested in models with and without that covariate, in the presence of as many as 5 other covariates; no covariates were allowed to exist in the same model if they had a correlation coefficient of at least 0.5 with the other covariate or covariates]

Covariate	ΔAIC	ΔSpearman's	ΔR^2
% Little sagebrush (r = 167)	30.1357	0.0580	0.0108
% Shrub cover (r = 439)	28.8457	0.0986	–0.0052
NDVI	28.7595	0.1290	0.0163
All stream density (r = 439)	28.6956	0.0621	0.0148
% Agricultural land (r = 167)	26.9363	0.0228	0.0034
% Non-sagebrush shrub (r = 1,451)	26.6691	0.0370	–0.0022
% Agricultural land (r = 1,451)	26.0982	0.0083	–0.0029
Heat load index (r = 439)	26.0934	0.0638	0.0062
Well density (r = 1,451)	23.5363	0.0104	–0.0011
% Non-sagebrush shrub (r = 439)	21.8871	0.0290	0.0202
All stream density (r = 167)	21.4560	0.0287	0.0076
Spring density (r = 167)	20.5854	0.0122	–0.0105
Heat load index (r = 167)	20.3274	0.0911	0.0117
Perennial stream density (r = 439)	19.9088	0.0272	0.0164
Intermittent stream density (r = 1,451)	19.6771	0.0468	0.0001
Distance to agricultural land	14.3910	0.0094	0.0080
% Non-sagebrush shrub (r = 167)	12.1077	0.0120	0.0216
Perennial stream density (r = 167)	9.5050	0.0138	0.0071
Distance to intermittent stream	6.1833	0.0624	0.0201
Distance to well	4.4906	–0.0084	0.0031
Curvature (r = 439)	4.1161	0.0232	0.0075
Distance to wet meadow	3.3525	–0.0051	–0.0106
Curvature (r = 167)	1.1763	0.0034	0.0064
Well density (r = 439)	0.5034	0.0004	–0.0003
Well density (r = 167)	–1.3869	0.0065	–0.0003

Table 6–3. Rankings of variable importance from preliminary variable screening, including change in AIC (ΔAIC), change in Spearman's rank coefficient (ΔSpearman's), and change in R^2 (ΔR^2) of observed versus predicted numbers of locations for sage-grouse winter telemetry locations.

[Variable importance was determined by repeatedly refitting GLM's with logit link and binomial family to response variable data indicating used vs. random locations. Each candidate covariate was tested in models with and without that covariate, in the presence of as many as 5 other covariates; no covariates were allowed to exist in the same model if they had a correlation coefficient of at least 0.5 with the other covariate or covariates]

Covariate	ΔAIC	ΔSpearman's	ΔR^2
All PJ (r = 439)	464.9993	0.2713	0.0540
% PJ–CC1 (r = 439)	438.2826	0.2399	0.0238
All PJ (r = 167)	412.0751	0.2164	0.0493
% PJ–CC1 (r = 167)	411.0159	0.2261	0.0476
% PJ–CC1 (r = 1,451)	403.0127	0.2158	–0.0144
All PJ (r = 1,451)	366.1952	0.2178	0.0567
Sagebrush height (r = 1,451)	284.7867	0.1252	0.0491
Slope (r = 439)	222.6762	0.2389	0.0044
Slope (r = 167)	215.4164	0.2260	0.0526
NDVI	202.8018	0.1285	–0.0118
Sagebrush height (r = 439)	200.2635	0.0900	0.0400
Distance to perennial stream	194.4803	0.1743	0.0371
NDVI (r = 439)	190.1386	0.1400	–0.0987
Slope (r = 1,451)	183.1140	0.0648	0.0030
Sagebrush height (r = 167)	181.1806	0.1174	0.0193
Roughness (r = 439)	163.4297	0.1470	0.0402
Roughness (r = 167)	161.3432	0.2138	0.0242
Roughness (r = 1,451)	160.0007	0.2694	0.0432
Elevation (r = 167)	154.4154	0.1388	–0.0308
NDVI (r = 1,451)	147.9914	0.0292	–0.0742
Elevation (r = 439)	138.0658	0.0939	–0.0361
Elevation (r = 1,451)	137.6968	0.0925	–0.0617
Compound topographic index (r = 439)	124.2172	0.1842	0.0140
Distance to all streams	118.0973	0.1423	0.0269
% Sagebrush (r = 1,451)	113.2254	0.2979	0.0088
% Big sagebrush (r = 1,451)	112.9036	0.1393	0.0175
Compound topographic index (r = 167)	106.1336	0.1848	0.0058
Compound topographic index (r = 1,451)	95.2362	0.1531	–0.0085
Distance to water body	93.8249	0.1791	0.0405
% Sagebrush (r = 439)	82.1460	0.0555	0.0056
Distance to agricultural land	80.1021	0.0725	–0.0173
% Shrub cover (r = 1,451)	76.2480	–0.0023	–0.0273
% Big sagebrush (r = 167)	73.9619	0.1074	0.0206
% Bare ground (r = 1,451)	72.8566	0.0273	–0.0250
% Big sagebrush (r = 439)	68.7715	0.1782	0.0737
Shrub height (r = 1,451)	63.3027	0.0463	0.0163
% Sagebrush (r = 167)	59.4742	0.0732	0.0246
Curvature (r = 1,451)	59.3060	0.0905	0.0126
% Annual grass (r = 439)	43.2944	0.1021	0.0098
Transformed aspect (r = 1,451)	35.7468	0.0984	0.0250
Transformed aspect (r = 439)	34.7531	0.0804	0.0312
Heat load index (r = 1,451)	34.4568	0.0924	–0.0026
% Annual grass (r = 167)	32.9165	0.0750	0.0121
% Non–sagebrush shrub (r = 167)	32.2422	0.1067	0.0134
% Bare ground (r = 439)	30.4008	0.0567	–0.0144
% Annual grass (r = 1,451)	29.5976	0.0840	0.0237
Distance to PJ–CC2	28.2154	0.0913	–0.0221
% Little sagebrush (r = 1,451)	28.0672	0.1211	0.0241
% Perennial grass (r = 1,451)	26.9205	0.0826	0.0244
% Non–sagebrush shrub (r = 439)	25.1783	0.0797	0.0132
Transformed aspect (r = 167)	24.9159	0.0772	0.0402
Distance to tree	24.3582	0.0924	–0.0189
Curvature (r = 439)	24.0018	0.0402	0.0022
Distance to ditch	23.9731	0.0216	0.0143
Distance to PJ–CC1	22.7121	0.1404	–0.0014
% Bare ground (r = 167)	20.9618	0.1580	0.0114
% Little sagebrush (r = 439)	19.6474	0.0686	0.0198
Heat load index (r = 439)	17.7674	0.0682	0.0123
% Herbaceous (r = 1,451)	17.2886	0.0429	0.0059
Shrub height (r = 439)	16.9114	0.0117	–0.0101
% Non–sagebrush shrub (r = 1,451)	16.6307	0.0927	0.0238
% Little sagebrush (r = 167)	16.0725	0.0868	0.0144
Distance to forest	15.0546	0.0195	0.0104
% Perennial grass (r = 439)	12.7536	0.0630	–0.0062
% Shrub cover (r = 167)	12.2470	0.0075	0.0048
% Perennial grass (r = 167)	11.4053	0.0334	0.0040
Well density (r = 1,451)	10.6114	0.0102	0.0015
Shrub height (r = 167)	10.5890	–0.0288	0.0043
% Shrub cover (r = 439)	10.2763	0.0144	–0.0132
Distance to wet meadow	9.4880	–0.0344	–0.0029
Heat load index (r = 167)	8.8475	0.0216	0.0050
Distance to intermittent stream	7.1437	0.0977	0.0233
Ditch density (r = 1,451)	6.7968	0.0298	0.0004

Table 6–3. Rankings of variable importance from preliminary variable screening, including change in AIC (ΔAIC), change in Spearman's rank coefficient (ΔSpearman's), and change in R^2 (ΔR^2) of observed versus predicted numbers of locations for sage-grouse winter telemetry locations.—Continued

[Variable importance was determined by repeatedly refitting GLM's with logit link and binomial family to response variable data indicating used vs. random locations. Each candidate covariate was tested in models with and without that covariate, in the presence of as many as 5 other covariates; no covariates were allowed to exist in the same model if they had a correlation coefficient of at least 0.5 with the other covariate or covariates]

Covariate	ΔAIC	ΔSpearman's	ΔR^2
Ditch density (r = 439)	6.0749	0.0239	–0.0004
Curvature (r = 167)	5.6549	0.0218	0.0051
Spring density (r = 1,451)	5.4979	0.0299	0.0095
Herbaceous (r = 167)	5.4713	0.0198	0.0083
Perennial stream density (r = 439)	4.7203	0.0233	0.0144
Perennial stream density (r = 167)	4.6709	0.0202	0.0018
All stream density (r = 439)	4.2968	0.0154	0.0093
% Agriculture (r = 1,451)	4.1993	0.0077	0.0035
All stream density (r = 167)	3.3281	0.0204	0.0020
All stream density (r = 1,451)	2.9972	0.0128	0.0091
% Herbaceous (r = 439)	2.9767	0.0107	0.0072
Perennial stream density (r = 1,451)	2.8976	0.0075	0.0082
% Wet meadow (r = 1,451)	2.3942	0.0003	0.0016
% Agriculture (r = 439)	2.0808	0.0210	0.0013
Intermittent stream density (r = 1,451)	1.8808	0.0089	0.0015
% Agriculture (r = 167)	1.5698	–0.0029	0.0011
Ditch density (r = 167)	1.4569	0.0086	–0.0015
% Wet meadow (r = 439)	1.1990	0.0075	0.0036
% Wet meadow (r = 167)	0.8828	0.0066	0.0045
Spring density (r = 439)	0.6648	0.0010	0.0014
Distance to well	0.6045	0.0006	0.0020
Intermittent stream density (r = 167)	0.3030	–0.0037	–0.0021
Well density (r = 439)	–0.4108	0.0021	–0.0006
Spring density (r = 167)	–0.6150	–0.0007	–0.0141
Intermittent stream density (r = 439)	–0.8782	0.0074	0.0019
Well density (r = 167)	–0.9395	0.0438	0.0032

Table 6–4. Rankings of variable importance from preliminary variable screening, including change in AIC (ΔAIC), change in Spearman's rank coefficient (ΔSpearman's), and change in R^2 (ΔR^2) of observed versus predicted numbers of locations for sage-grouse nest locations.

[Variable importance was determined by repeatedly refitting GLM's with logit link and binomial family to response variable data indicating used vs. random locations. Each candidate covariate was tested in models with and without that covariate, in the presence of as many as 5 other covariates; no covariates were allowed to exist in the same model if they had a correlation coefficient of at least 0.5 with the other covariate or covariates]

Covariate	ΔAIC	ΔSpearman's	ΔR^2
All PJ (r = 439)	257.3333	0.2255	0.0475
All PJ (r = 1,451)	250.3261	0.2385	0.0478
All PJ (r = 167)	221.5618	0.2255	0.0509
Sagebrush height (r = 1,451)	217.3599	0.2165	0.0447
Sagebrush height (r = 439)	201.6019	0.2377	0.0554
All PJ (r = 75)	195.9040	0.2091	0.0478
Sagebrush height (r = 167)	183.8527	0.2711	0.0675
Sagebrush height (r = 75)	178.7765	0.2469	0.0266
% PJ-CC1 (r = 1,451)	165.7709	0.1877	–0.0204
% Big sagebrush (r = 75)	148.0587	0.2248	0.0777
% PJ-CC1 (r = 439)	145.6135	0.1952	0.0411
% Big sagebrush (r = 167)	145.5843	0.2453	0.0830
% Big sagebrush (r = 1,451)	135.7630	0.1722	0.0440
% PJ-CC1 (r = 167)	135.3796	0.1951	0.0429
% Big sagebrush (r = 439)	130.0220	0.2169	0.0755
% Sagebrush (r = 1,451)	127.0239	0.2827	0.0065
% Sagebrush (r = 75)	119.3822	0.2356	0.0159
% Sagebrush (r = 167)	103.4651	0.1615	0.0265
% PJ-CC1 (r = 75)	98.5010	0.1627	0.0380
% Sagebrush (r = 439)	97.3172	0.1359	–0.0117
Distance to perennial stream	74.6503	0.1182	0.0140
Transformed aspect (r = 1,451)	64.8560	0.1262	0.0035
% Non-sagebrush shrub (r = 1,451)	61.5240	0.1787	–0.0352
% Non-sagebrush shrub (r = 439)	60.0450	0.1075	–0.0172
Elevation (r = 439)	57.6382	0.0721	–0.0122
Elevation (r = 167)	56.7809	0.0860	–0.0040
Distance to all streams	56.6126	0.1278	0.0247
Transformed aspect (r = 439)	51.2251	0.1851	0.0406
Elevation (r = 1,451)	50.2100	0.0618	0.0014
Elevation (r = 75)	49.5821	0.0458	–0.0048
% Non-sagebrush shrub (r = 167)	44.6517	0.0759	–0.0176
Distance to water body	43.4727	0.1277	0.0295
% Non-sagebrush shrub (r = 75)	38.6385	0.1306	0.0175
Transformed aspect (r = 167)	36.4909	0.1649	0.0440
% Bare ground (r = 1,451)	34.8850	0.0544	–0.0250
% Little sagebrush (r = 1,451)	31.1693	0.1026	–0.0292
Transformed aspect (r = 75)	30.6046	0.1179	0.0237
% Bare ground (r = 75)	27.7835	0.0980	0.0212
% Little sagebrush (r = 439)	25.7587	0.1266	–0.0029
% Bare ground (r = 167)	25.1834	0.0346	0.0255
Slope (r = 1,451)	24.1954	0.0539	0.0297
Roughness (r = 1,451)	23.8928	0.0539	0.0139
% Bare ground (r = 439)	23.7946	0.1553	–0.0163
Slope (r = 439)	23.2257	0.0417	0.0125
% Agricultural land (r = 1,451)	22.6549	0.0458	0.0099
NDVI (r = 439)	21.9877	0.0277	–0.0171
Perennial stream density (r = 439)	21.8462	0.0527	0.0170
% Little sagebrush (r = 75)	20.1694	0.1221	0.0121
NDVI (r = 1,451)	19.7965	0.0297	–0.0181
% Little sagebrush (r = 167)	19.6444	0.1015	0.0034
NVDI	19.1506	0.0600	0.0034
Roughness (r = 167)	18.6034	0.0352	0.0104
Perennial stream density (r = 167)	16.4785	0.0416	0.0063
Distance to forest	16.2911	0.0234	0.0173
Distance to agricultural land	15.7568	0.0540	–0.0099
Roughness (r = 439)	15.2911	0.0352	0.0094
All stream density (r = 167)	15.0227	0.0376	0.0035
Heat load index (r = 1,451)	14.5299	0.0739	0.0103
% Wet meadow (r = 439)	14.3112	0.0101	0.0030
Roughness (r = 75)	14.2978	0.0031	0.0091
Shrub height (r = 75)	14.2939	0.0670	0.0215
Perennial stream density (r = 1,451)	14.1237	0.0326	0.0236
% Shrub cover (r = 75)	14.0610	0.0154	–0.0084
Slope (r = 75)	13.9459	0.0123	0.0205
Curvature (r = 167)	13.9207	0.0595	0.0144
% Agricultural land (r = 439)	13.2496	0.0197	0.0101
Slope (r = 167)	13.0981	0.0364	0.0260
Shrub height (r = 167)	11.8562	–0.0059	–0.0197
Compound topographic index (r = 1,451)	11.5038	0.0074	–0.0039
Shrub height (r = 439)	11.3740	0.0446	0.0115

Table 6–4. Rankings of variable importance from preliminary variable screening, including change in AIC (ΔAIC), change in Spearman's rank coefficient (ΔSpearman's), and change in R^2 (ΔR^2) of observed versus predicted numbers of locations for sage-grouse nest locations.—Continued

[Variable importance was determined by repeatedly refitting GLM's with logit link and binomial family to response variable data indicating used vs. random locations. Each candidate covariate was tested in models with and without that covariate, in the presence of as many as 5 other covariates; no covariates were allowed to exist in the same model if they had a correlation coefficient of at least 0.5 with the other covariate or covariates]

Covariate	ΔAIC	ΔSpearman's	ΔR^2
All stream density (r = 439)	11.0487	0.0230	0.0124
All stream density (r = 75)	10.6379	0.0227	0.0035
All stream density (r = 1,451)	10.3324	0.0071	0.0118
Distance to PJ-CC2	10.0225	0.0329	–0.0026
Compound topographic index (r = 439)	9.8153	0.0189	0.0090
Perennial stream density (r = 75)	9.7407	0.0175	0.0022
Compound topographic index (r = 167)	9.7178	0.0346	0.0173
% Wet meadow (r = 167)	9.5738	0.0237	0.0039
Shrub height (r = 1,451)	9.3227	0.0057	–0.0026
% Shrub cover (r = 1,451)	8.7217	0.0225	–0.0211
% Perennial grass (r = 1,451)	7.8934	0.0389	–0.0203
% Annual grass (r = 439)	7.3940	0.0336	0.0079
% Herbaceous (r = 1,451)	7.2252	0.0740	0.0018
Distance to Tree	7.1741	0.0403	0.0073
% Wet meadow (r = 1,451)	6.9306	0.0122	0.0020
% Shrub cover (r = 167)	6.7339	0.0631	0.0226
Curvature (r = 1,451)	6.4076	0.0399	0.0060
Distance to PJ-CC1	6.3735	0.0447	0.0051
% Shrub cover (r = 439)	5.8677	0.0092	–0.0224
Heat load index (r = 439)	5.8495	0.0538	0.0089
% Annual grass (r = 167)	5.3117	0.0190	0.0053
Compound topographic index (r = 75)	5.3004	0.0312	0.0129
Distance to wet meadow	3.8952	–0.0062	0.0014
Distance to ditch	3.7838	0.0182	0.0028
Curvature (r = 75)	3.1143	0.0255	0.0102
% Agricultural land (r = 75)	3.0508	0.0112	0.0013
% Agricultural land (r = 167)	3.0220	0.0103	0.0026
Ditch density (r = 1,451)	2.9288	0.0085	0.0056
Intermittent stream density (r = 439)	2.8136	0.0164	–0.0010
% Annual grass (r = 75)	2.4493	0.0219	0.0128
% Perennial grass (r = 439)	2.3540	0.0460	0.0149
Heat load index (r = 75)	2.3251	0.0300	0.0083
Distance to intermittent stream	2.0978	0.0219	0.0077
Heat load index (r = 167)	2.0323	0.0477	0.0150
% Perennial grass (r = 167)	1.7266	0.0123	–0.0216
% Annual grass (r = 1,451)	1.5659	0.0029	0.0021
% Herbaceous (r = 439)	1.4095	0.0098	0.0042
Distance to well	1.2115	0.0036	–0.0026
% Herbaceous (r = 75)	0.9988	0.0181	0.0105
Curvature (r = 439)	0.8726	0.0019	0.0084
% Herbaceous (r = 167)	0.6386	0.0290	0.0178
% Perennial grass (r = 75)	0.0654	0.0278	0.0100
Intermittent stream density (r = 1,451)	0.0040	–0.0003	–0.0044
Spring density (r = 1,451)	–0.2783	0.0160	0.0015
Intermittent stream density (r = 75)	–0.6553	–0.0026	0.0010
Intermittent stream density (r = 167)	–1.4565	–0.0010	0.0024

Table 6–5. Rankings of variable importance from preliminary variable screening, including change in AIC (ΔAIC), change in Spearman's rank coefficient (ΔSpearman's), and change in R^2 (ΔR^2) of observed versus predicted numbers of locations for sage-grouse early brood locations.

[Variable importance was determined by repeatedly refitting GLM's with logit link and binomial family to response variable data indicating used vs. random locations. Each candidate covariate was tested in models with and without that covariate, in the presence of as many as 5 other covariates; no covariates were allowed to exist in the same model if they had a correlation coefficient of at least 0.5 with the other covariate or covariates]

Covariate	ΔAIC	ΔSpearman's	ΔR^2
% All PJ (r = 439)	196.6882	0.2566	0.1037
% All PJ (r = 167)	179.3213	0.2246	0.1007
% All PJ (r = 1,451)	175.3946	0.2418	0.0996
Saegbrush height (r = 1,451)	136.9557	0.0710	0.0956
% PJ-CC1 (r = 439)	135.2265	0.1618	0.0489
% PJ-CC1 (r = 167)	128.3528	0.2073	0.0781
Sagebrush height (r = 439)	124.2414	0.0489	0.1229
% PJ-CC1 (r = 1,451)	116.7861	0.2337	–0.0172
Sagebrush height (r = 167)	103.4636	0.1382	0.1182
% Big sagebrush (r = 1,451)	101.1434	0.1047	0.0907
Slope (r = 439)	96.5305	0.1255	0.0436
Roughness (r = 167)	91.5180	0.1165	0.0312
Slope (r = 167)	81.7925	0.0864	0.0423
Elevation (r = 439)	78.9733	0.1049	–0.0196
% Bare ground (r = 1,451)	77.3249	0.1243	0.0181
% Big sagebrush (r = 439)	75.8418	0.1211	0.1165
Roughness (r = 439)	75.8018	0.0829	0.0449
% Big sagebrush (r = 167)	73.7821	0.0582	0.1186
Elevation (r = 167)	73.0248	0.0866	–0.0652
Distance to perennial stream	72.1383	0.0717	0.0188
% Sagebrush (r = 439)	64.2552	0.0614	0.0335
Elevation (r = 1,451)	63.8608	0.0787	–0.0511
% Sagebrush (r = 167)	63.6740	0.1063	0.0865
% Sagebrush (r = 1,451)	62.0879	0.1031	0.0341
Distance to all streams	58.5149	0.1121	0.0260
Roughness (r = 1,451)	51.7196	0.0911	0.0189
Slope (r = 1,451)	48.0635	0.0705	0.0339
Transformed aspect (r = 439)	39.8619	0.1493	0.0342
% Bare ground (r = 439)	39.7696	0.0080	–0.0276
% Bare ground (r = 167)	37.7203	0.0673	0.0072
Transformed aspect (r = 167)	33.6640	0.0954	0.0513
Distance to agricultural land	33.1305	0.0636	0.0275
Distance to forest	28.9542	0.0193	0.0183
Curvature (r = 1,451)	28.9025	0.0997	0.0299
Distance to water body	28.1028	0.1110	0.0537
% Little sagebrush (r = 439)	27.9358	0.0279	0.0014
Transformed aspect (r = 1,451)	26.1674	0.0420	–0.0171
Compound topographic index (r = 439)	25.5537	0.0834	0.0145
% Non-sagebrush shrub (r = 1,451)	25.5512	0.0676	0.0123
Distance to ditch	21.8064	0.0315	0.0293
Compound topographic index (r = 167)	21.7070	0.0744	0.0082
% Perennial grass (r = 1,451)	21.3308	0.1132	–0.0054
% Non-sagebrush shrub (r = 439)	21.0366	0.0762	0.0288
% Little sagebrush (r = 1,451)	20.3892	0.0410	0.0201
% Little sagebrush (r = 167)	19.6830	0.0850	0.0539
% Herbaceous (r = 1,451)	18.6531	0.0846	0.0282
% Shrub cover (r = 439)	18.4603	0.0129	–0.0149
% Non-sagebrush shrub (r = 167)	18.3490	0.0878	0.0515
Shrub height (r = 1,451)	17.9732	0.0500	0.0124
Compound topographic index (r = 1,451)	16.4570	0.0841	–0.0083
Shrub height (r = 167)	16.0691	0.0669	0.0352
Spring density (r = 1,451)	15.8721	0.0644	0.0301
NDVI	15.3964	0.0746	–0.0020
Distance to intermittent stream	13.1838	0.0798	0.0028
Distance to PJ-CC2	11.2552	0.0168	–0.0062
Shrub height (r = 439)	10.8775	0.0448	–0.0039
Heat load index (r = 439)	10.4585	0.0547	0.0018
% Perennial grass (r = 439)	10.2875	0.0187	–0.0128
% Herbaceous (r = 439)	9.7307	0.0615	0.0114
% Shrub cover (r = 167)	9.0322	0.0520	0.0144
NDVI (r = 439)	8.4118	0.0106	0.0026
% Perennial grass (r = 167)	8.2708	0.0531	0.0051
% Agricultural land (r = 1,451)	7.0018	–0.0028	–0.0010
Perennial stream density (r = 439)	6.9680	0.0340	0.0276
Heat load index (r = 167)	6.9420	0.0412	0.0157
All stream density (r = 439)	6.9238	–0.0067	0.0232
Distance to tree	6.8756	0.0325	0.0072
Curvature (r = 439)	5.7436	0.0163	0.0090
Distance to wet meadow	5.5641	0.0018	0.0039
Distance to PJ-CC1	4.9902	0.0200	0.0050
Heat load index (r = 1,451)	4.8984	0.0162	–0.0068

Table 6–5. Rankings of variable importance from preliminary variable screening, including change in AIC (ΔAIC), change in Spearman's rank coefficient (ΔSpearman's), and change in R^2 (ΔR^2) of observed versus predicted numbers of locations for sage-grouse early brood locations.—Continued

[Variable importance was determined by repeatedly refitting GLM's with logit link and binomial family to response variable data indicating used vs. random locations. Each candidate covariate was tested in models with and without that covariate, in the presence of as many as 5 other covariates; no covariates were allowed to exist in the same model if they had a correlation coefficient of at least 0.5 with the other covariate or covariates]

Covariate	ΔAIC	ΔSpearman's	ΔR^2
NDVI (r = 1,451)	4.7780	0.0067	0.0108
% Herbaceous (r = 167)	4.7407	0.0448	–0.0045
Perennial stream density (r = 1,451)	4.0368	0.0013	0.0228
All stream density (r = 167)	3.1074	0.0050	0.0081
All stream density (r = 1,451)	3.0900	0.0035	0.0172
Distance to well	2.2385	0.0235	–0.0098
Perennial stream density (r = 167)	2.0020	0.0066	0.0057
% Annual grass (r = 167)	1.9635	0.0027	0.0103
% Agricultural land (r = 439)	1.8020	–0.0013	0.0032
Ditch density (r = 167)	1.8000	0.0034	0.0040
Ditch density (r = 1,451)	0.9484	–0.0015	0.0020
% Shrub cover (r = 1,451)	0.8660	0.0329	0.0013
% Agricultural land (r = 167)	0.7330	0.0004	–0.0007
% Annual grass (r = 1,451)	0.7126	–0.0045	0.0025
% Annual grass (r = 439)	0.6242	–0.0070	–0.0037
Spring density (r = 439)	0.0968	0.0006	–0.0059
% Wet meadow (r = 1,451)	0.0443	–0.0032	0.0008
Ditch density (r = 439)	–0.3949	–0.0046	0.0064
Intermittent stream density (r = 167)	–0.5258	–0.0085	–0.0031
Intermittent stream density (r = 1,451)	–0.6450	–0.0146	–0.0055
Curvature (r = 167)	–0.6856	0.0045	0.0005
% Wet meadow (r = 439)	–0.8349	–0.0061	0.0004
Spring density (r = 167)	–0.9589	–0.0059	–0.0030
Intermittent stream density (r = 439)	–0.9974	–0.0033	0.0038
% Wet meadow (r = 167)	–1.2278	0.0048	0.0060

Table 6–6. Rankings of variable importance from preliminary variable screening, including change in AIC (ΔAIC), change in Spearman's rank coefficient (ΔSpearman's), and change in R^2 (ΔR^2) of observed versus predicted numbers of locations for sage-grouse late brood locations.

[Variable importance was determined by repeatedly refitting GLM's with logit link and binomial family to response variable data indicating used vs. random locations. Each candidate covariate was tested in models with and without that covariate, in the presence of as many as 5 other covariates; no covariates were allowed to exist in the same model if they had a correlation coefficient of at least 0.5 with the other covariate or covariates]

Covariate	ΔAIC	ΔSpearman's	ΔR^2
All PJ (r = 1,451)	198.2483	0.1897	0.0485
All PJ (r = 439)	190.6226	0.2194	0.0950
PJ-CC1 (r = 1,451)	165.7056	0.2069	0.0326
All PJ (r = 167)	159.7507	0.1574	0.0478
PJ-CC1 (r = 439)	143.6294	0.1648	0.0476
Slope (r = 167)	134.8331	0.1810	0.0589
Sagebrush height (r = 1,451)	133.8118	0.1313	0.0755
Sagebrush height (r = 439)	123.8109	0.1196	0.0591
PJ-CC1 (r = 167)	120.0026	0.1487	0.0637
Sagebrush height (r = 167)	114.8426	0.1189	0.1076
Slope (r = 439)	111.5829	0.0936	0.0480
Roughness (r = 167)	109.9966	0.1324	0.0776
Distance to perennial stream	106.3650	0.1478	0.0466
Roughness (r = 439)	97.9271	0.1253	0.0437
% Big sagebrush (r = 1,451)	96.0423	0.1571	–0.0224
% Bare ground (r = 1,451)	93.1257	0.0691	0.0129
Distance to all streams	92.9051	0.1070	0.0368
% Sagebrush (r = 1,451)	92.5929	0.1423	0.0437
Roughness (r = 1,451)	92.2377	0.1082	0.0654
% Big sagebrush (r = 167)	87.6024	0.1300	0.0887
Elevation (r = 439)	81.9483	0.0793	0.0112
% Big sagebrush (r = 439)	81.2344	0.1842	0.1143
Elevation (r = 1,451)	80.7863	0.0773	0.0050
Elevation (r = 167)	76.8105	0.1042	0.0091
% Sagebrush (r = 167)	75.7310	0.1619	0.0682
% Sagebrush (r = 439)	73.8579	0.1400	0.0410
Slope (r = 1,451)	73.7664	0.0344	0.0687
% Bare ground (r = 439)	73.2716	0.0580	–0.0136
% Herbaceous (r = 1,451)	71.7289	0.1428	0.0258
% Bare ground (r = 167)	70.6829	0.1006	–0.0172
% Perennial grass (r = 1,451)	65.3027	0.0624	–0.0160
% Herbaceous (r = 439)	64.0867	0.1196	0.0711
Distance to agricultural land	57.0347	0.0524	0.0179
Transformed aspect (r = 439)	55.9461	0.1308	0.0108
% Herbaceous (r = 167)	53.1249	0.1355	0.0752
% Perennial grass (r = 439)	52.0185	0.1303	0.0555
% Perennial grass (r = 167)	51.2220	0.1364	0.0256
Transformed aspect (r = 167)	48.7304	0.1179	0.0245
Compound topographic index (r = 439)	48.4956	0.1005	–0.0211
Transformed aspect (r = 1,451)	44.7995	0.1261	0.0226
% Little sagebrush (r = 167)	43.9456	0.0839	0.0289
% Little sagebrush (r = 1,451)	42.0804	0.0752	0.0011
% Little sagebrush (r = 439)	41.2262	0.0430	–0.0050
Distance to ditch	39.8896	0.0255	0.0318
Distance to water body	38.9207	0.0833	0.0455
Compound topographic index (r = 167)	34.7752	0.0628	0.0261
Compound topographic index (r = 1,451)	33.4533	0.0203	0.0174
Distance to forest	32.5515	0.0197	0.0243
% Non-sagebrush shrub (r = 439)	30.4516	0.0403	0.0570
Heat load index (r = 439)	26.8947	0.0641	–0.0150
% Annual grass (r = 439)	25.8010	0.0108	0.0260
% Non-sagebrush shrub (r = 167)	24.0642	0.0613	0.0279
% Shrub cover (r = 1,451)	23.0102	0.0340	0.0079
% Annual grass (r = 1,451)	22.5038	0.0036	0.0101
Distance to tree	21.2647	0.0437	0.0157
Distance to PJ-CC1	19.9833	0.0227	0.0058
% Non-sagebrush shrub (r = 1,451)	18.6256	0.0405	0.0065
Heat load index (r = 167)	18.5458	0.0771	–0.0103
% Wet meadow (r = 1,451)	16.6489	0.0287	0.0156
Heat load index (r = 1,451)	15.6157	0.0471	0.0192
% Annual grass (r = 167)	15.2530	–0.0012	–0.0029
% Shrub cover (r = 439)	14.6134	–0.0127	–0.0091
Spring density (r = 1,451)	14.3323	0.0381	0.0065
Distance to PJ-CC2	13.2254	0.0868	0.0274
Curvature (r = 1,451)	12.3870	0.0487	0.0029
NDVI (r = 439)	9.8095	–0.0010	–0.0274
% Wet meadow (r = 439)	9.3138	0.0340	0.0102
Shrub height (r = 439)	8.2408	0.0477	0.0286
Shrub height (r = 167)	7.3283	0.0104	0.0192
Shrub height (r = 1,451)	6.7767	0.0561	–0.0028
% Wet meadow (r = 167)	6.0952	0.0238	0.0160
All stream density (r = 1,451)	5.6065	0.0286	0.0085
Ditch density (r = 1,451)	4.6093	0.0192	–0.0045
Distance to well	4.5879	0.0284	–0.0030

Table 6–6. Rankings of variable importance from preliminary variable screening, including change in AIC (ΔAIC), change in Spearman's rank coefficient (ΔSpearman's), and change in R^2 (ΔR^2) of observed versus predicted numbers of locations for sage-grouse late brood locations.—Continued

[Variable importance was determined by repeatedly refitting GLM's with logit link and binomial family to response variable data indicating used vs. random locations. Each candidate covariate was tested in models with and without that covariate, in the presence of as many as 5 other covariates; no covariates were allowed to exist in the same model if they had a correlation coefficient of at least 0.5 with the other covariate or covariates]

Covariate	ΔAIC	ΔSpearman's	ΔR^2
NDVI (r = 1,451)	4.5074	0.0255	0.0180
Perennial stream density (r = 1,451)	3.8749	0.0318	0.0104
% Shrub cover (r = 167)	3.8193	0.0665	0.0167
Distance to intermittent stream	3.7416	0.0647	0.0165
% Agriculture (r = 1,451)	2.9897	–0.0161	–0.0013
Ditch density (r = 439)	2.9065	0.0165	0.0049
Spring density (r = 439)	2.7327	0.0100	–0.0028
Spring density (r = 167)	1.9075	0.0028	–0.0043
NDVI	1.8395	0.0000	0.0171
All stream density (r = 439)	1.7582	–0.0096	–0.0006
Perennial stream density (r = 167)	1.6355	0.0148	0.0045
Distance to wet meadow	1.5433	0.0002	–0.0061
Perennial stream density (r = 439)	1.5229	0.0018	–0.0003
Intermittent stream density (r = 167)	1.2217	0.0027	0.0012
% Agricultural land (r = 439)	0.7325	–0.0025	0.0005
Ditch density (r = 167)	0.6796	0.0084	0.0014
All stream density (r = 167)	0.5697	0.0016	–0.0018
Curvature (r = 439)	0.4181	0.0083	–0.0017
% Agricultural land (r = 167)	0.1146	–0.0031	–0.0011
Intermittent stream density (r = 1,451)	0.0887	–0.0014	–0.0057
Intermittent stream density (r = 439)	–0.3828	–0.0041	–0.0013
Curvature (r = 167)	–1.2989	–0.0013	0.0018

For more information concerning the research in this report, contact the
Director, Western Ecological Research Center
U.S. Geological Survey
3020 State University Drive East
Sacramento, California 95819
https://www.usgs.gov/centers/werc

Publishing support provided by the U.S. Geological Survey
Science Publishing Network, Sacramento Publishing Service Center

ISSN 2331-1258(online)
https://doi.org/10.3133/ofr20191149